THE ROLE OF THE IMMUNE RESPONSE IN BRAIN METASTASIS

EDITED BY: Nicola Sibson, Frits Thorsen and Manuel Sarmiento Soto
PUBLISHED IN: Frontiers in Oncology and Frontiers in Immunology

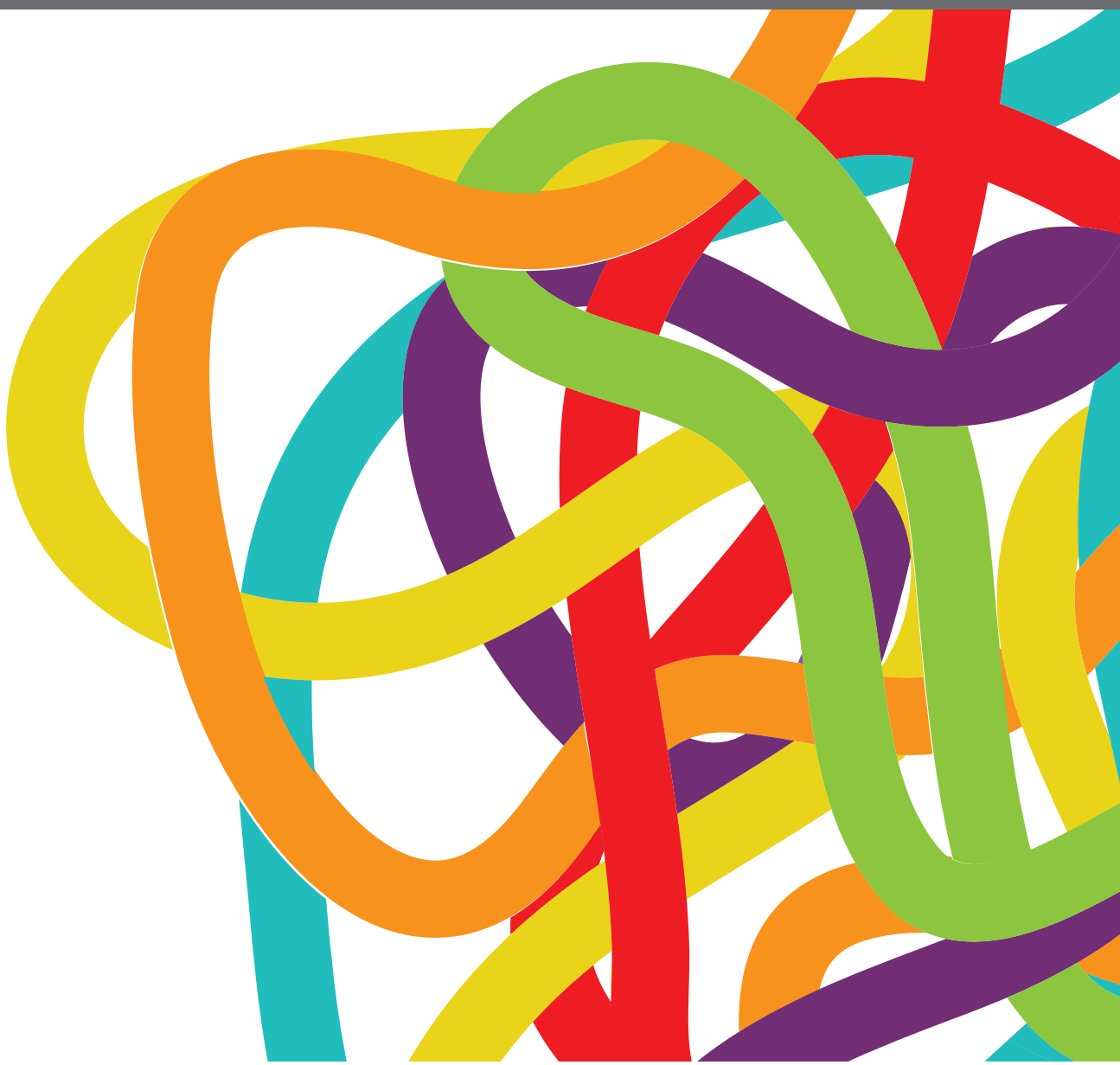

frontiers Research Topics

ISSN 1664-8714
ISBN 978-2-88976-287-3
DOI 10.3389/978-2-88976-287-3

About Frontiers

Frontiers is more than just an open-access publisher of scholarly articles: it is a pioneering approach to the world of academia, radically improving the way scholarly research is managed. The grand vision of Frontiers is a world where all people have an equal opportunity to seek, share and generate knowledge. Frontiers provides immediate and permanent online open access to all its publications, but this alone is not enough to realize our grand goals.

Frontiers Journal Series

The Frontiers Journal Series is a multi-tier and interdisciplinary set of open-access, online journals, promising a paradigm shift from the current review, selection and dissemination processes in academic publishing. All Frontiers journals are driven by researchers for researchers; therefore, they constitute a service to the scholarly community. At the same time, the Frontiers Journal Series operates on a revolutionary invention, the tiered publishing system, initially addressing specific communities of scholars, and gradually climbing up to broader public understanding, thus serving the interests of the lay society, too.

Dedication to Quality

Each Frontiers article is a landmark of the highest quality, thanks to genuinely collaborative interactions between authors and review editors, who include some of the world's best academicians. Research must be certified by peers before entering a stream of knowledge that may eventually reach the public - and shape society; therefore, Frontiers only applies the most rigorous and unbiased reviews.
Frontiers revolutionizes research publishing by freely delivering the most outstanding research, evaluated with no bias from both the academic and social point of view. By applying the most advanced information technologies, Frontiers is catapulting scholarly publishing into a new generation.

What are Frontiers Research Topics?

Frontiers Research Topics are very popular trademarks of the Frontiers Journals Series: they are collections of at least ten articles, all centered on a particular subject. With their unique mix of varied contributions from Original Research to Review Articles, Frontiers Research Topics unify the most influential researchers, the latest key findings and historical advances in a hot research area! Find out more on how to host your own Frontiers Research Topic or contribute to one as an author by contacting the Frontiers Editorial Office: frontiersin.org/about/contact

THE ROLE OF THE IMMUNE RESPONSE IN BRAIN METASTASIS

Topic Editors:
Nicola Sibson, University of Oxford, United Kingdom
Frits Thorsen, University of Bergen, Norway
Manuel Sarmiento Soto, Sevilla University, Spain

Citation: Sibson, N., Thorsen, F., Soto, M. S., eds. (2022). The Role of the Immune Response in Brain Metastasis. Lausanne: Frontiers Media SA.
doi: 10.3389/978-2-88976-287-3

Table of Contents

frontiers | Frontiers in Oncology

EDITORIAL
published: 10 May 2022
doi: 10.3389/fonc.2022.922700

Editorial: The Role of the Immune Response in Brain Metastasis

Nicola R. Sibson[1*], *Frits Thorsen*[2] *and Manuel Sarmiento Soto*[3,4]

[1] Department of Oncology, University of Oxford, Oxford, United Kingdom, [2] Molecular Imaging Center, Department of Biomedicine, University of Bergen, Bergen, Norway, [3] Department of Biochemistry and Molecular Biology, University of Seville, Seville, Spain, [4] Instituto de Biomedicina de Sevilla, Hospital Universitario Virgen del Rocío/CSIC/ Universidad de Sevilla and CIBERNED, Seville, Spain

Keywords: brain metastasis, immune response, tumour microenvironment, immunotherapy, imaging

Editorial on the Research Topic

The Role of the Immune Response in Brain Metastasis

OPEN ACCESS

Edited and reviewed by:
Catherine Sautes-Fridman, INSERM U1138 Centre de Recherche des Cordeliers (CRC), France

***Correspondence:**
Nicola R. Sibson
nicola.sibson@oncology.ox.ac.uk

Specialty section:
This article was submitted to Cancer Immunity and Immunotherapy, a section of the journal Frontiers in Oncology

Received: *18 April 2022*
Accepted: *25 April 2022*
Published: *10 May 2022*

Citation:
Sibson NR, Thorsen F and Soto MS (2022) Editorial: The Role of the Immune Response in Brain Metastasis. Front. Oncol. 12:922700. doi: 10.3389/fonc.2022.922700

Conventionally, metastases are treated using combinations of surgery, radiotherapy and systemic therapy. Nevertheless, survival amongst patients suffering metastatic spread to the brain remains extremely poor. Treatment failure frequently reflects the impact of complex and variable factors within the unique brain microenvironment, resulting in resistance to therapy and the onset of an immunosuppressive tumour microenvironment (TME). Thus, the development of new therapeutic strategies targeting brain-specific TME components has become one of the biggest challenges in the field.

It is becoming clear that the immune response to brain metastasis evolves over the time-course of tumour progression, and can have both tumour suppressive and tumour promoting effects. Nevertheless, as demonstrated by both Hu et al. and Xiao et al., despite issues of access across the blood-brain barrier, immunotherapy can confer a survival benefit in cancer patients with brain metastases. The overarching goal of this Research Topic, therefore, was to discuss the current state of knowledge with regards to the immune response to brain metastasis, and its potential role as a target for both diagnosis and treatment. From the available volumes on the Research Topic, we collected both original papers and review articles that addressed individual components of the brain immune response and TME, novel immunotherapeutic approaches and targeting of immune biomarkers for improved diagnosis or treatment planning.

It is undoubtedly the case that the complexity of the brain microenvironment contributes to the challenges encountered in treating brain metastases. Moreover, in the presence of a tumour, interactions between both the systemic and central immune responses and the normal brain environment only serve to compound these challenges. Understanding changes in the brain/tumour microenvironment at the cellular and molecular level is key to the development of new therapeutic strategies. In their primary research article, Economopoulos et al. evaluate the contribution of both blood-derived and brain resident macrophages (microglia) to brain metastasis development, with particular reference to their

pro-/anti-inflammatory state. The results of this study indicate that modulating both blood-derived macrophages and microglia towards a pro-inflammatory phenotype may provide a powerful therapeutic approach. Both Schulz and Sevenich, and Alvaro-Espinosa et al. expand this theme further at the molecular level, in mini-reviews. Schulz and Sevenich focus specifically on tumour associated macrophages, highlighting the similarities and differences between blood-derived and brain resident populations at the molecular level. This review focuses on RNA sequencing and mass cytometry data, and the authors discuss how increasing our understanding of transcriptional and translational programs that define disease-associated macrophage functions can help us to develop macrophage-targeted therapeutics. Alvaro-Espinosa et al. review the heterogeneity that can be seen within different cellular components in the healthy and injured brain, primarily at the single cell level, and discuss how understanding the diversity of the brain microenvironment could be exploited for translational purposes. Interestingly, as described by Randrian et al., the addition of artificial intelligence tools to histological analysis of immune cell infiltration could further enhance our understanding of the TME and aid stratification of brain metastasis patients.

Brain metastasis is an increasing clinical burden, and treatments for brain metastasis are frequently ineffective. New targeted therapies, tailored to the tumour and the specialised microenvironment of the brain are needed. Corroyer-Dulmont et al. and colleagues' mini-review evaluates the potential of radioimmunotherapy as a new approach to brain metastasis treatment. The review focuses on targeting inflammatory markers of brain metastasis for delivery of radionuclides to tumour sites. This paper also compares radioimmunotherapy with conventional whole brain radiotherapy, in terms of the balance between tumour control and healthy tissue complications. Of particular note, is the focus on treatment in the early micrometastatic stages of tumour development. Typically, brain metastases are only treated in the later stages of development, largely owing to limitations of current diagnostic imaging methods, and this is considered to be one of the main causes of ineffective treatment; treatment in the micrometastatic stages is likely to yield a much greater therapeutic response.

Imaging is frequently employed in the clinical diagnosis and management of brain metastasis. As the role of the brain's immune response comes under greater scrutiny, it is not surprising that attention has also turned to evaluating imaging readouts of this response. Zakaria et al. provide a comprehensive review of current imaging methods and their potential for predicting and measuring the response of brain metastases to immunotherapy; these methods include structural and physiological magnetic resonance imaging (MRI) methods, as well as molecular imaging approaches. Although it is relatively early days, and study numbers can be low, several of the methods discussed have potential and, of these, molecular imaging is perhaps the most promising. For example, in a primary research study, An et al. showed a significant correlation between increased uptake of the PET tracer ^{18}F-fluorodeoxyglucose (FDG) and CD68^{+} macrophages in brain metastases from primary breast cancer. Interestingly, however, increased ^{18}F-FDG did not correlate with the anti-inflammatory CD163^{+} subpopulation of macrophages. Given the work by Economopoulos et al. mentioned above, the ability to selectively image pro- and anti-inflammatory macrophages in brain metastases, may be an important goal, although other PET tracers, such as ^{18}F-DPA-713 (1), may provide more sensitive approaches than ^{18}F-FDG. Further, as noted by Zakaria et al., amino acid PET tracers or even specifically engineered PET tracers for monitoring cell trafficking (e.g. cytotoxic T cells), likely hold greater promise for the future of brain metastasis diagnosis and monitoring, as these do not suffer from the same sensitivity limitations as ^{18}F-FDG PET, owing to the high natural glucose consumption of the brain.

In recent years, one of the greatest advances in cancer therapy has been the development of therapies targeting the patient's immune defence against cancer cells, and it is becoming clear that this may also be a promising route to effective treatment of brain metastasis. Nevertheless, these immunotherapies must be developed with the specialised microenvironment of the brain in mind. Moreover, it seems logical that the development of sensitive and specific imaging tools must go hand-in-hand with the development of novel immune-targeted therapies for the most effective treatment of brain metastasis.

AUTHOR CONTRIBUTIONS

All authors listed have made a substantial, direct and intellectual contribution to the work, and approved it for publication.

FUNDING

This work was supported by Cancer Research UK (C5255/A15935) to NRS, The Norwegian Cancer Society (182716) to FT, and a Marie-Sklodowska Curie Action-IF (H2020-795695) to MSS.

REFERENCE

1. Pannell M, Economopoulos V, Wilson TC, Kersemans V, Isenegger PG, Larkin JR, et al. Imaging of Translocator Protein Upregulation is Selective for Pro-Inflammatory Polarised Astrocytes and Microglia. *Glia* (2019) 68:280–97. doi: 10.1002/glia.23716

Conflict of Interest: The authors declare that the research was conducted in the absence of any commercial or financial relationships that could be construed as a potential conflict of interest.

frontiers in Oncology

ORIGINAL RESEARCH
published: 24 June 2021
doi: 10.3389/fonc.2021.618705

Correlation Between ^{18}F-FDG Uptake and Immune Cell Infiltration in Metastatic Brain Lesions

*Young-Sil An[1], Se-Hyuk Kim[2], Tae Hoon Roh[2], So Hyun Park[3], Tae-Gyu Kim[3] and Jang-Hee Kim[3]**

[1] Department of Nuclear Medicine and Molecular Imaging, Ajou University School of Medicine, Suwon, South Korea, [2] Department of Neurosurgery, Ajou University School of Medicine, Suwon, South Korea, [3] Department of Pathology, Ajou University School of Medicine, Suwon, South Korea

OPEN ACCESS

Edited by:
Nicola Sibson,
University of Oxford, United Kingdom

Reviewed by:
Katsuhiko Kato,
Nagoya University, Japan
Eileen Parkes,
University of Oxford, United Kingdom

***Correspondence:**
Jang-Hee Kim
drjhk@ajou.ac.kr

Specialty section:
This article was submitted to Cancer Immunity and Immunotherapy, a section of the journal Frontiers in Oncology

Received: 18 October 2020
Accepted: 09 June 2021
Published: 24 June 2021

Citation:
An Y-S, Kim S-H, Roh TH, Park SH, Kim T-G and Kim J-H (2021) Correlation Between ^{18}F-FDG Uptake and Immune Cell Infiltration in Metastatic Brain Lesions. Front. Oncol. 11:618705. doi: 10.3389/fonc.2021.618705

Background: The purpose of this study was to investigate the correlation between ^{18}F-fluorodeoxyglucose (FDG) uptake and infiltrating immune cells in metastatic brain lesions.

Methods: This retrospective study included 34 patients with metastatic brain lesions who underwent brain ^{18}F-FDG positron emission tomography (PET)/computed tomography (CT) followed by surgery. ^{18}F-FDG uptake ratio was calculated by dividing the standardized uptake value (SUV) of the metastatic brain lesion by the contralateral normal white matter uptake value. We investigated the clinicopathological characteristics of the patients and analyzed the correlation between ^{18}F-FDG uptake and infiltration of various immune cells. In addition, we evaluated immune-expression levels of glucose transporter 1 (GLUT1), hexokinase 2 (HK2), and Ki-67 in metastatic brain lesions.

Results: The degree of ^{18}F-FDG uptake of metastatic brain lesions was not significantly correlated with clinical parameters. There was no significant relationship between the ^{18}F-FDG uptake and degree of immune cell infiltration in brain metastasis. Furthermore, other markers, such as GLUT1, HK2, and Ki-67, were not correlated with degree of ^{18}F-FDG uptake. In metastatic brain lesions that originated from breast cancer, a higher degree of ^{18}F-FDG uptake was observed in those with high expression of CD68.

Conclusions: In metastatic brain lesions, the degree of ^{18}F-FDG uptake was not significantly associated with infiltration of immune cells. The ^{18}F-FDG uptake of metastatic brain lesions from breast cancer, however, might be associated with macrophage activity.

Keywords: ^{18}F-fluorodeoxyglucose, positron emission tomography, brain metastasis, tumor microenvironment, immune cell

INTRODUCTION

Brain metastasis is a serious clinical manifestation in cancer patients and develops in approximately 20–30% of patients with solid cancers (1–3). Although management of brain metastasis has improved with multimodal therapies, effective management remains a challenge and the outcome of brain metastases is uniformly poor, with less than 10% of patients with brain metastasis surviving more than 2 years (2, 4). Cancer immunotherapies, i.e. immune-checkpoint inhibitors (ICIs), have enhanced the overall survival of cancer patients and dramatically changed therapeutic strategies for metastatic and other advanced stage of certain types of cancers (5–7). Furthermore, clinical trials have provided evidence that ICIs or ICI combined with radiation therapy could have sustained treatment efficacy for brain metastases (1, 2). However, these treatments can increase the risk of adverse effects, i.e. neurologic toxicity or radiation necrosis, in patients with brain metastases (1, 8). Moreover, no definitive biomarkers have been identified that can differentiate patients with brain metastases who may benefit from ICIs from those at risk for adverse effects (8).

^{18}F-Fluorodeoxyglucose (FDG) positron emission tomography (PET) is one of the fundamental imaging modalities for pre-therapeutic and therapeutic evaluation as well as end-of-treatment evaluations in clinical practice of many cancers (9–11). ^{18}F-FDG uptake is associated with elevated glycolysis in cancer cells. However, ^{18}F-FDG uptake can also be related to inflammation or immune reactions due to the consumption of glucose by immune cells (9, 11–13). Thus, ^{18}F-FDG uptake in cancer can reflect the tumor microenvironment, including not only the metabolic activity of cancer cells but also local immune reactions (11, 14–16). Since the response to immunotherapy can be associated with tumor infiltrating immune cells (17–20) and immune cell response can be visualized by ^{18}F-FDG PET (11, 14, 16), research has been conducted on the relationship between ^{18}F-FDG uptake and immunological features of the tumor microenvironment. In certain types of primary cancers, ^{18}F-FDG uptake is an additional biomarker that is predictive of immunological features and responses to ICIs (15, 21–24).

Since the microenvironment in brain metastases is different from the primary tumor (2, 25), to improve the efficiency of immunotherapy in brain metastases, a better understanding of the microenvironment in brain metastases, especially immune cell infiltration, is mandatory. However, few studies have used ^{18}F-FDG uptake for evaluation of immune cell infiltrate in brain metastases (26). Therefore, here we investigated the correlation between ^{18}F-FDG uptake and infiltration of various immune cells in brain metastases.

MATERIALS AND METHODS

Subjects

This study included 34 patients who underwent brain ^{18}F-FDG PET/computed tomography (CT) and were diagnosed with brain metastases at our institution between July 2005 and June 2019 with available brain tissue from surgery. We obtained clinical information (age, sex, primary cancer site, number of metastatic lesions in the brain, presence of metastatic lesions in regions other than brain and histologic type of metastatic brain lesion) from review of patient charts. This study was conducted retrospectively and was approved by the Institutional Review Board of Ajou University (AJIRB-MED-MDB-19-244). The need for informed consent was waived.

Brain ^{18}F-FDG PET/CT acquisition

After fasting for at least 6 h, patients were intravenously administered 300 MBq ^{18}F-FDG. The blood glucose level at the time of the ^{18}F-FDG injection was < 150 mg/dl in all patients. All subjects were instructed to rest comfortably for 30 min with their eyes closed before image acquisition. Brain PET/CT images were obtained with a Discovery ST 8 slice CT scanner or Discovery STE 16-slice CT scanner (GE Healthcare, Milwaukee, WI, USA). We first performed the non-contrast CT scan (100 kV, 95 mA; section width = 3.75 mm) in the brain region. Next, 10 min per frame of emission brain PET data were acquired in the three-dimensional mode. PET images were obtained by iterative reconstruction (i.e. ordered subsets of expectation maximization, with 2 iterations and 21 subsets), using CT images to correct attenuation.

Quantitative Analysis of PET Data

After fusion of the gadolinium-enhanced T1-weighted magnetic resonance imaging (MRI) and brain ^{18}F-FDG PET using the Fusion tool provided by PMOD software 3.0 (PMOD Technologies Ltd., Zurich, Switzerland), the volume of interest (VOI) was established by automatic delineation of the enhancing brain metastases lesions on MRI, which were removed by surgery. Edematous or necrotic areas of metastatic lesions, which could show considerably lower ^{18}F-FDG accumulation, were excluded from VOI. The VOI set for MRI was projected on the PET image, and the maximum and mean standardized uptake values normalized for body weight (SUVmax and SUVmean, respectively) of VOI were recorded (**Figures 1A–C**). All images were visually assessed for correct co-registration and appropriate VOIs that did not include adjacent normal brain activity. To set the reference value, a circular region of interest (ROI) with a 10mm diameter was circularly drawn on the frontal white matter area of the contralateral brain without any abnormal findings on MRI based on previous studies (27–29), and the SUVmean values were obtained (**Figure 1D**). The ^{18}F-FDG uptake ratio was calculated as the SUVs of the metastatic lesion divided by the SUVmean of the reference area. If multiple brain metastases were found in one patient, the lesion from which histological specimens were obtained was selected. We also measured the size of metastatic lesion, which had been excised and pathologically confirmed, on MRI images.

Histopathologic Analysis and Interpretation

Immunohistochemistry was conducted on representative sections of formalin-fixed, paraffin-embedded tissues using a BenchMark XT automated immunohistochemistry stainer (Ventana Medical Systems, Inc., Tucson, AZ, USA) according to the manufacturer's instructions. Briefly, after deparaffinization and rehydration, paraffin-embedded tissue sections (4-μm thick)

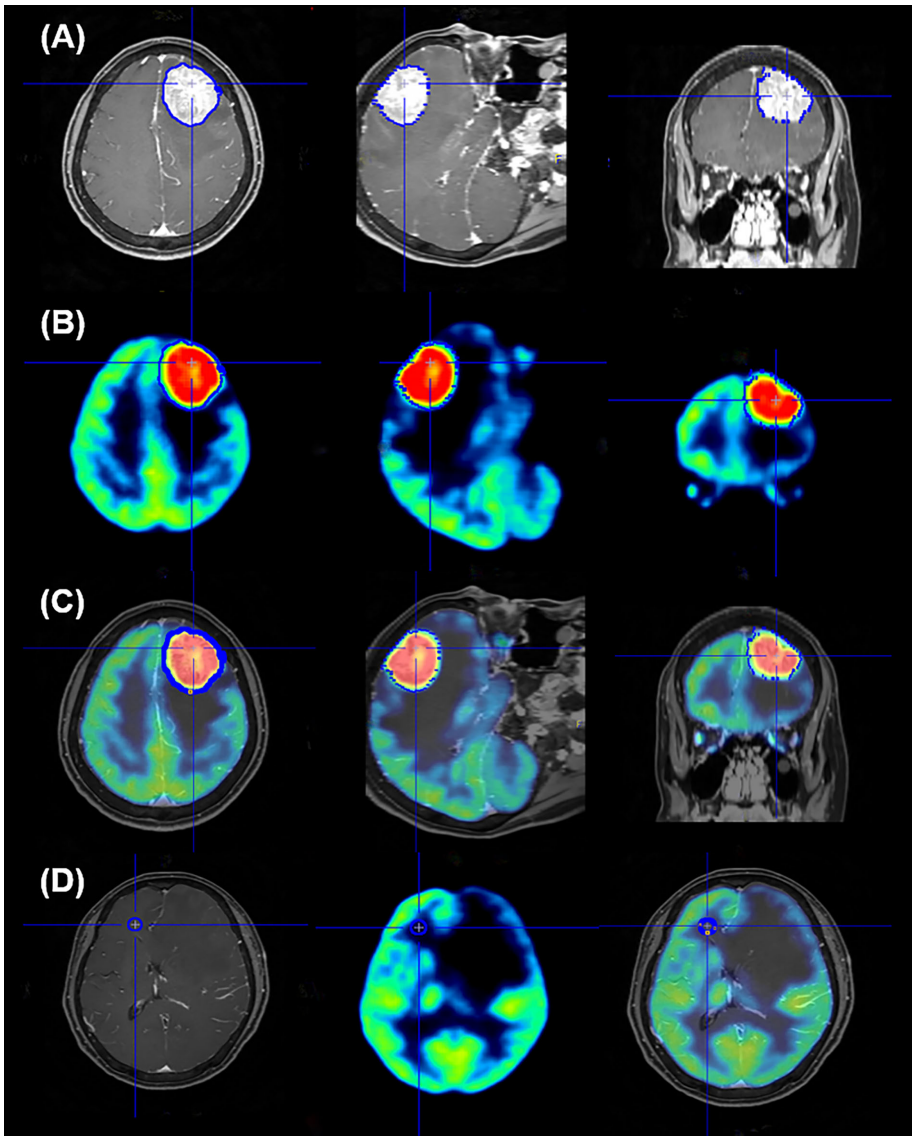

FIGURE 1 | Representative image of region of interest setting for quantification analysis of ^{18}F-FDG PET data. The volume of interest (VOI) was automatically delineated to brain lesions on MRI **(A)**; this edge of VOI was projected onto the PET image **(B)** and the VOI is seen in the image of the PET and MR fusion **(C)**. To set the reference area, the ROI is confirmed by setting the circular shape on the frontal white matter on the opposite side of the metastatic brain lesion and projecting it on the PET and PET/MR fusion images **(D)**.

were blocked with 3% hydrogen peroxide for 4 min at room temperature, treated with heat-induced antigen retrieval CC1 solution (Ventana Medical Systems) using the optimized antigen retrial condition, and incubated with primary antibodies. The primary antibodies are as follows: CD3, 1:100 (103R-95-RUO, Cell Marque, Rocklin, CA); CD8, pre-dilution (790-4460, Roche, Tucson, AZ); CD68, 1:50 (M0814, Dako, Denmark); CD163, 1:40 (163M-15-RUO, Cell Marque); myeloperoxidase (MPO), 1:100 (289A-75, Cell Marque); glucose transporter 1 (GLUT1), 1:200 (355A-14, Cell Marque); hexokinase 2 (HK2), 1:200 (E-AB-14706, Elabscience, Houston, TX) and Ki-67 (clone MIB-1) 1:60 (M7240, Dako). Detection was performed using the Ventana Optiview DAB Kit (Ventana Medical Systems). Counterstaining was performed with hematoxylin and bluing reagent for 4 min.

All histologic and immunohistochemical slides were reviewed by a single experienced pathologist (JH Kim) without prior knowledge of the clinical data and PET findings. Protein expression was evaluated based on intensity and proportion of positive cells. The intensity of expression was considered as positive if the intensity of membranous (GLUT1, CD3, and CD8), cytoplasmic (HK2, CD68, and CD163) or nuclear (Ki-67) staining was moderate or strong. Weak or nonspecific staining was considered as negative. For immune cell markers,

we used CD3 for T cells, CD68 for macrophages, and MPO for neutrophils and eosinophils. Infiltration of immune cells was scored as follows: Grade 1, focal mild infiltration of positive cells; Grade 2, multifocal mild infiltration; Grade 3, multifocal moderate to marked infiltration; and Grade 4, diffuse moderate to marked infiltration (**Figure 2**). GLUT1 and HK2 expressions were scored based on the percentage of positive tumor cells as follows: Grade 1, positive tumor cells <10%; Grade 2, 10¬–40%; Grade 3, 40–70%; and Grade 4, >70% (**Figure 3**). The Ki-67 proliferation index was measured by counting the percentage of Ki-67-positive nuclei per 500–1000 tumor cells in the region of the tumor with the greatest density of staining, indicating areas with the highest mitotic activity.

Statistical Analysis

The sample size required for this study using a significance (a) level of 5% and statistical power (1-b) of 80% was calculated using MedCalc software (version 18.11.3; MedCalc Software bvba, Ostend, Belgium). A sample size of 28 was required to obtain an appropriate confidence level; thus, the final sample size (n = 34) was sufficient.

Clinical characteristics are described as descriptive frequencies followed by percentages for categorical variables and means ± standard deviation (SD) for continuous variables. The difference in ^{18}F-FDG uptake of brain metastatic lesions according to clinical characteristics was analyzed using Mann–Whitney test and one-way analysis of variance (ANOVA) test. Mann–Whitney or ANOVA test was used to determine whether ^{18}F-FDG uptake varied according to the expression level of immune cell markers and biologic markers in metastatic brain lesions. Spearman's correlation coefficient (r) was calculated to evaluate the correlations parameters. Correlations were classified as poor ($|rho| < 0.29$), fair ($|rho| = 0.30–0.59$), moderate ($|rho| = 0.60–0.79$), and very strong ($|rho| \geq 0.80$) (30). If there was a significant correlation between pathologic parameters, the analysis of covariance (ANCOVA) test was used to adjust the covariates. All other statistics were analyzed using MedCalc software. P-values <0.05 were considered significant.

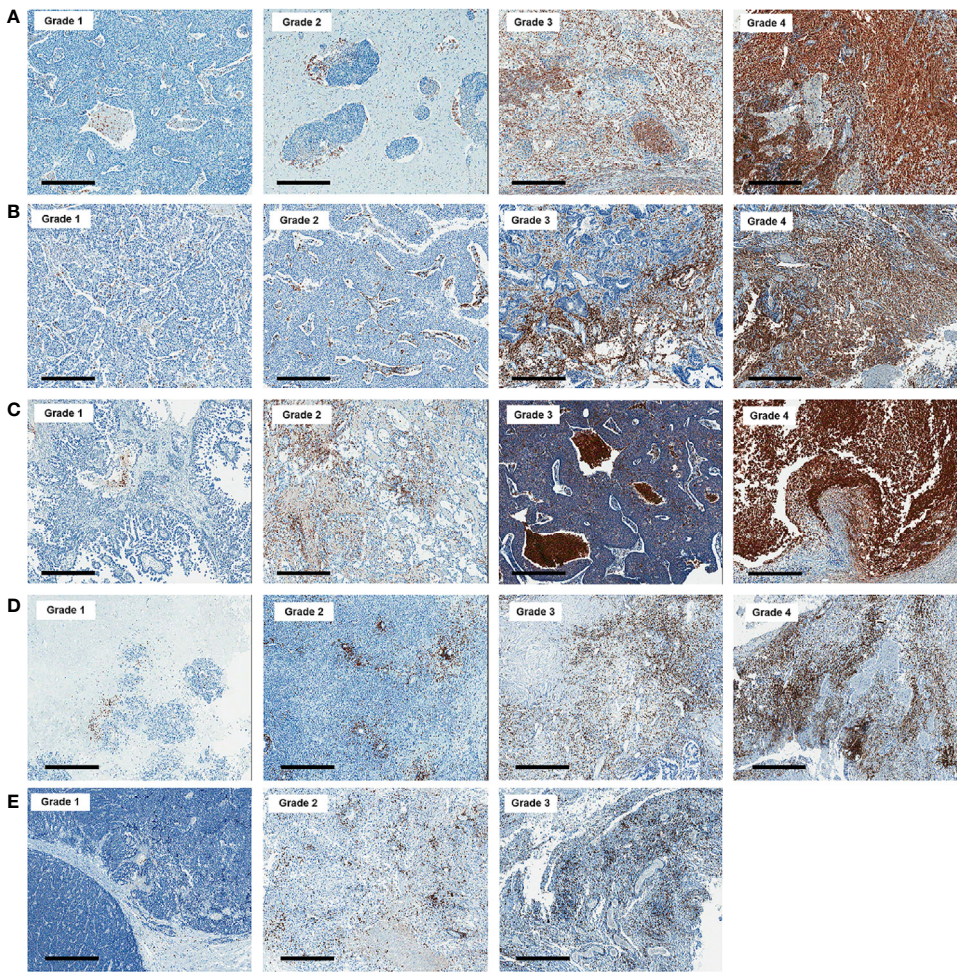

FIGURE 2 | Representative images of CD68 **(A)**, CD163 **(B)**, myeloperoxidase **(C)**, CD3 **(D)**, and CD8 **(E)** immunohistochemistry according to grades (x 50). Bar indicates 500 μm.

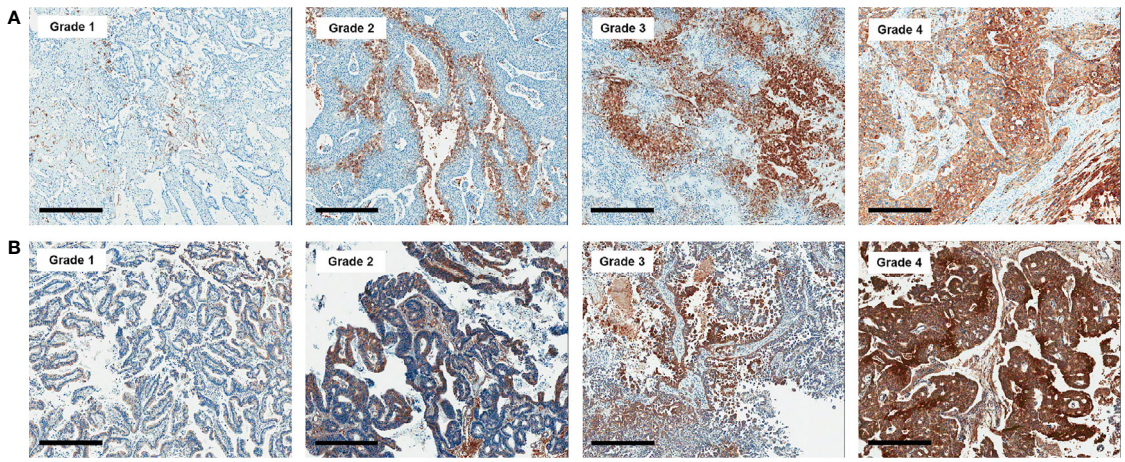

FIGURE 3 | Representative images of GLUT1 **(A)** and hexokinase 2 **(B)** immunohistochemistry according to grades (x 50). Bar indicates 500 μm.

RESULTS

Patient Characteristics and ^{18}F-FDG Uptake Ratio of Metastatic Brain Lesions

The average patient age was 63.7 years, and the patient group included 59% (20/34) males. Lung cancer (14/34, 41.2%) was the most common primary cancer site of metastatic brain lesions, followed by breast cancer (10/34, 29.4%). Twenty-one patients (21/34, 61.8%) had a single metastatic brain lesion. Approximately 44% of patients (15/34) also had metastases to other organs at the time of diagnosis of brain metastasis. Most of the histologic types of the metastatic lesions were adenocarcinoma (29/34, 85.4%). The mean diameter and VOI of brain metastases lesions were 3.10 cm and 13.08 cm^3, respectively. The mean value of maximum ^{18}F-FDG uptake ratio and of brain metastases was 3.02, and the average value of the mean ^{18}F-FDG uptake ratio was 1.70. The degree of ^{18}F-FDG uptake of brain metastasis lesions showed poor correlation with lesion size and VOI size (all $p > 0.05$) (**Table 1**). The mean and maximum ^{18}F-FDG uptake ratios were slightly lower in the metastatic brain lesions from the lung than those in other sites. However, the difference was not statistically significant. The other clinicopathological parameters, i.e. histologic type of the metastatic lesions, showed no significant correlation (all $p > 0.05$). **Table 1** lists the clinicopathological characteristics of patients and the difference in ^{18}F-FDG uptake of brain metastasis according to clinical parameters. The individual characteristics of each patient are presented in **Supplementary Table 1**.

Relationship Between ^{18}F-FDG Uptake and Grades of Immune Cell Infiltration

We next identified immune cells using specific markers. Macrophages, which are immune-positive for CD68 and/or CD163, were most abundantly identified in the metastatic brain lesions, followed by neutrophils, which are immune-positive for MPO. Diffuse strong infiltration (grade 4) of CD163+ macrophages was observed in 5 (14.7%) of metastatic lesions. Two (5.9%) cases showed diffuse strong infiltration of neutrophils, and both cases were associated with tumor necrosis. However, T lymphocytes in metastatic brain lesions were less frequently identified and only one case revealed diffuse strong infiltration (Grade 4) of CD3+ T lymphocytes. Moreover, most cases (27/34, 79.4%) showed only focal mild infiltration or no diffuse strong infiltration of CD8+ T lymphocytes (**Table 2**). We performed analysis of ^{18}F-FDG uptake ratio of brain metastases according to the grades of infiltration of each immune cell. To evaluate positive or negative effects between types of immune cells, we analyzed correlation between grades of immune markers. We observed a significantly positive correlation between markers for macrophages (CD68 and CD163) and T cells (CD3 and CD8). However, we could not find any significant differences between ^{18}F-FDG uptake ratio and grades of immune cell infiltration with or without adjustment for covariates (all $p > 0.05$) (**Table 2** and **Supplementary Table 2**).

Relationship Between ^{18}F-FDG Uptake and Grades of Immune Cell Infiltration According to the Primary Cancer Sites

We further investigated immune cell infiltration according to the sites of the primary cancers. We divided metastatic brain lesions into 3 groups (lung [n=14], breast [n=10], and GI and others [n=10]) according to the primary sites and analyzed immune cell infiltration in each group. Immune cell infiltration was more frequent in the metastatic lesions from the lung than the other two groups (**Table 3**). In particular, diffuse strong infiltration of macrophages (CD68 or CD163) was most commonly identified in the metastatic lesion from the lung. In the majority of metastatic lesions from the breast, immune cell infiltrations except for neutrophils (MPO) were mild (Grade 1 or 2). We analyzed the correlation between ^{18}F-FDG uptake ratio of brain metastases lesions and primary cancer sites. Interestingly, we found that the maximum ^{18}F-FDG uptake ratio and mean

TABLE 1 | Clinicopathologic characteristics and ^{18}F-FDG uptake ratio in patients with brain metastases.

Characteristics	Number	Maximum ^{18}F-FDG uptake ratio	*p*-value for difference of maximum ^{18}F-FDG uptake ratio between groups	Mean ^{18}F-FDG uptake ratio	*p*-value for difference of mean ^{18}F-FDG uptake ratio between groups
Age (years)	63.70 ± 9.90	3.02 ± 1.24	NA	1.70 ± 0.70	NA
Sex					
Male	20 (58.8%)	3.08 ± 1.39	0.743	1.58 ± 0.65	0.261
Female	14 (41.2%)	2.93 ± 1.05		1.86 ± 0.76	
Primary cancer sites					
Lung	14 (41.2%)	2.74 ± 0.95	0.547	1.51 ± 0.58	0.273
Breast	10 (29.4%)	3.12 ± 1.04		1.98 ± 0.82	
GI tract and others	10 (29.4%)	3.29 ± 1.75		1.67 ± 0.70	
Number of metastatic sites in the brain					
Single	21 (61.8%)	2.87 ± 0.96	0.375	1.64 ± 0.68	0.530
Multiple	13 (38.2%)	3.28 ± 1.66		1.80 ± 0.75	
Presence of extracranial metastasis					
Yes	15 (44.1%)	3.35 ± 1.42	0.165	1.73 ± 0.78	0.756
No	19 (55.9%)	2.75 ± 1.05		1.65 ± 0.60	
Histologic type of metastatic lesions					
Adenocarcinoma†	29 (85.4%)	3.08 ± 1.28	0.371	1.71 ± 0.69	0.118
Squamous cell carcinoma	3 (8.8%)	2.03 ± 0.16		1.17 ± 0.25	
Small cell carcinoma	1 (2.9%)	2.67		1.52	
Large cell neuroendocrine carcinoma	1 (2.9%)	4.38		3.11	

		Correlation with maximum ^{18}F-FDG uptake ratio		Correlation with mean ^{18}F-FDG uptake ratio	
		rho (95% CI)	*p*-value	rho (95% CI)	*p*-value
Size of brain metastasis (cm)	3.10 ± 0.94	0.27 (0.07 to 0.56)	0.114	0.03 (-0.31 to 0.36)	0.879
VOI size of brain metastasis (cm^3)	13.08 ± 9.94	0.23 (0.11 to 0.53)	0.175	0.02 (-0.35 to 0.32)	0.896

†*Category of adenocarcinoma included adenocarcinoma of the lung and gastrointestinal tracts, as well as ductal and lobular carcinoma of the breast.*
GI tract, Gastrointestinal tract; NA, Not available.

^{18}F-FDG uptake ratio were significantly correlated with infiltration of macrophages (CD68) in the metastatic lesions with breast origin (p = 0.002 and p =0.036, respectively). There were no associations between ^{18}F-FDG uptake ratios and infiltration of other types of immune cells (**Table 3**).

Relationship Between ^{18}F-FDG Uptake and Expression of Other Biologic Markers in the Metastatic Brain Lesions

We also examined immuno-expression of GLUT1, HK2 and Ki-67, which are known biologic markers associated with ^{18}F-FDG uptake. We found that 10 cases (29.4%) showed diffuse strong immuno-expression (grade 4) of HK2 in metastatic tumor cells and 7 cases (20.6%) revealed diffuse strong immuno-expression (grade 4) of GLUT1. However, the maximum ^{18}F-FDG uptake ratio and mean ^{18}F-FDG uptake ratio in metastatic brain lesions did not differ significantly according to the grades of GLUT1 and HK2 after adjustment for covariates (all $p > 0.05$) (**Table 4** and **Supplementary Table 2**). The absence of association between ^{18}F-FDG uptake ratio and degrees of GLUT1 and HK2 expression also was found within subgroups divided by primary cancer site (**Table 4**). The Ki-67 proliferation index of the metastatic brain lesions ranged widely from 0.3% to 96.1% (average: 35.0%). However, the Ki-67 proliferation index of the metastatic lesions showed not only poor correlation but also inverse tendency with ^{18}F-FDG uptake ratios (for maximum ^{18}F-FDG uptake ratio, rho = -0.21; for mean ^{18}F-FDG uptake ratio, rho = -0.25; **Figure 4** and **Table 5**). The Ki-67 proliferation index and ^{18}F-FDG uptake ratio did not show a significant correlation even within the subgroups by primary cancer site (all $p >$ 0.05, **Table 5**).

TABLE 2 | ^{18}F-FDG uptake ratio according to GLUT1, HK2 and immune cell markers in patients with brain metastasis.

	Maximum ^{18}F-FDG uptake ratio	*p*-value for difference of maximum ^{18}F-FDG uptake ratio between groups	Mean ^{18}F-FDG uptake ratio	*p*-value for difference of mean ^{18}F-FDG uptake ratio between groups
Expression of CD68				
Grade 1 (*n*=13)	3.02 ± 1.54		1.62 ± 0.70	
Grade 2 (*n*=10)	3.35 ± 1.09	0.384†	1.98 ± 0.77	0.216†
Grade 3 (*n*=6)	2.63 ± 1.09		1.36 ± 0.44	
Grade 4 (*n*=5)	2.80 ± 0.98		1.72 ± 0.79	
Expression of CD163				
Grade 1 (*n*=9)	3.21± 1.74		1.63 ± 0.77	
Grade 2 (*n*=12)	3.24± 1.10	0.865†	1.93 ± 0.72	0.748†
Grade 3 (*n*=8)	2.74 ± 1.00		1.40 ± 0.49	
Grade 4 (*n*=5)	2.58 ± 1.01		1.71 ± 0.79	
Expression of MPO				
Grade 1 (*n*=13)	3.46 ± 1.59		2.03 ± 0.83	
Grade 2 (*n*=10)	2.44 ± 0.68	0.271†	1.42 ± 0.38	0.074†
Grade 3 (*n*=9)	3.23 ± 1.01		1.66 ± 0.66	
Grade 4 (*n*=2)	2.02 ± 0.07		1.09 ± 0.12	
Expression of CD3				
Grade 1 (*n*=18)	3.25 ± 1.39		1.78 ± 0.74	
Grade 2 (*n*=14)	2.85 ± 1.06	0.350†	1.64 ± 0.69	0.279†
Grade 3 (*n*=1)	2.02		1.40	
Grade 4 (*n*=1)	2.05		1.26	
Expression of CD8				
Grade 1 (*n*=27)	3.01 ± 1.29		1.68 ± 0.68	
Grade 2 (*n*=5)	3.47 ± 1.06	0.312†	1.93 ± 0.92	0.529†
Grade 3 (*n*=2)	2.03 ± 0.02		1.33 ± 0.09	

†*adjusted values for covariates; MPO, Myeloperoxidase, marker for neutrophils; CD3/CD8, Marker for T cells; CD68/CD163, Marker for macrophages.*

DISCUSSION

The tumor microenvironment of brain metastases is unique and distinct from other sites of the body not only in terms of cellular components but also in metabolism (25, 31, 32). The cellular components of brain include astrocytes, microglia, oligodendrocytes, and neurons that are not present elsewhere in the body (2, 25, 32). In addition, parenchymal cells of the normal brain show high levels of glucose metabolism (33) and this metabolic characteristic of normal brain hampers the delineation of tumors from normal brain by ^{18}F-FDG compared with amino acid tracers, such as ^{11}C-methionine (MET) and 6-[18F]-L-fluoro-L-3, 4-dihydroxyphenylalanine (FDOPA) (34). Nevertheless, ^{18}F-FDG is clinically preferred because commercially available ^{18}F-FDG is the easiest to - perform in facilities without cyclotrons and costs are mostly covered by health insurance, though this can vary from country to country, but also shows cost benefits. In addition, previous studies reported that ^{18}F-FDG PET provides valuable information on the metabolic status of the tumor microenvironment as well as local immune reactions (14, 15, 21–24, 35). To overcome the weakness of ^{18}F-FDG in the brain and enhance the delineation of tumor from normal brain, we defined the reference value; the ROI was circularly drawn on the frontal white matter area of

TABLE 3 | ^{18}F-FDG uptake ratio and expression of immune cell markers according to the primary cancer

Primary cancer	Immune cell markers	Maximum ^{18}F-FDG uptake ratio	*p*-value for difference of maximum ^{18}F-FDG uptake ratio between groups	Mean ^{18}F-FDG uptake ratio	*p*-value for difference of mean ^{18}F-FDG uptake ratio between groups
Lung	Expression of CD68				
	Grade 1 (*n*=4)	3.03 ± 1.04		1.64 ± 0.51	
	Grade 2 (*n*=2)	2.28 ± 0.61	0.909†	1.24 ± 0.45	0.688†
	Grade 3 (*n*=3)	2.56 ± 1.31		1.17 ± 0.29	
	Grade 4 (*n*=5)	2.80 ± 0.98		1.72 ± 0.79	
	Expression of CD163				
	Grade 1 (*n*=2)	3.19 ± 0.74		1.56 ± 0.06	
	Grade 2 (*n*=3)	2.53 ± 1.28	0.764†	1.45 ± 0.77	0.632†
	Grade 3 (*n*=4)	2.88 ± 1.02		1.27 ± 0.31	
	Grade 4 (*n*=5)	2.58 ± 1.01		1.71 ± 0.79	
	Expression of MPO				
	Grade 1 (*n*=3)	2.80 ± 1.14		1.65 ± 0.63	
	Grade 2 (*n*=5)	2.47 ± 0.77	0.722†	1.35 ± 0.27	0.767†
	Grade 3 (*n*=5)	3.11 ± 1.15		1.65 ± 0.86	
	Grade 4 (*n*=1)	2.08		1.18	
	Expression of CD3				
	Grade 1 (*n*=5)	2.79 ± 1.04		1.49 ± 0.55	
	Grade 2 (*n*=7)	2.91 ± 1.02	0.253†	1.57 ± 0.72	0.452†
	Grade 3 (*n*=1)	2.02		1.40	
	Grade 4 (*n*=1)	2.05		1.26	
	Expression of CD8				
	Grade 1 (*n*=9)	2.57 ± 0.88		1.39 ± 0.45	
	Grade 2 (*n*=3)	3.72 ± 0.88	0.190†	1.98 ± 0.98	0.307†
	Grade 3 (*n*=2)	2.03 ± 0.02		1.33 ± 0.09	
Breast	Expression of CD68				
	Grade 1 (*n*=6)	2.36 ± 0.40*		1.47 ± 0.60*	
	Grade 2 (*n*=4)	4.27 ± 0.28*	0.002†*	2.75 ± 0.29*	0.036†*
	Expression of CD163				
	Grade 1 (*n*=4)	2.39 ± 0.42		1.45 ± 0.73	
	Grade 2 (*n*=6)	3.61 ± 1.06	0.818†	2.33 ± 0.72	0.927†
	Expression of MPO				
	Grade 1 (*n*=8)	3.37 ± 1.01		2.08 ± 0.87	
	Grade 2 (*n*=1)	2.32	0.348	2.03	0.628
	Grade 3 (*n*=1)	1.95		1.16	
	Expression of CD3				
	Grade 1 (*n*=7)	3.02 ± 1.03		1.94 ± 0.88	
	Grade 2 (*n*=3)	3.37 ± 1.23	0.659	2.08 ± 0.81	0.827
	Expression of CD8				
	Grade 1 (*n*=9)	3.00 ± 1.02		1.90 ± 0.82	
	Grade 2 (*n*=1)	4.22	0.295	2.72	0.377
GI tract and others	Expression of CD68				
	Grade 1 (*n*=3)	4.32 ± 2.90		1.92 ± 1.18	
	Grade 2 (*n*=4)	2.97 ± 1.13	0.974†	1.58 ± 0.49	0.980†
	Grade 3 (*n*=3)	2.71 ± 1.11		1.55 ± 0.54	
	Expression of CD163				
	Grade 1 (*n*=3)	4.32 ± 2.90		1.92 ± 1.18	
	Grade 2 (*n*=3)	3.19 ± 1.03	0.967†	1.61 ± 1.11	0.970†
	Grade 3 (*n*=4)	2.61 ± 1.11		1.53 ± 0.66	
	Expression of MPO				
	Grade 1 (*n*=2)	4.82 ± 3.97		2.41 ± 1.22	
	Grade 2 (*n*=4)	2.45 ± 0.77	0.400	1.35 ± 0.46	0.262
	Grade 3 (*n*=3)	3.86 ± 0.16		1.84 ± 0.34	
	Grade 4 (*n*=1)	1.97		1.00	
	Expression of CD3				
	Grade 1 (*n*=6)	3.91 ± 1.91		1.84 ± 0.76	
	Grade 2 (*n*=4)	2.37 ± 1.11	0.487†	1.42 ± 0.59	0.594†
	Expression of CD8				
	Grade 1 (*n*=9)	3.44 ± 1.79		1.75 ± 0.69	
	Grade 2 (*n*=1)	1.97	0.459	1.00	0.262

*†adjusted values for covariates, *p < 0.05; GI tract: Gastrointestinal tract; MPO, Myeloperoxidase, marker for neutrophils; CD3/CD8, Marker for T cells; CD68/CD163, Marker for macrophages.*

the contralateral brain without any abnormal findings on MRI based on previous studies (27–29). We found a wide range of ^{18}F-FDG uptake in metastatic brain lesions.

^{18}F-FDG can be taken up by many tumor-associated immune cells, such as tumor-infiltrating lymphocytes (TILs), tumor-associated macrophages (TAMs) and granulocytes such as neutrophils (11, 14, 16). ^{18}F-FDG uptake is correlated with PDL-1 expression and TILs, especially CD8+ cytotoxic T cells in primary cancers (14, 22–24). Furthermore, abundant infiltration of TILs including CD8+ T cells in primary cancers is associated with better response to immunotherapy (18, 20, 36, 37). Here we investigated the correlation between ^{18}F-FDG uptake and immune cell infiltration with various immune cell markers in brain metastases. In contrast to previous reports with primary cancers (14, 22–24), there were no significant correlations between ^{18}F-FDG uptake and T cell infiltration grade in brain metastases.

^{18}F-FDG uptake of immune cells in brain metastases can differ from uptake in other sites of the body. Immune cells including lymphocytes, neutrophils and the monocyte/macrophage family express high levels of glucose transporters and hexokinase activity with increased ^{18}F-FDG uptake (12, 13). However, immune cells in metastatic brain lesions compete to utilize glucose not only with tumor cells but also brain parenchymal cells, because brain parenchymal cells have also high glucose metabolism (33, 38). This difference of the metabolic environment in brain makes the mechanism of ^{18}F-FDG uptake in brain metastases highly complex. We suggest the possibility that such a unique tumor microenvironment may be one of possible explanations of our negative results.

In brain metastases, T cell infiltration tends to be less frequent than in peripherally located primary lesions whereas infiltration of microglia and monocytes can be abundant (39–41). We found that among immune cells, macrophages most frequently showed diffuse strong infiltration in brain metastases (14.7%, 5/34 cases) followed by neutrophils (5.9%, 2/34 cases). We observed a significantly positive correlation between grades of macrophages markers (CD68 and CD163) and T cell markers (CD3 and CD8). Interestingly, infiltration of macrophages (CD68+) was significantly associated with increased ^{18}F-FDG uptake in metastatic lesions from the breast, although the number of patients was as small at 10. Contrary to our expectation, the majority of metastatic lesions from the breast revealed only focal mild or multifocal mild infiltration of immune cell infiltration except for neutrophils. In addition, different from other types of metastatic tumors, infiltration of macrophages (CD68) in metastatic breast tumor showed no significant correlation with T cell markers but revealed a negative correlation with Ki-67 proliferative index, suggesting that a less complex immune environment and a low proliferation rate of tumor cells could explain the result. The association of ^{18}F-FDG uptake with immune cell infiltration in primary breast cancers is controversial. Kajary et al. (42) reported no correlation between TILs and kinetic parameters using whole-body ^{18}F-FDG PET. However, other studies revealed a significant correlation between ^{18}F-FDG uptake and TILs in breast cancers (21, 22, 43). Furthermore, all of these studies have focused only on TILs in primary tumors and did not investigate other immune cells such as macrophages. In brain metastases, similar to brain tumors, the majority of immune cells are macrophages that may hinder the cell mediated immune response in metastasis (39–41). Macrophages can polarize as either M1 macrophages or M2 macrophages. M1 macrophages can produce inflammatory mediators directed against pathogens and tumor cells, while M2 macrophages are involved in immunosuppression and repair. Tumor associated macrophages (TAMs) take on a pro-tumoral M2 phenotype involved in growth, extracellular matrix remodeling, angiogenesis and immunosuppression (32, 39, 40, 44). However, such an oversimplification of macrophage phenotype has been disputed because the status of macrophage activation reveals a much wider range *in vivo* (32, 39). In addition to CD68, we also analyzed macrophages using CD163, which is one of the markers suggesting M2 macrophages. Infiltration of CD163+ macrophages was slightly higher than that of CD68+ macrophages. However, we could not find a significant correlation between the infiltration of CD163+ macrophages and ^{18}F-FDG uptake.

Pukrop T et al. (45) reported that microglia/macrophages can be identified in brain metastases from the breast, ranging from only few to up to 50% of all cells. TAMs within the brain tend to be pro-tumorigenic and TAM depletion strategies may provide a survival advantage in several types of cancer (32). Activated TAMs promoted cancer cell invasion and colonization of the brain tissue *in vitro* whereas blocking microglia function reduced cancer cell invasion. However, TAMs can be activated by cancer cells without polarization to M2 macrophages (45). We found that infiltration of CD68+ macrophages in brain metastases was only significantly correlated with maximum and mean ^{18}F-FDG uptake ratios at the metastatic lesions ($p < 0.001$ and $p = 0.005$, respectively). Since TAM density is associated with poor prognosis in breast cancer patients and eliminating macrophages from the tumor site in mouse models of breast cancer induced a delay of tumor progression, targeting TAM in brain metastases from the breast may provide a new therapeutic strategy (25, 40, 41, 46).

In addition to immune cell infiltration in brain metastases, we also analyzed additional biologic makers related to ^{18}F-FDG uptake. ^{18}F-FDG uptake in cancer tissues from primary malignant lesions is commonly associated with high levels of HK and GLUT (47–50). In addition, the Ki-67 proliferation index, which indicates the growth rate of tumor cells, is also associated with tumor ^{18}F-FDG uptake (51). However, we could not find associations of ^{18}F-FDG uptake in brain metastases with GLUT1 or HK2 or the Ki-67 proliferation index. We cannot explain these negative results. However, we suggest that the mechanism involving ^{18}F-FDG uptake in the brain metastases may be more complex than in the primary cancer due to a unique tumor microenvironment in which not only cancer cells but also immune cells and brain parenchymal cells compete to utilize glucose for survival (25, 52). The complex mechanisms that influence ^{18}F-FDG uptake in brain metastasis remain to be determined. Therefore, our study may provide reference data for subsequent studies to address the mechanism of ^{18}F-FDG uptake in brain metastases.

TABLE 4 | ^{18}F-FDG uptake ratio according to the expression of GLUT1 and HK2 in patients with brain metastasis.

Primary cancer		Maximum ^{18}F-FDG uptake ratio	*p*-value for difference of maximum ^{18}F-FDG uptake ratio between groups	Mean ^{18}F-FDG uptake ratio	*p*-value for difference of mean ^{18}F-FDG uptake ratio between groups
Total	Expression of GLUT1				
	Grade 1 (*n*=8)	3.26 ± 0.91		2.02 ± 0.69	
	Grade 2 (*n*=11)	2.85 ± 1.75	0.978†	1.49 ± 0.74	0.755†
	Grade 3 (*n*=8)	2.95 ± 0.89		1.63 ± 0.58	
	Grade 4 (*n*=7)	3.07 ± 1.18		1.70 ± 0.77	
	Expression of HK2				
	Grade 1 (*n*=6)	2.71 ± 0.93		1.60 ± 0.76	
	Grade 2 (*n*=9)	2.97 ± 0.87	0.641	1.72 ± 0.55	0.988
	Grade 3 (*n*=9)	2.80 ± 1.06		1.73 ± 0.65	
	Grade 4 (*n*=10)	3.44 ± 1.79		1.70 ± 0.90	
Lung	Expression of GLUT1				
	Grade 1 (*n*=2)	2.59 ± 0.81		1.41 ± 0.01	
	Grade 2 (*n*=4)	2.08 ± 0.21	0.410	1.25 ± 0.29	0.612
	Grade 3 (*n*=3)	3.15 ± 0.79		1.45 ± 0.15	
	Grade 4 (*n*=5)	3.08 ± 1.32		1.79 ± 0.93	
	Expression of HK2				
	Grade 1 (*n*=5)	2.86 ± 0.96		1.72 ± 0.78	
	Grade 2 (*n*=1)	1.85	0.733	0.92	0.307
	Grade 3 (*n*=5)	2.97 ± 0.85		1.68 ± 0.39	
	Grade 4 (*n*=3)	2.46 ± 1.38		1.09 ± 0.22	
Breast	Expression of GLUT1				
	Grade 1 (*n*=6)	3.49 ± 0.90		2.23 ± 0.69	
	Grade 2 (*n*=2)	1.89 ± 0.08	0.166	0.84 ± 0.44	0.067
	Grade 3 (*n*=2)	3.27 ± 1.34		2.37 ± 0.48	
	Expression of HK2				
	Grade 2 (*n*=2)	3.45 ± 1.08		2.28 ± 0.62	
	Grade 3 (*n*=3)	2.96 ± 1.45	0.900	2.08 ± 0.95	0.811
	Grade 4 (*n*=5)	3.09 ± 1.01		1.81 ± 0.94	
GI tract and others	Expression of GLUT1				
	Grade 2 (*n*=5)	3.86 ± 2.30			
	Grade 3 (*n*=3)	2.54 ± 0.91	0.631		0.483
	Grade 4 (*n*=2)	3.03 ± 1.21			
	Expression of HK2				
	Grade 1 (*n*=1)	1.97			
	Grade 2 (*n*=6)	3.00 ± 0.79	0.091		0.248

(Continued)

TABLE 4 | Continued

Primary cancer		Maximum ^{18}F-FDG uptake ratio	*p*-value for difference of maximum ^{18}F-FDG uptake ratio between groups	Mean ^{18}F-FDG uptake ratio	*p*-value for difference of mean ^{18}F-FDG uptake ratio between groups
	Grade 3 (*n*=1)	1.49			
	Grade 4 (*n*=2)	5.76 ± 2.64			

†adjusted values for covariates; GLUT1, Glucose transporter 1; HK2, Hexokinase 2.

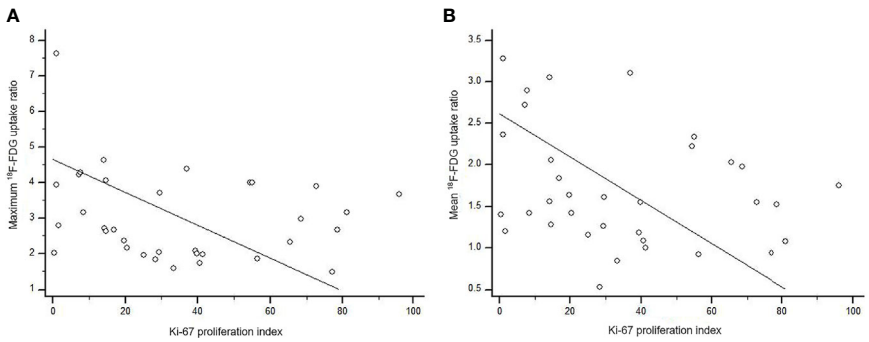

FIGURE 4 | Scatter diagram of the correlation between Ki-67 proliferation index and ^{18}F-FDG uptake ratio in metastatic brain lesion (total, n = 34). **(A)** The maximum ^{18}F-FDG uptake ratio of brain metastatic lesions poorly correlated with Ki-67 proliferation index without statistical significance (rho = -0.21, p = 0.227). **(B)** There was no significant correlation between Ki-67 proliferation index and mean 18F-FDG uptake ratio (rho = -0.25, p = 0.143).

TABLE 5 | Correlation between ^{18}F-FDG uptake ratio and Ki-67 proliferation index in patients with brain metastasis.

Primary cancer	Ki-67 proliferation index (%)	Correlation with maximum ^{18}F-FDG uptake ratio		Correlation with mean ^{18}F-FDG uptake ratio	
		rho (95% CI)	*p*-value	rho (95% CI)	*p*-value
Total	35.0 ± 26.9	-0.21 (-0.56 to 0.06)	0.112	-0.25 (-0.57 to 0.05)	0.094
Lung	32.6 ± 21.1	-0.14 (-0.62 to 0.42)	0.637	-0.13 (-0.61 to 0.43)	0.670
Breast	18.2 ± 18.9	-0.27 (-0.49 to 0.16)	0.721	-0.18 (-0.75 to 0.20)	0.491
GI tract and others	55.3 ± 29.6	-0.24 (-0.66 to 0.09)	0.581	-0.26 (-0.77 to 0.38)	0.423

CI, Confidence Interval.

The small number of patients included in this study may be a limitation to our study. It was not easy to find cancer patients available for brain ^{18}F-FDG PET and with pathological data of metastatic brain lesion. Although we confirmed that the number of patients in this study satisfied the statistically meaningful sample size, we also acknowledge that the sample number is small. In particular, the number of samples in subgroups according to primary cancer site was very small. Therefore, future studies including large samples are needed to validate our study results.

In conclusion, we investigated the degree of ^{18}F-FDG uptake in brain metastases and its correlation with immune cell infiltration and several biologic markers. ^{18}F-FDG uptake was not correlated with immune cells and other biologic markers. However, in certain types of metastatic cancer, ^{18}F-FDG uptake may be a non-invasive tool for predicting immunological features of brain metastases.

DATA AVAILABILITY STATEMENT

The raw data supporting the conclusions of this article will be made available by the authors, without undue reservation.

ETHICS STATEMENT

This study was conducted retrospectively and was approved by the Institutional Review Board of Ajou University (AJIRB-MED-MDB-19-244). Written informed consent for participation was not required for this study in accordance with the national legislation and the institutional requirements.

AUTHOR CONTRIBUTIONS

Y-SA and J-HK conceived of the presented idea. Y-SA and J-HK developed the theory and performed the computations. S-HK,

TR, SP, and T-GK verified the analytical methods. J-HK encouraged SP and T-GK to investigate histologic aspect and supervised the findings of this work. All authors contributed to the article and approved the submitted version.

FUNDING

This work was supported by the faculty research fund of Ajou University School of Medicine to S-HK and J-HK, National Research Foundation of Korea to J-HK (NRF-2016R1D1A1B02010452), and Basic Science Research Program through the National Research Foundation of Korea (NRF) funded by the Ministry of Education (NRF-2020R1A6A1A03043539) to J-HK.

SUPPLEMENTARY MATERIAL

The Supplementary Material for this article can be found online at: https://www.frontiersin.org/articles/10.3389/fonc.2021.618705/full#supplementary-material

REFERENCES

1. Suh JH, Kotecha R, Chao ST, Ahluwalia MS, Sahgal A, Chang EL. Current Approaches to the Management of Brain Metastases. *Nat Rev Clin Oncol* (2020) 17(5):279–99. doi: 10.1038/s41571-019-0320-3
2. Achrol AS, Rennert RC, Anders C, Soffietti R, Ahluwalia MS, Nayak L, et al. Brain Metastases. *Nat Rev Dis Primers* (2019) 5(1):5. doi: 10.1038/s41572-018-0055-y
3. Cagney DN, Martin AM, Catalano PJ, Redig AJ, Lin NU, Lee EQ, et al. Incidence and Prognosis of Patients With Brain Metastases at Diagnosis of Systemic Malignancy: A Population-Based Study. *Neuro Oncol* (2017) 19 (11):1511–21. doi: 10.1093/neuonc/nox077
4. Hall WA, Djalilian HR, Nussbaum ES, Cho KH. Long-Term Survival With Metastatic Cancer to the Brain. *Med Oncol* (2000) 17(4):279–86. doi: 10.1007/BF02782192
5. Gauci ML, Lanoy E, Champiat S, Caramella C, Ammari S, Aspeslagh S, et al. Long-Term Survival in Patients Responding to Anti-PD-1/PD-L1 Therapy and Disease Outcome Upon Treatment Discontinuation. *Clin Cancer Res* (2019) 25(3):946–56. doi: 10.1158/1078-0432.CCR-18-0793
6. Topalian SL, Sznol M, McDermott DF, Kluger HM, Carvajal RD, Sharfman WH, et al. Survival, Durable Tumor Remission, and Long-Term Safety in Patients With Advanced Melanoma Receiving Nivolumab. *J Clin Oncol* (2014) 32(10):1020–30. doi: 10.1200/JCO.2013.53.0105
7. Topalian SL, Hodi FS, Brahmer JR, Gettinger SN, Smith DC, McDermott DF, et al. Safety, Activity, and Immune Correlates of Anti-PD-1 Antibody in Cancer. *N Engl J Med* (2012) 366(26):2443–54. doi: 10.1056/NEJMoa1200690
8. Tran TT, Jilaveanu LB, Omuro A, Chiang VL, Huttner A, Kluger HM. Complications Associated With Immunotherapy for Brain Metastases. *Curr Opin Neurol* (2019) 32(6):907–16. doi: 10.1097/WCO.0000000000000756
9. Decazes P, Bohn P. Immunotherapy by Immune Checkpoint Inhibitors and Nuclear Medicine Imaging: Current and Future Applications. *Cancers (Basel)* (2020) 12(2):371. doi: 10.3390/cancers12020371
10. Ben-Haim S, Ell P. 18f-Fdg PET and PET/CT in the Evaluation of Cancer Treatment Response. *J Nucl Med* (2009) 50(1):88–99. doi: 10.2967/jnumed.108.054205
11. Laing RE, Nair-Gill E, Witte ON, Radu CG. Visualizing Cancer and Immune Cell Function With Metabolic Positron Emission Tomography. *Curr Opin Genet Dev* (2010) 20(1):100–5. doi: 10.1016/j.gde.2009.10.008
12. Treglia G. Diagnostic Performance of (18)F-FDG PET/CT in Infectious and Inflammatory Diseases According to Published Meta-Analyses. *Contrast Media Mol Imaging* (2019) 2019:3018349. doi: 10.1155/2019/3018349
13. Jamar F, Buscombe J, Chiti A, Christian PE, Delbeke D, Donohoe KJ, et al. EANM/SNMMI Guideline for 18F-FDG Use in Inflammation and Infection. *J Nucl Med* (2013) 54(4):647–58. doi: 10.2967/jnumed.112.112524
14. Tomita M, Suzuki M, Kono Y, Nakajima K, Matsuda T, Kuge Y, et al. Influence on [(18)F]FDG Uptake by Cancer Cells After Anti-PD-1 Therapy in an Enforced-Immune Activated Mouse Tumor. *EJNMMI Res* (2020) 10(1):24. doi: 10.1186/s13550-020-0608-4
15. Lee S, Choi S, Kim SY, Yun MJ, Kim HI. Potential Utility of FDG Pet-CT as a non-Invasive Tool for Monitoring Local Immune Responses. *J Gastric Cancer* (2017) 17(4):384–93. doi: 10.5230/jgc.2017.17.e43
16. Shu CJ, Guo S, Kim YJ, Shelly SM, Nijagal A, Ray P, et al. Visualization of a Primary Anti-Tumor Immune Response by Positron Emission Tomography. *Proc Natl Acad Sci USA* (2005) 102(48):17412–7. doi: 10.1073/pnas.0508698102
17. Mazzaschi G, Madeddu D, Falco A, Bocchialini G, Goldoni M, Sogni F, et al. Low PD-1 Expression in Cytotoxic Cd8(+) Tumor-Infiltrating Lymphocytes Confers an Immune-Privileged Tissue Microenvironment in NSCLC With a Prognostic and Predictive Value. *Clin Cancer Res* (2018) 24(2):407–19. doi: 10.1158/1078-0432.CCR-17-2156
18. Tumeh PC, Harview CL, Yearley JH, Shintaku IP, Taylor EJ, Robert L, et al. PD-1 Blockade Induces Responses by Inhibiting Adaptive Immune Resistance. *Nature* (2014) 515(7528):568–71. doi: 10.1038/nature13954
19. Horne ZD, Jack R, Gray ZT, Siegfried JM, Wilson DO, Yousem SA, et al. Increased Levels of Tumor-Infiltrating Lymphocytes are Associated With Improved Recurrence-Free Survival in Stage 1A non-Small-Cell Lung Cancer. *J Surg Res* (2011) 171(1):1–5. doi: 10.1016/j.jss.2011.03.068
20. Kluger HM, Zito CR, Barr ML, Baine MK, Chiang VL, Sznol M, et al. Characterization of PD-L1 Expression and Associated T-Cell Infiltrates in Metastatic Melanoma Samples From Variable Anatomic Sites. *Clin Cancer Res* (2015) 21(13):3052–60. doi: 10.1158/1078-0432.CCR-14-3073
21. Murakami W, Tozaki M, Sasaki M, Hida AI, Ohi Y, Kubota K, et al. Correlation Between (18)F-FDG Uptake on PET/MRI and the Level of Tumor-Infiltrating Lymphocytes (Tils) in Triple-Negative and HER2-Positive Breast Cancer. *Eur J Radiol* (2020) 123:108773. doi: 10.1016/j.ejrad.2019.108773
22. Hirakata T, Fujii T, Kurozumi S, Katayama A, Honda C, Yanai K, et al. FDG Uptake Reflects Breast Cancer Immunological Features: The PD-L1 Expression and Degree of Tils in Primary Breast Cancer. *Breast Cancer Res Treat* (2020) 181(2):331–8. doi: 10.1007/s10549-020-05619-0
23. Wang Y, Zhao N, Wu Z, Pan N, Shen X, Liu T, et al. New Insight on the Correlation of Metabolic Status on (18)F-FDG PET/CT With Immune Marker Expression in Patients With Non-Small Cell Lung Cancer. *Eur J Nucl Med Mol Imaging* (2020) 47(5):1127–36. doi: 10.1007/s00259-019-04500-7
24. Lopci E, Toschi L, Grizzi F, Rahal D, Olivari L, Castino GF, et al. Correlation of Metabolic Information on FDG-PET With Tissue Expression of Immune Markers in Patients With non-Small Cell Lung Cancer (NSCLC) Who are Candidates for Upfront Surgery. *Eur J Nucl Med Mol Imaging* (2016) 43 (11):1954–61. doi: 10.1007/s00259-016-3425-2
25. Cacho-Diaz B, Garcia-Botello DR, Wegman-Ostrosky T, Reyes-Soto G, Ortiz-Sanchez E, Herrera-Montalvo LA. Tumor Microenvironment Differences Between Primary Tumor and Brain Metastases. *J Transl Med* (2020) 18 (1):1. doi: 10.1186/s12967-019-02189-8
26. Galldiks N, Langen KJ, Albert NL, Chamberlain M, Soffietti R, Kim MM, et al. PET Imaging in Patients With Brain Metastasis-Report of the RANO/PET Group. *Neuro Oncol* (2019) 21(5):585–95. doi: 10.1093/neuonc/noz003
27. Das K, Mittal BR, Vasistha RK, Singh P, Mathuriya SN. Role of (18)F-Fluorodeoxyglucose Positron Emission Tomography Scan in Differentiating Enhancing Brain Tumors. *Indian J Nucl Med* (2011) 26(4):171–6. doi: 10.4103/0972-3919.106698
28. Utriainen M, Metsahonkala L, Salmi TT, Utriainen T, Kalimo H, Pihko H, et al. Metabolic Characterization of Childhood Brain Tumors: Comparison of 18F-Fluorodeoxyglucose and 11C-Methionine Positron Emission Tomography. *Cancer* (2002) 95(6):1376–86. doi: 10.1002/cncr.10798
29. Kosaka N, Tsuchida T, Uematsu H, Kimura H, Okazawa H, Itoh H. 18f-Fdg PET of Common Enhancing Malignant Brain Tumors. *AJR Am J Roentgenol* (2008) 190(6):W365–9. doi: 10.2214/AJR.07.2660

30. Akoglu H. User's Guide to Correlation Coefficients. *Turk J Emerg Med* (2018) 18(3):91–3. doi: 10.1016/j.tjem.2018.08.001
31. Di Giacomo AM, Valente M, Cerase A, Lofiego MF, Piazzini F, Calabro L, et al. Immunotherapy of Brain Metastases: Breaking a "Dogma". *J Exp Clin Cancer Res* (2019) 38(1):419. doi: 10.1186/s13046-019-1426-2
32. Quail DF, Joyce JA. The Microenvironmental Landscape of Brain Tumors. *Cancer Cell* (2017) 31(3):326–41. doi: 10.1016/j.ccell.2017.02.009
33. Berti V, Mosconi L, Pupi A. Brain: Normal Variations and Benign Findings in Fluorodeoxyglucose-PET/Computed Tomography Imaging. *PET Clin* (2014) 9(2):129–40. doi: 10.1016/j.cpet.2013.10.006
34. Juhasz C, Dwivedi S, Kamson DO, Michelhaugh SK, Mittal S. Comparison of Amino Acid Positron Emission Tomographic Radiotracers for Molecular Imaging of Primary and Metastatic Brain Tumors. *Mol Imaging* (2014) 13:10.2310/7290.2014.00015. doi: 10.2310/7290.2014.00015
35. Kasahara N, Kaira K, Yamaguchi K, Masubuchi H, Tsurumaki H, Hara K, et al. Fluorodeoxyglucose Uptake is Associated With Low Tumor-Infiltrating Lymphocyte Levels in Patients With Small Cell Lung Cancer. *Lung Cancer* (2019) 134:180–6. doi: 10.1016/j.lungcan.2019.06.009
36. Herbst RS, Soria JC, Kowanetz M, Fine GD, Hamid O, Gordon MS, et al. Predictive Correlates of Response to the Anti-PD-L1 Antibody MPDL3280A in Cancer Patients. *Nature* (2014) 515(7528):563–7. doi: 10.1038/nature14011
37. Rossi S, Toschi L, Castello A, Grizzi F, Mansi L, Lopci E. Clinical Characteristics of Patient Selection and Imaging Predictors of Outcome in Solid Tumors Treated With Checkpoint-Inhibitors. *Eur J Nucl Med Mol Imaging* (2017) 44(13):2310–25. doi: 10.1007/s00259-017-3802-5
38. Chang CH, Qiu J, O'Sullivan D, Buck MD, Noguchi T, Curtis JD, et al. Metabolic Competition in the Tumor Microenvironment Is a Driver of Cancer Progression. *Cell* (2015) 162(6):1229–41. doi: 10.1016/j.cell.2015.08.016
39. Sampson JH, Gunn MD, Fecci PE, Ashley DM. Brain Immunology and Immunotherapy in Brain Tumours. *Nat Rev Cancer* (2020) 20(1):12–25. doi: 10.1038/s41568-019-0224-7
40. Farber SH, Tsvankin V, Narloch JL, Kim GJ, Salama AK, Vlahovic G, et al. Embracing Rejection: Immunologic Trends in Brain Metastasis. *Oncoimmunology* (2016) 5(7):e1172153. doi: 10.1080/2162402X.2016.1172153
41. You H, Baluszek S, Kaminska B. Immune Microenvironment of Brain Metastases-are Microglia and Other Brain Macrophages Little Helpers? *Front Immunol* (2019) 10:1941. doi: 10.3389/fimmu.2019.01941
42. Kajary K, Lengyel Z, Tokes AM, Kulka J, Dank M, Tokes T. Dynamic FDG-PET/CT in the Initial Staging of Primary Breast Cancer: Clinicopathological Correlations. *Pathol Oncol Res* (2020) 26(2):997–1006. doi: 10.1007/s12253-019-00641-0
43. Sasada S, Shiroma N, Goda N, Kajitani K, Emi A, Masumoto N, et al. The Relationship Between Ring-Type Dedicated Breast PET and Immune Microenvironment in Early Breast Cancer. *Breast Cancer Res Treat* (2019) 177(3):651–7. doi: 10.1007/s10549-019-05339-0
44. Galdiero MR, Bonavita E, Barajon I, Garlanda C, Mantovani A, Jaillon S. Tumor Associated Macrophages and Neutrophils in Cancer. *Immunobiology* (2013) 218(11):1402–10. doi: 10.1016/j.imbio.2013.06.003
45. Pukrop T, Dehghani F, Chuang HN, Lohaus R, Bayanga K, Heermann S, et al. Microglia Promote Colonization of Brain Tissue by Breast Cancer Cells in a Wnt-Dependent Way. *Glia* (2010) 58(12):1477–89. doi: 10.1002/glia.21022
46. Laoui D, Movahedi K, Van Overmeire E, Van den Bossche J, Schouppe E, Mommer C, et al. Tumor-Associated Macrophages in Breast Cancer: Distinct Subsets, Distinct Functions. *Int J Dev Biol* (2011) 55(7-9):861–7. doi: 10.1387/ijdb.113371dl
47. Park SG, Lee JH, Lee WA, Han KM. Biologic Correlation Between Glucose Transporters, Hexokinase-II, Ki-67 and FDG Uptake in Malignant Melanoma. *Nucl Med Biol* (2012) 39(8):1167–72. doi: 10.1016/j.nucmedbio.2012.07.003
48. Tohma T, Okazumi S, Makino H, Cho A, Mochiduki R, Shuto K, et al. Relationship Between Glucose Transporter, Hexokinase and FDG-PET in Esophageal Cancer. *Hepatogastroenterology* (2005) 52(62):486–90.
49. Izuishi K, Yamamoto Y, Sano T, Takebayashi R, Nishiyama Y, Mori H, et al. Molecular Mechanism Underlying the Detection of Colorectal Cancer by 18F-2-Fluoro-2-Deoxy-D-Glucose Positron Emission Tomography. *J Gastrointest Surg* (2012) 16(2):394–400. doi: 10.1007/s11605-011-1727-z
50. Mamede M, Higashi T, Kitaichi M, Ishizu K, Ishimori T, Nakamoto Y, et al. [18F]FDG Uptake and PCNA, Glut-1, and Hexokinase-II Expressions in Cancers and Inflammatory Lesions of the Lung. *Neoplasia* (2005) 7(4):369–79. doi: 10.1593/neo.04577
51. Deng SM, Zhang W, Zhang B, Chen YY, Li JH, Wu YW. Correlation Between the Uptake of 18F-Fluorodeoxyglucose (18f-FDG) and the Expression of Proliferation-Associated Antigen Ki-67 in Cancer Patients: A Meta-Analysis. *PloS One* (2015) 10(6):e0129028. doi: 10.1371/journal.pone.0129028
52. Szekely B, Bossuyt V, Li X, Wali VB, Patwardhan GA, Frederick C, et al. Immunological Differences Between Primary and Metastatic Breast Cancer. *Ann Oncol* (2018) 29(11):2232–9. doi: 10.1093/annonc/mdy399

Conflict of Interest: The authors declare that the research was conducted in the absence of any commercial or financial relationships that could be construed as a potential conflict of interest.

frontiers in Immunology

SYSTEMATIC REVIEW
published: 14 July 2021
doi: 10.3389/fimmu.2021.669398

Brain Metastases Status and Immunotherapy Efficacy in Advanced Lung Cancer: A Systematic Review and Meta-Analysis

Hao Hu[1†], Zhi-Yong Xu[2†], Qian Zhu[3†], Xi Liu[4], Si-Cong Jiang[4] and Ji-Hua Zheng[1]*

[1] Department of Radiation Therapy, General Hospital of Southern Theater Command, Guangzhou, China, [2] The Second Clinical Medical School, Guangzhou University of Chinese Medicine, Guangzhou, China, [3] Department of Intensive Care Unit, Sun Yat-sen University Cancer Center, Guangzhou, China, [4] Department of Thoracic Surgery, Jiangxi Cancer Hospital of Nanchang University, Nanchang, China

OPEN ACCESS

Edited by:
Frits Thorsen,
University of Bergen, Norway

Reviewed by:
Raffaella Bonecchi,
Humanitas University, Italy
Michele Ghidini,
Unit of Medical Oncology, Foundation Ca 'Granda Ospedale Maggiore Policlinico (IRCCS), Italy

****Correspondence:***
Ji-Hua Zheng
zjz19930901@163.com

[†]These authors have contributed equally to this work and share first authorship

Specialty section:
This article was submitted to Cancer Immunity and Immunotherapy, a section of the journal Frontiers in Immunology

Received: *18 February 2021*
Accepted: *25 June 2021*
Published: *14 July 2021*

Citation:
Hu H, Xu Z-Y, Zhu Q, Liu X, Jiang S-C and Zheng J-H (2021) Brain Metastases Status and Immunotherapy Efficacy in Advanced Lung Cancer: A Systematic Review and Meta-Analysis. Front. Immunol. 12:669398. doi: 10.3389/fimmu.2021.669398

Background: Brain metastases (BMs) indicate poor outcomes and are commonly excluded in immunotherapy clinical trials in advanced lung cancer; moreover, the effect of BM status on immunotherapy efficacy is inconsistent and inconclusive. Therefore, we conducted a meta-analysis to assess the influence of BM status on immunotherapy efficacy in advanced lung cancer.

Methods: Electronic databases and all major conference proceedings were searched without language restrictions according to the Preferred Reporting Items for Systematic Reviews and Meta-analyses guidelines. We extracted randomized clinical trials on lung cancer immunotherapy that had available overall survival (OS) and/or progression-free survival (PFS) data based on the BM status. All analyses were performed using random effects models.

Results: Fourteen randomized clinical trials with 9,089 patients were identified. Immunotherapy conferred a survival advantage to BM patients [OS-hazard ratio (HR), 0.72; 95% confidence interval (CI), 0.58–0.90; P = 0.004; and PFS-HR, 0.68; 95% CI, 0.52–0.87, P = 0.003]. Non-BM patients could also derive a survival benefit from immunotherapy (OS-HR, 0.76; 95% CI, 0.71–0.80; P <0.001; and PFS-HR, 0.68; 95% CI, 0.56–0.82, P <0.001). The pooled ratios of OS-HRs and PFS-HRs reported in BM patients *versus* non-BM patients were 0.96 (95% CI, 0.78–1.18; P = 0.72) and 0.97 (95% CI, 0.79–1.20; P = 0.78), respectively, indicating no statistically significant difference between them. Subsequent sensitivity analyses did not alter the results. Subgroup analyses according to tumor type, line of therapy, immunotherapy type, study design, and representation of BM patients reconfirmed these findings.

Conclusion: We demonstrated that BM status did not significantly influence the immunotherapy efficacy in lung cancer, suggesting that both BM and non-BM patients could obtain comparable benefits.

Systematic Review Registration: https://www.crd.york.ac.uk/prospero/, identifier (CRD42020207446).

Keywords: brain metastases, efficacy, immunotherapy, lung cancer, programmed cell death ligand 1

INTRODUCTION

Brain metastases (BMs) are common (approximately 20–40% of cases) and potentially devastating complications in advanced lung cancer, leading to a decreased quality of life and extremely poor prognosis (1, 2). Moreover, the survival benefit of conventional treatment options (e.g. radiotherapy, surgery, and systemic therapy) for BMs patients is limited (3). Thus, new effective therapies to improve the outcomes of BMs patients in lung cancer are warranted.

Recently, immunotherapy has revolutionized lung cancer treatment, resulting in global regulatory approvals and widespread use of such agents in the current clinical practice (4–8). Although many literatures focus on immunotherapy in lung cancer, whether the efficacy of lung cancer immunotherapy differs based on the BM status remains unclear, mainly because of limited data in this area, particularly on the BM patients. First, the low enrollment rate of BM patients makes it unfeasible to recruit sufficient participants to observe the differences. Second, BMs may negatively affect outcomes in patients treated with immunotherapy, and these patients are typically excluded in clinical trials, partly due to poor drug transport across the blood–brain barrier, the risk of brain pseudo-progression, and the use of high-dose corticosteroids (9–11). Third, few studies have conducted a subgroup analysis based on BM status even if the BM patients are included in the immunotherapy trials. Given the poor prognosis of BM patients and potential negative effect on outcomes, there is a clear need to evaluate whether immunotherapy has comparable efficacy between BM and non-BM patients.

Previous randomized controlled trials (RCTs) have presented conflicting findings in the BM patients with lung cancer (4–6). A prior meta-analysis (12) evaluated the clinical efficacy of lung cancer immunotherapy in the BM patients; however, whether the benefits of these agents vary between BM and non-BM patients has not been adequately assessed, largely because of the scarce trials published, as well as the small sample sizes analyzed. Moreover, an analysis of disproportionately fewer BM patients (6.2–17.5%) in trials may result in unreliable or even false results (13, 14). Nevertheless, the statistical power of meta-analyses of such trials may be enhanced by integrating these small subgroup analyses, hence drawing more accurate results.

Now that the results of several RCTs on immunotherapy according to BM status have become increasingly available, we therefore conducted a meta-analysis to examine the effect of BM status on immunotherapy efficacy in advanced lung cancer.

METHODS

Search Strategy

We made a predetermined protocol (PROSPERO registration number: CRD42020207446) to perform a systematic literature search and meta-analysis according to the Preferred Reporting Items for Systematic Reviews and Meta-Analyses guidelines (15). The PubMed, Cochrane Library, and EMBASE databases were searched for phase 2 and 3 RCTs on lung cancer immunotherapy [i.e., anti-programmed cell death 1 or programmed cell death ligand 1 (PD-1/PD-L1) inhibitors] from the inception to June 1, 2020 without language restrictions. The abstracts and presentations from the American Society of Clinical Oncology, World Conference on Lung Cancer, European Society for Medical Oncology, and American Association for Cancer Research were also reviewed from January 1, 2015 to December 1, 2020. Moreover, the references of the identified articles were reviewed (further information is listed in **Supplementary Table 1**).

Study Selection

The inclusion criteria were: 1) phase 2 and 3 RCTs investigating new immunotherapy agents against a control regimen (conventional standard therapy) in patients with advanced lung cancer; and 2) available data on hazard ratios (HRs) for overall survival (OS) and/or progression-free survival (PFS) based on BM status (with or without BMs). Conversely, the exclusion criteria were: 1) studies that explored only BM or non-BM patients; 2) single-arm and non-randomized studies (i.e., retrospective or prospective observational cohort); 3) studies without OS and PFS outcomes data according to BM status; and 4) an immunotherapy agent in both arms. We included the most recent and/or most complete trial if duplicate clinical trials were identified.

Data Extraction and Risk of Bias Assessment

For each study, the study name, phase, stage, blinding, histological type, number of patients, BM distribution, treatment characteristics (line of therapy, study drugs, median follow-up time), and survival outcomes data (OS and PFS) according to the BM status were extracted. We adopted the Cochrane Collaboration tool to estimate the risk of bias (16), and applied the 5-point Jadad score to evaluate the methodological quality of the studies (an overall score of 0 indicated the worst methodological quality, and 5 indicated optimal methodological quality) (17). Funnel plots, Egger's test, and Begg's test were conducted to test the risk of publication bias.

Statistical Analyses

We used the same method of determining the difference in immunotherapy efficacy between BM and non-BM patients to avoid the risk of ecological bias, as previously reported (18, 19). First, we calculated an interaction trial-specific HR for each study (the ratio of HR in BM patients to HR in non-BM patients). Then, we used a random effects model to combine the trial-

specific HR ratios across trials. Study heterogeneity was investigated with the Q test, which was quantified using the I^2 test (20). All analyses were performed using random effects models and Stata version 14.0 (StataCorp, College Station, TX). Statistically significant was set at *P* values <0.05 in the two-tailed tests.

Subgroup and Sensitivity Analyses

The pre-specified subgroup analyses included tumor type [non-small cell lung cancer (NSCLC) *vs*. small cell lung cancer (SCLC)], study design [immunotherapy *vs*. standard of care (SOC) alone, immunotherapy + SOC *vs*. SOC alone], line of therapy (first-line *vs*. second- or later-line), immunotherapy type (anti-PD-1 *vs*. anti-PD-L1), and the proportion of BM patients in each study (<10% *vs*. ≥10 of the study cohort). We tested the subgroups using the χ^2 test and excluded subgroups that included less than two studies to avoid possible selection bias. Sensitivity analysis was conducted by excluding the trials that recruited patients with particular conditions, trials with a unique study design, and trials that used a fixed-effects model.

RESULTS

Search Results

Database and manual searches yielded a total of 6,205 references, and 1,454 studies were excluded because of duplications. We then checked the titles and abstracts, and 4,715 studies were excluded because they were not in line with the inclusion criteria. After screening the full-text of the remaining 36 potentially eligible studies, we identified 14 relevant clinical trials for the final analysis (4, 6–8, 21–30). Of these, one trial (26) reported two treatment arms with different regimens (durvalumab plus platinum–etoposide with or without tremelimumab). Finally, a total of 15 independent cohorts from the 14 included trials were recorded (**Table 1**). **Figure 1** presents the study selection flowchart.

Main Characteristics of the Identified Trials

All included trials were randomized multi-center international phase 3 trials; four were double-blind trials (7, 8, 28, 30), and only one trial performed randomization stratified by BM status (8). There were 11 trials (78.6%) with patients with NSCLC (4, 6, 7, 21–25, 27, 29, 30), and three (27.3%) with those with SCLC (8, 26, 28). Most studies (71.4%) evaluated immunotherapy in the first-line setting (7, 8, 22, 23, 25–30), whereas four trials (28.6%) assessed the efficacy in the second- or later-line setting (4, 6, 21, 24). Seven trials (50%) included the immunotherapy-chemotherapy combination *vs*. SOC alone (7, 8, 25–28, 30), both of which recruited patients with advanced or metastatic disease.

The study size ranged from 305 to 1,225 patients. Among all the 9,089 patients included, 1,051 (11.6%) were BM patients, and 8,038 (88.4%) were non-BM patients; notably, the proportion of BM patients differ widely between studies (4.1% to 17.5% of all cancers). The median follow-up duration varied between 8.8 months and 29.3 months, and most trials (78.6%) had a more than 12-months median follow-up (4, 6–8, 21–23, 26–29). Seven studies (50%) evaluated OS as the primary endpoint (4, 6, 21, 22, 24, 26, 27), three (23, 25, 30) assessed OS as the secondary endpoint (the primary endpoint was PFS), and four (7, 8, 28, 29) chose OS and PFS as dual primary endpoints. Moreover, 50% of the included studies allowed patients who presented disease progression in the control group to crossover to the immunotherapy group. The main characteristics of the 14 included trials are listed in **Table 1** and **Supplementary Table 2**.

Bias Assessment

As summarized in **Supplementary Table 3**, all trials received moderate-to-high quality (Jadad scores of 3–5). Minimal or no publication bias for OS and PFS were detected *via* the funnel plots, respectively (**Supplementary Figure 1**). Moreover, additional tests failed to find any publication bias for the outcome OS (Egger's test P = 0.34; Begg's test P = 0.43) or PFS (Egger's test P = 0.65; Begg's test P = 1).

The Relationship Between BM Status and OS Outcomes

All trials except two (25, 30) had available OS data according to the BM status and were included in the pooled estimates for such an endpoint. As shown in **Figure 2**, immunotherapy could reduce the risk of death for BM patients, as compared with SOC systemic therapies (HR, 0.72; 95% CI, 0.58–0.90; P = 0.004). A similar result was uncovered for non-BM patients (HR, 0.76; 95% CI, 0.71–0.80; P <0.001). However, a statistically significant heterogeneity was found in the BM patients (χ^2 = 22.79; P = 0.03; I^2 = 47.3%), but not in the non-BM patients (χ^2 = 11.74; P = 0.467; I^2 = 0%). The pooled HR for OS in all patients, including both BM and non-BM patients, was 0.74 (95% CI, 0.69–0.79; P <0.001). However, we failed to discover any statistically significant differences in OS between BM and non-BM patients (P = 0.72 for interaction) (**Table 2**). The pooled ratio of OS-HRs in BM *versus* non-BM patients reported in each trial was 0.96 (95% CI, 0.78–1.18) (**Supplementary Figure 2**). Moreover, the sensitivity analysis using a fixed-effects model showed that the results did not change. KEYNOTE-024 (23) recruited only patients with PD-L1 ≥50%, whereas CheckMate 227 (22), CASPIAN (26), and Checkmate 9LA (27) have unique study designs, which included an anti-cytotoxic T-lymphocyte antigen 4 agents (tremelimumab or ipilimumab). The sensitivity analysis was performed to separately exclude KEYNOTE-024 (23), CheckMate 227 (22), CASPIAN (26), and Checkmate 9LA (27); nevertheless, the results remained unchanged (**Supplementary Table 4**). The results of the subgroup analyses for OS outcomes are summarized in **Table 2**. No statistically significant differences in the OS outcome were demonstrated between BM and non-BM patients based on tumor type, line of therapy, immunotherapy type, and study design. Finally, we further evaluated the effect of the prevalence of BMs in the study cohort and found no statistically significant differences between these subgroups.

TABLE 1 | Main Characteristics of the Included 14 Trials.

Study name (phase, dominant ethnicity)	Tumor type	Line of therapy	Intervention (No.)	Control treatment (No.)	Age, median (Range or IQR), y	Follow-up, median (Range or IQR), mo	Randomization stratified by BMs status	BMs status (No.)		Jadad score
								No	Yes	
CheckMate 057 (4), (3, White)	NSCLC	>1	Nivolumab (n = 292)	Docetaxel (n = 290)	62 (21–85)	13.2 (NR)	No	514	68	3
KEYNOTE-024 (23), (3, White)	NSCLC	1	Pembrolizumab (n = 154)	CTx (n = 151)	65 (33–90)	25.2 (20.4–33.7)	No	277	28	3
JAVELIN Lung 200 (21), (3, White)	NSCLC	>1	Avelumab (n = 396)	Docetaxel (n = 396)	63 (57–69)	18.3 (12.9–22.9)	No	713	79	3
OAK (6), (3, White)	NSCLC	>1	Atezolizumab (n = 613)	Docetaxel (n = 612)	64 (25–85)	26 (NR)	No	1,107	118	3
KEYNOTE-189 (7), (3, White)	NSCLC	1	Pembrolizumab+CTx (n = 410)	CTx (n = 206)	64 (34–84)	23.1 (18.6–30.9)	No	508	108	5
CheckMate 227 (22), (3, White)	NSCLC	1	Nivolumab+ ipilimumab (n = 583)	CTx (n = 583)	64 (26–87)	29.3 (NR)	No	1,051	115	3
CheckMate 078 (24), (3, Asian)	NSCLC	>1	Nivolumab (n = 338)	Docetaxel (n = 166)	60 (27–78)	8.8 (NR)	No	432	72	3
SHR-1210-303 (25), (3, Asian)	NSCLC	1	Camrelizumab+CTx (n = 205)	CTx (n = 207)	60 (24–71)	11.9 (NR)	No	395	17	3
Checkmate 9LA (27), (3, White)	NSCLC	1	Nivolumab+ ipilimumab +CTx (n = 361)	CTx (n = 358)	65 (26–86)	12.7 (NR)	No	597	122	3
IMpower133 (8), (3, White)	SCLC	1	Atezolizumab+ CTx (n = 201)	CTx (n = 202)	64 (26–90)	13.9 (NR)	Yes	368	35	5
CASPIAN (26), (3, White)	SCLC	1	Durvalumab+ CTx (268)	CTx (n = 269)	63 (28–88)	25.1 (0.1–33.7)	No	482	55	3
			Durvalumab+ tremelimumab+ CTx (n = 268)					472	65	
Keynote 604 (28), (3, White)	SCLC	1	Pembrolizumab + CTx (n = 228)	CTx (n = 225)	65 (24–83)	21.6 (16.1–30.6)	No	398	55	5
ORIENT-11 (30), (3, Asian)	NSCLC	1	Sintilimab +CTx (n = 266)	CTx (n = 131)	61 (30–75)	8.9 (NR)	No	339	58	5
EMPOWER-Lung 1 (29), (3, Asian)	NSCLC	1	Cemiplimab (n = 356)	CTx (n = 356)	63 (31–84)	13.1 (NR)	No	627	83	3

Data are presented as n (%), and median (range), unless otherwise stated.

BMs, brain metastases; CTx, chemotherapy; NR, not reported; IQR, interquartile range; NSCLC, non-small-cell lung cancer; SCLC, small-cell lung cancer; HR, hazard ratio; CI, confidence interval.

The Relationship Between BM Status and PFS Outcomes

Ten of the 14 RCTs were included in the pooled estimation because they had available PFS data according to the BM status (4, 7, 8, 21, 23–25, 28–30). As shown in **Figure 3**, BM patients treated with immunotherapy experienced a significantly lower risk of progression as compared with those treated with SOC systemic therapies (HR, 0.68; 95% CI, 0.52–0.87; P = 0.003). In non-BM patients, the PFS benefit obtained with immunotherapy compared to that with SOC systemic therapies was similar (HR, 0.68; 95% CI, 0.56–0.82; P <0.001). However, a substantial heterogeneity was detected in non-BM patients (χ^2 = 76.17; P <0.001; I^2 = 85.4%), but not in BM patients (χ^2 = 13.98; P = 0.12; I^2 = 35.6%). Overall, the pooled HR for PFS in all patients, including both BM and non-BM patients, was 0.68 (95% CI, 0.56–0.82; P <0.001). However, no PFS benefit difference between BM and non-BM patients was found (P = 0.78 for interaction) (**Table 2**). The pooled ratio of PFS-HRs in BM *versus* non-BM patients reported in each trial was 0.97 (95% CI, 0.79–1.20) (**Supplementary Figure 3**). As shown in **Supplementary Table 4**, sensitivity analysis with a fixed-effects model demonstrated that the results were not altered. The results of the sensitivity analysis were also consistent after omitting the trial by KEYNOTE-024 (23). **Table 3** shows the results of the subgroup analyses for the association between BM status and PFS outcomes. For subgroups including tumor type, line of therapy, immunotherapy type, and study design, the PFS benefit obtained from immunotherapy *vs*. SOC did not differ between BM- and non-BM patients. In addition, the prevalence of BM in the study cohort did not show significant differences within the subgroups (**Table 3**).

DISCUSSION

To the best of our knowledge, the present study is the first meta-analysis to compare the long-term outcomes of immunotherapy between BM and non-BM patients with advanced lung cancer. The results demonstrated no difference in OS and PFS between BM and non-BM patients. Moreover, subsequent sensitivity analyses did not alter the results. Furthermore, subgroup analyses according to tumor type, line of therapy, immunotherapy type, and study design also demonstrated no significant BM-associated differences in the efficacy. Hence, our study suggests that immunotherapy is preferable to conventional SOC therapy for treating both BM and non-BM patients with advanced lung cancer. Moreover, the BM status did not significantly affect the efficacy of PD-L1-based immunotherapy, indicating that both BM and non-BM patients could obtain comparable survival benefits from lung cancer immunotherapy. Therefore, the BM status should not be the only decisive factor for the use of PD-L1-based immunotherapy treatment during routine clinical practice and in future research.

Despite lung cancer immunotherapy has received extensive attention, the efficacy of these agents in BM patients was still uncertain, mainly because of limited information available in published trials. A previously published meta-analysis (12)

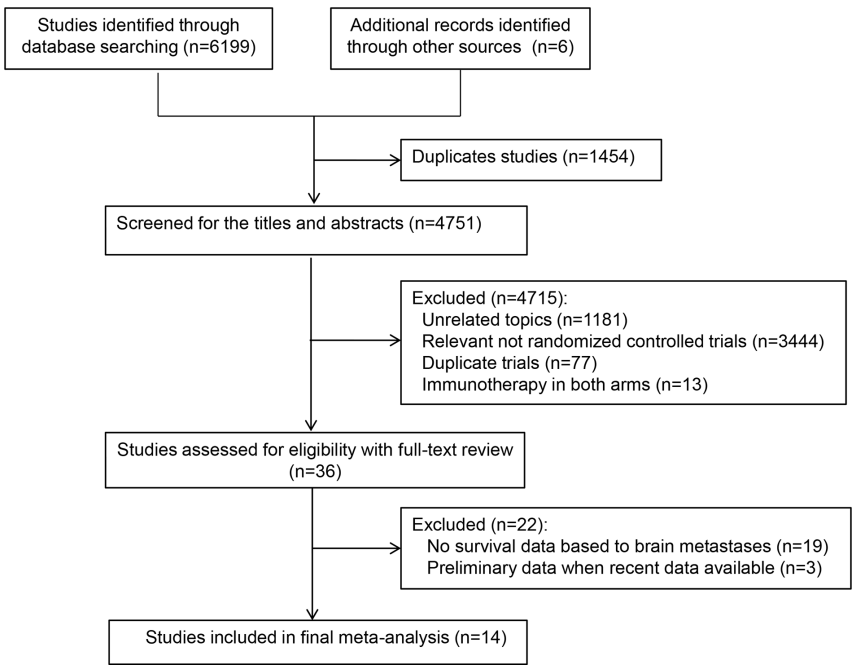

FIGURE 1 | Preferred Reporting Items for Systematic Reviews and Meta-analyses diagram.

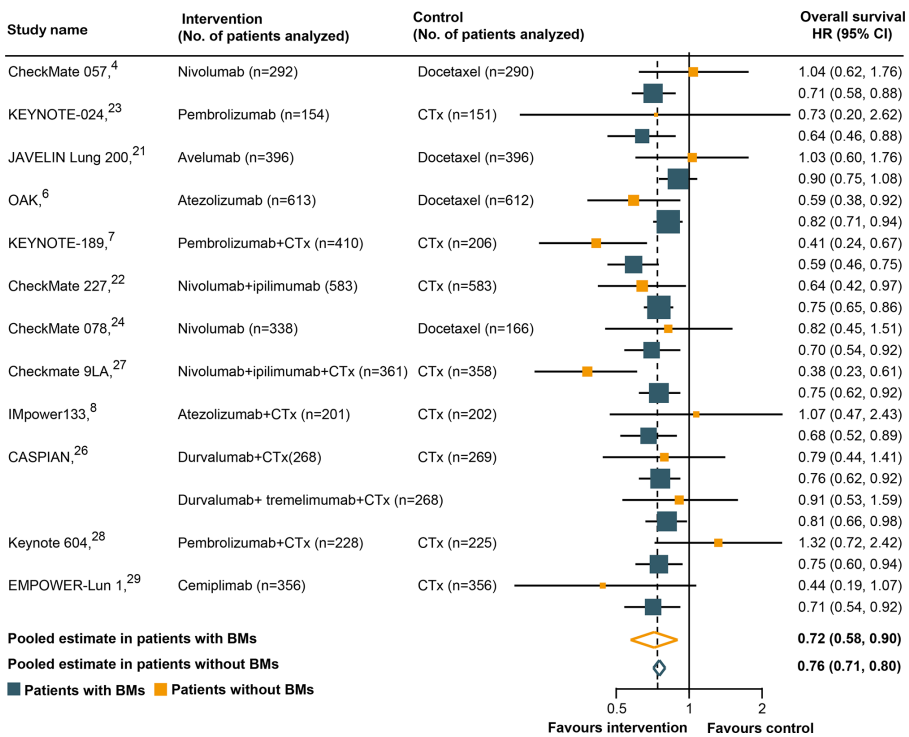

FIGURE 2 | Hazard ratios for overall survival when comparing immunotherapy to control treatment.

TABLE 2 | Analyses of Pooled Hazard Ratios for OS Outcomes by Subgroup.

Variables	Study, No. (%)	Participants, No.		Pooled HR (95% CI) for immunotherapy *vs* SOC		P value for interaction
		BMs	non-BMs	BMs	non-BMs	
Overall	13	976	7,304	0.72 (0.58–0.90)	0.76 (0.71–0.80)	0.72
Tumor type						
NSCLC	9 (69)	793	5,826	0.63 (0.49–0.82)	0.75 (0.69–0.81)	0.19
SCLC	4 (31)	183	1,478	0.99 (0.72–1.34)	0.76 (0.68–0.85)	0.13
Study design						
immunotherapy *vs* SOC	7 (54)	563	4,721	0.74 (0.60–0.91)	0.77 (0.71–0.83)	0.73
immunotherapy + SOC *vs* SOC	6 (46)	413	2,583	0.71 (0.46–1.09)	0.73 (0.67–0.80)	0.91
Line of therapy						
first-line	9 (69)	639	4,538	0.67 (0.49–0.90)	0.73 (0.68–0.78)	0.54
second- or later-line	4 (31)	337	2,766	0.83 (0.62–1.10)	0.80 (0.72–0.89)	0.75
Immunotherapy type						
anti-PD-1	8 (62)	651	4,404	0.66 (0.47–0.92)	0.71 (0.66–0.77)	0.66
anti-PD-L1	5 (38)	325	2,900	0.81 (0.63–1.03)	0.81 (0.74–0.88)	0.97
BMs proportion						
<10	5 (38)	375	3,516	0.73 (0.57–0.93)	0.78 (0.71–0.86)	0.52
≥10	8 (62)	601	3,788	0.70 (0.50–0.98)	0.73 (0.67–0.79)	0.87

NSCLC, non–small cell lung cancer; SCLC, small cell lung cancer; PD-1, programmed cell death 1; PD-L1, programmed cell death ligand 1; SOC, standard of care chemotherapy; BMs, brain metastases; OS, overall survival; HR, hazard ratio; CI, confidence interval.

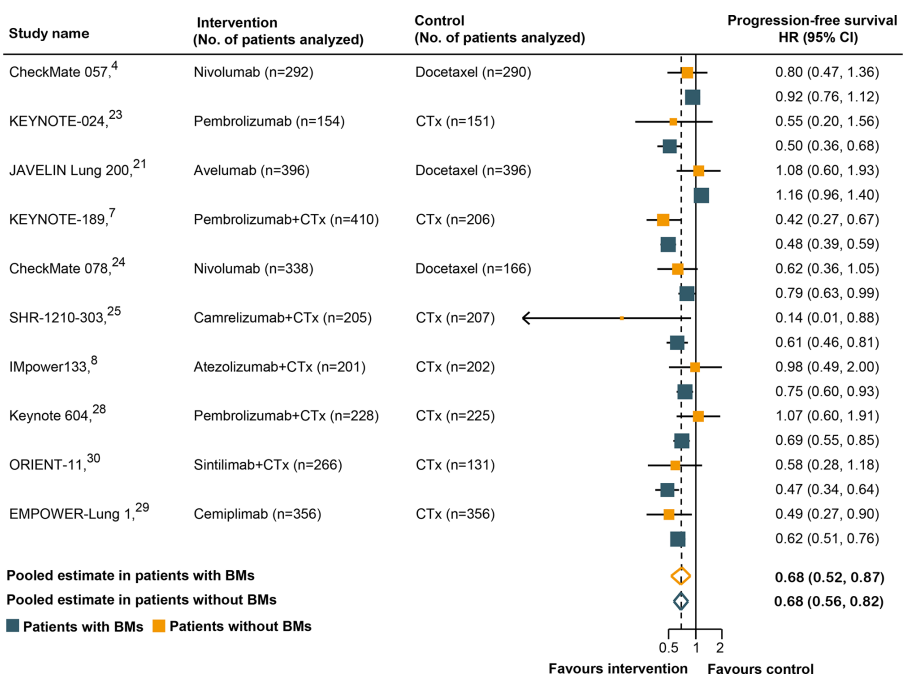

FIGURE 3 | Hazard ratios for progression-free survival when comparing immunotherapy to control treatment.

included only three trials with 259 BM patients with NSCLC, and concluded that BM patients could obtain OS benefit from immunotherapy in combination with chemotherapy rather than immunotherapy alone. Nevertheless, their study may have been biased by the small sample sizes, with limited trials analyzed. Our study, which included 13 cohorts with 976 BM patients, is the largest study to test the immunotherapy efficacy of lung cancer among BM patients. We found that the risk of death in BM patients was significantly reduced by 26% when treated with immunotherapy monotherapy (**Table 2**); however, the OS benefit of immunotherapy in combination with chemotherapy was marginal (HR, 0.71; 95% CI, 0.46–1.09), partially due to the relatively small sample size, and the lack of statistical power to discover a significant difference. However, there are also few studies inconsistent with our results. A recent multicenter retrospective study enrolled patients with several types of metastatic cancer,

TABLE 3 | Analyses of Pooled Hazard Ratios for PFS Outcomes by Subgroup.

Variables	Study, No. (%)	Patients, No.		Pooled HR (95% CI) for immunotherapy *vs* SOC		P value for interaction
		BMs	non-BMs	BMs	non-BMs	
Overall	10	603	4,571	0.68 (0.52–0.87)	0.68 (0.56–0.82)	0.78
Tumor type						
NSCLC	8 (80)	513	3,805	0.61 (0.46–0.79)	0.67 (0.52–0.85)	0.25
SCLC	2 (20)	90	766	1.03 (0.66–1.61)	0.72 (0.62–0.84)	0.13
Study design						
immunotherapy *vs* SOC	5 (50)	330	2,563	0.71 (0.54–0.93)	0.78 (0.59–1.02)	0.25
immunotherapy + SOC *vs* SOC	5 (50)	273	2,008	0.65 (0.40–1.06)	0.60 (0.49–0.72)	0.47
Line of therapy						
first-line	7 (70)	384	2,912	0.61 (0.43–0.87)	0.59 (0.51–0.68)	0.74
second- or later-line	3 (30)	219	1,659	0.80 (0.58–1.10)	0.95 (0.77–1.18)	0.37
Immunotherapy type						
anti-PD-1	8 (80)	489	3,490	0.61 (0.47–0.79)	0.63 (0.53–0.75)	0.61
anti-PD-L1	2 (20)	114	1,081	1.04 (0.66–1.63)	0.94 (0.61–1.44)	0.77
BMs proportion						
<10	4 (40)	159	1,753	0.83 (0.51–1.37)	0.73 (0.50–1.05)	0.97
≥10	6 (60)	444	2,818	0.62 (0.47–0.83)	0.65 (0.52–0.80)	0.70

NSCLC, non–small cell lung cancer; SCLC, small cell lung cancer; PD-1, programmed cell death 1; PD-L1, programmed cell death ligand 1; SOC, standard of care chemotherapy; BMs, brain metastases; PFS, progression-free survival; HR, hazard ratio; CI, confidence interval.

including NSCLC who received immunotherapy (31). The study demonstrated that patients with BM had worse PFS and OS than did those without BMs. Similarly, a prior systematic review and meta-analysis inferred that BM were independent predictors of the poor survival outcomes in advanced NSCLC patients treated with PD-1-based immunotherapy (32). However, their conclusions might be limited by the heterogeneity of treatment characteristics between different studies and the inherent biases owing to the retrospective nature of most of the included studies in these reviews. BM patients are known to have an unfavorable prognosis in lung cancer, with a 1-year survival rate of <10% (33). They tend to have a range of symptoms (e.g., altered mental status, visual impairments with headaches, and fatigue), which can lead to psychological, social, and physical debilitation, as well as greater social and economic burdens (34). Therefore, this challenge emphasizes the further clinical implication and importance of the current research. BMs are commonly considered to be a predictor of poor outcomes in patients with advanced lung cancer treated with PD-L1-based immunotherapy (32). In this study, we demonstrated that BMs did not negatively influence the efficacy of lung cancer immunotherapy. Our findings may be explained in several ways. First, the normal brain has been long recognized as an "immune privileged" organ in the body because the blood–brain barrier could prevent it from immune cell entry (35). However, the blood–brain barrier is damaged or influenced in BM patients and can allow substantial immune cells (e.g., peripherally activated T cells) to enter and/or infiltrate (36). In addition, the change in the blood–brain barrier makes it possible for immunotherapy agents to function in the brain. In support of this, specimens of BMs exhibit dense infiltrates of tumor-infiltrating lymphocytes and is correlated with favorable survival outcomes, further providing the basis for treating BM patients with these agents (37, 38). Second, resected BMs have a higher tumor mutation burden (TMB) than paired primary lung tumors (39, 40). Prior studies (41, 42) have suggested that TMB is a promising predictive biomarker for immunotherapy in diverse cancers, including lung cancer. Hence, high tumor mutation load in BMs and increased frequency of neoantigens may contribute to an improved response to lung cancer immunotherapy (39). Third, higher PD-L1 expression in tumor cells has been noted in lung cancer BM than in matched primary tumors (43). As previously demonstrated (19), the survival benefit from immunotherapy is PD-L1-dependent, and patients with high-level PD-L1 expression had a greater survival advantage. Accordingly, our results may be partly attributable to the overexpression of PD-L1 in BM patients. Fourth, patients with active or untreated BMs and patients who require systemic steroids (poorer prognostic factors) are usually excluded from immunotherapy trials (10, 44). The observed survival benefits in BM patients cannot be ruled out because of the more favorable prognostic profile in these patients. Consistently, several previous retrospective studies demonstrated that BMs did not significantly correlate with survival outcomes in advanced NSCLC patients treated with nivolumab, an anti-PD1 agent (45–47).

Previous studies (48, 49) have also demonstrated that anti-PD-1 agents show better anti-cancer effect than anti-PD-L1 agents in the treatment of advanced cancer, including lung cancer, partly owing to the inherent discrepancy among them. In the present study, we found a consistently better efficacy in BM patients treated with anti-PD-1 agents: anti-PD-1 agents significantly improved OS and PFS outcomes compared with conventional SOC therapy in BM patients, whereas anti-PD-L1 agents did not (**Tables 2** and **3**). Our results suggest a possible superior anti-tumor effect of anti-PD-1 agents in the treatment of BM patients, although this finding remains unclear from the sample size in this analysis. Therefore, large RCTs are essential for investigating the relative survival advantage of different immunotherapy agents in BM patients to identify best treatment. Notably, in SCLC, immunotherapy was not effective in improving OS and PFS in BM patients. Nevertheless, the available data were only from a small number of BM patients,

and the observed wide CIs for the calculated HRs in these patients prevented us from drawing definitive conclusions.

This study has some limitations. Of note, our findings are based on published trials, rather than individual patient data. Furthermore, patients included in our study had treatable, stable, and asymptomatic BMs, rather than having untreatable, active, or symptomatic BMs. However, a recent phase II trial (50) has revealed that pembrolizumab, an anti-PD-1 inhibitor, showed consistent brain and extra-cerebral responses in patients with NSCLC, indicating that immunotherapy can be active in patients with active BMs. Other trials (51–53) have also found that immunotherapy agents are active in patients with active melanoma BMs. Additionally, we cannot rule out that some factors other than BMs are distributed differently between BM and non-BM patients, and that these factors might affect our results. Finally, previous reports have investigated the prognosis of BM patients in several types of metastatic cancer, and the prognostic factors varied between different tumor types. For instance, a study established a nomogram based on 3,522 patients from the Surveillance, Epidemiology, and End Results database, and demonstrated that age, marital status, T stage, N stage, race, and gender were independent predictors of survival in SCLC patients with BM (54). Meanwhile, a cohort of 227 patients with BM from colorectal cancer proposed that age, performance status, BM site, and BM number were independent prognostic factors for survival (55). However, evidences from NSCLC patients with BM suggested that BM number did not influence the survival outcome (56, 57). In our study unfortunately, the included trials were not conducted specifically to evaluate the intracranial efficacy of lung cancer immunotherapy, and thus several detail data related to BM had not been reported in published clinical trials. Therefore, we could not assess the effect of immunotherapy on the reduced size and severity of BM. Future studies on BM patients are needed to evaluate the intracranial efficacy of immunotherapy in advanced lung cancer.

In the current meta-analysis of all available randomized trials of lung cancer immunotherapy, we demonstrated that BM and non-BM patients could derive similar survival advantages. We recommend that BM status may not be the only consideration when deciding whether to offer immunotherapy to patients with advanced lung cancer in routine clinical practice and future clinical trial designs.

DATA AVAILABILITY STATEMENT

The original contributions presented in the study are included in the article/**Supplementary Material**. Further inquiries can be directed to the corresponding author.

AUTHOR CONTRIBUTIONS

J-HZ had full access to all of the data in this study and accepts responsibility for the integrity of the data and the accuracy of the data analysis. Concept and design: HH, ZY-X, and QZ. Acquisition, analysis, or interpretation of data: All authors. Drafting of the manuscript: All authors. Critical revision of the manuscript for important intellectual content: All authors. Statistical analysis: All authors. Administrative, technical, or material support: All authors. Supervision: HH, J-HZ. All authors contributed to the article and approved the submitted version.

FUNDING

This study was supported by the Science and Technology Planning Project of Guangzhou, China (No. 202102080513), and the Medical Scientific Research Foundation of Guangdong Province, China (No. A2021279).

ACKNOWLEDGMENTS

We would like to thank Merck and Pfizer for data provision in JAVELIN Lung 200 trial. We also would like to thank Editage (www.editage.cn) for English language editing.

SUPPLEMENTARY MATERIAL

The Supplementary Material for this article can be found online at: https://www.frontiersin.org/articles/10.3389/fimmu.2021.669398/full#supplementary-material

REFERENCES

1. Sul J, Posner JB. Brain Metastases: Epidemiology and Pathophysiology. *Cancer Treat Res* (2007) 136:1–21. doi: 10.1007/978-0-387-69222-7_1
2. Riihimäki M, Hemminki A, Fallah M, Thomsen H, Sundquist K, Sundquist J, et al. Metastatic Sites and Survival in Lung Cancer. *Lung Cancer (Amst Neth)* (2014) 86(1):78–84. doi: 10.1016/j.lungcan.2014.07.020
3. Jindal V, Gupta S. Expected Paradigm Shift in Brain Metastases Therapy-Immune Checkpoint Inhibitors. *Mol Neurobiol* (2018) 55(8):7072–8. doi: 10.1007/s12035-018-0905-3
4. Borghaei H, Paz-Ares L, Horn L, Spigel DR, Steins M, Ready NE, et al. Nivolumab Versus Docetaxel in Advanced Nonsquamous Non-Small-Cell Lung Cancer. *New Engl J Med* (2015) 373(17):1627–39. doi: 10.1056/NEJMoa1507643
5. Brahmer J, Reckamp KL, Baas P, Crino L, Eberhardt WE, Poddubskaya E, et al. Nivolumab Versus Docetaxel in Advanced Squamous-Cell Non-Small-Cell Lung Cancer. *N Engl J Med* (2015) 373(2):123–35. doi: 10.1056/NEJMoa1504627
6. Fehrenbacher L, von Pawel J, Park K, Rittmeyer A, Gandara DR, Ponce Aix S, et al. Updated Efficacy Analysis Including Secondary Population Results for OAK: A Randomized Phase III Study of Atezolizumab Versus Docetaxel in Patients With Previously Treated Advanced Non-Small Cell Lung Cancer. *J Thoracic Oncol Off Publ Int Assoc Study Lung Cancer* (2018) 13(8):1156–70. doi: 10.1016/j.jtho.2018.04.039
7. Gadgeel S, Rodríguez-Abreu D, Speranza G, Esteban E, Felip E, Dómine M, et al. Updated Analysis From KEYNOTE-189: Pembrolizumab or Placebo Plus Pemetrexed and Platinum for Previously Untreated Metastatic Nonsquamous Non-Small-Cell Lung Cancer. *J Clin Oncol* (2020) 38 (14):1505–17. doi: 10.1200/jco.19.03136
8. Horn L, Mansfield AS, Szczesna A, Havel L, Krzakowski M, Hochmair MJ, et al. First-Line Atezolizumab Plus Chemotherapy in Extensive-Stage Small-

Cell Lung Cancer. *N Engl J Med* (2018) 379(23):2220–9. doi: 10.1056/NEJMoa1809064
9. Arbour KC, Mezquita L, Long N, Rizvi H, Auclin E, Ni A, et al. Impact of Baseline Steroids on Efficacy of Programmed Cell Death-1 and Programmed Death-Ligand 1 Blockade in Patients With Non-Small-Cell Lung Cancer. *J Clin Oncol* (2018) 36(28):2872–8. doi: 10.1200/jco.2018.79.0006
10. Ricciuti B, Dahlberg SE, Adeni A, Sholl LM, Nishino M, Awad MM. Immune Checkpoint Inhibitor Outcomes for Patients With Non–Small-Cell Lung Cancer Receiving Baseline Corticosteroids for Palliative Versus Nonpalliative Indications. *J Clin Oncol* (2019) 37(22):1927–34. doi: 10.1200/jco.19.00189
11. Hendriks LEL, Henon C, Auclin E, Mezquita L, Ferrara R, Audigier-Valette C, et al. Outcome of Patients With Non-Small Cell Lung Cancer and Brain Metastases Treated With Checkpoint Inhibitors. *J Thorac Oncol* (2019) 14 (7):1244–54. doi: 10.1016/j.jtho.2019.02.009
12. Yang K, Li J, Bai C, Sun Z, Zhao L. Efficacy of Immune Checkpoint Inhibitors in Non-small-cell Lung Cancer Patients With Different Metastatic Sites: A Systematic Review and Meta-Analysis. *Front Oncol* (2020) 10:1098. doi: 10.3389/fonc.2020.01098
13. Hackshaw A. Small Studies: Strengths and Limitations. *Eur Respir J* (2008) 32 (5):1141–3. doi: 10.1183/09031936.00136408
14. Button KS, Ioannidis JP, Mokrysz C, Nosek BA, Flint J, Robinson ES, et al. Power Failure: Why Small Sample Size Undermines the Reliability of Neuroscience. *Nat Rev Neurosci* (2013) 14(5):365–76. doi: 10.1038/nrn3475
15. Moher D, Liberati A, Tetzlaff J, Altman DG. Preferred Reporting Items for Systematic Reviews and Meta-Analyses: The PRISMA Statement. *Int J Surg* (2010) 8(5):336–41. doi: 10.1016/j.ijsu.2010.02.007
16. Higgins JPT, Altman DG, Gøtzsche PC, Jüni P, Moher D, Oxman AD, et al. The Cochrane Collaboration's Tool for Assessing Risk of Bias in Randomised Trials. *BMJ* (2011) 343:d5928. doi: 10.1136/bmj.d5928
17. Jadad AR, Moore RA, Carroll D, Jenkinson C, Reynolds DJM, Gavaghan DJ, et al. Assessing the Quality of Reports of Randomized Clinical Trials: Is Blinding Necessary? *Control Clin Trials* (1996) 17(1):1–12. doi: 10.1016/0197-2456(95)00134-4
18. Conforti F, Pala L, Bagnardi V, De Pas T, Martinetti M, Viale G, et al. Cancer Immunotherapy Efficacy and Patients' Sex: A Systematic Review and Meta-Analysis. *Lancet Oncol* (2018) 19(6):737–46. doi: 10.1016/s1470-2045(18)30261-4
19. Liu X, Guo CY, Tou FF, Wen XM, Kuang YK, Zhu Q, et al. Association of PD-L1 Expression Status With the Efficacy of PD-1/PD-L1 Inhibitors and Overall Survival in Solid Tumours: A Systematic Review and Meta-Analysis. *Int J Cancer* (2020) 147(1):116–27. doi: 10.1002/ijc.32744
20. Higgins JP, Thompson SG, Deeks JJ, Altman DG. Measuring Inconsistency in Meta-Analyses. *BMJ* (2003) 327(7414):557–60. doi: 10.1136/bmj.327.7414.557
21. Barlesi F, Vansteenkiste J, Spigel D, Ishii H, Garassino M, de Marinis F, et al. Avelumab Versus Docetaxel in Patients With Platinum-Treated Advanced non-Small-Cell Lung Cancer (JAVELIN Lung 200): An Open-Label, Randomised, Phase 3 Study. *Lancet Oncol* (2018) 19(11):1468–79. doi: 10.1016/s1470-2045(18)30673-9
22. Hellmann MD, Paz-Ares L, Bernabe Caro R, Zurawski B, Kim SW, Carcereny Costa E, et al. Nivolumab Plus Ipilimumab in Advanced Non-Small-Cell Lung Cancer. *N Engl J Med* (2019) 381(21):2020–31. doi: 10.1056/NEJMoa1910231
23. Reck M, Rodriguez-Abreu D, Robinson AG, Hui R, Csoszi T, Fulop A, et al. Updated Analysis of KEYNOTE-024: Pembrolizumab Versus Platinum-Based Chemotherapy for Advanced Non-Small-Cell Lung Cancer With Pd-L1 Tumor Proportion Score of 50% or Greater. *J Clin Oncol* (2019) 37(7):537–46. doi: 10.1200/jco.18.00149
24. Wu YL, Lu S, Cheng Y, Zhou C, Wang J, Mok T, et al. Nivolumab Versus Docetaxel in a Predominantly Chinese Patient Population With Previously Treated Advanced NSCLC: CheckMate 078 Randomized Phase III Clinical Trial. *J Thorac Oncol* (2019) 14(5):867–75. doi: 10.1016/j.jtho.2019.01.006
25. Zhou C, Chen G, Huang Y, Zhou J, Lin L, Feng J, et al. A Randomized Phase 3 Study of Camrelizumab Plus Chemotherapy as 1st Line Therapy for Advanced/Metastatic non-Squamous Non-Small Cell Lung Cancer. *J Thoracic Oncol* (2019) 14(10):S215–S6. doi: 10.1016/j.jtho.2019.08.425
26. Paz-Ares LG, Dvorkin M, Chen YB, Reinmuth N, Hotta K, Trukhin D, et al. Durvalumab +/- Tremelimumab Plus Platinum-Etoposide in First-Line Extensive-Stage SCLC (Es-Sclc): Updated Results From the Phase III CASPIAN Study. *J Clin Oncol* (2020) 38(15):9002. doi: 10.1200/jco.2020.38.15_supp.9002
27. Reck M, Ciuleanu TE, Dols MC, Schenker M, Zurawski B, Menezes J, et al. Nivolumab (NIVO) Plus Ipilimumab (IPI)+2 Cycles of Platinum-Doublet Chemotherapy (Chemo) vs 4 Cycles Chemo as First-Line (1L) Treatment (Tx) for Stage IV/Recurrent Non-Small Cell Lung Cancer (NSCLC): CheckMate 9la. *J Clin Oncol* (2020) 38(15):9501. doi: 10.1200/jco.2020.38.15_supp.9501
28. Rudin CM, Awad MM, Navarro A, Gottfried M, Peters S, Csőszi T, et al. Pembrolizumab or Placebo Plus Etoposide and Platinum as First-Line Therapy for Extensive-Stage Small-Cell Lung Cancer: Randomized, Double-Blind, Phase Iii KEYNOTE-604 Study. *J Clin Oncol* (2020) 38(21):2369–79. doi: 10.1200/jco.20.00793
29. Sezer A, Kilickap S, Gumus M, Bondarenko I, Ozguroglu M, Gogishvili M, et al. Empower-Lung 1: Phase III First-Line (1L) Cemiplimab Monotherapy vs Platinum-Doublet Chemotherapy (Chemo) in Advanced Non-Small Cell Lung Cancer (NSCLC) With Programmed Cell Death-Ligand 1 (PD-L1) >= 50%. *Ann Oncol* (2020) 31:S1182–S3. doi: 10.1016/j.annonc.2020.08.2285
30. Zhang L, Yang Y, Wang Z, Fang J, Yu Q, Han B, et al. Orient-11: Sintilimab Plus Pemetrexed Plus Platinum as First-Line Therapy for Locally Advanced or Metastatic Non-Squamous Nsclc. *J Thoracic Oncol* (2020) 15(10):e41. doi: 10.1016/j.jtho.2020.08.002
31. Botticelli A, Cirillo A, Scagnoli S, Cerbelli B, Strigari L, Cortellini A, et al. The Agnostic Role of Site of Metastasis in Predicting Outcomes in Cancer Patients Treated With Immunotherapy. *Vaccines* (2020) 8(2):203. doi: 10.3390/vaccines8020203
32. Huang Y, Zhu L, Guo T, Chen W, Zhang Z, Li W, et al. Metastatic Sites as Predictors in Advanced NSCLC Treated With PD-1 Inhibitors: A Systematic Review and Meta-Analysis. *Hum Vaccines Immunotherapeutics* (2021) 17 (5):1278–87. doi: 10.1080/21645515.2020.1823779
33. Jacot W, Quantin X, Boher JM, Andre F, Moreau L, Gainet M, et al. Brain Metastases at the Time of Presentation of Non-Small Cell Lung Cancer: A Multi-Centric AERIO Analysis of Prognostic Factors. *Br J Cancer* (2001) 84 (7):903–9. doi: 10.1054/bjoc.2000.1706
34. Wong E, Zhang L, Rowbottom L, Chiu N, Chiu L, McDonald R, et al. Symptoms and Quality of Life in Patients With Brain Metastases Receiving Whole-Brain Radiation Therapy. *Supportive Care Cancer* (2016) 24(11):4747–59. doi: 10.1007/s00520-016-3326-8
35. Engelhardt B, Vajkoczy P, Weller RO. The Movers and Shapers in Immune Privilege of the CNS. *Nat Immunol* (2017) 18(2):123–31. doi: 10.1038/ni.3666
36. Quail DF, Joyce JA. The Microenvironmental Landscape of Brain Tumors. *Cancer Cell* (2017) 31(3):326–41. doi: 10.1016/j.ccell.2017.02.009
37. Berghoff AS, Fuchs E, Ricken G, Mlecnik B, Bindea G, Spanberger T, et al. Density of Tumor-Infiltrating Lymphocytes Correlates With Extent of Brain Edema and Overall Survival Time in Patients With Brain Metastases. *Oncoimmunology* (2016) 5(1):e1057388. doi: 10.1080/2162402x.2015.1057388
38. Berghoff AS, Ricken G, Wilhelm D, Rajky O, Widhalm G, Dieckmann K, et al. Tumor Infiltrating Lymphocytes and PD-L1 Expression in Brain Metastases of Small Cell Lung Cancer (SCLC). *J Neuro-Oncol* (2016) 130(1):19–29. doi: 10.1007/s11060-016-2216-8
39. Stein MK, Pandey M, Xiu J, Tae H, Swensen J, Mittal S, et al. Tumor Mutational Burden Is Site Specific in Non–Small-Cell Lung Cancer and Is Highest in Lung Adenocarcinoma Brain Metastases. *JCO Precis Oncol* (2019) 3):1–13. doi: 10.1200/po.18.00376
40. Wang H, Ou Q, Li D, Qin T, Bao H, Hou X, et al. Genes Associated With Increased Brain Metastasis Risk in non-Small Cell Lung Cancer: Comprehensive Genomic Profiling of 61 Resected Brain Metastases Versus Primary Non-Small Cell Lung Cancer (Guangdong Association Study of Thoracic Oncology 1036). *Cancer* (2019) 125(20):3535–44. doi: 10.1002/cncr.32372
41. Goodman AM, Kato S, Bazhenova L, Patel SP, Frampton GM, Miller V, et al. Tumor Mutational Burden as an Independent Predictor of Response to Immunotherapy in Diverse Cancers. *Mol Cancer Ther* (2017) 16(11):2598–608. doi: 10.1158/1535-7163.mct-17-0386
42. Wang Z, Duan J, Cai S, Han M, Dong H, Zhao J, et al. Assessment of Blood Tumor Mutational Burden as a Potential Biomarker for Immunotherapy in Patients With Non-Small Cell Lung Cancer With Use of a Next-Generation Sequencing Cancer Gene Panel. *JAMA Oncol* (2019) 5(5):696–702. doi: 10.1001/jamaoncol.2018.7098
43. Berghoff A, Inan C, Ricken G, Widhalm G, Dieckmann K, Birner P, et al. 1324ptumor-Infiltrating Lymphocytes (Tils) And Pd-L1 Expression in Non-Small Cell Lung Cancer Brain Metastases (Bm) And Matched Primary

Tumors (Pt). *Ann Oncol Off J Eur Soc Med Oncol* (2014) 25:iv465–6. doi: 10.1093/annonc/mdu349.103
44. Hendriks LEL, Henon C, Auclin E, Mezquita L, Ferrara R, Audigier-Valette C, et al. Outcome of Patients With Non-Small Cell Lung Cancer and Brain Metastases Treated With Checkpoint Inhibitors. *J Thoracic Oncol Off Publ Int Assoc Study Lung Cancer* (2019) 14(7):1244–54. doi: 10.1016/j.jtho.2019.02.009
45. Botticelli A, Salati M, Di Pietro FR, Strigari L, Cerbelli B, Zizzari IG, et al. A Nomogram to Predict Survival in Non-Small Cell Lung Cancer Patients Treated With Nivolumab. *J Trans Med* (2019) 17(1):99. doi: 10.1186/s12967-019-1847-x
46. Garde-Noguera J, Martin-Martorell P, De Julián M, Perez-Altozano J, Salvador-Coloma C, García-Sanchez J, et al. Predictive and Prognostic Clinical and Pathological Factors of Nivolumab Efficacy in Non-Small-Cell Lung Cancer Patients. *Clin Trans Oncol Off Publ Fed Spanish Oncol Soc Natl Cancer Institute Mexico* (2018) 20(8):1072–9. doi: 10.1007/s12094-017-1829-5
47. Tamiya M, Tamiya A, Inoue T, Kimura M, Kunimasa K, Nakahama K, et al. Metastatic Site as a Predictor of Nivolumab Efficacy in Patients With Advanced non-Small Cell Lung Cancer: A Retrospective Multicenter Trial. *PloS One* (2018) 13(2):e0192227–e. doi: 10.1371/journal.pone.0192227
48. Duan J, Cui L, Zhao X, Bai H, Wang J. Use of Immunotherapy With Programmed Cell Death 1 vs Programmed Cell Death Ligand 1 Inhibitors in Patients With Cancer: A Systematic Review and Meta-Analysis. *JAMA Oncol* (2020) 6(3):375–84. doi: 10.2139/ssrn.3384914
49. Yi K, Zhu Q, Kuang Y-K, Jiang S-C, Hu H. The Relative and Absolute Benefit of Programmed Death Receptor-1 vs Programmed Death Ligand 1 Therapy in Advanced non-Small-Cell Lung Cancer: A Systematic Review and Meta-Analysis. *Int Immunopharmacol* (2020) 87:106852. doi: 10.1016/j.intimp.2020.106852
50. Goldberg SB, Schalper KA, Gettinger SN, Mahajan A, Herbst RS, Chiang AC, et al. Pembrolizumab for Management of Patients With NSCLC and Brain Metastases: Long-Term Results and Biomarker Analysis From a Non-Randomised, Open-Label, Phase 2 Trial. *Lancet Oncol* (2020) 21(5):655–63. doi: 10.1016/s1470-2045(20)30111-x
51. Kluger HM, Chiang V, Mahajan A, Zito CR, Sznol M, Tran T, et al. Long-Term Survival of Patients With Melanoma With Active Brain Metastases Treated With Pembrolizumab on a Phase Ii Trial. *J Clin Oncol Off J Am Soc Clin Oncol* (2019) 37(1):52–60. doi: 10.1200/jco.18.00204
52. Long GV, Atkinson V, Lo S, Sandhu S, Guminski AD, Brown MP, et al. Combination Nivolumab and Ipilimumab or Nivolumab Alone in Melanoma Brain Metastases: A Multicentre Randomised Phase 2 Study. *Lancet Oncol* (2018) 19(5):672–81. doi: 10.1016/s1470-2045(18)30139-6
53. Tawbi HA, Forsyth PA, Algazi A, Hamid O, Hodi FS, Moschos SJ, et al. Combined Nivolumab and Ipilimumab in Melanoma Metastatic to the Brain. *New Engl J Med* (2018) 379(8):722–30. doi: 10.1056/NEJMoa1805453
54. Shan Q, Shi J, Wang X, Guo J, Han X, Wang Z, et al. A New Nomogram and Risk Classification System for Predicting Survival in Small Cell Lung Cancer Patients Diagnosed With Brain Metastasis: A Large Population-Based Study. *BMC Cancer* (2021) 21(1):640. doi: 10.1186/s12885-021-08384-5
55. Pietrantonio F, Aprile G, Rimassa L, Franco P, Lonardi S, Cremolini C, et al. A New Nomogram for Estimating Survival in Patients With Brain Metastases Secondary to Colorectal Cancer. *Radiother Oncol J Eur Soc Ther Radiol Oncol* (2015) 117(2):315–21. doi: 10.1016/j.radonc.2015.08.023
56. Huang Z, Hu C, Tong Y, Fan Z, Zhao C. Construction of a Nomogram to Predict the Prognosis of Non-Small-Cell Lung Cancer With Brain Metastases. *Medicine* (2020) 99(31):e21339. doi: 10.1097/md.0000000000021339
57. Kim J, Lee SM, Yim JJ, Yoo CG, Kim YW, Han SK, et al. Prognosis for non-Small Cell Lung Cancer Patients With Brain Metastases. *Thoracic Cancer* (2013) 4(2):167–73. doi: 10.1111/j.1759-7714.2012.00164.x

Conflict of Interest: The authors declare that the research was conducted in the absence of any commercial or financial relationships that could be construed as a potential conflict of interest.

frontiers in Oncology

MINI REVIEW
published: 24 August 2021
doi: 10.3389/fonc.2021.714514

Radioimmunotherapy for Brain Metastases: The Potential for Inflammation as a Target of Choice

Aurélien Corroyer-Dulmont[1,2], Cyril Jaudet[1†], Anne-Marie Frelin[3†], Jade Fantin[2], Kathleen Weyts[4], Katherine A. Vallis[5], Nadia Falzone[6], Nicola R. Sibson[5], Michel Chérel[7], Françoise Kraeber-Bodéré[7,8], Alain Batalla[1], Stéphane Bardet[4], Myriam Bernaudin[2†] and Samuel Valable[2†]*

[1] Medical Physics Department, CLCC François Baclesse, Caen, France, [2] Normandie Univ, UNICAEN, CEA, CNRS, ISTCT/CERVOxy Group, GIP CYCERON, Caen, France, [3] Grand accélérateur National d'Ions Lourds (GANIL), CEA/DRF-CNRS/IN2P3, Caen, France, [4] Nuclear Medicine Department, CLCC François Baclesse, Caen, France, [5] Medical Research Council, Department of Oncology, Oxford Institute for Radiation Oncology, University of Oxford, Oxford, United Kingdom, [6] GenesisCare, Alexandria, NSW, Australia, [7] Team 13-Nuclear Oncology, CRCINA, INSERM, CNRS, Nantes University, Nantes, France, [8] Nuclear Medicine Department, University Hospital, Nantes, France

Brain metastases (BM) are frequently detected during the follow-up of patients with malignant tumors, particularly in those with advanced disease. Despite a major progress in systemic anti-cancer treatments, the average overall survival of these patients remains limited (6 months from diagnosis). Also, cognitive decline is regularly reported especially in patients treated with whole brain external beam radiotherapy (WBRT), due to the absorbed radiation dose in healthy brain tissue. New targeted therapies, for an earlier and/or more specific treatment of the tumor and its microenvironment, are needed. Radioimmunotherapy (RIT), a combination of a radionuclide to a specific antibody, appears to be a promising tool. Inflammation, which is involved in multiple steps, including the early phase, of BM development is attractive as a relevant target for RIT. This review will focus on the (1) early biomarkers of inflammation in BM pertinent for RIT, (2) state of the art studies on RIT for BM, and (3) the importance of dosimetry to RIT in BM. These two last points will be addressed in comparison to the conventional EBRT treatment, particularly with respect to the balance between tumor control and healthy tissue complications. Finally, because new diagnostic imaging techniques show a potential for the detection of BM at an early stage of the disease, we focus particularly on this therapeutic window.

Keywords: brain metastases, radio-immunotherapy, microenvironment, alpha-particle therapy, inflammation, VCAM-1, 212Pb

OPEN ACCESS

Edited by:
Giovanna Schiavoni, National Institute of Health (ISS), Italy

Reviewed by:
Andrew Nisbet, University College London, United Kingdom
Mark Konijnenberg, Erasmus Medical Center, Netherlands

****Correspondence:***
Aurélien Corroyer-Dulmont
a.corroyer-dulmont@baclesse.unicancer.fr

†These authors have contributed equally to this work

Specialty section:
This article was submitted to Cancer Immunity and Immunotherapy, a section of the journal Frontiers in Oncology

Received: *25 May 2021*
Accepted: *03 August 2021*
Published: *24 August 2021*

Citation:
Corroyer-Dulmont A, Jaudet C, Frelin A-M, Fantin J, Weyts K, Vallis KA, Falzone N, Sibson NR, Chérel M, Kraeber-Bodéré F, Batalla A, Bardet S, Bernaudin M and Valable S (2021) Radioimmunotherapy for Brain Metastases: The Potential for Inflammation as a Target of Choice. Front. Oncol. 11:714514. doi: 10.3389/fonc.2021.714514

INTRODUCTION

Current Management of Brain Metastases

Owing to advances in primary cancer control, the incidence of brain metastases (BM) is increasing (1). Lung cancer, the main cause of death from cancer, and breast cancer, the most common cancer in women in developed countries, carry 40% and 20% risk of BM, respectively (2). Depending on the Karnofsky performance status (KPS) factor, molecular features, and number of BM of the patient, conventional treatment comprises surgical resection when possible and image-guided stereotactic radiosurgery (SRS), with or without whole-brain radiotherapy (WBRT) (1).

Therapeutic Challenges

Despite these treatments, and even in cases where control of the primary cancer has a favorable impact on the overall survival (OS), a significant proportion of patients die as a result of BM (3), with an average OS of 6 months. For WBRT, 30 Gy in 10 fractions is conventionally given which can lead to cognitive decline owing to the radiation absorbed dose in healthy brain tissue. Indeed, cognitive changes were observed in children after a WBRT dose of greater or equal to 18 Gy. However the effect of WBRT in the adult brain is less well defined, with the incidence and severity of cognitive decline dependent on the dose per fraction, fractionation frequency, and volume irradiated (4). Therefore, increasing the dose of external radiotherapy (RT) in an effort to improve tumour control is currently not possible.

The balance between Tumour Control Probability (TCP) and Normal Tissue Complication Probability (NTCP) are, therefore, sub-optimal with the current treatments. One explanation may be the fact that BM are often diagnosed when locally advanced, as conventional MRI only detects the late disruption of the blood-brain-barrier (BBB) (5), when tumours are large and frequently beyond effective treatment. In contrast, treatment in the earlier stages of BM development is likely to yield a better tumour control, as fewer tumour cells have invaded the brain parenchyma and those that have remain within easier reach of systemic therapies if access across the BBB can be negotiated. Thus, the pressing unmet therapeutic challenges are to treat (i) at an early stage when relatively few metastatic tumour cells have invaded the brain parenchyma, and (ii) in a targeted manner to avoid healthy brain toxicity.

Radioimmunotherapy (RIT) enables targeted dose delivery by systemically administered radiopharmaceuticals to disseminated cancer cells. RIT uses the combination of a radionuclide emitting ionizing particulate radiation coupled to an antibody that targets a specific antigen expressed on tumour cells or their local microenvironment. For this reason, unlike conventional RT, RIT specifically affects cells that express the relevant molecular target (6), limiting dose deposition in healthy tissues, even those close to the tumour mass. The potential of RIT has been shown, for example, in non-Hoddgkin's lymphoma where ^{131}I was combined with an anti-CD20 antibody (7).

However, to the best of our knowledge, only one clinical study with four patients has evaluated the therapeutic relevance of RIT in BM. Poli and colleagues used a fully humanized antibody L19, which targets an epitope contained in the extra-domain B (EDB) of fibronectin (8). EDB-containing fibronectin molecules are highly expressed in the extracellular matrix surrounding newly formed blood vessels. Since most solid tumours and hematologic malignancies rely on neoangiogenesis for their growth and metastatic spread, it makes EDB-containing fibronectin an ideal target for RIT. ^{131}I-L19SIP (Radretumab) administration resulted in a decrease in tumour glucose metabolism with a significant BM/background uptake ratio > 4. From these studies, the attributes of RIT make it a promising approach to early BM management and could lead to a better TCP/NTCP ratio. Given the high linear energy transfer (LET), especially for alpha particles, and local dose deposition of radiation emitting particles, the specificity of the target is crucial. To this end, exploring the biomarkers of early BM or the microenvironment of early BM development could be a first step in providing an alternative target for RIT.

EARLY BIOMARKERS OF BM

Biomarkers of Tumour Cells

For about 30% of the patients, BM resulting from some lung and breast cancers, as well as the primary cancer cells themselves, exhibit an overexpression of the epidermal growth factor receptor (EGFR) and HER2. For this reason, tyrosine kinase inhibitors (TKI), such as ALK inhibitor, are used as systemic treatments in both the early and late disease stages and improve the progression-free survival of patients compared to chemotherapy. Thus, the combination of a TKI and RIT, in a way to transport the RIT, may have a potential as a new therapeutic strategy. However, the expression of EGFR and HER2 is highly heterogeneous, and TKI cannot be proposed for all patients (2). Another useful target for RIT could be the overexpression of certain genes that are implicated in early BM. Duchnowska and colleagues have shown, in 84 patients with breast cancer, that the expression of RAD51, HDGF, and TPR could predict early BM development and could be used as intracellular targets (9). Intracellular targets for RIT are relevant as their close proximity to DNA means that even radionuclides with very short-range emissions, such as the Auger-emitting ^{125}I, become candidates for therapy. Nevertheless, these targets require the radiopharmaceutical to traverse the BBB and cancer cell plasma membrane, yielding a significant delivery challenge. Alternatively, αv-integrins which play a role in tumour cell adhesion, invasion, and growth, have also been proposed as early biomarkers of BM. In a preclinical study, administration of intetumab, an anti-αv-integrin-targeted monoclonal antibody, was shown to decrease BM formation and increase the overall survival in a breast cancer BM rat model (10).

Abbreviations: BM, brain metastases; RIT, radio-immunotherapy; TCP, tumor control probability; NTCP, normal tissue complication probability; MRI, magnetic resonance imaging; PET, positron emission tomography; SPECT, single photon emission computed tomography; TKI, tyrosine kinase inhibitors; BBB, blood-brain-barrier; WBRT, whole brain radiotherapy; SF, survival fraction; MIRD, medical internal radiation Dose; EBRT, external beam radiotherapy; LET, linear energy transfer.

Importantly, αv-integrins are expressed on the cell membrane surface and are therefore more accessible for RIT targeting than intracellular targets.

All of these cancer cell biomarkers are promising as therapeutic targets, but to date, most systemically administrated agents have failed to provide effective treatment for BM owing to the presence of the BBB, which remains effective when addressing the early phase of BM. Puttemans and colleagues have shown that even the early phases of BM growth are characterized by a functional BBB (11). RIT agents directed against cancer cell biomarkers must be delivered efficiently so that sufficient radioactivity accumulates intratumourally to cause radiotoxicity. An alternative approach, however, is to use more accessible molecular targets, even if these are not on or immediately adjacent to cancer cells. This option is feasible because of the penetration of particulate radiation in tissue, resulting in radial radiation dose deposition from the decay site itself. Thus, RIT can be targeted to compartments relatively close to the tumour and still remain effective in treating tumour cells.

Biomarkers of the Tumour Microenvironment

Vascularisation

Kienast and colleagues have demonstrated, in preclinical models, the importance of vascular remodelling at the very early stages of BM invasion into the brain parenchyma. Using a multiphoton laser scanning microscopy, these investigators demonstrated the onset of BM formation through real-time tracking of individual human melanoma and lung cancer cells that had been injected *via* the mouse heart into the circulation (12). Early BM development appears to be strongly correlated with the ability to stimulate angiogenesis. Interestingly, it was shown that anti-angiogenic treatments (e.g., anti-VEGF, bevacizumab) could decrease the establishment of BM from lung carcinoma. These findings are consistent with the ability of bevacizumab to prevent BM development from nsNSCLC (AVAiL trial), but not BM from breast cancer (AVADO and AVEREL trials) (13). Whereas angiogenesis occurs after tumour cell invasion into the brain parenchyma, endothelial cells may express markers such as connexion as a direct result of tumour cell extravasation, providing targets indicative of an even earlier stage of BM (14).

The vascular compartment appears to be a rational target for RIT of early BM and the combination with anti-angiogenic treatments, such as bevacizumab, merits investigation. However, depending on the choice of the radionuclide, radio-toxicity in healthy tissue could be an issue. Angiogenesis is not only observed within the tumour microenvironment, VEGF is also expressed in healthy endothelial cells, macrophages, and platelets, whilst VEGF also plays a role in normal physiological functions such as bone formation, haematopoiesis, and development. In the tumour microenvironment, on the other hand, radio-toxicity on the vasculature could increase vessel permeability and provide a means to improve systemic drug delivery to BM. As an example, ^{225}Ac coupled to a monoclonal antibody directed against monomeric vascular endothelial cadherin, which is expressed on the tumour neovasculature (E4G10), induces vascular remodelling in a preclinical model of glioblastoma (15). This remodelling impacted the biodistribution of a systemic treatment, with an increase of dasatinib (TKI) concentration observed within the tumour when given in combination with the RIT agent. Vascular remodelling using RIT increased tumour permeability by 58% and was concomitant with an increase in the overall survival in mice from 9 to 21 days in comparison to the control. Finally, targeting fibronectin may be promising, as the molecule is present in the extracellular matrix surrounding newly formed blood vessels in BM and is undetectable in almost all healthy adult tissues (with the exception of female reproductive organs), which has a potential for healthy tissue preservation in the case of targeting RIT (8, 16).

Inflammation

Inflammatory processes are known to play a key role in the early invasion of the brain parenchyma by metastatic cancer cells. Leukocyte recruitment after tumour cell invasion is well characterized, and therapeutic trials using immunomodulation have yielded promising results, despite the notable heterogeneity between patients (17, 18). The endothelial cellular adhesion molecules (CAMs), which are implicated in the adhesion and transendothelial migration of macrophages and T cells, are also co-opted for tumour cell traversal through the endothelium. ALCAM, E-selectin, ICAM/LFA-1, and VCAM-1/VLA-4 have all been shown to play a part in the tumour cell invasion into the brain parenchyma (19). For this reason, these proteins have a considerable potential as biomarkers of early BM. In preclinical studies, blocking VLA-4 or ALCAM on tumour cells (*via* incubation with neutralizing antibodies) resulted in a significant decrease in the number and volume of BM in comparison to the unblocked cells (19). Importantly, endothelial CAM overexpression has been observed in early BM in both preclinical studies and human tissue (20, 21). VCAM-1, in particular, has been presented as a major biomarker of tumorigenesis in many types of cancers, further reinforcing its early biomarker status (22). On this basis, a novel MRI contrast agent, comprised of microparticles of iron oxide (MPIO) conjugated to anti-VCAM-1 antibodies (VCAM-MPIO), has been proposed as a diagnostic tool for the detection of early BM (23), and has been shown to enable detection of BM from breast, lung, and melanoma human cancers in preclinical models (24).

For these reasons, RIT targeted to BM *via* VCAM-1 may be promising, as it allows the targeting of the very early phase of BM. However, it is important to keep in mind that CAMs are also expressed in normal tissue, such as the kidney and bone marrow, and so toxicity profiles should be evaluated with care.

RADIOIMMUNOTHERAPY OF EARLY BM

RIT is the combination of a specific targeting moiety with a specific payload. In terms of payload, a range of radionuclides with different physicochemical properties can be used in RIT, each with different advantages and limitations (**Table 1**). This diversity of available radionuclides provides a means of matching

TABLE 1 | Early biomarkers of BM and potential radionuclides to combined.

Biomarkers (study reference)	Potential radionuclides for RIT (type of emission)	Therapeutic particle range	Radionuclide allowing biodistribution/dosimetry evaluation?	Advantages	Limitations
RAD51, HDGF and TPR gene overexpression in primary cancer cells (8)	^{125}I, ^{111}In (e-/γ)	2-5 nm	yes	•No need to pass throught the BBB •Early stage of BM •Possible biodistribution/dosimetry evaluation	•Need to be internalized into the cells •Low energy deposition
Tyrosine kinase inhibitors (2)	^{212}Pb, ^{225}Ac, ^{211}As, ^{213}Bi (α/β-/γ)	40-100µm	no	•Early stage of BM	•Need to pass throught the BBB •Difficult biodistribution/dosimetry evaluation
αv-integrin (9)	^{212}Pb, ^{225}Ac, ^{211}As, ^{213}Bi (α/β-/γ)	40-100µm	no	•Early stage of BM	•Need to pass throught the BBB •Difficult biodistribution/dosimetry evaluation
VEGF (12)	^{212}Pb, ^{225}Ac, ^{211}As, ^{213}Bi (α/β-/γ)	40-100µm	no	•Early stage of BM •No need to pass throught the BBB	•Difficult biodistribution/dosimetry evaluation •VEGF expression in healthy tissue could induce radiotoxicity
VCAM-1 (21)	^{212}Pb, ^{225}Ac, ^{211}As, ^{213}Bi (α/β-/γ)	40-100µm	no	•Early stage of BM •No need to pass throught the BBB	•Difficult biodistribution/dosimetry evaluation •VCAM-1 expression in kidney, spleen and bone marrow could induce radiotoxicity

treatment to the tumour characteristics. As previously discussed, early BM exhibits a functional BBB, which prevents an easy direct contact between the systemically administered RIT and tumour cells. Radionuclides can damage the tumour DNA from a distance. This distance depends on the energy and, therefore, track length in tissue, of the particulate emissions. Ranges are of the order of a few nm–µm for Auger e^-, µm for α particles, or mm for β particles. Energy deposition also depends on the type of particles: dozen of keV for Auger e^-, hundreds of keV for β particles, and MeV for α particles (25). Given these properties, RIT targeting of VCAM-1 expression on endothelial cells could result in the irradiation of adjacent early BM. However, which radionuclide is most suitable for this application has yet to be investigated.

Based on the two-photon and immunohistochemistry images from a preclinical model of breast cancer BM (MDA-231-Br cell line), an *in silico* model was constructed to evaluate several radionuclides to identify which would provide the best radiation dose distribution in the context of early BM formation. In this study, Monte Carlo simulations were performed with ^{149}Tb, ^{211}At, ^{212}Pb, ^{213}Bi, and ^{225}Ac (α-emitting radionuclides); ^{90}Y, ^{161}Tb, and ^{177}Lu (β-emitting radionuclides); and ^{67}Ga, ^{89}Zr, ^{111}In, and ^{124}I (auger e^- emitting radionuclides) enabling evaluation of dose deposition in the DNA specifically. This study showed that α particle emitters, with a short range and a high dose deposition, are the most appropriate for RIT targeting *via* VCAM-1 expression in early BM. Among these α particles emitters, ^{212}Pb has the attributes of a theranostic radionuclide since it can be used for SPECT imaging and showed a favourable dose profile and RBE (26).

On the basis of the above study, the therapeutic value of RIT for early BM was assessed in a preclinical study, in which the added-value of RIT using ^{212}Pb combined with an anti-VCAM-1 antibody (^{212}Pb-αVCAM-1) was assessed in comparison to conventional WBRT (27). In this preclinical study, BM were induced by intracardiac injection of human breast cancer cells (MDA-231-Br). ^{212}Pb-αVCAM-1 showed a favourable biodistribution in the whole body with a high uptake in BM compared to healthy tissues. In addition, low toxicity was observed, highlighting the added value of ^{212}Pb-αVCAM-1 in comparison to WBRT with respect to the avoidance of dose deposition in healthy brain. In terms of tumour control, tumour volume and the number of BM were both decreased in comparison to the WBRT group, and the OS was significantly increased (**Figure 1**). To understand the different therapeutic effects of ^{212}Pb-αVCAM-1 and WBRT, clonogenic assays were performed and showed higher radiosensitivity parameters, such as the survival fraction at 2 Gy or the dose that decreased the survival fraction by 50% (28), for ^{212}Pb-αVCAM-1 compared to WBRT. However, such an evaluation of radiosensitivity requires complex experiments with clonogenic assays that are not possible in clinical practice. Thus, evaluation of the added value of targeted RIT, in comparison to conventional WBRT for the treatment of BM, requires a detailed dosimetry as performed for external beam RT.

Dosimetry of Radioimmunotherapy

Administered activity is either based on a fixed amount or adjusted taking the body weight or body surface area of the

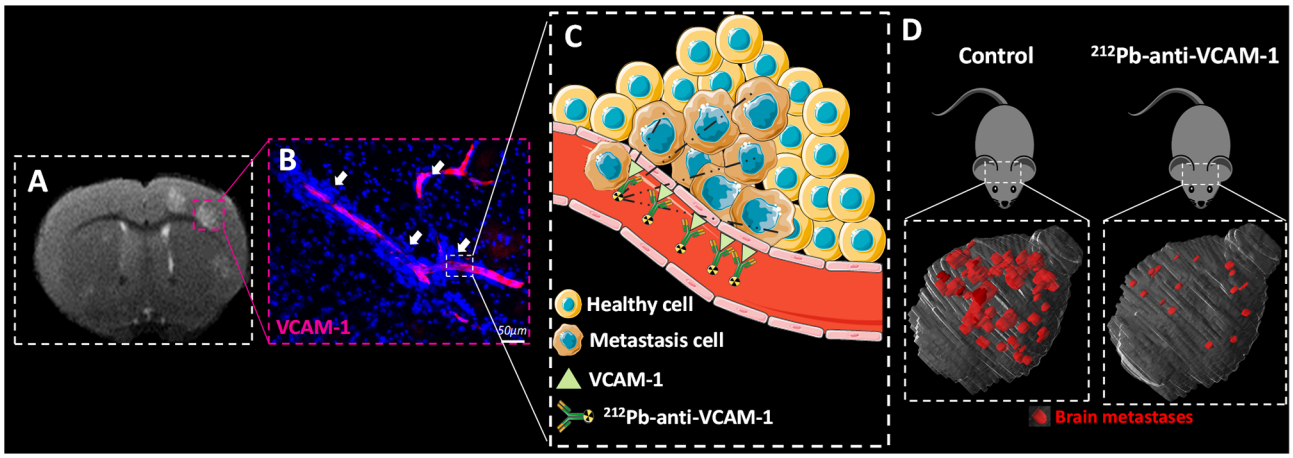

FIGURE 1 | RIT in early brain metastases. **(A)** MRI of a brain mouse with early brain metastases (BM). **(B)** VCAM-1 immunostaining showing the small distance between VCAM-1 activated endothelial cells and BM (pink staining and with arrow). **(C)** Representation of radioimmunotherapy targeting VCAM-1 for the early treatment of BM. **(D)** 3D representation of BM (red) in the brain (grey) in the control and 212Pb-anti-VCAM-1 treated group.

patient into consideration and not planned to maximise the tumour dose, whilst sparing the organs at risk. Nevertheless, a substantial effort is being made to individualise patient treatments and to improve the accuracy of dosimetry procedures in the clinic. Important initiatives to standardise dosimetry include the internal dosimetry task force linked to EANM (29, 30), the Medical Internal Radiation Dose committee (31), or the EU consortium MEDIRAD (32, 33). Dosimetry should play an important role when a new agent for RIT undergoes clinical testing, alongside the assessment of the maximum tolerated dose and side effects, similar to clinical trials of nonradioactive oncological drugs (34).

In the case of BM, only one study has reported dosimetry for the purpose of RIT. Poli and colleagues evaluated the biodistribution of ^{124}I-L19SIP in patients with BM to compute the ^{131}I-L19SIP dosimetry (8) With ^{124}I, PET imaging can be performed, providing a more precise spatial information than SPECT, and its half-life of 4.18 days is compatible with a biodistribution study of ^{131}I-L19SIP. PET imaging was performed at 1, 2, 24, 48, and 96 hours after an injected activity of (^{124}I-L19SIP). Time activity curves were obtained and the cumulated activity over time (AUC) was computed. Using OLINDA/EXM (35) and MIRD formalism, the authors evaluated the dose in Gy per injected MBq in different organs. This study suggested that immuno-PET diagnostic imaging with ^{124}I-L19SIP could actually predict the dose that would be delivered to the tumour *vs.* healthy organs by a subsequent therapeutic ^{131}I-L19SIP dose. Those authors also measured the red bone marrow dose. The estimated dose was similar during both the diagnostic scanning and treatment. However, significant heterogeneity in the dose delivered to different tumours in the same patient was apparent. This tumour heterogeneity highlights the importance of preliminary dosimetry before RIT (8).

The biological distribution of ^{212}Pb-αVCAM-1 has not yet been studied in humans. Two approaches to dosimetry can be considered, either during or before treatment. Concerning the first approach, the temporal and spatial distribution of ^{212}Pb-αVCAM-1 can be evaluated through the γ-emissions of ^{212}Pb with multiple time-point SPECT acquisitions. The second approach, similar to Poli et al. consists of performing pre-treatment imaging with ^{203}Pb-αVCAM-1 (36), emitting γ-rays with a half-life of 51.87 h, to compute a predictive dose distribution of ^{212}Pb-αVCAM-1. As the physical half-life of ^{212}Pb is shorter (10.4 h) than that of ^{131}I-L19SIP (37), all of the imaging acquisitions and blood sampling could be performed within one day instead of four. This imaging procedure would enable a dose computation to be made before treatment and, consequently, allow the possibility of adapting the injected activity to reach the desired dose to the tumour whilst minimising the risk of complication. Additionally, the injected activity or number of cycles could be tailored to reach the best TCP, whilst lowering the NTCP as in WBRT. For instance, the TCP model of WBRT is based on a biologically effective dose of about 40 Gy (38). Usually, a fractionation of 10 times 3 Gy is delivered to the patient after a CT planning scan. Calculation of the absorbed dose is relatively straightforward in EBRT with constant dose rates and photon beams of widely used energies, and the biological effects are mainly produced by low LET particles. It is hazardous to extrapolate doses from EBRT to RIT owing to the fundamental differences in the dose rate and the mechanisms of DNA damage and repair. Consequently, preclinical studies to characterise the biodistribution of ^{212}Pb-αVCAM-1 with ^{203}Pb-αVCAM-1 in BM is the next step to determining a predictive dose.

Radioimmunotherapy of Late Stage BM

Most patients are treated when their BM are advanced due to the diagnostic insensitivity of the currently available imaging. Advanced BM are associated with larger tumour sizes and the microenvironment is different with marked angiogenesis

suggesting BBB disruption, chaotic and heterogeneous vascularisation. Hypoxic features have been shown in the BM microenvironment from lung, breast, renal, and colorectal cancers (39), as well as at the preclinical level for BM from lung cancer (40). All of these changes negatively affect the performance of RIT, and fewer abnormal vessels (per tumour volume) is likely to reduce the accumulation of RIT at the tumour site. Poor concentration of RIT limits irradiation of the tumour by short range α-emitting. Imaging studies prior to RIT are, therefore, very important to evaluate biodistribution. However, RIT using α-emitting isotopes could still be very effective in combination with external RT for late BM, because α-particle radiation effects are not impacted by radioresistance factors such as hypoxia. The maximum relative radiosensitivity of cells to oxygen concentration, or the oxygen enhancement ratio (OER), is commonly thought to be about 3 for x-rays that induce secondary electrons with LET of 1.3 keV/μm. For α-particles with LET of 60–110 keV/μm, the OER decreases to 1.3–2.1 between the particle emission point and the Bragg peak, and to about 1.0 in the Bragg peak area, and thus leads to a no effect of hypoxia on RIT efficacy (41). However, this potential of the α-particle RIT for the treatment of hypoxic BM has first to be confirmed in preclinical studies, and then in clinical studies.

CONCLUSION

Treatment of BM at the early stage of development is likely to yield optimal tumour control. However, owing to the small size of BM at this early stage, and limited detection, external RT is not suitable and molecularly targeted treatment is needed. RIT using α-particles (e.g., ^{212}Pb) combined with biomarkers of early disease, such as cell adhesion molecules (e.g., VCAM-1), has shown promising results at the preclinical level for treatment of early BM. The treatment of well-established BM exhibiting hypoxic features with RIT using a combination of α-particles with a hypoxia biomarker may have a potential, but requires validation. Finally, because α-particles have a very high LET and a very short range, the distribution of α-particle RIT to the BM site is crucial. Consequently, imaging enabling the characterisation of biodistribution and dosimetry are needed to fully evaluate the potential benefit of α-particle RIT for the treatment of BM.

AUTHOR CONTRIBUTIONS

Manuscript drafting or manuscript revision for important intellectual content: all authors. All authors contributed to the article and approved the submitted version. Literature research: AC-D, CJ, NF, A-MF. Manuscript editing: All authors. Figure preparation: AC-D.

FUNDING

This study was funded by the Région Normandie, the Centre National de la Recherche Scientifique (CNRS), the Université de Caen Normandie (UNICAEN), the European Union-Fonds Européen de Développement Régional (FEDER), the Ministère de l'Enseignement Supérieur et de la Recherche and the French National Agency for Research "Investissements d'Avenir" n° ANR-11-LABEX-0018-01 and n°ANR-10-EQPX1401 and The HABIONOR European project, and co-funded by the Normandy County Council, the French State in the framework of the interregional development Contract "Vallée de la Seine" 2015-2020 and the FRC. NS and KV were supported by a Cancer Research UK core award (C5255/A15935).

REFERENCES

1. Ostrom QT, Wright CH, Barnholtz-Sloan JS. Brain Metastases: Epidemiology. *Handb Clin Neurol* (2018) 149:3–23. doi: 10.1016/B978-0-12-811161-1.00002-5
2. Mao Y, Yang D, He J, Krasna MJ. Epidemiology of Lung Cancer. *Semin Interv Radiol* (2016) 25:439–45. doi: 10.1016/j.soc.2016.02.001
3. Robinson AG, Young K, Balchin K, Ashworth A, Owen T. Causes of Death and Subsequent Treatment After Initial Radical or Palliative Therapy of Stage III Non-Small-Cell Lung Cancer. *Curr Oncol* (2015) 22:333. doi: 10.3747/co.22.2432
4. Lawrence YR, Li XA, el Naqa I, Hahn CA, Marks LB, Merchant TE, et al. Radiation Dose-Volume Effects in the Brain. *Int J Radiat Oncol Biol Phys* (2010) 76:20–7. doi: 10.1016/j.ijrobp.2009.02.091
5. Tong E, McCullagh KL, Iv M. Advanced Imaging of Brain Metastases: From Augmenting Visualization and Improving Diagnosis to Evaluating Treatment Response. *Front Neurol* (2020) 11:270. doi: 10.3389/fneur.2020.00270
6. Gill MR, Falzone N, Du Y, Vallis KA. Targeted Radionuclide Therapy in Combined-Modality Regimens. *Lancet Oncol* (2017) 18:e414–23. doi: 10.1016/S1470-2045(17)30379-0
7. Chow VA, Rajendran JG, Fisher DR, Appelbaum FR, Cassaday RD, Martin PS, et al. A Phase II Trial Evaluating the Efficacy of High-Dose Radioiodinated Tositumomab (Anti-CD20) Antibody, Etoposide and Cyclophosphamide Followed by Autologous Transplantation, for High-Risk Relapsed or Refractory Non-Hodgkin Lymphoma. *Am J Hematol* (2020) 95:775–83. doi: 10.1002/ajh.25818
8. Poli GL, Bianchi C, Virotta G, Bettini A, Moretti R, Trachsel E, et al. Radretumab Radioimmunotherapy in Patients With Brain Metastasis: A 124I-L19SIP Dosimetric PET Study. *Cancer Immunol Res* (2013) 1:134–43. doi: 10.1158/2326-6066.CIR-13-0007
9. Duchnowska R, Jassem J, Goswami CP, Dundar M, Gökmen-Polar Y, Li L, et al. Predicting Early Brain Metastases Based on Clinicopathological Factors and Gene Expression Analysis in Advanced HER2-Positive Breast Cancer Patients. *J Neurooncol* (2015) 122:205–16. doi: 10.1007/s11060-014-1704-y
10. Wu YJ, Muldoon LL, Gahramanov S, Kraemer DF, Marshall DJ, Neuwelt EA. Targeting alphaV-Integrins Decreased Metastasis and Increased Survival in a Nude Rat Breast Cancer Brain Metastasis Model. *J Neurooncol* (2012) 110:27–36. doi: 10.1007/s11060-012-0942-0
11. Puttemans J, Lahoutte T, D'huyvetter M, Devoogdt N. Beyond the Barrier: Targeted Radionuclide Therapy in Brain Tumors and Metastases. *Pharmaceutics* (2019) 11:1–23. doi: 10.3390/pharmaceutics11080376
12. Kienast Y, von Baumgarten L, Fuhrmann M, Klinkert WEF, Goldbrunner R, Herms J, et al. Real-Time Imaging Reveals the Single Steps of Brain Metastasis Formation. *Nat Med* (2010) 16:116–22. doi: 10.1038/nm.2072
13. Ilhan-Mutlu A, Osswald M, Liao Y, Gömmel M, Reck M, Miles D, et al. Bevacizumab Prevents Brain Metastases Formation in Lung Adenocarcinoma. *Mol Cancer Ther* (2016) 15:702–10. doi: 10.1158/1535-7163.MCT-15-0582

14. Stoletov K, Strnadel J, Zardouzian E, Momiyama M, Park FD, Kelber JA, et al. Role of Connexins in Metastatic Breast Cancer and Melanoma Brain Colonization. *J Cell Sci* (2013) 126:904–13. doi: 10.1242/jcs.112748
15. Behling K, DiGialleonardo V, Maguire WF, Heeb LEM, Hassan IF, Veach DR, et al. Remodelling the Vascular Microenvironment of Glioblastoma With Alpha-Particles. *J Nucl Med* (2016) 57(11):1771–8. doi: 10.2967/jnumed.116.173559
16. Schittenhelm J, Klein A, Tatagiba MS, Meyermann R, Fend F, Goodman SL, et al. Comparing the Expression of Integrins αvβ3, αvβ5, αvβ6, αvβ8, Fibronectin and Fibrinogen in Human Brain Metastases and Their Corresponding Primary Tumors. *Int J Clin Exp Pathol* (2013) 6:2719–32.
17. Fernandes GNC. Immunotherapy for Melanoma Brain Metastases. *Discoveries* (2019) 7:e93. doi: 10.15190/d.2019.6
18. Hamilton A, Sibson NR. Role of the Systemic Immune System in Brain Metastasis. *Mol Cell Neurosci* (2013) 53:42–51. doi: 10.1016/j.mcn.2012.10.004
19. Soto MS, Serres S, Anthony DC, Sibson NR. Functional Role of Endothelial Adhesion Molecules in the Early Stages of Brain Metastasis. *Neuro Oncol* (2014) 16:540–51. doi: 10.1093/neuonc/not222
20. Zarghami N, Soto MS, Perez-Balderas F, Khrapitchev AA, Karali CS, Johanssen VA, et al. A Novel Molecular Magnetic Resonance Imaging Agent Targeting Activated Leukocyte Cell Adhesion Molecule as Demonstrated in Mouse Brain Metastasis Models. *J Cereb Blood Flow Metab* (2020) 41(7):1592–607. doi: 10.1177/0271678X20968943
21. Soto MS, O'Brien ER, Andreou K, Scrace SF, Zakaria R, Jenkinson MD, et al. Disruption of Tumour-Host Communication by Downregulation of LFA-1 Reduces COX-2 and E-NOS Expression and Inhibits Brain Metastasis Growth. *Oncotarget* (2016) 7:52375. doi: 10.18632/oncotarget.10737
22. Schlesinger M, Bendas G. Vascular Cell Adhesion Molecule-1 (VCAM-1) - An Increasing Insight Into its Role in Tumorigenicity and Metastasis. *Int J Cancer* (2015) 136:2504–14. doi: 10.1002/ijc.28927
23. Serres S, Soto MS, Hamilton A, McAteer MA, Carbonell WS, Robson MD, et al. Molecular MRI Enables Early and Sensitive Detection of Brain Metastases. *Proc Natl Acad Sci USA* (2012) 109:6674–9. doi: 10.1073/pnas.1117412109
24. Cheng VWT, Sarmiento Soto M, Khrapitchev AA, Perez-Balderas F, Zakaria R, Jenkinson MD, et al. VCAM-1 Targeted Magnetic Resonance Imaging Enables Detection of Brain Micrometastases From Different Primary Tumours. *Clin Cancer Res* (2018) 25(2):clincanres.1889.2018. doi: 10.1158/1078-0432.CCR-18-1889
25. Barbet J, Bardiès M, Bourgeois M, Chatal JF, Chérel M, Davodeau F, et al. Radiolabeled Antibodies for Cancer Imaging and Therapy. *Methods Mol Biol* (2012) 907:681–97. doi: 10.1007/978-1-61779-974-7-38
26. Falzone N, Ackerman NL, de la Rosales LF, Bernal MA, Liu X, Peeters SG, et al. Dosimetric Evaluation of Radionuclides for VCAM-1-Targeted Radionuclide Therapy of Early Brain Metastases. *Theranostics* (2018) 8:292–303. doi: 10.7150/thno.22217
27. Corroyer-Dulmont A, Valable S, Falzone N, Frelin-Labalme AM, Tietz O, Toutain J, et al. VCAM-1 Targeted Alpha-Particle Therapy for Early Brain Metastases. *Neuro Oncol* (2020) 22:357–68. doi: 10.1093/neuonc/noz169
28. Frelin-Labalme A-M, Roger T, Falzone N, Quan Lee B, Sibson NR, Vallis KA, et al. Radionuclide Spatial Distribution and Dose Deposition for *In Vitro* Assessments of 212 Pb-αvcam-1 Targeted Alpha Therapy. *Med Phys* (2020) 47:1317–26. doi: 10.1002/mp.13969
29. Kratochwil C, Fendler WP, Eiber M, Baum R, Bozkurt MF, Czernin J, et al. EANM Procedure Guidelines for Radionuclide Therapy With 177Lu-Labelled PSMA-Ligands (177Lu-PSMA-RLT). *Eur J Nucl Med Mol Imaging* (2019) 46:2536–44. doi: 10.1007/s00259-019-04485-3
30. Lassmann M, Chiesa C, Flux G, Bardiès M. EANM Dosimetry Committee Guidance Document: Good Practice of Clinical Dosimetry Reporting. *Eur J Nucl Med Mol Imaging* (2011) 38:192–200. doi: 10.1007/s00259-010-1549-3
31. Ljungberg M, Celler A, Konijnenberg MW, Eckerman KF, Dewaraja YK, Sjögreen-Gleisner K. MIRD Pamphlet No. 26: Joint EANM/MIRD Guidelines for Quantitative 177Lu SPECT Applied for Dosimetry of Radiopharmaceutical Therapy. *J Nucl Med* (2016) 57:151–62. doi: 10.2967/jnumed.115.159012
32. Taprogge J, Murray I, Gear J, Chittenden SJ, Parker CC, Flux GD. Compartmental Model for 223Ra-Dichloride in Patients With Metastatic Bone Disease From Castration-Resistant Prostate Cancer. *Int J Radiat Oncol Biol Phys* (2019) 105:884–92. doi: 10.1016/j.ijrobp.2019.07.022
33. Taprogge J, Leek F, Schurrat T, Tran-Gia J, Vallot D, Bardiès M, et al. Setting Up a Quantitative SPECT Imaging Network for a European Multi-Centre Dosimetry Study of Radioiodine Treatment for Thyroid Cancer as Part of the MEDIRAD Project. *EJNMMI Phys* (2020) 7(1):1–14. doi: 10.1186/s40658-020-00332-9
34. Giammarile F, Muylle K, Bolton RD, Kunikowska J, Haberkorn U, Oyen W. Dosimetry in Clinical Radionuclide Therapy: The Devil is in the Detail. *Eur J Nucl Med Mol Imaging* (2017) 7(1):3–5. doi: 10.1007/s00259-017-3820-3
35. Stabin MG, Sparks RB, Crowe E. OLINDA/EXM: The Second-Generation Personal Computer Software for Internal Dose Assessment in Nuclear Medicine. *J Nucl Med* (2005) 46:1023–7.
36. dos Santos JC, Schäfer M, Bauder-Wüst U, Lehnert W, Leotta K, Morgenstern A, et al. Development and Dosimetry of 203 Pb/212 Pb-Labelled PSMA Ligands: Bringing "The Lead" Into PSMA-Targeted Alpha Therapy? *Eur J Nucl Med Mol Imaging* (2019) 46:1081–91. doi: 10.1007/s00259-018-4220-z
37. Corroyer-Dulmont A, Valable S, Falzone N, Frelin-Labalme A-M, Tietz O, Toutain J, et al. VCAM-1 Targeted Alpha-Particle Therapy for Early Brain Metastases. *Neuro Oncol* (2019) 22(3):1–12. doi: 10.1093/neuonc/noz169
38. Zhuang QY, Li JL, Lin FF, Lin XJ, -lin H, Wang Y, et al. High Biologically Effective Dose Radiotherapy for Brain Metastases May Improve Survival and Decrease Risk for Local Relapse Among Patients With Small-Cell Lung Cancer: A Propensity-Matching Analysis. *Cancer Control* (2020) 27:1–11. doi: 10.1177/1073274820936287
39. Berghoff AS, Ilhan-Mutlu A, Dinhof C, Magerle M, Hackl M, Widhalm G, et al. Differential Role of Angiogenesis and Tumour Cell Proliferation in Brain Metastases According to Primary Tumour Type: Analysis of 639 Cases. *Neuropathol Appl Neurobiol* (2015) 41:e41–55. doi: 10.1111/nan.12185
40. Corroyer-dulmont A, Valable S, Fantin J, Chatre L, Toutain J, Teulier S, et al. Multimodal Evaluation of Hypoxia in Brain Metastases of Lung Cancer and Interest of Hypoxia Image-Guided Radiotherapy. *Sci Rep* (2021) 11(1):1–15. doi: 10.1038/s41598-021-90662-0
41. Sgouros G, Roeske JC, McDevitt MR, Palm S, Allen BJ, Fisher DR, et al. MIRD Pamphlet No. 22 (Abridged): Radiobiology and Dosimetry of α-Particle Emitters for Targeted Radionuclide Therapy. *J Nucl Med* (2010) 51:311–28. doi: 10.2967/jnumed.108.058651

Conflict of Interest: Author NF was employed by GenesisCare.

The remaining authors declare that the research was conducted in the absence of any commercial or financial relationships that could be construed as a potential conflict of interest.

Publisher's Note: All claims expressed in this article are solely those of the authors and do not necessarily represent those of their affiliated organizations, or those of the publisher, the editors and the reviewers. Any product that may be evaluated in this article, or claim that may be made by its manufacturer, is not guaranteed or endorsed by the publisher.

frontiers in Oncology

PERSPECTIVE
published: 01 September 2021
doi: 10.3389/fonc.2021.714428

Brain Microenvironment Heterogeneity: Potential Value for Brain Tumors

Laura Álvaro-Espinosa, Ana de Pablos-Aragoneses, Manuel Valiente and Neibla Priego *

Brain Metastasis Group, Molecular Oncology Programme, Spanish National Cancer Research Centre (CNIO), Madrid, Spain

Uncovering the complexity of the microenvironment that emerges in brain disorders is key to identify potential vulnerabilities that might help challenging diseases affecting this organ. Recently, genomic and proteomic analyses, especially at the single cell level, have reported previously unrecognized diversity within brain cell types. The complexity of the brain microenvironment increases during disease partly due to the immune infiltration from the periphery that contributes to redefine the brain connectome by establishing a new crosstalk with resident brain cell types. Within the rewired brain ecosystem, glial cell subpopulations are emerging hubs modulating the dialogue between the Immune System and the Central Nervous System with important consequences in the progression of brain tumors and other disorders. Single cell technologies are crucial not only to define and track the origin of disease-associated cell types, but also to identify their molecular similarities and differences that might be linked to specific brain injuries. These altered molecular patterns derived from reprogramming the healthy brain into an injured organ, might provide a new generation of therapeutic targets to challenge highly prevalent and lethal brain disorders that remain incurable with unprecedented specificity and limited toxicities. In this perspective, we present the most relevant clinical and pre-clinical work regarding the characterization of the heterogeneity within different components of the microenvironment in the healthy and injured brain with a special interest on single cell analysis. Finally, we discuss how understanding the diversity of the brain microenvironment could be exploited for translational purposes, particularly in primary and secondary tumors affecting the brain.

Keywords: brain, brain metastasis, microenvironment, heterogeneity, single-cell analysis

OPEN ACCESS

Edited by:
Frits Thorsen,
University of Bergen, Norway

Reviewed by:
Monika Vishnoi,
Houston Methodist Research Institute, United States
Sivan Izraely,
Tel Aviv University, Israel

***Correspondence:**
Neibla Priego
npriego@cnio.es

Specialty section:
This article was submitted to Cancer Immunity and Immunotherapy, a section of the journal Frontiers in Oncology

Received: *25 May 2021*
Accepted: *16 August 2021*
Published: *01 September 2021*

Citation:
Álvaro-Espinosa L, de Pablos-Aragoneses A, Valiente M and Priego N (2021) Brain Microenvironment Heterogeneity: Potential Value for Brain Tumors. Front. Oncol. 11:714428. doi: 10.3389/fonc.2021.714428

INTRODUCTION

The brain microenvironment represents a complex habitat that notably differs from the microenvironment associated with other tumors (1). In addition to the still incomplete understanding of brain homeostasis and the structural heterogeneity of this organ, the presence of any insult, such as a tumor, might contribute to amplify the pre-existing diversity within the microenvironment.

Imaging, genomic and proteomic analyses have been valuable tools for dissecting inter- and intra-regional heterogeneity within the brain. Initially applied to uncover neuronal subtypes across brain

regions (2–5), single-cell RNA sequencing (scRNAseq), single-nucleus RNA sequencing (snRNAseq), mass cytometry (CyTOF) and spatial transcriptomics, have also proved to be a powerful tool beyond non-neuronal cells, revolutionizing the way we interrogate cancer-associated heterogeneity. Recently, the principles of scRNAseq have been expanded to elucidate *in vivo* networks based on cell-to-single cell interactions (6–8). These studies are dramatically expanding the complexity of the brain that should be translated into comprehensive pharmacologic approaches overcoming initial technical difficulties associated with this organ (9).

Although the characterization of altered molecular pathways within the brain microenvironment at the single cell level in brain tumors, especially in brain metastasis, is still limited, in this perspective we take advantage of findings obtained from other contexts (**Figure 1**) to discuss how exploiting heterogeneity could be translated into novel therapeutic strategies also for brain tumors.

DIVERSITY OF MACROPHAGES WITHIN THE BRAIN MICROENVIRONMENT

Health and Aging

scRNA-seq approaches have uncovered specific transcriptomic profiles that distinguish brain microglia and macrophages (2, 10–13). Additionally, different microglial states have been found at embryonic and early postnatal time points (14–16), while aging modulates inflammatory and interferon response signatures in microglia (14), as detailed in **Table 1**.

Brain Disorders

During Alzheimer disease (AD), disease-associated microglia (DAM) and late-response microglia are defined by the expression of genes related to lipid metabolism and phagocytosis (*ApoE, Lpl, Trem2, Tyrobp, Ctsd*) and interferon response (17, 18). By combining CyTOF with lineage tracing models Mrdjen et al. identified a subset of microglia during AD characterized by the upregulation of phagocytic markers CD11c and CD14. However, the specific functional contribution of DAMs during AD remains unclear (17, 19). During Experimental Autoimmune Encephalomyelitis (EAE) microglia showed a similar signature, except for decreased CD14 and increased MHCII and Sca-1 expression (11). In the same line, Ajami et al. identified two CNS-resident myeloid populations increased in frequency during EAE, Amyotrophic Lateral Sclerosis (ALS) and Huntington's disease (HD) (20) and Jordao et al. described four disease-associated microglia in EAE (**Table 1** details defining gene signatures). Peripheral monocyte populations present in the EAE model, but absent in AD and HD, express CD49e and show higher expression of pSTAT3 and lower of pCREB and NFκ-B in comparison to resident myeloid cells.

Remarkably, high-throughput technological pipelines are now available to profile novel cell-to-cell interactions at a single cell level. Clark et al. combines molecular barcoding, viral tracing and scRNASeq *in vivo* (RABID-seq) to map the microglia-astrocyte crosstalk during EAE, being responsible of inducing a pro-inflammatory microenvironment through two main axes: *Sema4D-PlexinB2* and *Ephrin-B3/EphB3* (8).

As summarized in **Table 1**, analysis of human and mouse microglia suggests high correlation in their transcriptomic profiles (i.e. upregulation of *Apoe)* and highlight the broader heterogeneity of human microglia (15, 21–23).

Brain Tumors

Recent sc-RNAseq analysis found that the interaction of tumor-associated macrophages (TAMs) and glioma cells occurs mainly through CXCL chemokines and their receptors (24). Furthermore, scRNA-seq analysis of CD11b+ myeloid cells isolated from murine experimental GL261 gliomas unveiled that activated microglia and BMDM significantly change their transcriptional networks, with upregulation of MHCII related proteins (25). In glioma patients, TAM BMDM invade the tumor core displaying an anti-inflammatory and pro-angiogenic phenotype, expressing immunosuppressive cytokines (i.e. *Il10* and *Tgfβ2*) and markers of active phagocytosis (*CD93*). Meanwhile, microglia located in the surrounding space is characterized by the expression of pro-inflammatory molecules (i.e. C*CL4, CCL3, IL1A/B*) (25–27).

Recently this heterogeneity has also been addressed in brain metastasis in comparison to gliomas. Friebel et al. found that, while the glioma microenvironment is predominantly composed by activated microglia, brain metastases are characterized by the infiltration of BMDM (28). Similarly, Guldner et al. identified myeloid clusters characterized by the expression of complement genes, while BMDMs express higher levels of inflammatory genes (*S100a11, Lgals, Il1b*) in brain metastasis. Furthermore, it was shown that loss of *Cx3cr1* in CNS-myeloid cells triggers upregulation of *Cxcl10*, which in turn drives an immunosuppressive pro-metastatic microenvironment through PD-L1 and VISTA. Interestingly, co-inhibition of both molecules reduced the brain metastatic burden (29).

LYMPHOCYTES AND NATURAL KILLER CELLS HETEROGENEITY WITHIN THE BRAIN MICROENVIRONMENT

Health and Ageing

Applying CyTOF to the naïve mouse brain, Korine et al. found that CD4+ and CD8+ infiltrating T cells express markers of memory T cells (CD44+CD62L-) and could be characterized by the increased expression of CD86 and CX3CR1 in comparison to their blood counterparts. Indeed, CD44 was suggested to be a general marker for brain infiltrating immune populations (30). Brain B cells and NK cells, which are found in lower numbers than in peripheral blood, particularly IgM+ B cells, are also defined by CX3CR1 expression (30). In the aged brain, using cellular indexing of transcriptomes and epitopes by sequencing (CITE-seq), T cells were found to express a T cell memory stemness signature characterize by CD3+ and Thy1+/Itga2+/Klrb1- mRNA expression and additional gene signatures associated with chemotaxis and ribosomal proteins, including Ly6a and Dusp2 expression. These findings suggest that

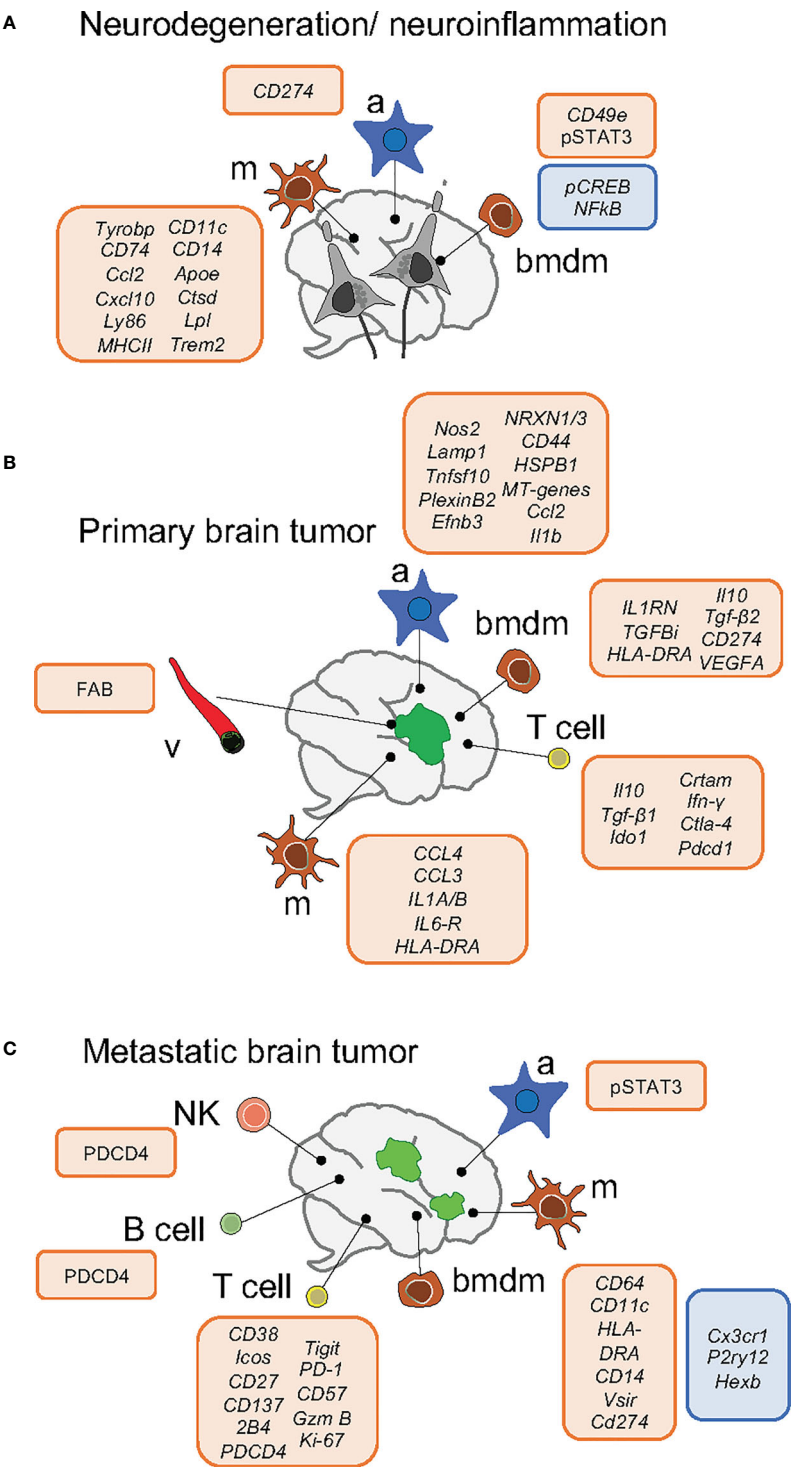

FIGURE 1 | Schema of key markers deregulated within the brain microenvironment in neurodegeneration/neuroinflammation **(A)** and primary **(B)** and secondary **(C)** brain tumors. Upregulation is indicated by the box in red and downregulation by the box in blue. Neurodegeneration/neuroinflammation comprises the following brain disorders: Alzheimer, Huntington disease, Amyotrophic Lateral Sclerosis and Experimental Autoimmune Encephalomyelitis. a, astrocytes; m, microglia; bmdm, bone marrow-derived macrophages; v, vasculature.

TABLE 1 | Key signatures and markers found in microglia/macrophages, T cells, astrocytes and endothelial cells subpopulations within the brain in preclinical models and/or patients of brain disorders and primary and secondary brain tumors.

Paper	PMID	Context	Cell type	Gene	Up/Down	Validated in patients	Notes
Masuda et al.	30760929	Health	Microglia	*TMEM119, P2RY12, CX3CR1, P2RY13, SLC2A5*	Defining signature	Yes (Human samples)	
Zeisel et al.	25700174	Health	Microglia	*Aif1 (Iba1), Cx3cr1*	Defining signature	No	
Zeisel et al.	25700174	Health	pvMΦ	*Aif1 (Iba-1), Cx3CR1, Mrc1 (CD206), Lyve1, Lyl1, Spic*	Defining signature	No	
Goldmann et al.	27135602	Health	pvMΦ	*Aif1 (Iba-1), Cx3CR1, Csf1r, CD45 (Ptprc)high, Mrc1, CD36*	Defining signature	No	
Goldmann et al.	27135602	Health	Microglia	*Aif1 (Iba-1), Cx3CR1, Csf1r, CD45low, P2ry12*	Defining signature	No	
Jordao et al.	30679343	Health	Microglia	*P2ry12, Tmem119, Sparc, Olfml3, Sall1*	Defining signature	No	
Jordao et al.	30679343	Health	BAMs/CAMs	*Mrc1, Pf4, Ms4a7, Cbr2*	Defining signature	No	
Jordao et al.	30679343	Health	mMΦ	*Mrc1, Pf4,Ms4a7, Stab1, Cbr2, Cd163, Fcrl, Siglec1*	Defining signature	No	
Van Hove et al.	31061494	Health	BAMs/CAMs	*Apoe, Ms4a7, Ms4a6c, Lyz2, Tgfbi*	Defining signature	No	
Li et al.	30606613	Health	Microglia	*Tmem119, P2ry12*	Defining signature	No	
Mrdjen et al.	29426702	Aging	Microglia	*CD11c, CD14* (phagocytosis markers), *CD44, CD86, PD-L1*	Up	No	
Mrdjen et al.	29426702	Aging	Microglia	*CX3CR1, MerTK, and Siglec-H* (core microglia genes)	Down	No	
Hammond et al.	30471926	Aging	Microglia	*OA2: Lgals3, Cst7, Ccl3, Ccl4, Il1b* (pro-inflammatory) *2) OA3: Ifitm3, Trp4, Oasl2* (IFN-response genes)	Up	No	
Keren-Shaul et al.	28602351	Alzheimer	Microglia (DAM)	*Apoe, Ctsd, Lpl, Tyrobp, Trem2, CD11c (Itgax)*	Up	No	
Keren-Shaul et al.	28602351	Alzheimer	Microglia (DAM)	*P2ry12/P2ry13, Cx3cr1, Tmem119* (core microglia genes)	Down	No	
Mathys et al.	29020624	Alzheimer	Microglia (late-response)	*Apoe, Axl, Lgals3bp + H2-Ab1, H2-D1, CD74* (antigen presentation-related genes)	Up	No	
Mathys et al.	29020624	Alzheimer	Microglia	*Cx3cR1, P2ry12, TMEM119* (core microglia genes)	Down	No	
Mrdjen et al.	29426702	Alzheimer	Microglia	*CD11c, CD14* (phagocytosis markers), *CD44, CD86, PD-L1*	Up	No	
Mrdjen et al.	29426702	Alzheimer	Microglia	*CX3CR1, MerTK, and Siglec-H* (core microglia genes)	Down	No	
Habib et al.	32341542	Alzheimer	Microglia	*Apoe, Ctsd, Ctsb, Ctsl*	Up	No	
Mathys et al.	31042697	Alzheimer	Microglia (DAM)	*Apoe, Trem2, CD74, Hla-drb1/5*	Up	Yes	
Olah et al.	33257666	Alzheimer	Microglia	*CD74, ISG15, CD83*	Up	Yes	Several microglia clusters, each one characterized (and validated) with these genes
Keren-Shaul et al.	28602351	Amyotrophic Lateral Sclerosis	Microglia	*Tmem119, P2ry12 (core microglia genes)*	Down	No	
Masuda et al.	30760929	Multiple sclerosis	Microglia	*TMEM119, P2RY12, P2RY13, CX3CR1, SLC2A5* (core microglia genes)	Down	Yes	
Masuda et al.	30760929	Multiple sclerosis	Microglia	*APOE, MAFB*	Up	Yes	
Mrdjen et al.	29426702	Multiple sclerosis (EAE)	Microglia	*CX3CR1, MerTK* and *Siglec-H* (core microglia genes)	Down	No	
Mrdjen et al.	29426702	Multiple sclerosis (EAE)	Microglia	*MHCII, Sca-1, PDL1, CD11c, CD44, CD86*	Up	No	
Mrdjen et al.	29426702	Multiple sclerosis (EAE)	Microglia	*CD14*	Down	No	
Jordao et al.	30679343	Multiple sclerosis (EAE)	Microglia	*P2ry12, Tmem119, Selplg, Siglech, Gpr34, Sall1* (core microglia genes)	Down	No	
Jordao et al.	30679343	Multiple sclerosis (EAE)	Microglia	*Ly86, CCl2, Cxcl10, Mki67*	Up	No	
Jordao et al.	30679343	Multiple sclerosis (EAE)	Microglia	*Sparc, Olfml3*	Up	No	
Jordao et al.	30679343	Multiple sclerosis (EAE)	Microglia	*1) damicroglia2: Cd74, Ctsb, Apoe 2) damicroglia3: Cxcl10, Tnf, Ccl4 3) damicroglia4: Ccl5, Ctss, Itm2b*	Up	No	3 clusters
Jordao et al.	30679343	Multiple sclerosis (EAE)	BMDM	*Mertk, Mrc1, Zbtb46, Cd209a*	Up	No	

(Continued)

TABLE 1 | Continued

Paper	PMID	Context	Cell type	Gene	Up/Down	Validated in patients	Notes
Ajami et al.	29507414	Multiple sclerosis (EAE)	CNS-resident myeloid cells (microglia, pvMΦ, mMΦ)	*MHCII, CD86, CD80, Axl, Tim4, CD274 (Pd-l1), CD195 (Ccr5), CD194 (Ccr4), CD11c (Itgax)*	Up	No	
Ajami et al.	29507414	Multiple sclerosis (EAE)	BMDM	*CD80, CD86, CD38, CD39, MerTK, Axl, CD206, TREM2, CD274*	Up	No	
Ajami et al.	29507414	Multiple sclerosis (EAE)	BMDM	pSTAT3	Up	No	
Ajami et al.	29507414	Multiple sclerosis (EAE)	BMDM	pCREB, *NFkB*	Down	No	
Ajami et al.	29507414	Multiple sclerosis (EAE)	BMDM	*CD49e (itga5)*	Up	No	
Hammond et al.	30471926	Multiple sclerosis (LPC-induced demyelination)	Microglia	*P2ry12, Cx3cr1 (core microglia genes)*	Down	No	
Hammond et al.	30471926	Multiple sclerosis (LPC-induced demyelination)	Microglia	*CxCl10, Ccl4, Ifi204, Apoe, Lpl, Spp1*	Up	No	
Rothhammer et al.	29769726	Multiple sclerosis (EAE)	Microglia	*AHR*	Up	Yes	Functional validation
Rothhammer et al.	29769726	Multiple sclerosis (EAE)	Microglia	*TGF-alpha*	Up	Yes	Functional validation
Rothhammer et al.	29769726	Multiple sclerosis (EAE)	Microglia	*VEGF-B*	Up	Yes	Functional validation
Clark et al.	33888612	Multiple sclerosis (EAE)	Microglia	*Semad4d*	Expressed in EAE	Yes	Functional validation
Clark et al.	33888612	Multiple sclerosis (EAE)	Microglia	*Ephb3*	Expressed in EAE	Yes	Functional validation
Friebel et al.	32470397	Glioma	Microglia and BMDM	*CD64, CD11c, HLA-DR, CD14*	Up	Yes	
Friebel et al.	32470397	Glioma	BMDM	*CD45RA, CD141, Icam*	Up	Yes	
Friebel et al.	32470397	Glioma	BMDM	*CD38, PD-L1, PD-L2*	Up	Yes	
Darmanis et al.	29091775	Glioma	Microglia	*CCL3, CCL4, CCL2,TNF (*Cks). *IL1A/B, IL6-R* (pro-inflammatory)	Up	Yes	
Darmanis et al.	29091775	Glioma	BMDM	*VEGFA, VEGFB* (angiogenesis), *IL1RN, TGFBi* (anti-inflammatory)	Up	Yes	
Ochocka et al.	33809675	Glioma	Microglia and BMDM	*H2-Aa, H2-Ab1, H2-D1, H2K1(MHCII), Ifitm3*	Up	No	
Ochocka et al.	33809675	Glioma	Microglia	*Ccl3, Ccl4, Ccl12*	Up	No	
Ochocka et al.	33809675	Glioma	BMDM	*Cd274, il1rn, il18b*,	Up	No	
Sankowski et al.	31740814	Glioma	Microglia	*CX3CR1, CSF1R*	Down	Yes	
Sankowski et al.	31740814	Glioma	Microglia	*CD163, APOE, SPP1, TREM2 LPL, IFI27, IFITM3, HIF1A, VEGFA*	Up	Yes	
Friebel et al.	32470397	Brain Metastasis	CNS resident (microglia) and BMDM	*CD64, CD11c, HLA-DR, CD14*	Up	Yes	
Friebel et al.	32470397	Brain Metastasis	BMDM	*CD45RA, CD141, ICAM*	Up	Yes	
Friebel et al.	32470397	Brain Metastasis	BMDM	*CD38, PD-L1, PD-L2*	Up	Yes	
Guldner et al.	33113353	Brain Metastasis	CNS-myeloids (microglia+BAMs)	*S100a11, Lgals, Il1b*	Up	No	
Guldner et al.	33113353	Brain Metastasis	CNS-myeloids (microglia+BAMs)	*Cx3cr1, P2ry12, Hexb* (core microglia genes)	Down	No	
Guldner et al.	33113353	Brain Metastasis	CNS-myeloids (microglia+BAMs)	*Vsir, Cd274*	Up	No	

(Continued)

TABLE 1 | Continued

Paper	PMID	Context	Cell type	Gene	Up/Down	Validated in patients	Notes
Guldner et al.	33113353	Brain Metastasis	BMDM	*Tspo, Isg15, Ifitm2, Anxa2, Irf7* (inflammation),*Ifitm1, Il1b, S100a10, Lgals1*	Up	No	
Guldner et al.	33113353	Brain Metastasis	BMDM	*Hbb-bs, Serinc3, CD81, Klf2*	Down	No	
Korin et al.	28758994	Health	Brain infiltrated leukocytes	*CXCR1*	Up (compared with blood)	No	
Korin et al.	28758994	Health	Brain infiltrated leukocytes	*CD44*	Up (compared with blood)	No	
Korin et al.	28758994	Health	CD8+ T cells	*CD86*	Up (compared with blood)	No	
Golomb et al.	33264626	Ageing	CD4+/CD8+ T cells	T memory stemness (Tscm) signature: CD3+ *and Thy1+/Itga2+/Klrb1-* mRNA	Up (compared with young mice)	No	
Caruso et al.	33155039	Glioma	CD8+ T cells	*CRTAM*	Up	Patients data	
Friebel et al.	32470397	Brain Metastasis	CD8+ T cells	*CD38*	Up (compared with the cluster of low immune infiltrates and worse survival)	Patients data	
Friebel et al.	32470397	Brain Metastasis	CD8+ T cells	Co-stimulatory receptors: *Icos, CD27 and CD137*	Up (compared with the cluster of low immune infiltrates and worse survival)	Patients data	
Friebel et al.	32470397	Brain Metastasis	CD8+ T cells	Co-inhibitory receptors: *2B4, Tigit and Pd-1*	Up (compared with the cluster of low immune infiltrates and worse survival)	Patients data	
Friebel et al.	32470397	Brain Metastasis	CD8+ T cells	Effector function: *CD57* and *gzmB*	Up (compared with the cluster of low immune infiltrates and worse survival)	Patients data	
Friebel et al.	32470397	Brain Metastasis	CD8+ T cells	*Ki-67*	Up (compared with the cluster of low immune infiltrates and worse survival)	Patients data	
Boisvert et al.	29298427	Aging	Astrocytes	*Casp1*	Up	No	
Boisvert et al.	29298427	Aging	Astrocytes	*Casp12*	Up	No	
Boisvert et al.	29298427	Aging	Astrocytes	*Cxcl5*	Up	No	
Boisvert et al.	29298427	Aging	Astrocytes	*Tlr2*	Up	No	
Boisvert et al.	29298427	Aging	Astrocytes	*Tlr4*	Up	No	
Lau et al.	32989152	Alzheimer	Astrocytes	*ADGRV1*	Defining signature	Yes	
Lau et al.	32989152	Alzheimer	Astrocytes	*GPC5*	Defining signature	Yes	
Lau et al.	32989152	Alzheimer	Astrocytes	*RYR3*	Novel gene signature identifying astrocytes	Yes	
Lau et al.	32989152	Alzheimer	Astrocytes	*NRXN1*	Down	Yes	
Lau et al.	32989152	Alzheimer	Astrocytes	*NRXN3*	Down	Yes	
Leng et al.	33432193	Alzheimer	Astrocytes	*HSPB1*	Up	Yes	Expression validated in a mouse model of spinal cord injury

(Continued)

TABLE 1 | Continued

Paper	PMID	Context	Cell type	Gene	Up/Down	Validated in patients	Notes
Leng et al.	33432193	Alzheimer	Astrocytes	*TNC*	Up	Yes	Expression validated in a mouse model of spinal cord injury
Leng et al.	33432193	Alzheimer	Astrocytes	*HSP90AA1*	Up	Yes	Expression validated in a mouse model of spinal cord injury
Leng et al.	33432193	Alzheimer	Astrocytes	Glutamate/GABA-signalling associated genes	Down	Yes	Expression validated in a mouse model of spinal cord injury
Al-Dalahmah et al.	32070434	Huntington disease	Astrocytes	*MT-genes*	Up	Yes	
Al-Dalahmah et al.	32070434	Huntington disease	Astrocytes	Protoplasmic genes	Down	Yes	
Rothhammer et al.	29769726	Multiple sclerosis (EAE)	Astrocytes	*Ccl2*	Upregulated upon AHR deletion	No	Functional validation
Rothhammer et al.	29769726	Multiple sclerosis (EAE)	Astrocytes	*Il1b*	Upregulated upon AHR deletion	No	
Rothhammer et al.	29769726	Multiple sclerosis (EAE)	Astrocytes	*Nos2*	Upregulated upon AHR deletion	No	
Sanmarco et al.	33408417	Multiple sclerosis (EAE)	Astrocytes	*CD107a (Lamp1)*	Upregulated upon CNS inflammation	Yes	Functional validation
Sanmarco et al.	33408417	Multiple sclerosis (EAE)	Astrocytes	*Tnfsf10* (TRAIL death receptor ligand)	Upregulated upon CNS inflammation	Yes	Functional validation
Clark et al.	33888612	Multiple sclerosis (EAE)	Astrocytes	*PlexinB2*	Expressed in EAE	Yes	Functional validation
Clark et al.	33888612	Multiple sclerosis (EAE)	Astrocytes	*Efnb3*	Expressed in EAE	Yes	Functional validation
Heiland et al.	31186414	Glioblastoma	Reactive astrocytes	*CD274*	Up	Yes (human samples)	
Priego et al.	29921958	Brain Metastasis	Reactive astrocytes	STAT3 (phosphorilation)	Up	Yes	Functional validation
Ebert et al.	33082953	Glioblastoma	Pericytes	CD73 CD105	Up	Yes (human samples)	
Ebert et al.	33082953	Glioblastoma	Tumor associated endothelial cells	Fab	Up	Yes (human samples)	
Carlson et al.	33367832	Glioblastoma	Tumor associated endothelial cells	*Jcad, Spop* and *Ctnnb1* (in all clusters), clusters 2–5: *Malat1, Jun* and *Arhgap*, cluster 3: *Mgp, Stmn2, Sema3g* and *Gja4*, cluster 4: *Nr2f2, Vwf, Aldh1a1* and *Junb*, cluster 5: *CD74* and *Cxcl10*	Up	No	Validation in patient derived orthotopic xenograft
Carlson et al.	33367832	Glioblastoma	Tumor derived endothelial cells	*Pdpn* and *Flt4* Lymphatic endothelial cells: *Icam1, Dcn, Tgfbi and CD74*	Up	No	Validation in patient derived orthotopic xenograft

BAM, Barrier-associated macrophages; CAM, Central Nervous System (CNS)-associated macrophages; BMDM, Bone Marrow-Derived Macrophages; DAM, Disease-associated microglia; mMφ, meningeal macrophages; pvMφ, perivascular macrophages.

organismal aging correlates with the enrichment of specific lymphocytes populations within the brain (31).

Brain Tumors

Single-cell transcriptomics uncovered a gene signature in glioma composed by immune effector molecules and inhibitory feedback mechanisms (genes such as *Ifn-γ, Ctla-4, Pdcd1, IL-10, Tgf-β1 or Ido1*) that lead to the reprogramming of T cells subsets that become unable to target the cancer cells (32). A more specific dissection of the crosstalk between glioma cells and T cells in patients was achieved by applying single-cell Tumor-Host Interaction (scTHI) analysis of scRNA sequencing data. In particular, Caruso et al. found that the cross-talk between CD8+ T cells and tumor cells included components belonging to major histocompatibility complex Class I, chemokines, interleukins, IFN-γ and TNF. This study also described paracrine interactions with myeloid cells involving immune checkpoint genes, TNF family members and chemoattractant chemokine ligands, such as CXCR6 receptor on T cells and its ligand CXCL16 secreted by macrophages that are upregulated in glioma (7).

Cy-TOF of surgical resections have characterized the lymphocyte landscape in primary and secondary brain tumor entities (28).Compared to primary brain tumors, metastases favor T and B cell infiltration and T regulatory cells (T regs) present higher accumulation in brain metastasis and IDH1 *wt* gliomas. Moreover, CD8+ T cells present an increased expression of co-stimulatory and co-inhibitory receptors, the activation marker CD38 and effector and proliferation functions in metastases, while glioma samples show less activation (28). The activation/exhaustion phenotypic state of T cells in metastatic tumors could explain their favorable clinical response to immune checkpoint inhibitors compared to those of primary origin.

Recent papers shed light on the stromal and immune landscape in human multiple sclerosis and brain tumors, focusing on the analysis by scRNAseq and set enrichment analysis of cerebrospinal fluid (CSF) leukocytes (33), and CSF from patients (34, 35). Specifically, Rubio-Perez et al. have described an inflammatory status independently of the primary tumor source of the metastasis and a cluster characterized by active proliferation of T cells. Noteworthy, identical T cell receptor sequences between the CSF and the metastatic lesions were detected in 66.7% of patients, indicating a partial connection of the immune profiles from both compartments (34). This work suggests the potential value of CSF to characterize the immune microenvironment and T cells subclonal evolution in brain metastasis to monitor patients during tumor progression or treatment.

ASTROCYTES DIVERSITY WITHIN THE BRAIN MICROENVIRONMENT

Health and Aging

Different studies have shown that astrocytic transcriptome heterogeneity encompasses well-recognized astrocyte functions and happens both between and within brain regions (9, 36). In aged brains, cerebellar astrocytes were characterized by the upregulation of inflammatory factors that can damage synapses (*caspase-1* and *-12*, Cxcl5) and key inflammasome receptors *Tlr2* and *4*. This demonstrates that dependency of the glial cell type correlates with more severe or less synaptic dysfunction (37).

Brain Disorders

Astrocytes can be rapidly activated in response to various insults, by a process known as "reactive astrogliosis" which aims to limit the damage that occurs locally. Three states of reactive astrocytes (RAs) can be found in HD, defined by different levels of GFAP, metallothionein (MT) genes and quiescent protoplasmic genes. The upregulation of MTs by RAs could be a protective response to combat oxidative stress, which is characteristic of the HD brain (38). Interestingly, astrocytes in AD were found to express a unique and novel signature (*Adgrv1*, *Gpc5* and *Ryr3 genes*). Down-regulated genes in AD-astrocytes are associated mainly with synaptic signaling (i.e. *NRXN1* and *NRXN3*) and glutamate secretion (39). An independent study, showed that high *GFAP* astrocytes from AD, which lose homeostatic functions, also express pan-astrocytes and reactive markers such as *CD44*, *HSPB1*, *TNC* and *HSP90AA1* (40). Remarkably, some recent studies emphasize the gut-brain axis as an important player during the course of CNS disease that fine-tunes inflammation and neurodegeneration. In EAE, the deletion of aryl hydrocarbon receptor (AHR) in microglia, upregulated the expression of genes in astrocytes associated with inflammation and neurodegeneration (*Ccl2, Il1b* and *Nos2*) (41). A later study described a subset of LAMP1+ astrocytes limiting inflammation, driven by IFNγ produced by meningeal natural killer cells, which is modulated by the commensal flora in mice (42). Notably, Clark et al. use the RABID-seq technology to identify pro-inflammatory astrocytes connected to T cells that exhibited high TNFα signaling *via* NF-κB (8).

Brain Tumors

In malignant brain tumors, knowledge related to astrocyte function and crosstalk to other components of the environment requires further investigation. Tumor-occupying astrocytes analyzed in three glioblastoma patients revealed similarities to highly proliferative astrocyte precursor cells from fetal brains (43). JAK/STAT pathway activation and *CD274* expression was present in RAs, in a set of *de-novo* and recurrent glioblastoma specimens, inducing immunological cold tumor environment (44). Notably, in the context of brain metastasis, a pro-metastatic program driven by STAT3 signaling in a subpopulation of RAs surrounding metastatic lesions promotes an immunosuppressive microenvironment, being an interesting target (45).

HETEROGENEITY OF ENDOTHELIAL CELLS WITHIN THE BRAIN MICROENVIRONMENT

Health

The lack of a molecular understanding of the constituent cell types of the brain vasculature could be solved by using single cell

approaches. In murine models, single-cell transcriptomics distinguished different molecular signatures and phenotypic changes in endothelial and mural cells (46). Moreover, brain-specific endothelial transcripts have been identified, mainly cell surface transporters and intracellular enzymes (47).

Brain Tumors

In a glioblastoma mouse model, single cell sequencing identified three separated clusters of brain endothelium with a distinct molecular signature, differentiating tumor associated vessels and tumor derived endothelial cells (detailed in **Table 1**) (48). Moreover, in human samples, heterogeneity was reported within pericytes and endothelial cells (49). These pioneer studies describe molecular inter and intra-heterogeneity within the primary brain tumor vasculature.

In human brain metastasis patients, clusters of endothelial cells have been identified using the marker CLDN5+, being in higher proportion in melanoma than in breast cancer brain metastasis (50).

THERAPEUTIC STRATEGIES EXPLOITING THE HETEROGENEITY WITHIN THE BRAIN MICROENVIRONMENT

Uncovering functional and molecular diversity of glial and brain immune cells in preclinical models and patients affected by disease has a remarkable translational potential, including brain tumors. However, an important effort in the field is needed to validate the contribution of disease-associated alterations and cellular cross-talk between the various reactive states described.

Brain Disorders

Ajami et al. proposed the surface marker CD49e found in peripheral monocytes, to be a therapeutic target in EAE since the treatment with anti-CD49e antibody significantly reduced disease severity (20). Interestingly, in the treatment of brain neurodegeneration, targeted immunotherapies may be used against B cell clusters responsible for disease-specific antibody production (51). Mapping the cross-talk between identified cell populations that shape the local microenvironment in brain disorders is key to uncover potential targets (8). Clark et al. have shown that in a EAE model, inactivating the interaction between *Sema4d-Plxnb2 or Ephb3-Efnb3* in microglia-astrocytes, respectively, ameliorates the disease (8). Interestingly, as a proof of concept in traumatic brain injury models (mTBI), Arneson et al. focused on the thyroid hormone pathway based on its differential expression across cell types in mTBI. Injecting T4 immediately after the damage improved cognitive deficits in a mouse model of concussive injury (52). In addition, specific gene expression programs related to endosome, plasma membrane, mitochondrion and autophagy have been shown to be relevant for the progression of neurodegeneration in humans, especially when enriched in neurons and microglia (53, 54). This finding emphasizes the emerging vulnerability of dysfunctional bioenergetics for brain disorders.

Brain Tumors

Understanding the diversity within the microenvironment of clinically-relevant experimental models of brain tumors will help to identify altered pathways not essential for brain homeostasis. To illustrate this point, using single cell transcriptomics in the DNp53-PDGFB glioma model, Weng et al. have been able to identify the RNA-binding protein Zfp36l1 to be necessary for malignant oligodendrocyte-astrocyte lineage transition and glioma growth (55). In human primary and secondary tumors, candidate immunosuppressive molecules could be used to potentiate immunotherapy by designing customized strategies for brain tumors. For instance, by using single-cell gene expression Caruso et al. found TLR2 to be exclusively upregulated in glioma-associated microglia and CRTAM receptor in CD8+ T cells, confirming previous studies (56, 57) that have proposed these molecules as targets for adjuvant immunotherapies in glioma. Additionally, the same scRNAseq study defined ligand-receptor interactions between the microenvironment and cancer cells such as HBEGF-EGFR, MIF-CD74 and CD11B/CD18-CD90, that could be potential targets given their role in immunosuppression. FAB, identified mainly in endothelial cells and pericytes by scRNAseq, has been proposed as a potential antigen for (CAR)-T cells therapy to target tumor cells and tumor associated vessels in glioblastoma (49).

Intrinsic properties of cancer cells could indirectly influence response to therapy by modulating the brain microenvironment. Whether the mutational status of cancer cells could influence the brain microenvironment in secondary brain tumors, as it does in primary brain tumors (58–62), is still unexplored. However changes in the immune infiltrate have been reported depending on the primary origin of brain metastases. For example, melanoma brain metastasis present higher frequencies of T cells than carcinoma brain metastasis, except for Tregs (28, 61). Notably, tumor location influences microenvironmental landscapes (63, 64). Meningiomas have higher TAM infiltration and less presence of T regs than gliomas (64), while in secondary brain tumors, scRNAseq revealed a distinct immune-suppressed T-cell microenvironment in leptomeningeal metastasis compared with brain metastasis derived from melanoma (63).

Furthermore, a deep knowledge of immune diversity induced by the presence of tumor cells is critical to predict immunotherapeutic outcomes since it might help to explain the different response to checkpoint inhibitors reported in primary and secondary brain tumors. For instance, Close et al. suggest that the presence of immune signatures with anti-tumor effector functions (i.e. granzyme B or IFN-γ) in a subset of patients with GBM will predispose to better benefit from combination immunotherapies (32). In addition, immune evasion signatures have been defined and novel targets, such as CDK4/6, have been proposed to overcome the resistance to immune checkpoint blockade in cancer metastatic to the brain (65, 66). scRNAseq of a melanoma brain metastasis patient found *PDCD4* to be expressed on CD8 Tcells, NK cells, B cells and mast cells, associated with cytotoxicity (Gzm expression), suggesting a role to potentiate immune response (67). Other very interesting tools are predictive studies of brain metastatic tumors to classify

patients into potential good or bad responders to immunotherapy. This approach is able to determine specific molecules as targets for adjuvant immunotherapies according to the immune profile, which allows to narrow down candidates to specific biomarkers. For instance, the expression of CD74 in the microenvironment of brain metastases fulfilled the *in silico* criteria (68). Uncovering functional and dysfunctional CD8+ T cell activation states in brain tumors is key to establish more accurate immune signatures to stratify patients. Transposase-accessible chromatin sequencing (ATAC-seq) and RNA-seq could be applied to preclinical models of brain metastasis and human data to achieve this goal, as it has been done for hepatocarcinoma and melanoma (69). Other important aspect to consider is the reprogramming of the brain immune landscape by therapy. i.e. TMZ in primary tumors (60) and WBRT in brain metastasis (70).

Finally, due to the limited availability of brain tissue from patients, profiling the mutational landscape and evolutionary patterns of tumor and microenvironment using non-invasive biopsies, could be key to establish predictive biomarkers of therapeutic response. In this sense, pioneer studies using CSF as a relative non-invasive surrogate to be processed by single-cell techniques could help to define the heterogeneity of the immune microenvironment and its link to clinically meaningful correlations (34, 35). Analysis of this liquid biopsy in patients with positive and negative local responses to immunotherapy has started to be explored (61). Moreover, considering the important role of meningeal lymphatics in regulating brain tumor immunity, other plausible source of cancer-derived material is the regional lymphatic drainage (71), although in-depth analysis is needed to characterize the immune landscape in this liquid biopsy.

DISCUSSION

In conclusion, the data reviewed lays a firm foundation for considering vulnerabilities generated in the brain metastasis microenvironment relevant to predict and improve responses to immune based therapies that are effective only in a limited percentage of patients, especially when asymptomatic (72, 73). Overall, we consider a key aspect to embrace the emerging complexity and to dissect functionally relevant hubs within the local microenvironment, providing the avenues to transform the clinical management of brain metastasis patients within the years to come.

DATA AVAILABILITY STATEMENT

The original contributions presented in the study are included in the article/supplementary material. Further inquiries can be directed to the corresponding author.

AUTHOR CONTRIBUTIONS

LÁ-E, AP-A, MV, and NP conceptualized and wrote the manuscript. All authors contributed to the article and approved the submitted version.

FUNDING

Research in the Brain Metastasis Group is supported by MINECO (SAF2017-89643-R) (MV), Fundació La Marató de TV3 (141) (MV), Fundación Ramón Areces (CIVP19S8163) (MV), Worldwide Cancer Research (19–0177) (MV), H2020-FETOPEN (828972) (MV), Cancer Research Institute (Clinic and Laboratory Integration Program CRI Award 2018 (54545) (MV), AECC (Coordinated Translational Groups 2017 (GCTRA16015SEOA) (MV), LAB AECC 2019 (LABAE19002VALI) (MV), ERC CoG (864759) (MV), La Caixa INPhINIT Fellowship (LCF/BQ/DI19/11730044) (AP-A), MINECO-Severo Ochoa PhD Fellowship (BES-2017-081995) (LA-E), AECC Postdoctoral Fellowship (POSTD19016PRIE) (NP). MV is an EMBO YIP investigator (4053).

ACKNOWLEDGMENTS

The authors want to thank the members of the Brain Metastasis Group for their comments on the manuscript.

REFERENCES

1. Boire A, Brastianos PK, Garzia L, Valiente M. Brain Metastasis. *Nat Rev Cancer* (2020) 20:4–11. doi: 10.1038/s41568-019-0220-y
2. Zeisel A, Muñoz-Manchado AB, Codeluppi S, Lönnerberg P, La Manno G, Juréus A, et al. Brain Structure. Cell Types in the Mouse Cortex and Hippocampus Revealed by Single-Cell RNA-Seq. *Science* (2015) 347:1138–42. doi: 10.1126/science.aaa1934
3. Llorens-Bobadilla E, Zhao S, Baser A, Saiz-Castro G, Zwadlo K, Martin-Villalba A. Single-Cell Transcriptomics Reveals a Population of Dormant Neural Stem Cells That Become Activated Upon Brain Injury. *Cell Stem Cell* (2015) 17:329–40. doi: 10.1016/j.stem.2015.07.002
4. Prasad JA, Balwani AH, Johnson EC, Miano JD, Sampathkumar V, De Andrade V, et al. A Three-Dimensional Thalamocortical Dataset for Characterizing Brain Heterogeneity. *Sci Data* (2020) 7:358. doi: 10.1038/s41597-020-00692-y
5. Lake BB, Chen S, Sos BC, Fan J, Kaeser GE, Yung YC, et al. Integrative Single-Cell Analysis of Transcriptional and Epigenetic States in the Human Adult Brain. *Nat Biotechnol* (2018) 36:70–80. doi: 10.1038/nbt.4038
6. Pasqual G, Chudnovskiy A, Tas JMJ, Agudelo M, Schweitzer LD, Cui A, et al. Monitoring T Cell-Dendritic Cell Interactions *In Vivo* by Intercellular Enzymatic Labelling. *Nature* (2018) 553:496–500. doi: 10.1038/nature25442
7. Caruso FP, Garofano L, D'Angelo F, Yu K, Tang F, Yuan J, et al. A Map of Tumor-Host Interactions in Glioma at Single-Cell Resolution. *Gigascience* (2020) 9(10). doi: 10.1093/gigascience/giaa109
8. Clark IC, Gutiérrez-Vázquez C, Wheeler MA, Li Z, Rothhammer V, Linnerbauer M, et al. Barcoded Viral Tracing of Single-Cell Interactions in Central Nervous System Inflammation. *Science* (2021) 372(6540). doi: 10.1126/science.abf1230
9. Batiuk MY, Martirosyan A, Wahis J, de Vin F, Marneffe C, Kusserow C, et al. Identification of Region-Specific Astrocyte Subtypes at Single Cell Resolution. *Nat Commun* (2020) 11:1220. doi: 10.1038/s41467-019-14198-8

10. Goldmann T, Wieghofer P, Jordão MJC, Prutek F, Hagemeyer N, Frenzel K, et al. Origin, Fate and Dynamics of Macrophages at Central Nervous System Interfaces. *Nat Immunol* (2016) 17:797–805. doi: 10.1038/ni.3423
11. Mrdjen D, Pavlovic A, Hartmann FJ, Schreiner B, Utz SG, Leung BP, et al. High-Dimensional Single-Cell Mapping of Central Nervous System Immune Cells Reveals Distinct Myeloid Subsets in Health, Aging, and Disease. *Immunity* (2018) 48:380–95.e6. doi: 10.1016/j.immuni.2018.01.011
12. Jordão MJC, Sankowski R, Brendecke SM, Sagar, Locatelli G, Tai Y-H, et al. Single-Cell Profiling Identifies Myeloid Cell Subsets With Distinct Fates During Neuroinflammation. *Science* (2019) 363(6425). doi: 10.1126/science.aat7554
13. Van Hove H, Martens L, Scheyltjens I, De Vlaminck K, Pombo Antunes AR, De Prijck S, et al. A Single-Cell Atlas of Mouse Brain Macrophages Reveals Unique Transcriptional Identities Shaped by Ontogeny and Tissue Environment. *Nat Neurosci* (2019) 22:1021–35. doi: 10.1038/s41593-019-0393-4
14. Hammond TR, Dufort C, Dissing-Olesen L, Giera S, Young A, Wysoker A, et al. Single-Cell RNA Sequencing of Microglia Throughout the Mouse Lifespan and in the Injured Brain Reveals Complex Cell-State Changes. *Immunity* (2019) 50:253–71.e6. doi: 10.1016/j.immuni.2018.11.004
15. Masuda T, Sankowski R, Staszewski O, Böttcher C, Amann L, Sagar, et al. Spatial and Temporal Heterogeneity of Mouse and Human Microglia at Single-Cell Resolution. *Nature* (2019) 566:388–92. doi: 10.1038/s41586-019-0924-x
16. Li Q, Cheng Z, Zhou L, Darmanis S, Neff NF, Okamoto J, et al. Developmental Heterogeneity of Microglia and Brain Myeloid Cells Revealed by Deep Single-Cell RNA Sequencing. *Neuron* (2019) 101:207–23.e10. doi: 10.1016/j.neuron.2018.12.006
17. Keren-Shaul H, Spinrad A, Weiner A, Matcovitch-Natan O, Dvir-Szternfeld R, Ulland TK, et al. A Unique Microglia Type Associated With Restricting Development of Alzheimer's Disease. *Cell* (2017) 169:1276–90.e17. doi: 10.1016/j.cell.2017.05.018
18. Mathys H, Davila-Velderrain J, Peng Z, Gao F, Mohammadi S, Young JZ, et al. Single-Cell Transcriptomic Analysis of Alzheimer's Disease. *Nature* (2019) 570:332–7. doi: 10.1038/s41586-019-1195-2
19. Krasemann S, Madore C, Cialic R, Baufeld C, Calcagno N, El Fatimy R, et al. The TREM2-APOE Pathway Drives the Transcriptional Phenotype of Dysfunctional Microglia in Neurodegenerative Diseases. *Immunity* (2017) 47:566–81.e9. doi: 10.1016/j.immuni.2017.08.008
20. Ajami B, Samusik N, Wieghofer P, Ho PP, Crotti A, Bjornson Z, et al. Single-Cell Mass Cytometry Reveals Distinct Populations of Brain Myeloid Cells in Mouse Neuroinflammation and Neurodegeneration Models. *Nat Neurosci* (2018) 21:541–51. doi: 10.1038/s41593-018-0100-x
21. Gosselin D, Skola D, Coufal NG, Holtman IR, Schlachetzki JCM, Sajti E, et al. An Environment-Dependent Transcriptional Network Specifies Human Microglia Identity. *Science* (2017) 356(6344). doi: 10.1126/science.aal3222
22. Böttcher C, Schlickeiser S, Sneeboer MAM, Kunkel D, Knop A, Paza E, et al. Human Microglia Regional Heterogeneity and Phenotypes Determined by Multiplexed Single-Cell Mass Cytometry. *Nat Neurosci* (2019) 22:78–90. doi: 10.1038/s41593-018-0290-2
23. Sankowski R, Böttcher C, Masuda T, Geirsdottir L, Sagar, Sindram E, et al. Mapping Microglia States in the Human Brain Through the Integration of High-Dimensional Techniques. *Nat Neurosci* (2019) 22:2098–110. doi: 10.1038/s41593-019-0532-y
24. Yu K, Hu Y, Wu F, Guo Q, Qian Z, Hu W, et al. Surveying Brain Tumor Heterogeneity by Single-Cell RNA Sequencing of Multi-Sector Biopsies. *Natl Sci Rev* (2020) 7(8):1306–18. doi: 10.1093/nsr/nwaa099
25. Ochocka N, Segit P, Walentynowicz KA, Wojnicki K, Cyranowski S, Swatler J, et al. Single-Cell RNA Sequencing Reveals Functional Heterogeneity of Glioma-Associated Brain Macrophages. *Nat Commun* (2021) 12:1151. doi: 10.1038/s41467-021-21407-w
26. Müller S, Kohanbash G, Liu SJ, Alvarado B, Carrera D, Bhaduri A, et al. Single-Cell Profiling of Human Gliomas Reveals Macrophage Ontogeny as a Basis for Regional Differences in Macrophage Activation in the Tumor Microenvironment. *Genome Biol* (2017) 18:234. doi: 10.1186/s13059-017-1362-4
27. Darmanis S, Sloan SA, Croote D, Mignardi M, Chernikova S, Samghababi P, et al. Single-Cell RNA-Seq Analysis of Infiltrating Neoplastic Cells at the Migrating Front of Human Glioblastoma. *Cell Rep* (2017) 21:1399–410. doi: 10.1016/j.celrep.2017.10.030
28. Friebel E, Kapolou K, Unger S, Núñez NG, Utz S, Rushing EJ, et al. Single-Cell Mapping of Human Brain Cancer Reveals Tumor-Specific Instruction of Tissue-Invading Leukocytes. *Cell* (2020) 181:1626–42.e20. doi: 10.1016/j.cell.2020.04.055
29. Guldner IH, Wang Q, Yang L, Golomb SM, Zhao Z, Lopez JA, et al. CNS-Native Myeloid Cells Drive Immune Suppression in the Brain Metastatic Niche Through Cxcl10. *Cell* (2020) 183:1234–48.e25. doi: 10.1016/j.cell.2020.09.064
30. Korin B, Ben-Shaanan TL, Schiller M, Dubovik T, Azulay-Debby H, Boshnak NT, et al. High-Dimensional, Single-Cell Characterization of the Brain's Immune Compartment. *Nat Neurosci* (2017) 20:1300–9. doi: 10.1038/nn.4610
31. Golomb SM, Guldner IH, Zhao A, Wang Q, Palakurthi B, Aleksandrovic EA, et al. Multi-Modal Single-Cell Analysis Reveals Brain Immune Landscape Plasticity During Aging and Gut Microbiota Dysbiosis. *Cell Rep* (2020) 33:108438. doi: 10.1016/j.celrep.2020.108438
32. Close HJ, Stead LF, Nsengimana J, Reilly KA, Droop A, Wurdak H, et al. Expression Profiling of Single Cells and Patient Cohorts Identifies Multiple Immunosuppressive Pathways and an Altered NK Cell Phenotype in Glioblastoma. *Clin Exp Immunol* (2020) 200:33–44. doi: 10.1111/cei.13403
33. Schafflick D, Xu CA, Hartlehnert M, Cole M, Schulte-Mecklenbeck A, Lautwein T, et al. Integrated Single Cell Analysis of Blood and Cerebrospinal Fluid Leukocytes in Multiple Sclerosis. *Nat Commun* (2020) 11:247. doi: 10.1038/s41467-019-14118-w
34. Rubio-Perez C, Planas-Rigol E, Trincado JL, Bonfill-Teixidor E, Arias A, Marchese D, et al. Immune Cell Profiling of the Cerebrospinal Fluid Enables the Characterization of the Brain Metastasis Microenvironment. *Nat Commun* (2021) 12:1503. doi: 10.1038/s41467-021-21789-x
35. Miller AM, Shah RH, Pentsova EI, Pourmaleki M, Briggs S, Distefano N, et al. Tracking Tumour Evolution in Glioma Through Liquid Biopsies of Cerebrospinal Fluid. *Nature* (2019) 565:654–8. doi: 10.1038/s41586-019-0882-3
36. Bayraktar OA, Bartels T, Holmqvist S, Kleshchevnikov V, Martirosyan A, Polioudakis D, et al. Astrocyte Layers in the Mammalian Cerebral Cortex Revealed by a Single-Cell *in Situ* Transcriptomic Map. *Nat Neurosci* (2020) 23:500–9. doi: 10.1038/s41593-020-0602-1
37. Boisvert MM, Erikson GA, Shokhirev MN, Allen NJ. The Aging Astrocyte Transcriptome From Multiple Regions of the Mouse Brain. *Cell Rep* (2018) 22:269–85. doi: 10.1016/j.celrep.2017.12.039
38. Al-Dalahmah O, Sosunov AA, Shaik A, Ofori K, Liu Y, Vonsattel JP, et al. Single-Nucleus RNA-Seq Identifies Huntington Disease Astrocyte States. *Acta Neuropathol Commun* (2020) 8:19. doi: 10.1186/s40478-020-0880-6
39. Lau S-F, Cao H, Fu AKY, Ip NY. Single-Nucleus Transcriptome Analysis Reveals Dysregulation of Angiogenic Endothelial Cells and Neuroprotective Glia in Alzheimer's Disease. *Proc Natl Acad Sci U S A* (2020) 117:25800–9. doi: 10.1073/pnas.2008762117
40. Leng K, Li E, Eser R, Piergies A, Sit R, Tan M, et al. Molecular Characterization of Selectively Vulnerable Neurons in Alzheimer's Disease. *Nat Neurosci* (2021) 24:276–87. doi: 10.1038/s41593-020-00764-7
41. Rothhammer V, Borucki DM, Tjon EC, Takenaka MC, Chao C-C, Ardura-Fabregat A, et al. Microglial Control of Astrocytes in Response to Microbial Metabolites. *Nature* (2018) 557:724–8. doi: 10.1038/s41586-018-0119-x
42. Sanmarco LM, Wheeler MA, Gutiérrez-Vázquez C, Polonio CM, Linnerbauer M, Pinho-Ribeiro FA, et al. Gut-Licensed Ifnγ+ NK Cells Drive LAMP1 +TRAIL+ Anti-Inflammatory Astrocytes. *Nature* (2021) 590:473–9. doi: 10.1038/s41586-020-03116-4
43. Zhang Y, Sloan SA, Clarke LE, Caneda C, Plaza CA, Blumenthal PD, et al. Purification and Characterization of Progenitor and Mature Human Astrocytes Reveals Transcriptional and Functional Differences With Mouse. *Neuron* (2016) 89:37–53. doi: 10.1016/j.neuron.2015.11.013
44. Henrik Heiland D, Ravi VM, Behringer SP, Frenking JH, Wurm J, Joseph K, et al. Tumor-Associated Reactive Astrocytes Aid the Evolution of Immunosuppressive Environment in Glioblastoma. *Nat Commun* (2019) 10:2541. doi: 10.1038/s41467-019-10493-6
45. Priego N, Zhu L, Monteiro C, Mulders M, Wasilewski D, Bindeman W, et al. STAT3 Labels a Subpopulation of Reactive Astrocytes Required for Brain Metastasis. *Nat Med* (2018) 24:1024–35. doi: 10.1038/s41591-018-0044-4

46. Vanlandewijck M, He L, Mäe MA, Andrae J, Ando K, Del Gaudio F, et al. A Molecular Atlas of Cell Types and Zonation in the Brain Vasculature. *Nature* (2018) 554:475–80. doi: 10.1038/nature25739
47. Seaman S, Stevens J, Yang MY, Logsdon D, Graff-Cherry C, St Croix B. Genes That Distinguish Physiological and Pathological Angiogenesis. *Cancer Cell* (2007) 11:539–54. doi: 10.1016/j.ccr.2007.04.017
48. Carlson JC, Cantu Gutierrez M, Lozzi B, Huang-Hobbs E, Turner WD, Tepe B, et al. Identification of Diverse Tumor Endothelial Cell Populations in Malignant Glioma. *Neuro Oncol* (2021) 23:932–44. doi: 10.1093/neuonc/noaa297
49. Ebert LM, Yu W, Gargett T, Toubia J, Kollis PM, Tea MN, et al. Endothelial, Pericyte and Tumor Cell Expression in Glioblastoma Identifies Fibroblast Activation Protein (FAP) as an Excellent Target for Immunotherapy. *Clin Transl Immunol* (2020) 9:e1191. doi: 10.1002/cti2.1191
50. Dankner M, Caron M, Al-Saadi T, Yu W, Ouellet V, Ezzeddine R, et al. Invasive Growth Associated With Cold-Inducible RNA-Binding Protein Expression Drives Recurrence of Surgically Resected Brain Metastases. *Neuro Oncol* (2021) noab002. doi: 10.1093/neuonc/noab002
51. Zou A, Ramanathan S, Dale RC, Brilot F. Single-Cell Approaches to Investigate B Cells and Antibodies in Autoimmune Neurological Disorders. *Cell Mol Immunol* (2021) 18:294–306. doi: 10.1038/s41423-020-0510-z
52. Arneson D, Zhang G, Ying Z, Zhuang Y, Byun HR, Ahn IS, et al. Single Cell Molecular Alterations Reveal Target Cells and Pathways of Concussive Brain Injury. *Nat Commun* (2018) 9:3894. doi: 10.1038/s41467-018-06222-0
53. Capurro A, Bodea L-G, Schaefer P, Luthi-Carter R, Perreau VM. Computational Deconvolution of Genome Wide Expression Data From Parkinson's and Huntington's Disease Brain Tissues Using Population-Specific Expression Analysis. *Front Neurosci* (2014) 8:441. doi: 10.3389/fnins.2014.00441
54. Skene NG, Grant SGN. Identification of Vulnerable Cell Types in Major Brain Disorders Using Single Cell Transcriptomes and Expression Weighted Cell Type Enrichment. *Front Neurosci* (2016) 10:16. doi: 10.3389/fnins.2016.00016
55. Weng Q, Wang J, Wang J, He D, Cheng Z, Zhang F, et al. Single-Cell Transcriptomics Uncovers Glial Progenitor Diversity and Cell Fate Determinants During Development and Gliomagenesis. *Cell Stem Cell* (2019) 24:707–23.e8. doi: 10.1016/j.stem.2019.03.006
56. Hu F, Dzaye OD, Hahn A, Yu Y, Scavetta RJ, Dittmar G, et al. Glioma-Derived Versican Promotes Tumor Expansion via Glioma-Associated Microglial/Macrophages Toll-Like Receptor 2 Signaling. *Neuro Oncol* (2015) 17:200–10. doi: 10.1093/neuonc/nou324
57. Boles KS, Barchet W, Diacovo T, Cella M, Colonna M. The Tumor Suppressor TSLC1/NECL-2 Triggers NK-Cell and CD8+ T-Cell Responses Through the Cell-Surface Receptor CRTAM. *Blood* (2005) 106:779–86. doi: 10.1182/blood-2005-02-0817
58. Gargini R, Segura-Collar B, Herránz B, García-Escudero V, Romero-Bravo A, Núñez FJ, et al. The IDH-TAU-EGFR Triad Defines the Neovascular Landscape of Diffuse Gliomas. *Sci Transl Med* (2020) 12(527). doi: 10.1126/scitranslmed.aax1501
59. Miroshnikova YA, Mouw JK, Barnes JM, Pickup MW, Lakins JN, Kim Y, et al. Tissue Mechanics Promote IDH1-Dependent HIF1α-Tenascin C Feedback to Regulate Glioblastoma Aggression. *Nat Cell Biol* (2016) 18:1336–45. doi: 10.1038/ncb3429
60. Kohanbash G, Carrera DA, Shrivastav S, Ahn BJ, Jahan N, Mazor T, et al. Isocitrate Dehydrogenase Mutations Suppress STAT1 and CD8+ T Cell Accumulation in Gliomas. *J Clin Invest* (2017) 127:1425–37. doi: 10.1172/JCI90644
61. Klemm F, Maas RR, Bowman RL, Kornete M, Soukup K, Nassiri S, et al. Interrogation of the Microenvironmental Landscape in Brain Tumors Reveals Disease-Specific Alterations of Immune Cells. *Cell* (2020) 181:1643–60.e17. doi: 10.1016/j.cell.2020.05.007
62. Wang Q, Hu B, Hu X, Kim H, Squatrito M, Scarpace L, et al. Tumor Evolution of Glioma-Intrinsic Gene Expression Subtypes Associates With Immunological Changes in the Microenvironment. *Cancer Cell* (2017) 32:42–56.e6. doi: 10.1016/j.ccell.2017.06.003
63. Smalley I, Chen Z, Phadke M, Li J, Yu X, Wyatt C, et al. Single-Cell Characterization of the Immune Microenvironment of Melanoma Brain and Leptomeningeal Metastases. *Clin Cancer Res* (2021) 27:4109–25. doi: 10.1158/1078-0432.CCR-21-1694
64. Domingues P, González-Tablas M, Otero Á, Pascual D, Miranda D, Ruiz L, et al. Tumor Infiltrating Immune Cells in Gliomas and Meningiomas. *Brain Behav Immun* (2016) 53:1–15. doi: 10.1016/j.bbi.2015.07.019
65. Jerby-Arnon L, Shah P, Cuoco MS, Rodman C, Su M-J, Melms JC, et al. A Cancer Cell Program Promotes T Cell Exclusion and Resistance to Checkpoint Blockade. *Cell* (2018) 175:984–97.e24. doi: 10.1016/j.cell.2018.09.006
66. Zhao J, Chen AX, Gartrell RD, Silverman AM, Aparicio L, Chu T, et al. Immune and Genomic Correlates of Response to Anti-PD-1 Immunotherapy in Glioblastoma. *Nat Med* (2019) 25:462–9. doi: 10.1038/s41591-019-0349-y
67. Tran TT, Rane CK, Zito CR, Weiss SA, Jessel S, Lucca L, et al. Clinical Significance of PDCD4 in Melanoma by Subcellular Expression and in Tumor-Associated Immune Cells. *Cancers (Basel)* (2021) 13(5):1049. doi: 10.3390/cancers13051049
68. García-Mulero S, Alonso MH, Pardo J, Santos C, Sanjuan X, Salazar R, et al. Lung Metastases Share Common Immune Features Regardless of Primary Tumor Origin. *J Immunother Cancer* (2020) 8(1):e000491. doi: 10.1136/jitc-2019-000491
69. Pritykin Y, van der Veeken J, Pine AR, Zhong Y, Sahin M, Mazutis L, et al. A Unified Atlas of CD8 T Cell Dysfunctional States in Cancer and Infection. *Mol Cell* (2021) 81:2477–93.e10. doi: 10.1016/j.molcel.2021.03.045
70. Niesel K, Schulz M, Anthes J, Alekseeva T, Macas J, Salamero-Boix A, et al. The Immune Suppressive Microenvironment Affects Efficacy of Radio-Immunotherapy in Brain Metastasis. *EMBO Mol Med* (2021) 13:e13412. doi: 10.15252/emmm.202013412
71. García-Silva S, Benito-Martín A, Sánchez-Redondo S, Hernández-Barranco A, Ximénez-Embún P, Nogués L, et al. Use of Extracellular Vesicles From Lymphatic Drainage as Surrogate Markers of Melanoma Progression and BRAFV600E Mutation. *J Exp Med* (2019) 216:1061–70. doi: 10.1084/jem.20181522
72. Tawbi HA, Forsyth PA, Algazi A, Hamid O, Hodi FS, Moschos SJ, et al. Combined Nivolumab and Ipilimumab in Melanoma Metastatic to the Brain. *N Engl J Med* (2018) 379:722–30. doi: 10.1056/NEJMoa1805453
73. Goldberg SB, Schalper KA, Gettinger SN, Mahajan A, Herbst RS, Chiang AC, et al. Pembrolizumab for Management of Patients With NSCLC and Brain Metastases: Long-Term Results and Biomarker Analysis From a non-Randomised, Open-Label, Phase 2 Trial. *Lancet Oncol* (2020) 21:655–63. doi: 10.1016/S1470-2045(20)30111-X

Conflict of Interest: The authors declare that the research was conducted in the absence of any commercial or financial relationships that could be construed as a potential conflict of interest.

frontiers in Immunology

REVIEW
published: 03 September 2021
doi: 10.3389/fimmu.2021.716504

TAMs in Brain Metastasis: Molecular Signatures in Mouse and Man

Michael Schulz[1,2] *and Lisa Sevenich*[1,3,4,5]*

[1] Institute for Tumor Biology and Experimental Therapy, Georg-Speyer-Haus, Frankfurt am Main, Germany, [2] Biological Sciences, Faculty 15, Goethe University Frankfurt, Frankfurt am Main, Germany, [3] German Cancer Consortium (DKTK), Partner Site Frankfurt/Mainz, Frankfurt am Main, Germany, [4] German Cancer Research Center (DKFZ), Heidelberg, Germany, [5] Frankfurt Cancer Institute (FCI), Goethe University Frankfurt, Frankfurt am Main, Germany

Macrophages not only represent an integral part of innate immunity but also critically contribute to tissue and organ homeostasis. Moreover, disease progression is accompanied by macrophage accumulation in many cancer types and is often associated with poor prognosis and therapy resistance. Given their critical role in modulating tumor immunity in primary and metastatic brain cancers, macrophages are emerging as promising therapeutic targets. Different types of macrophages infiltrate brain cancers, including (i) CNS resident macrophages that comprise microglia (TAM-MG) as well as border-associated macrophages and (ii) monocyte-derived macrophages (TAM-MDM) that are recruited from the periphery. Controversy remained about their disease-associated functions since classical approaches did not reliably distinguish between macrophage subpopulations. Recent conceptual and technological advances, such as large-scale omic approaches, provided new insight into molecular profiles of TAMs based on their cellular origin. In this review, we summarize insight from recent studies highlighting similarities and differences of TAM-MG and TAM-MDM at the molecular level. We will focus on data obtained from RNA sequencing and mass cytometry approaches. Together, this knowledge significantly contributes to our understanding of transcriptional and translational programs that define disease-associated TAM functions. Cross-species meta-analyses will further help to evaluate the translational significance of preclinical findings as part of the effort to identify candidates for macrophage-targeted therapy against brain metastasis.

Keywords: cerebral metastasis, brain cancer, tumor microenvironment, tumor-associated macrophages, microglia, tumor immunology, targeted therapy

OPEN ACCESS

Edited by:
Frits Thorsen, University of Bergen, Norway

Reviewed by:
Markus Biburger, Friedrich-Alexander-University Erlangen-Nürnberg, Germany
Andoni Garitano, University Hospital Würzburg, Germany

***Correspondence:**
Lisa Sevenich
sevenich@gsh.uni-frankfurt.de

Specialty section:
This article was submitted to Cancer Immunity and Immunotherapy, a section of the journal Frontiers in Immunology

Received: *28 May 2021*
Accepted: *13 August 2021*
Published: *03 September 2021*

Citation:
Schulz M and Sevenich L (2021) TAMs in Brain Metastasis: Molecular Signatures in Mouse and Man. Front. Immunol. 12:716504. doi: 10.3389/fimmu.2021.716504

INTRODUCTION

Mononuclear phagocytes comprise bone marrow-derived progenitors, blood monocytes, and tissue-specific macrophage populations of embryonic origin (1). Fate-mapping studies in mice revealed that macrophage populations of distinct organs (e.g., lung, spleen, liver, brain, skin) are established early during development and are self-maintained during adulthood (2). The cellular identity of tissue resident macrophages is shaped by the local environment of specific organs (3–5). Moreover, the presence of a diverse range of receptors (6) allows macrophages to receive a broad spectrum of

signals and thus contribute in autocrine and paracrine interactions. Hence, this functional plasticity places them at the interface of developmental processes, tissue homeostasis, and immunity (1).

As the sole immune cell type within the immune-privileged brain parenchyma, yolk sac-derived microglia (MG) exert critical functions in immune surveillance and host defense (7, 8). In contrast to the brain parenchyma, where the entry of systemic immune cells is strictly controlled, areas surrounding the brain (e.g., meninges) are constantly patrolled by different classes of lymphoid and myeloid cells (9, 10) (**Figure 1**). In addition to the heterogeneous MG populations that have been identified throughout the brain parenchyma (11, 12), nonparenchymal macrophages found in border regions [= border-associated macrophages (BAMs)] represent a distinct population of central nervous system (CNS) phagocytes (13). Similar to microglia, they derive from yolk sac progenitors during early development (14) and populate the meninges (m), the perivascular areas (pv), and the choroid plexus (cp). Each population is classified based on a specific set of genes, and functional adaptation is driven by local traits. Compared with MG, BAMs exhibit distinct transcriptional signatures (10, 14, 15). Under homeostatic conditions, the structures adjacent to the parenchyma maintain physical and immunological separation of the CNS, but at the same time allow restricted exchange and access of cells and molecules (16).

Neurological disorders disrupt the tissue homeostasis of the brain and lead to the recruitment of cells from the periphery, mostly of myeloid origin (17). Accumulation of myeloid cells within the parenchyma impacts the severity and disease outcome of neurological disorders. Hence, understanding the biology of specific myeloid subpopulations at spatiotemporal resolution is crucial for the development of therapeutic strategies that resolve underlying insults.

A prominent example is the development of brain malignancies. Cerebral or cerebellar tumor formation is accompanied by a massive recruitment of macrophages from the periphery, which together with resident microglia represent the most abundant stromal cell types in primary (18) and secondary (19) brain tumors [brain metastasis (BrM)]. Although every tumor type can metastasize to the brain, the highest incidence is associated to melanoma, lung and breast cancer. Adding up relative numbers, BrM originating from lung or breast cancer contribute to more than 75% of all BrM (20–23).

The brain tumor-associated macrophage (TAM) population consists of cells originating from resident microglia (TAM-MG) and cells of monocytic origin, i.e., monocytes and monocyte-derived macrophages (MDM). However, due to the lack of definitive markers that discriminate both lineages within brain tumors, it was (24, 25) challenging to determine quantitative and qualitative contributions of both TAM populations to brain

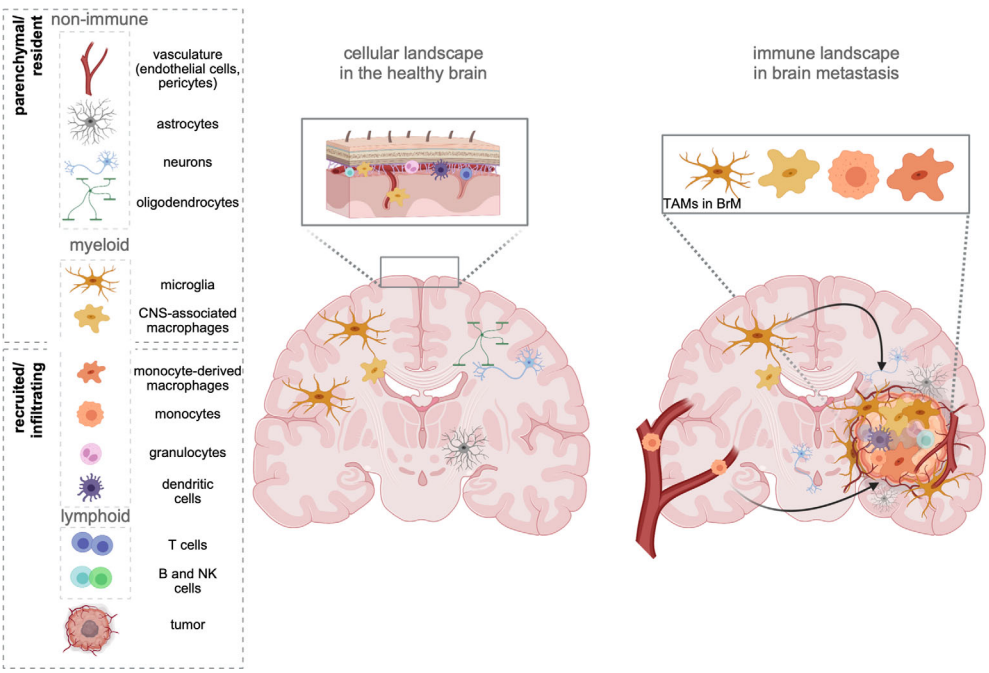

FIGURE 1 | The cellular environment in the healthy brain and BrM. The healthy brain parenchyma consists of resident cell types, including neurons, astrocytes, oligodendrocytes, and cells forming the vasculature (endothelial cells, pericytes). While microglia represent the sole immune cells within the parenchyma, border-associated areas of the brain (e.g., meninges, perivascular areas) harbor every other cell type of the immune system. In contrast, brain metastasis (right) induce the recruitment of all types of myeloid and lymphoid immune cells from the periphery. Tumor-associated macrophages (TAMs) represent a heterogeneous pool of myeloid cells, which consist of brain-resident microglia, as well as monocytes, and monocyte-derived macrophages from the periphery. Recent studies further suggest a partial involvement of recruited CNS/border-associated macrophages (BAMs).

tumor biology in the past without the need of transplantation models or lineage-tracing approaches. Bowman et al. employed two lineage tracing models in combination with RNA sequencing to identify markers, which reliably allow the discrimination of TAM-MGs and TAM-MDMs in mouse and human primary and metastatic brain tumors. This study led to the identification of the integrin alpha subunit CD49d (encoded by *Itga4*) that is specifically repressed in MG but highly expressed in MDMs. Importantly, this expression pattern remains conserved within brain tumors. In addition, the authors identified CD11a (encoded by *Itgal*) as similarly differently regulated between both major TAM populations (26).

The biggest differences between both TAM subpopulations are determined by their different ontogenetic origin. Since brain TAMs are known to critically influence the progression and outcome of brain tumor biology (24, 25), understanding their quantitative contributions under different conditions and associated putative different functions is key in order to develop novel strategies targeting distinct disease-associated phenotypes in BrM.

TAMs AS CENTRAL PART OF THE BRAIN METASTASIS MICROENVIRONMENT

TAMs are known to represent a highly abundant cell population in primary and metastatic brain tumors with different quantitative contribution to the myeloid cell pool depending on primary tumor entity (18, 19). However, controversy remained on the functional contribution of macrophage populations depending on their ontogeny. Technical integration of lineage-restricted markers or the use of single cell-based techniques to characterize myeloid cells in brain tumors has significantly broadened our knowledge on TAM heterogeneity in experimental BrM models and patient-derived data from various brain malignancies (**Table 1**).

Two recent studies explored the cellular heterogeneity of myeloid cells in experimental brain metastasis models by multicolor flow cytometry (FCM) integrating CD49d as a marker to distinguish TAM-MG and TAM-MDM. Although approximately 75% of all $CD45^+$ cells of the syngeneic breast cancer model 99LN-BrM were of myeloid origin, only 5%–10% of all TAMs were MDMs (30). By comparison, the xenograft lung cancer BrM model H2030-BrM induced stronger TAM-MDM recruitment (32), which constantly increased across different stages of tumor progression leading to 10% and 20% of TAM-MDMs in small or large BrM, respectively (32). Moreover, it was demonstrated that the TAM population within the H2030-BrM model changed in response to whole brain radiotherapy (WBRT), applied as a standard-of-care treatment modality (32). A relative reduction of TAM-MDM contribution to the total TAM pool was observed 3 days after hypofractionated as well as classically fractionated WBRT. Interestingly, this effect was transient and constant reinfiltration resulted in a steadily increasing TAM-MDM population, as examined within the total myeloid cell pool in H2030-BrM at several time points after WBRT. Hence, the application of radiotherapy represents a useful strategy to modulate the TAM pool by causing radiation-mediated cell elimination on the one hand, but enhancing infiltration of naïve cells from the periphery on the other hand. A similar way of interfering with MDM recruitment has been shown in mouse models of glioma in response to radiation (33).

Collectively, these data suggest that the TAM pool in preclinical BrM models is highly dynamic. Moreover, recent studies highlighted the contribution of each TAM population to total TAMs. The relative contribution of each TAM population to the total TAM pool is influenced by the primary tumor entity and can be modulated by radiotherapy. TAMs of peripheral origin have been found to be more abundant in recurrent glioma samples upon surgery (34), further illustrating the impact of antitumor therapy on the immune landscape. Interestingly, the diversity of the TAM pool is similarly regulated by the origin of the primary tumor in human BrM (27, 29, 31). Within the studies by Friebel et al. and Klemm et al. the authors performed comprehensive in-depth analysis of patient-derived primary and secondary brain tumor tissue by integrating high-dimensional techniques, such as, FCM, RNA sequencing, or mass cytometry by time of flight (CyToF) to gain insight into cellular and molecular aspects of the brain tumor immune landscape. In contrast to primary brain tumors, BrM induced higher infiltration of myeloid cells from the periphery, and the majority of $CD45^+$ cells was composed of neutrophils and MDMs (27, 29). Lower abundance of macrophages from the

TABLE 1 | Overview of recent studies, examining the tumor microenvironment (TME) of preclinical models of brain metastasis (BrM), and human patient samples.

Reference	Species	Tumor	Main methodology	TAM differentiation		Treatment of individuals	Main targets
				Prior	Post		
Friebel et al. (27)	*H. sapiens*	Various	Single-cell mass cytometry	No	Yes	Treated various (CT, RT, IT)	Protein
Guldner et al. (28)	*M. musculus*	Syngeneic, B2B	CyTOF, CITE-Seq, scRNA seq	No	Yes	Major analyses from untreated	Gene/protein
Klemm et al. (29)	*H. sapiens*	Various	Sorted bulk RNA seq, FCM	Yes, FCM, CD49d		Untreated and treated (CT, RT, IT, others)	Gene
Niesel et al. (30)	*M. musculus*	Syngeneic, B2B	Sorted bulk RNA seq, FCM	Yes, FCM, CD49d		Untreated	Gene
Rubio-Perez et al. (31)	*H. sapiens*	Various	scRNA seq, TCR seq	No	Yes	Treated various (CT, RT, IT)	Gene
Schulz et al. (32)	*M. musculus*	Xenograft, L2B	Sorted bulk RNA seq, scRNA seq, FCM	Yes, FCM, CD49d		Untreated and treated (RT)	Gene

H. sapiens, Homo sapiens; M. musculus, Mus musculus; FCM, flow cytometry; CT, chemotherapy; IT, immunotherapy; RT, radiotherapy; B2B, breast-to-brain; L2B, lung-to-brain.

periphery was observed in melanoma BrM compared with breast and lung cancers (**Figure 2**).

MOLECULAR PROFILES OF TAMs IN BrM

TAMs are malignancy instructed and have been described as key players at the interface between tumors and cells of the immune landscape. This can be attributed to their high capacity of integrating a broad range of external stimuli, resulting in diverse activation states and highly plastic phenotypes (35, 36). In the following paragraphs, we will provide an overview of molecular alterations observed in both major TAM populations of mouse and human BrM and highlight representative markers that have been identified to be differentially expressed in TAM-MG and TAM-MDM. Moreover, we will discuss candidate factors that have been identified as core signatures of disease-associated macrophages and are commonly up- or downregulated in both major TAM populations. An overview of the representative factors can be found in **Table 2**.

Transition From Normal to Disease-Associated Cell States

It is increasingly appreciated that tumor-associated immune cells are significantly different compared with their normal cellular counterparts. However, it remains less well understood how normal cells transition into disease-associated cell types upon initial contact to tumor cells and within different stages of tumor progression. Interestingly, Schulz et al. observed that the instruction and education of TAMs represents an early event during formation of the BrM-TME and occurs rapidly after recruitment of resident TAM-MG or peripheral-derived TAM-MDMs. Analyses of transcriptional program in TAMs isolated from small- *vs*. large-stage BrM revealed an almost complete absence of differences in gene expression in each population, suggesting stable transcriptomes during BrM progression (32). However, further dissection of potential transition stages based on single-cell approaches are needed to characterize the acquisition of diseases-associated signatures across a broader range of different stages of tumor progression and to identify the progenitor cells that contribute to tumor-associated myeloid cell pool for more precise comparison. In the following paragraph, we will therefore highlight recent insight on signatures of transition states based on trajectory analyses. Interesting observations on the cellular differentiation route of TAM-MDMs were made in a recent study in which the authors dissected the myeloid cell pool in different stages of murine and human glioma by single-cell RNA-Seq (scRNA-Seq) approaches in combination with lineage-tracing experiments in mouse models (34). By adoptively transferring classical or nonclassical monocytes from Cx3cr1$^{GFP/+}$ mice into *Ccr2*-KO mice harboring orthotopically transplanted gliomas, the authors demonstrated that only classical monocytes were able to differentiate into MDMs within the tumor. If this applies to TAM-MDM in BrM requires further investigation.

Disease-Associated Transcriptional Signatures of TAM-MG in BrM

Microglia under homeostatic conditions represent a heterogeneous cell population depending on their localization within the brain parenchyma. Moreover, MG heterogeneity is modulated by developmental stages with lower heterogeneity found in adults compared with embryonic stages. Given the inherent MG heterogeneity, it is not surprising that brain pathologies induce an even higher degree of heterogeneity (12, 37), which was demonstrated with single cell RNA-seq for TAM-MG (28, 32). For example, by using t-distributed stochastic neighbor embedding (tSNE), a dimensionality reduction method, of RNA-Seq data from single cells, Schulz et al. reported that the majority of TAM-MG from the H2030-BrM

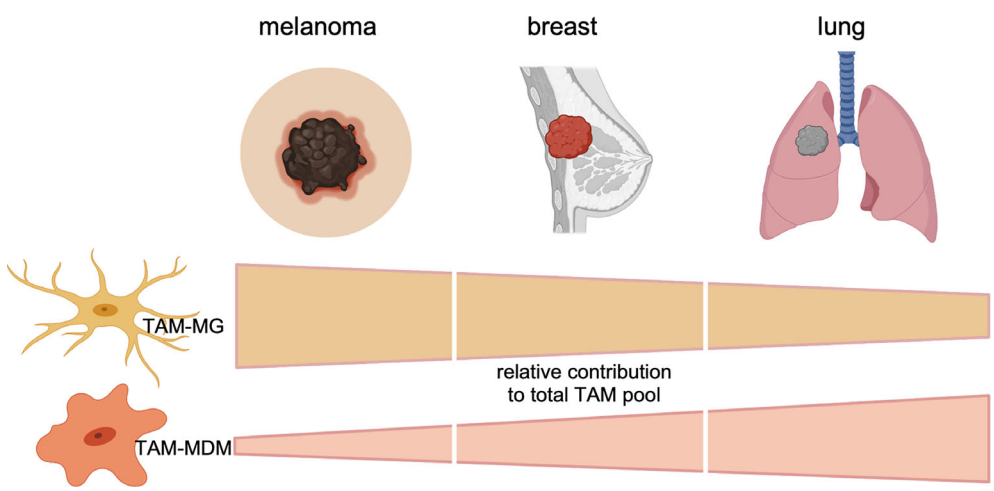

FIGURE 2 | Relative contribution of each TAM subpopulation to the total TAM pool in BrMs derived from melanoma, breast cancer, or lung cancer. Data represent cumulative, relative data derived from preclinical (mouse models) and clinical (human) findings.

TABLE 2 | Selected markers and their regulation within murine (left) and human (right) TAM-MG and TAM-MDMs.

Category	Target (depending on study, referred to gene or protein)	Mouse		Human	
		TAM-MG	TAM-MDM	TAM-MG	TAM-MDM
Microglia lineage	CX3CR1	(28, 30, 32)	(30, 32)	(28, 29)	(27, 29)
	P2RY12	(28, 30, 32)	(30, 32)	(28, 29)	(29)
	SALL1	(30, 32)	Slightly up (30, 32)	(29)	Low (29)
	TMEM119	(28, 30, 32)	(30, 32)	(28, 29)	Unchanged (29)
Macrophage lineage	CCR2	Lower in MG (30, 32)	Higher in MDM (30, 32)	Lower in MG (27, 29)	Higher in MDM but downregulated (27) or upregulated (29)
	CD49d	Lower in MG (30, 32)	Higher in MDM (30, 32)	Lower in MG (27, 29)	Higher in MDM (27, 29)
Antigen presentation	H2-Aa (only mouse)	Lower than MDM, but upregulated (30, 32)	Higher than MG (28, 30, 32)		
	H2-Ab (only mouse)	Lower than MDM, but upregulated (30, 32)	Higher than MG (28, 30, 32)		
	H2-Eb (only mouse)	Lower than MDM, but upregulated (30, 32)	Higher than MG (28, 30, 32)		
	H2-D1 (only mouse)	(30, 32)	Strongly upregulated (30), slightly regulated (32)		
	B2M	(30, 32)	(30, 32) (higher than MG)	Strong upregulation (29)	Slight upregulation and higher than MG (32)
	HLA-A (only human)			(29)	(29)
	HLA-DR (only human)			(27) [high but slightly decreased expression in (29)]	Higher presence than MG (27, 29)
	CD74	(30, 32)	Higher than MG (28, 30, 32)	Slight downregulation (29)	(29)
T cell interaction	CD275/ICOSLG/B7-H2	Unchanged (30) or slightly upregulated (32)	Upregulated (30, 32)	No expression change (29)	(29)
	PD-L1	Unchanged (30) or slightly upregulated (32)	Higher than MG (28, 30, 32)	No expression change but higher than MDM (27, 29)	Upregulated in MDM-3 (27), no expression change (29)
Complement	C1Q	(28, 30, 32) (but higher than MDM)	(28, 30, 32)	Slight downregulation (29)	(29) C1QB high (31)
	C3	(30, 32)	Unchanged (30) or slightly upregulated (32)	(28, 29)	(29)
	C3AR1	(30, 32)	(30, 32)	(29)	Strong upregulation (29)
	C4B	(30, 32)	(30, 32)	Slight upregulation (29)	Slight upregulation (29)
	C5AR1	(30, 32)	(30, 32)	Slight downregulation (29)	Slight downregulation (29)
Cytokine	CCL2	(30, 32)	(30, 32)	(29)	Unchanged (29)
	CCL3	(30, 32)	(30, 32)	(29)	Strong upregulation (29), high expression (31)
	CCL4	(30, 32)	(30, 32)	(29)	Strong upregulation (29), high expression (31)
	IL1A	(30, 32)	(30, 32)	Slight downregulation, high level (29)	Strong upregulation (29)
	IL1B	(30, 32)	(28, 30, 32)	Slight downregulation, high level (29)	Strong upregulation (29), high expression (31)
	TNF	(30, 32)	(30, 32)	Slight downregulation, high level (29)	Strong upregulation (29)
TAM signaling	AXL	(30, 32)	(30, 32)	(29)	(27, 29)

(Continued)

TABLE 2 | Continued

Category	Target (depending on study, referred to gene or protein)	Mouse		Human	
		TAM-MG	TAM-MDM	TAM-MG	TAM-MDM
	MERTK	Downregulated (30), unchanged (32)	(30, 32)	Moderate (27)	Partially (27) or strong upregulated (29)
	GAS6	(30, 32)	(30, 32)	(29)	Strong upregulation (29)
Growth factor and ECM organizer	APOE	(30, 32) (higher than MDM)	(28, 30, 32)	Mixed acc. to primary (29), higher expressed than MDM (31)	Unchanged/slightly downregulated (29)
	CTSB	(30, 32)	(30, 32)	Unchanged (29)	Downregulated, but higher levels than MG (29)
	LGALS3	(28, 30, 32)	Not regulated (30) or downregulated (32), higher than MG (28)	Strong upregulation (29)	Slightly downregulated, but higher than MG (29)
	SEMA4B	(30, 32)	Slightly up (30) or down (32)	(29)	(29)
	SPARC	Slightly upregulated (30, 32)	(30, 32)	Strong upregulation (29)	(29)
	VEGFA	Slightly upregulated (30, 32)	(30, 32)	Moderately upregulated (29)	Strong upregulation (29)
Receptors	CD33/SIGLEC3	Downregulated (30), unchanged high expression (32)	(30, 32)	Absent (27)	Down on protein level (27), up on RNA (29)
	CD64/FCGR1	Unchanged (30, 32)	Upregulated (30), no change (32)	(29)	(27, 29)
	CD163	No expression (30, 32)	No expression (30), upregulated (32)	Low (27) or upregulated (29, 31)	(27, 29, 31)
	MARCO	No expression (30, 32)	No expression (30, 32)	Low expression (29)	Strong upregulation (29)
	NR4A2	(30, 32)	(30) (slightly) (32),	(29)	Strong upregulation (29)
	CD206/MRC1	Downregulated (30) or slightly upregulated (32)	(30, 32)	(29)	(27, 29, 31)
	P2RX4	(30, 32)	(30, 32)	Unchanged high expression (29)	Slight downregulation (29)
	TREM2	Slightly upregulated (30, 32)	Strongly upregulated (30, 32)	Slight downregulation (29)	Unchanged high expression (29)
Others	CD209/CLEC4L	No expression (30) or slightly upregulated (32)	High expression (30, 32)	Low (27, 29)	High on MDM-3 (27) or downregulated (29)
	MS4A family members				
	MS4A4C	Slight upregulation (30, 32)	No change (30, 32), upregulated (28)	In *H. sapiens*: MS4A4E, low expression (29)	In *H. sapiens*: MS4A4E, strong upregulation (29)
	MS4A6C	(28, 30, 32)	Unchanged high expression (30, 32); slightly upregulated (28)	In *H. sapiens*: MS4A6E, low expression (29)	In *H. sapiens*: MS4A6E (29)
	MS4A7	(30, 32)	High expression (30, 32)	Slight downregulation (29)	(29)
	S100A family members				
		Higher then MDM in (28): S100a4, S100a6, S100a10	S100a6, S100a10 (32)	(29): S100A4, S100A6 [high in (31)], S100A10 [high in (31)]	(29): high expression level but down in TAM-MDM (S100A4, S100A6)
		Not expressed: S100a4 (30, 32), S100a6 (32); S100a10 [slightly down (32)]		(31): low expression of S100A8, S100A9	(31): slight expression of S100A8, S100A9

(Continued)

TABLE 2 | Continued

Category	Target (depending on study, referred to gene or protein)	Mouse		Human	
		TAM-MG	TAM-MDM	TAM-MG	TAM-MDM
		S100a6, S100a10 (30)			
	S100A16	Slightly upregulated (30), downregulated (32)	Upregulated (30), no expression (32)	(29): strong upregulation	(29): slight upregulation
	SPP1	(30, 32)	(30, 32)	High expression, but unchanged in TAM-MG (29)	(29): slight upregulation

Red cell, upregulated; blue cell, downregulated; grey cell, comment within the corresponding cell. In addition, each cell contains information of the respective reference. Note that if not stated otherwise, up/downregulation is referring to the comparison of BrM-associated cells vs. their normal counterpart.

model were contributing to three transcriptionally distinct cell cluster in treatment-naïve BrM. The cluster comprising most of the TAM-MG (cluster 9) was represented by high expression of cytokines (*Ccl3*, *Ccl4*, *Cxcl13*), cathepsin Z (*Ctsz*), the epidermal growth factor receptor 1 (*Egfr1*), as well as MG typical marker (*C1qa*, *Hexb*) (38, 39). The complement member and MG lineage marker *C1qa* was found to be upregulated in TAM-MG in several studies (**Table 2**), whereas other members of the MG-specific "sensome" core signature (*Cx3cr1*, *P2ry12*, *Tmem119*) (11, 38, 39) were consequently downregulated in murine and human TAM-MG (**Table 2**). While an increased expression of *C1q* members in MG belongs to their activation profile (40, 41), downregulation of homeostatic markers most likely is a consequence concomitantly occurring with downregulation of the homeostatic regulatory gene *Sall1*/*SALL1* in murine and human TAM-MG. This further mirrors a classical activation response of MG associated to any damage of the brain, as observed under neuroinflammatory conditions (42).

Once activated and educated by tumor cells, TAM-MG upregulate several markers known to be crucial for inflammation in the injured brain, thereby probably contributing to BrM progression, e.g., *via* exerting immune-suppressive functions. Presumably, this is accompanied with profound metabolic changes as seen in an apparent deregulation of members of solute carrier (*Slc*) genes (32).

Some of the frequently observed markers in MG associated to neurological damage are apolipoprotein E (*Apoe/APOE*) and the triggered receptor expressed on myeloid cells 2, *Trem2/TREM2*, which were highly expressed/upregulated in TAM-MG of murine BrM models, whereas the expression of both members only slightly varied in human TAM-MG. The APOE-TREM2 axis has been described to drive activated MG states in neurodegenerative diseases along with downregulation of homeostatic markers (39, 43). However, especially TAM-MDMs showed elevated expression levels of *Trem2/TREM2* in preclinical BrM models or patient material of BrM derived from various primary tumors (**Table 2**). The contributions of TREM2 and APOE to neurological diseases [e.g., Alzheimer's disease (AD) or multiple sclerosis (MS)] have been extensively described with regard to MG (44, 45). Importantly, it was shown that targeting $TREM2^+$ MG represents an interesting approach to attenuate disease progression. In addition to the broadly studied APOE-TREM2 axis, another key player of MG-mediated neurological dysfunction, and ligand for TREM2, is Galectin-3, encoded by *Lgals3/LGALS3*. Galectin-3 shows a multitude of functions in MG. Elevated extracellular levels within the BrM-TME might drive inflammatory responses in a Toll-like receptor (TLR) 4 binding-mediated self-sustaining manner (46, 47). In line with this, TLR4 expression was found to be upregulated in TAM-MG of H2030-BrM (32). In a recent study, Siew et al. analyzed the contribution of MG-derived Galectin-3 signaling in a mouse model of Huntington's disease (48). Elevated cytokine levels were attributed to high Galectin-3 signaling, and strategies targeting its expression have been shown to be sufficient in decreasing levels of inflammatory cytokines, thereby ameliorating MG-mediated pathogenesis (48).

While profiling across different conditions revealed that *Lgals3/LGALS3* expression levels are strongly increased in TAM-MG,

varying but high levels within TAM-MDMs have been found in murine or human BrM as well (**Table 2**). Similarly, high expression levels were rather associated to TAM-MDMs of murine (49), or human recurrent glioma (34), as revealed in high-dimensional single-cell profiling studies. Therefore, contribution of elevated *Lgals3/LGALS3* levels need to be carefully evaluated in a context-specific manner. Another group of genes (S100 family members) shows an interesting alternating pattern across TAMs in mouse and human BrM. S100 members are small, Ca^{2+}-binding proteins, which regulate several cellular functions in an autocrine, or paracrine fashion, and can act as damage-associated molecular pattern (DAMP) (50). For example, S100β has been shown to serve as a noninvasive, astrocytic marker of blood-brain barrier (BBB) integrity and function, also in brain tumors (51), whereas several S100A members have been implicated in neurodegenerative diseases like AD (52). In addition, distinct S100 proteins have been associated to the regulation of inflammatory responses and TAM migration and invasion in tumors (50). Hence, upregulation or high expression especially in TAM-MG of BrM (e.g., *S100A6*, *S100A10*) (**Table 2**) (28, 31), might reflect a central mediator of BrM-associated inflammation. In contrast, in glioma elevated expression level of *S100A6* has been implicated in a transitory TAM-MDM state in mouse and humans (34) or was part of a strong "macrophage signature" (49). Since S100A6, which was implicated in tumor progression in several other cancers (53), can either act on MG in a cell-restricted manner or can be secreted, elevated expression levels of *S100A6* and other S100 members need further examination. To date, it remains unclear if the regulation of S100 members represents a cause or consequence of progressing BrM.

Direct comparison of both TAM populations on the single cell (27, 28, 31), and bulk population level (29, 30, 32) revealed further cell type-restricted molecular profiles in mouse models and human patient samples. TAM-MG showed higher upregulation of distinct proinflammatory cytokines (e.g., *CXCL5*, *CXCL8*, *IL6*) (29), or genes belonging to cell migration, e.g., *Vim/VIM* (28, 31) within a changing environment.

Cathepsins (*Cts/CTS*) encompass a family of proteases known to play several protumorigeneic roles in the tumor context by, e.g., remodeling the extracellular matrix (ECM) (54). In the brain, cathepsin S has been described as BrM-promoting *via* enhancing transmigration through the BBB (19). High expression levels of different cathepsins within TAMs of established BrM further suggest profound remodeling of the TME in outgrowing tumors. Among them, *Ctsd* (28) and *CTSL* (31) exhibited higher expression levels in TAM-MG, while *Ctsb* was strongly upregulated in both TAM populations of different murine BrM models (30, 32), but in human BrM was, together with *CTSW*, rather enriched in TAM-MDM (29). Hence, different highly expressed members of this family of ECM modulators further suggest an involvement for generating a BrM-promoting environment, but specific contributions for/with each TAM population in BrM have not been elucidated yet.

Disease-Associated Transcriptional Signatures of TAM-MDM in BrM

Recruitment of monocytes to the CNS has been predominantly attributed to the chemokine axis including the receptors Ccr2/CCR2 and Cx3cr1/CX3CR1 (17), which was shown in the brain tumor context using lineage-tracing approaches in glioma mouse models (26, 55). Interestingly, while *Ccr2/CCR2* is dramatically downregulated upon entry into the parenchyma and during the monocyte-to-macrophage transition in glioma (55), and also BrM (27), *Cx3cr1/CX3CR1* levels are upregulated in TAM-MDMs (**Table 2**), whereas the protein was downregulated on the majority of MDM subsets but remained abundant on only a small subset (27). These data suggest that high levels of Cx3cr1/CX3CR1 are partially required to integrate into the CNS parenchyma, since the axis is usually involved in glia-neuronal crosstalk (56). Comparing TAM data for the expression of another potent chemokine receptor known to be involved in cell migration, it became apparent that especially TAM-MDMs possess high levels or strongly upregulated the C3A receptor, *C3ar1/C3AR1* in murine and human BrM (**Table 2**). This suggests the contribution of a conserved mechanism of recruitment *via* the anaphylatoxin/chemokine axis.

Given the fact that bulk analysis usually masks different expression/antigen density levels, Friebel et al. comprehensively dissected the heterogeneity of TAMs derived from different human brain malignancies, and showed that TAM instruction is not a random process, but rather driven by the underlying tumor, both in primary and secondary brain malignancies (27). By combining in total 38 markers for their myeloid panel, the authors captured a broad range of cellular states as depicted by distinct lineage-specific, but also activation markers. Upon merging all TAM CyTOF data from both, glioma and BrM samples, the authors created a detailed relationship and trajectory analyses focusing on abundance of typical monocyte/macrophage markers *in silico*. One of the common features they found was downregulation of CCR2 and the SIGLEC family member, SIGLEC3 (CD33), which represents a transmembrane receptor implicated in pattern recognition and regulation of phagocytosis, and in that regard has been described to be a risk factor for AD (57). Moreover, transitioning cells were found to commonly upregulate the innate immune sensor receptor CD163, together with the TAM receptor MERTK (**Table 2**). Monocytes transition to macrophages through a more common MDM state (termed MDM 1), and finally develop into three distinct MDM subpopulations (MDM 2, 3, 4), and this transition was driven by differential regulation of certain markers, including CD169, CD206 (mannose receptor c-type I, MRC1), CD209 (C-type lectin receptor, CLEC4L), CD38, and PD-L1. Some of these markers were further used in combination with IBA1 to specifically stain for MDMs in the TAM compartment (27). Since not only CD206 but also CD209 usually are associated to alternative macrophage activation, it is not surprising that those markers have been found to be predominantly upregulated in TAM-MDMs of murine and human BrM across different conditions (**Table 2**). MERTK upregulation was found to be gradual, and highest antigen density was allocated to the MDM 4 population (27), whereas bulk RNA-Seq of murine and human TAM-MDMs revealed in general elevated expression levels (**Table 2**). MERTK and AXL, which were also found to be significantly upregulated especially in TAM-MDMs (**Table 2**), represent two of the three TAM (*T*YRO3, *A*XL, *M*ERTK)

receptor tyrosine kinases, which are involved in phagocytosis and regulation of inflammatory responses (58). Interestingly, one of the ligands for AXL, *Gas6/GAS6*, was also highly expressed within both TAM populations in murine BrM, but rather upregulated in TAM-MDMs of human BrM samples (**Table 2**). Although GAS6-AXL signaling is present in the healthy CNS, and is associated to phagocytosing MG (59), deregulation can cause enhanced inflammation in the CNS (60). Moreover, this signaling axis can lead to a protumorigenic TME (61) and has been found to be coexpressed in TAMs with high *C1QC* levels in various primary tumors (62).

Despite several differences between the same TAM population within both mouse and human, further commonly regulated markers of TAM-MDMs included *Nr4a2/NR4A2*. This nuclear receptor family is known to control macrophage gene expression during inflammation (63) but is implicated in maintaining normal functions of dopaminergic neurons in the healthy brain. Interestingly, *NR4A2* has been found particularly upregulated in a transitory monocyte population in glioma (34), further suggesting regulatory involvement in inducing inflammatory phenotypes during MDM development.

While certain patterns associated to these inflammatory states of TAMs seem to be conserved between species, other families of proteins are rather restricted to either a species, or a cell type. One interesting group encompasses the membrane-spanning (MS) protein family of MS4A members (**Table 2**). While for some of the family members (e.g., MS4A1 = CD20) their functions are well described, most of them remain poorly understood. In a recent study, Liu et al. generated new lineage-tracing mouse models targeting Ms4a3 (*Ms4a3*^{Cre} and *Ms4a3*^{CreERT2}) and validated lineage specificity of this marker, which specifically distinguishes monocytes and granulocytes from embryonically derived resident macrophage populations, including MG, under steady state but also inflammatory conditions (64). MG possess strong expression levels of certain Ms4a members (*Ms4a6b*, *Ms4a6c*, *Ms4a6d*, *Ms4a7*) during early development, while these high expression levels are not found in adult MG or in response to injury. Nevertheless, MG of that specific subpopulation of MG identified during early development cluster also showed overlapping features to BAMs (37). Several genes of the MS4A family appeared in all of the BrM-omics studies among the top regulated genes, and some of them have been described as risk factors for AD (65), including *Ms4a4c (mouse)/MS4A4E (human)*, *Ms4a6c/MS4A6E*, and *Ms4a7/MS4A7*. Interestingly, all of them were found at high expression levels or strongly upregulated across both TAM populations of murine BrM with slightly higher levels in TAM-MDM (**Table 2**). Contrary, in human TAMs, MS4A members were found predominantly upregulated or higher expressed *per se* in TAM-MDMs. Similarly, high and stable expression of *Ms4a7* was reported as part of a core signature for BAMs in steady state and under neuroinflammatory conditions (42). Taken together, this data is in line with the situation in glioma TAMs (34) and further corroborate strong similarities in transcriptional profiles between each TAM population derived from distinct diseases. These findings are strengthened by higher intersect levels of each TAM pool between glioma and BrM (29).

Aiming to describe heterogeneity within certain TAM subsets, all of the recent studies looking into the TME by single-cell approaches confirmed that especially the TAM-MDM pool consists of a more diverse range of cellular states (27, 28, 32). Whereas, Guldner et al. even described BAMs to contribute to the TAM-MDM pool within their model. With respect to identity of cell types within cell populations that were FACS purified prior to transcriptomic analyses, it is important to carefully consider procedures of sample preparation and marker selection. Macrodissection of tumor lesions is critical to reduce the risk of diluting the disease-associated cell pool with normal cell types. Moreover, the use of different marker combinations can lead to different assignment of cell types to certain subpopulations. For example, several commonly used markers to discriminate MG and MDM including CD45, SALL1, and TMEM119 (30, 66) are known to show assimilation of expression levels in both populations in brain tumors. Hence, the choice of marker combinations can lead to differences in population assignment. This determines the classification of subpopulations and consequently significantly affects the respective transcriptional programs. Nevertheless, typical non-MG clusters (TAM-MDMs/BAMs) were shown to be dominated by the expression of genes belonging to antigen processing and presentation particularly associated to MHC class II presentation, including *H2-Aa*, *H2-Ab1*, *H2-Eb*, and *CD74* (**Table 2**) in several independent studies (28, 30, 32). Expression of the MHC class II member HLA-DR in human TAMs was similarly higher in TAM-MDMs (**Table 2**), and upregulated expression can be attributed to the transition from monocytes to MDMs (27), similarly as in the glioma situation (34). Interestingly, this raises the question to which extent each TAM population contributes to T-cell interaction, hence influencing a cancer-promoting, or immunosuppressive TME. Using multiplexed immunostaining, spatial organization of TAMs with respect to T cells was examined in murine (30) and human BrM (29). Both studies found a close proximity of both TAM populations to $CD4^+$ and $CD8^+$ T cells, yet Niesel et al. observed closer proximity of TAM-MDM to T cells compared with TAM-MG based on discrimination by TMEM119 (30). Moreover, it was observed that PD-L1 was almost absent in tumor-free brains, whereas BrM induced the recruitment of PD-$L1^+$ myeloid cells, and levels of PD-L1 were highest among TAM-MDMs (30). On the gene expression level, several costimulatory and also inhibitory markers were found to be present among both TAM populations, whereas most of them were expressed at higher levels in TAM-MDMs (30). Representative comparison of different T-cell regulatory markers across TAMs revealed that both, activating *Icosl/ICOSL*, and inhibitory *Pd-l1/PD-L1* markers are present in TAMs with slight higher levels in the TAM-MDM compartment (**Table 2**). Given the spatial organization of TAMs within the BrM-TME, one can assume that TAM-MGs in the BrM periphery are in contact with T cells at the tumor-stroma interface, while immunosuppression within the BrM core is fostered by TAM-MDMs once T cells have entered the tumor mass. Furthermore, T-cell profiles confirm exhaustion states within the

TME (27, 30). Additional immunoregulatory mediators within BrMs predominantly derived from TAM-MDMs were the chemokines *CCL8*, *CCL13*, *CCL17*, and *CCL18* (29). Together, all of them are attributed to an alternative, rather tumor-promoting phenotype (= M2) of macrophages, which is found in many tumors (35). Despite this fact, both TAM-MG and TAM-MDMs upregulate a broad range of inflammatory mediators (29, 32), and hence cannot be classified into the conservative M1–M2 scheme, but rather exist within a continuum, depending on their current local environment.

Finally, in order to understand putative dichotomous functions of TAMs, and their relevance for the inflammatory TME in BrM (**Figure 3**), detailed annotation and pathway analyses of differently regulated genes were performed based on results obtained from RNA-Seq experiments (28–30, 32).

To delineate functional changes upon TAM instruction, comparative analyses of significantly differently regulated genes of TAMs *vs.* their healthy counterparts (i.e., normal MG, or blood monocytes) in breast cancer BrM (30), and lung cancer BrM (32) were performed. Together, both studies showed that altered transcriptional profiles in TAM-MG resulted in upregulation of pathways and signaling cascades associated to inflammation, regulation of cytokine production, type I interferon (IFN) signaling, cell migration and motility, and proliferation. Interestingly, TAM-MG were found to be involved in the recruitment and interaction with neutrophils, in both mouse models of BrM (30, 32), and also in human BrM (29). Concurrently, TAM-MG downregulates genes involved in housekeeping functions, such as synapse organization or regulation of neuronal organization.

TAMs derived from the periphery are more plastic than MG as described above. Thus, their altered transcriptional profiles need to be evaluated more carefully in a context-dependent manner. Compared with their normal cellular counterparts, TAM-MDMs upregulated pathways involved in inflammatory responses, cytokine production and interaction, migration, mitosis and cell cycle, and also organization of the ECM (30, 32). In addition, human BrM TAM-MDMs showed slightly higher relevance of genes related to mitosis and cell division, compared with TAM-MGs; however, staining of human BrM samples for proliferation markers indicated proliferation in both cell types (29). However, if this results from an environment promoting local proliferation, or is caused by other stimuli, e.g., prior treatment remains to be elucidated. Analyses of patient samples stratified based on treatment history will be required to gain further insight whether different intervention strategies modulate recruitment and expansion of TAM-MDMs as previously shown in a lung-to-brain model in response to radiotherapy (32). Both human TAM populations showed an enrichment for genes related to type I IFN, and NF-kB signaling (29). Not surprisingly upon entering the BrM-TME, and transitioning from monocytes, TAM-MDMs downregulated genes related to chromatin organization, and intracellular reorganization of, e.g., the cytoskeleton (30).

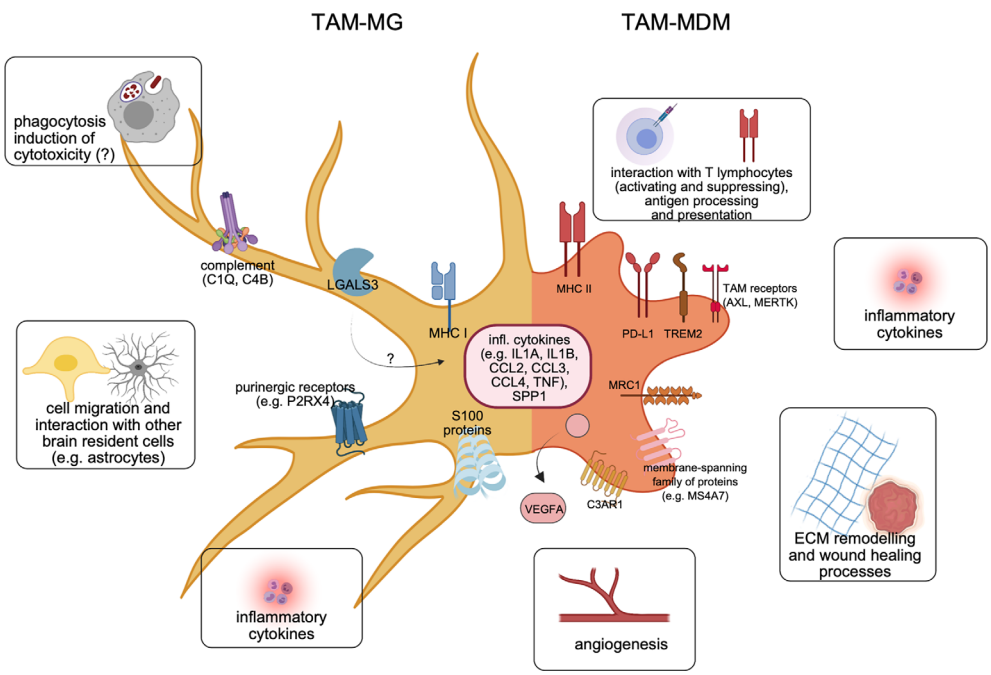

FIGURE 3 | Molecular features of both major TAM populations in BrM. Recent cellular and molecular findings underline the differences of TAM-MG (left) *vs*. TAM-MDM (right) within the BrM microenvironment. Representative markers shared between TAMs from murine or human BrM are illustrated, together with major functional annotations.

Transcriptional Programs Shared in TAM-MG and TAM-MDM

In addition to lineage-restricted transcriptional programs in TAM populations, it became clear that both TAM populations also share a significant proportion of similarly regulated markers by Top marker principal component, and overlapping gene analysis in human TAMs (29), or by comparison of all differently regulated genes (DEGs) (32).

In H2030-BrM, approximately 300 DEGs were found to be commonly upregulated, and around 900 DEGs commonly downregulated between both TAM populations (32). Functional annotation of all jointly regulated markers revealed the induction of inflammatory pathways, as well as regulation of cell adhesion and cell migration. Downregulated DEGs were mostly associated to homeostatic functions in the brain, e.g., synapse organization. In contrast to the results obtained from experimental BrM models, the number of shared genes between TAM-MG and TAM-MDM was rather small in the human situation (29). The difference can potentially be explained by the fact that human RNA-seq data in this study were not stratified based on primary tumor type thereby possibly missing important similarly regulated genes. Comparison of typical inflammatory cytokines (e.g., *CCL2*, *CCL3*, *CCL4*, *IL1B*) across mice and human BrM-TAMs revealed that although most of them exhibited much higher expression levels in the BrM situation in mice, it rather were TAM-MDMs upregulating them in the human scenario (**Table 2**). RNA velocity analysis of single-cell RNA-Seq data of mouse TAMs further showed that *Il1b* and also *Tgfb* were genes similarly regulated at convergence points between TAM-MG and TAM-MDM clusters (28).

Osteopontin which is encoded by *Spp1/SPP1* is a marker usually associated to MG of early development or has been described as one key marker of all disease-associated MG (DAM) subcluster (37). In BrM, *Spp1/SPP1* was found highly expressed or upregulated in both TAM populations across species (**Table 2**), however with slightly higher expression levels in TAM-MG, similar as in primary brain tumors (34). Although a broad range of cellular functions has been assigned to osteopontin, under inflammatory conditions it most likely regulates inflammation itself *via* enhancing the recruitment of not only myeloid but also lymphoid cells (67) to the TME. Aiming to reduce or dampen inflammation within the BrM TME, osteopontin hence might represent an interesting target.

In addition to the high expression levels of the complement cascade-initiating member *C1q/C1Q* within the BrM-TME, two other inflammatory factors, *Il1a/IL1A* and *Tnf/TNF*, showed broad abundance and were highly expressed or upregulated in TAMs of murine or human BrMs (**Table 2**). Together, the presence of all three molecules strongly raises the possibility of TAM-mediated astrocyte activation towards a neurotoxic phenotype (termed A1), which partially would be sustained due to constant factor availability. This mechanism of astrocyte activation has been described in mouse models of neuroinflammatory conditions, and A1 astrocytes were found in samples of various human diseases. A characteristic marker for A1 astrocytes is the central complement component C3 (68). Interestingly, next to C1q/C1Q, other members of the complement system were apparently deregulated in BrM (32), and cross-conditional comparison revealed upregulation of, for example, *C4b/C4B* among all TAMs in mice and human (**Table 2**). While oligodendrocyte-derived *C4b* in mice has been associated to pathogenicity in an AD model (69), its functions within the TAM pool of BrM remain to be shown.

In summary, recent discoveries and previously unknown molecular insights into macrophages/microglia associated to BrM have dramatically shifted the paradigm of BrM-TAMs representing one homogeneous population. In comparison with data derived from recent "*omics*" studies involving glioma, it became clear that TAMs in brain malignancies constitute a heterogeneous mixture of resident and recruited mononuclear phagocytes, with multifaceted activation states (**Figure 3**). Moreover, each major subpopulation contributes to the inflammatory TME in a unique way, and disease-specific manner. The discovery of molecular markers present in both TAM populations or conserved between species opens novel avenues to develop targeted approaches in order to fight this deadly disease.

TRANSLATIONAL ASPECTS

TAM-targeted therapies have attracted attention as promising therapeutic strategies for a variety of different primary cancers (**Table 3**). Besides their high abundance, TAMs have been shown to critically influence tumor biology, often in a protumorigenic fashion by exerting immune-suppressive functions, and at the same time interacting with tumor cells to reciprocally support each other (35). However, in the brain, targeted approaches have to be carefully designed, in order to address modulation within specific TAM populations, without affecting resident macrophage populations (i.e., adjacent MGs) to prevent side effects.

Given the central role of CSF1-CSF1R signaling for survival and proliferation of macrophages, it is not surprising that specifically this axis has been targeted by antibodies, or small inhibitory molecules in order to reduce macrophage infiltration or deplete resident, tumor-promoting populations. Aiming to suppress tumor-promoting TAM functions, Pyonteck et al. utilized a CSF1R inhibitor in preclinical glioma models (18). Interestingly, CSF1R inhibition as monotherapy resulted in improved survival and even tumor regression, accompanied by re-education of TAMs into a rather antitumor phenotype. Long-term treatment however resulted in acquired resistance driven by IGF signaling between TAMs and tumor cells, which resulted in prolonged glioma cell survival and invasive capacities (71). Improved efficacy however can be obtained by combining CSF1R inhibition with radiotherapy in glioma (33). CSF1R inhibition was shown to reduce to breast cancer cell invasion (79) and lead to antitumor efficacy in melanoma-BrM and intracerebrally inoculated breast cancer cells (72, 80). However, therapeutic efficacy of CSF1R inhibition still needs to be carefully evaluated with regard to long-term efficacy and potential resistance mechanisms as observed in glioma.

TABLE 3 | Examples of preclinical and clinical studies targeting certain TAM-related receptors/factors as mono- or combination therapies in various types of extra- and intracranial tumors.

Target	Tumor/model	Species	Treatment/drug/resource	Major effects	Study reference
C3AR	Leptomeningeal metastasis (LeptoM) models from breast and lung cancer	*M. musculus*	Nonpeptide antagonist SB290157/Santa Cruz	Prolonged survival and reduced LeptoM burden	(70)
CSF1R	Glioma	*M. musculus*	BLZ945/Novartis	Improved survival of glioma-bearing mice, tumor regression, TAM repolarization, tumor relapse observed after the period of tumor stasis	(18)
	Glioma	*M. musculus*	BLZ945/Novartis + Pi3K inhibition BLZ945/Novartis + IGF-1R inhibition	Combination delays glioma relapse	(71)
	Glioma	*M. musculus*	BLZ945/Novartis + 5 × 2 Gy WBRT	Combination delays glioma relapse	(33)
	Intracerebral induced melanoma BrM	*M. musculus*	PLX3397/Selleck Chemicals	Reduction of BrM burden and BrM size	(72)
	Different primary tumors, including glioma	*H. sapiens*	Cabiralizumab (anti-CSF-1R mAB)/Five Prime Therapeutics (± nivolumab)	Ongoing study	NCT02526017
CXCR4	Adult glioblastoma (and other primary CNS tumors)	*H. sapiens*	AMD3100/Plerixafor/	Improved local tumor recurrence control	(73) (NCT01977677)
TREM2	Different primary solid tumors	*M. musculus*	Anti-TREM2 mAB clone 178	Reduced tumor growth and remodeling of myeloid landscape within the TME, enhanced immunotherapy (e.g., anti-PD-L1)	(74)
	Different primary solid tumors	*H. sapiens*	PY314/mAB against TREM2 on myeloid cells in the TME/Pionyr Immunoherapeutics	Ongoing study	NCT04691375
VEGF	Glioma	*M. musculus*	Aflibercept/VEGF-trap/Sanofi (in combination with antiangiogenic therapy, Ang-1/Ang-2 peptibody, and immunotherapy, anti-PD-1/ BioXCell)	Improved survival, tumor vessel normalization, immunostimulatory reprogramming	(75)
	Breast cancer BrM	*M. musculus*	Bevacizumab/anti-VEGF mAB (in combination with anti-Ang2 L1-10)	Reduced BrM burden and permeability of blood vessels associated to BrM	(76)
	Breast cancer BrM	*H. sapiens*	Bevacizumab/anti-VEGF mAB (in combination with carboplatin)	High rate of durable objective CNS response	(77) (NCT01004172)
	Solid tumor BrM	*H. sapiens*	Bevacizumab/anti-VEGF mAB (after failure of WBRT)	About 80% of patients showed disease response, defined as stable disease or better	(78) (NCT01898130)
VISTA	Breast cancer BrM	*M. musculus*	Anti-VISTA/13F3, mAB//BioXCell (in combination with anti-PD-L1)	Reduction of BrM burden and increase of CD3 + cell abundance	(28)
	Various types of solid tumors, however exclusively without BrM	*H. sapiens*	CI-8993/anti-VISTA mAB/CURIS, Inc.	Ongoing study	NCT04475523

H. sapiens, Homo sapiens; M. musculus, Mus musculus; BrM, brain metastases; mAB, monoclonal antibody; WBRT, whole brain radiotherapy. Information on National Clinical Trial (NCT) data can be found at: www.clinicaltrials.gov.

Another strategy of limiting TAM functions within the TME includes blockade of their recruitment, *via* interfering with chemokines (81) or chemokine receptors, e.g., CCR2 or CXCR4 to inhibit general TAM recruitment (73) or by targeting newly identified markers that are implicated in the recruitment of TAM subpopulations such as CD49d (33). Given the high abundance of the anaphylatoxin receptor C3ar1/C3AR1 predominantly on TAM-MDMs of murine and human origin, blockade of this axis could also be used to inhibit monocyte/macrophage recruitment to the brain. Antibody- or small molecule-mediated inhibition of the C3-C3AR1 axis could have strong inhibitory effects and furthermore might impact the permeability of the BBB at sites of malignant inflammation. In leptomeningeal metastasis, this axis has been shown particularly important for enhancing the permeability at the choroid plexus epithelium, in order to trophically support metastasized cancer cells within the CSF (70). By interfering with the C3-C3AR1 axis, one might even trigger another antitumoral response due to blockade of the interaction of astrocytes and MG as shown by Litvinchuk et al. in a mouse model of neurodegeneration. While astrocyte-derived C3 *via* C3AR1 on MG induces proinflammatory programs *via* STAT3 signaling (82), activation of astrocytes could in part be mediated *via* C1Q plus two other cytokines, IL1A and TNF (68), which seem to be broadly present within the BrM-TME. Since astrocytes have been shown to exert multiple BrM-promoting functions (83–86) and elimination of the three aforementioned factors was beneficial in an ALS mouse model by attenuating gliosis (87), targeting one or several steps within the complement cascade seems promising and has the potential to reverse or block the immunosuppressive, cancer-permissive TME in BrM.

Although some of the markers in TAMs seem to be regulated in a more conditional manner (e.g., by different model, primary tumor entity, genetic background, species), a distinct set of genes was

conservatively regulated, and similarly across TAM populations and species (e.g., MS4A proteins, TAM receptors AXL and MERTK, TREM2). While little is known about the specific functions of individual MS4A members, they might play a central role in regulating cellular functions, including cell growth, survival, and activation by serving as family of ion channels and/or adaptor proteins facilitating intracellular protein-protein interaction (41). For example, MS4A4A has been described as a key marker of BAMs (14, 15, 42) and was described as a novel M2-like marker of metastasis-associated macrophages (88). Hence future studies need to address the consequences on the inflammatory state upon interfering with, e.g., MS4A7, which was highly upregulated on both, murine and human TAM-MDMs in BrM. Given their surface exposure, MS4A members are potentially druggable by, e.g., antibodies (41).

Interestingly, within the study form Mattiola et al., the authors showed that MS4A4A interacts with a ß-glucan receptor dectin-1 in lipid rafts of the cell membrane. The dectin-1 pathway transmits intracellular signals similar to those of TREM2. Hence, TREM2 deficiency can be compensated by enhanced dectin-1 signaling (89). TREM2 signaling is essential for MG function and disease-associated phenotypes in MG can be induced by the APOE-TREM2 pathway (43). In AD, TREM2-deficient MG undergoes autophagy due to impaired mTOR signaling and metabolism (89). Since TREM2 seems to be dramatically upregulated in all TAMs across different conditions, antibody-mediated blockade of this receptor signaling pathway represents a promising approach. Within a recent study, the authors examined TREM2 function in TAMs of distinct tumor models (74). Interestingly, they found that both, mice deficient for TREM2, or antibody-mediated blockade of TREM2 signaling, resulted in delayed tumor growth. Simultaneously, the immune landscape within their model was altered including an increase of intratumoral $CD8^+$ T cells, which consequently led to enhanced efficacy of anti-PD1 immunotherapy. More importantly, the authors showed ubiquitous abundance of $TREM2^+$ macrophages across distinct human tumor samples, and that TREM2 expression inversely correlated with greater overall, and relapse-free survival in colorectal carcinoma and triple negative breast cancer patients (74). Given the negative correlation between MDMs and T-cell frequencies in BrM (29), it is tempting to speculate that high expression of TREM2 in TAM-MDM as seen under various BrM conditions might be an interesting candidate for combination therapies. If this furthermore leads to remodeling of the TME with enhanced T cell recruitment, also in BrM, needs to be evaluated. In summary, targeting TREM2 in combination with immunotherapy (e.g., anti-PD-L1), or radiotherapy, might represent an attractive strategy to overcome immunosuppression. It was previously shown that radiotherapy has the potential to transiently lift immunosuppressive features of the TAM pool by enhancing the recruitment of naïve monocytes/MDMs to BrM in a lung-to-brain metastasis model (32). However, acquired resistance to combined radioimmunotherapy was partially mediated by PD-L1 expression from infiltrated myeloid cells (30), which rapidly undergo tumor education. In addition to targeting the PD1-PD-L1 axis in order to enhance antitumor responses, targeting different TAM populations showed promising results in glioma and BrM models. For example, Guldner et al. inhibited the negative immune checkpoint VISTA (encoded by *Vsir*) on TAMs which similar as targeting TREM2 enhanced the $CD3^+$ cell abundance within BrM leading to improved efficacy of anti-PD-L1 (28). Given the high abundance and strong expression of *Vegfa/VEGFA* in TAMs, interference with VEGF signaling could furthermore lead to enhanced antitumor responses, as shown in a triple treatment approach of murine glioma (75). The authors blocked the angiogenic factors VEGF and ANG-2 in combination with PD-1, which resulted in extended survival of mice compared with anti-VEGF as monotherapy (75). However, targeting VEGF in BrM is not indicated for every primary tumor type which gives rise to BrM. While double inhibition of VEGF and ANG-2 reduced BrM burden in preclinical models of breast-to-brain metastasis (76), VEGFA inhibition can induce long-term dormancy in lung-to-brain metastasis (90). For breast-to-brain metastasis patients, combination of VEGFA inhibition with bevacizumab in combination with carboplatin resulted in a high rate of durable responses (77). Moreover, VEGFA inhibition resulted in a 25% disease response rate in 80% of solid cancer patients with current brain metastasis that failed whole-brain radiotherapy (78).

In summary, novel targeted therapeutic approaches need to be carefully evaluated in a context-specific manner upon spatiotemporal determination of leukocytic subsets within the TME. This is particularly important for targeting specific phenotypic features of TAMs, but at the same time spare homeostatic features of adjacent, non-BrM-associated populations. Furthermore, it will be critical to evaluate to which extent altered gene expression also translates into altered protein abundance, which in addition requires evaluation on a spatial level. In combination with standard therapy, targeting distinct TAM subsets represents a promising strategy. Combination therapies are expected to induce synergy by on the one hand repressing tumor-promoting traits, and on the other hand lifting immunosuppression, thereby enhancing antitumor immunity.

CONCLUDING REMARKS

Driven by technical advances, as well as scientific and clinical interest in understanding cellular and molecular landscapes in health and disease, recent research has resulted in tremendous insight into the heterogeneity of TAM of primary and secondary BrMs.

RNA sequencing, multiplexed flow, and mass cytometry revealed the dichotomous nature of TAMs in BrM, wherein resident microglia as well as recruited monocyte-derived macrophages represent the two major populations and contribute significantly to the entire immune cell landscape. Although both TAMs quantitatively differentially contribute to the local TAM pool and populate different niches within the TME, their phenotypic changes occur early upon disease-specific instruction in a highly plastic manner. Together, both TAM populations contribute to the establishment of an immunosuppressive and tumor-promoting environment in BrM. In order to evaluate the applicability of novel targeted approaches, further research needs to determine

molecular pattern in spatiotemporal resolution. Detailed mechanistic understanding how standard therapy can be used as an immune modulator in addition to the identification of transcriptional programs that drive disease-promoting states in TAMs to provide scientific rationale for the development of improved therapeutic avenues against BrM is needed.

AUTHOR CONTRIBUTIONS

MS and LS conceptualized and wrote the manuscript. All authors contributed to the article and approved the submitted version.

FUNDING

Research in the lab of LS is supported by institutional funds from the Georg-Speyer-Haus jointly funded by the German Federal Ministry of Health and the Ministry of Higher Education, Research and the Arts of the State of Hesse (HMWK), as well as grants from the German Cancer Aid (Max-Eder Junior Group Leader Program 70111752) and German Research Foundation (SE2234/3-1).

ACKNOWLEDGMENTS

We thank all members from the Sevenich Lab and from the Georg-Speyer-Haus for insightful feedback on our work. Furthermore, we are thankful to all authors of the main recent studies involved in providing material and information regarding novel insights into the TME of BrM, in particular supplementary files from Guldner et al. and Klemm et al. Data from Klemm et al. were accessed *via* supplementary files and their RNA-Seq database at https://joycelab.shinyapps.io/braintime/. Figures were created with Biorender (www.biorender.com).

REFERENCES

1. Wynn TA, Chawla A, Pollard JW. Macrophage Biology in Development, Homeostasis and Disease. *Nature* (2013) 496(7446):445–55. doi: 10.1038/nature12034
2. Yona S, Kim KW, Wolf Y, Mildner A, Varol D, Breker M, et al. Fate Mapping Reveals Origins and Dynamics of Monocytes and Tissue Macrophages Under Homeostasis. *Immunity* (2013) 38(1):79–91. doi: 10.1016/j.immuni.2012.12.001
3. Gautier EL, Shay T, Miller J, Greter M, Jakubzick C, Ivanov S, et al. Gene-Expression Profiles and Transcriptional Regulatory Pathways That Underlie the Identity and Diversity of Mouse Tissue Macrophages. *Nat Immunol* (2012) 13(11):1118–28. doi: 10.1038/ni.2419
4. Gosselin D, Link VM, Romanoski CE, Fonseca GJ, Eichenfield DZ, Spann NJ, et al. Environment Drives Selection and Function of Enhancers Controlling Tissue-Specific Macrophage Identities. *Cell* (2014) 159(6):1327–40. doi: 10.1016/j.cell.2014.11.023
5. Lavin Y, Winter D, Blecher-Gonen R, David E, Keren-Shaul H, Merad M, et al. Tissue-Resident Macrophage Enhancer Landscapes Are Shaped by the Local Microenvironment. *Cell* (2014) 159(6):1312–26. doi: 10.1016/j.cell.2014.11.018
6. Taylor PR, Martinez-Pomares L, Stacey M, Lin HH, Brown GD, Gordon S. Macrophage Receptors and Immune Recognition. *Annu Rev Immunol* (2005) 23:901–44. doi: 10.1146/annurev.immunol.23.021704.115816
7. Alliot F, Godin I, Pessac B. Microglia Derive From Progenitors, Originating From the Yolk Sac, and Which Proliferate in the Brain. *Brain Res Dev Brain Res* (1999) 117(2):145–52. doi: 10.1016/s0165-3806(99)00113-3
8. Ginhoux F, Greter M, Leboeuf M, Nandi S, See P, Gokhan S, et al. Fate Mapping Analysis Reveals That Adult Microglia Derive From Primitive Macrophages. *Science* (2010) 330(6005):841–5. doi: 10.1126/science.1194637
9. Korin B, Ben-Shaanan TL, Schiller M, Dubovik T, Azulay-Debby H, Boshnak NT, et al. High-Dimensional, Single-Cell Characterization of the Brain's Immune Compartment. *Nat Neurosci* (2017) 20(9):1300–9. doi: 10.1038/nn.4610
10. Mrdjen D, Pavlovic A, Hartmann FJ, Schreiner B, Utz SG, Leung BP, et al. High-Dimensional Single-Cell Mapping of Central Nervous System Immune Cells Reveals Distinct Myeloid Subsets in Health, Aging, and Disease. *Immunity* (2018) 48(2):380–395 e6. doi: 10.1016/j.immuni.2018.01.011
11. Geirsdottir L, David E, Keren-Shaul H, Weiner A, Bohlen SC, Neuber J, et al. Cross-Species Single-Cell Analysis Reveals Divergence of the Primate Microglia Program. *Cell* (2019) 179(7):1609–22.e16. doi: 10.1016/j.cell.2019.11.010
12. Masuda T, Sankowski R, Staszewski O, Bottcher C, Amann L, Sagar C, et al. Spatial and Temporal Heterogeneity of Mouse and Human Microglia at Single-Cell Resolution. *Nature* (2019) 566(7744):388–92. doi: 10.1038/s41586-019-0924-x
13. Zeisel A, Munoz-Manchado AB, Codeluppi S, Lonnerberg P, La Manno G, Jureus A, et al. Brain Structure. Cell Types in the Mouse Cortex and Hippocampus Revealed by Single-Cell RNA-Seq. *Science* (2015) 347(6226):1138–42. doi: 10.1126/science.aaa1934
14. Utz SG, See P, Mildenberger W, Thion MS, Silvin A, Lutz M, et al. Early Fate Defines Microglia and Non-Parenchymal Brain Macrophage Development. *Cell* (2020) 181(3):557–73.e18. doi: 10.1016/j.cell.2020.03.021
15. Van Hove H, Martens L, Scheyltjens I, De Vlaminck K, Pombo Antunes AR, De Prijck S, et al. A Single-Cell Atlas of Mouse Brain Macrophages Reveals Unique Transcriptional Identities Shaped by Ontogeny and Tissue Environment. *Nat Neurosci* (2019) 22(6):1021–35. doi: 10.1038/s41593-019-0393-4
16. Kierdorf K, Masuda T, Jordao MJC, Prinz M. Macrophages at CNS Interfaces: Ontogeny and Function in Health and Disease. *Nat Rev Neurosci* (2019) 20(9):547–62. doi: 10.1038/s41583-019-0201-x
17. Prinz M, Priller J. Tickets to the Brain: Role of CCR2 and CX3CR1 in Myeloid Cell Entry in the CNS. *J Neuroimmunol* (2010) 224(1-2):80–4. doi: 10.1016/j.jneuroim.2010.05.015
18. Pyonteck SM, Akkari L, Schuhmacher AJ, Bowman RL, Sevenich L, Quail DF, et al. CSF-1R Inhibition Alters Macrophage Polarization and Blocks Glioma Progression. *Nat Med* (2013) 19(10):1264–72. doi: 10.1038/nm.3337
19. Sevenich L, Bowman RL, Mason SD, Quail DF, Rapaport F, Elie BT, et al. Analysis of Tumour- and Stroma-Supplied Proteolytic Networks Reveals a Brain-Metastasis-Promoting Role for Cathepsin s. *Nat Cell Biol* (2014) 16(9):876–88. doi: 10.1038/ncb3011
20. Gavrilovic IT, Posner JB. Brain Metastases: Epidemiology and Pathophysiology. *J Neurooncol* (2005) 75(1):5–14. doi: 10.1007/s11060-004-8093-6
21. Nayak L, Lee EQ, Wen PY. Epidemiology of Brain Metastases. *Curr Oncol Rep* (2012) 14(1):48–54. doi: 10.1007/s11912-011-0203-y
22. Suh JH, Kotecha R, Chao ST, Ahluwalia MS, Sahgal A, Chang EL. Current Approaches to the Management of Brain Metastases. *Nat Rev Clin Oncol* (2020) 17(5):279–99. doi: 10.1038/s41571-019-0320-3
23. Valiente M, Ahluwalia MS, Boire A, Brastianos PK, Goldberg SB, Lee EQ, et al. The Evolving Landscape of Brain Metastasis. *Trends Cancer* (2018) 4(3):176–96. doi: 10.1016/j.trecan.2018.01.003
24. Gutmann DH, Kettenmann H. Microglia/Brain Macrophages as Central Drivers of Brain Tumor Pathobiology. *Neuron* (2019) 104(3):442–9. doi: 10.1016/j.neuron.2019.08.028
25. Sevenich L. Brain-Resident Microglia and Blood-Borne Macrophages Orchestrate Central Nervous System Inflammation in Neurodegenerative Disorders and Brain Cancer. *Front Immunol* (2018) 9:697. doi: 10.3389/fimmu.2018.00697
26. Bowman RL, Klemm F, Akkari L, Pyonteck SM, Sevenich L, Quail DF, et al. Macrophage Ontogeny Underlies Differences in Tumor-Specific Education in

Brain Malignancies. *Cell Rep* (2016) 17(9):2445–59. doi: 10.1016/j.celrep.2016.10.052
27. Friebel E, Kapolou K, Unger S, Nunez NG, Utz S, Rushing EJ, et al. Single-Cell Mapping of Human Brain Cancer Reveals Tumor-Specific Instruction of Tissue-Invading Leukocytes. *Cell* (2020) 181(7):1626–1642 e20. doi: 10.1016/j.cell.2020.04.055
28. Guldner IH, Wang Q, Yang L, Golomb SM, Zhao Z, Lopez JA, et al. CNS-Native Myeloid Cells Drive Immune Suppression in the Brain Metastatic Niche Through Cxcl10. *Cell* (2020) 183(5):1234–48.e25. doi: 10.1016/j.cell.2020.09.064
29. Klemm F, Maas RR, Bowman RL, Kornete M, Soukup K, Nassiri S, et al. Interrogation of the Microenvironmental Landscape in Brain Tumors Reveals Disease-Specific Alterations of Immune Cells. *Cell* (2020) 181(7):1643–1660 e17. doi: 10.1016/j.cell.2020.05.007
30. Niesel K, Schulz M, Anthes J, Alekseeva T, Macas J, Salamero-Boix A, et al. The Immune Suppressive Microenvironment Affects Efficacy of Radio-Immunotherapy in Brain Metastasis. *EMBO Mol Med* (2021) 13(5):e13412. doi: 10.15252/emmm.202013412
31. Rubio-Perez C, Planas-Rigol E, Trincado JL, Bonfill-Teixidor E, Arias A, Marchese D, et al. Immune Cell Profiling of the Cerebrospinal Fluid Enables the Characterization of the Brain Metastasis Microenvironment. *Nat Commun* (2021) 12(1):1503. doi: 10.1038/s41467-021-21789-x
32. Schulz M, Michels B, Niesel K, Stein S, Farin H, Rodel F, et al. Cellular and Molecular Changes of Brain Metastases-Associated Myeloid Cells During Disease Progression and Therapeutic Response. *iScience* (2020) 23(6):101178. doi: 10.1016/j.isci.2020.101178
33. Akkari L, Bowman RL, Tessier J, Klemm F, Handgraaf SM, de Groot M, et al. Dynamic Changes in Glioma Macrophage Populations After Radiotherapy Reveal CSF-1R Inhibition as a Strategy to Overcome Resistance. *Sci Transl Med* (2020) 12(552). doi: 10.1126/scitranslmed.aaw7843
34. Pombo Antunes AR, Scheyltjens I, Lodi F, Messiaen J, Antoranz A, Duerinck J, et al. Single-Cell Profiling of Myeloid Cells in Glioblastoma Across Species and Disease Stage Reveals Macrophage Competition and Specialization. *Nat Neurosci* (2021) 24(4):595–610. doi: 10.1038/s41593-020-00789-y
35. Mantovani A, Sozzani S, Locati M, Allavena P, Sica A. Macrophage Polarization: Tumor-Associated Macrophages as a Paradigm for Polarized M2 Mononuclear Phagocytes. *Trends Immunol* (2002) 23(11):549–55. doi: 10.1016/s1471-4906(02)02302-5
36. Noy R, Pollard JW. Tumor-Associated Macrophages: From Mechanisms to Therapy. *Immunity* (2014) 41(1):49–61. doi: 10.1016/j.immuni.2014.06.010
37. Hammond TR, Dufort C, Dissing-Olesen L, Giera S, Young A, Wysoker A, et al. Single-Cell RNA Sequencing of Microglia Throughout the Mouse Lifespan and in the Injured Brain Reveals Complex Cell-State Changes. *Immunity* (2019) 50(1):253–271 e6. doi: 10.1016/j.immuni.2018.11.004
38. Butovsky O, Jedrychowski MP, Moore CS, Cialic R, Lanser AJ, Gabriely G, et al. Identification of a Unique TGF-Beta-Dependent Molecular and Functional Signature in Microglia. *Nat Neurosci* (2014) 17(1):131–43. doi: 10.1038/nn.3599
39. Hickman SE, Kingery ND, Ohsumi TK, Borowsky ML, Wang LC, Means TK, et al. The Microglial Sensome Revealed by Direct RNA Sequencing. *Nat Neurosci* (2013) 16(12):1896–905. doi: 10.1038/nn.3554
40. Farber K, Cheung G, Mitchell D, Wallis R, Weihe E, Schwaeble W, et al. C1q, the Recognition Subcomponent of the Classical Pathway of Complement, Drives Microglial Activation. *J Neurosci Res* (2009) 87(3):644–52. doi: 10.1002/jnr.21875
41. Eon Kuek L, Leffler M, Mackay GA, Hulett MD. The MS4A Family: Counting Past 1, 2 and 3. *Immunol Cell Biol* (2016) 94(1):11–23. doi: 10.1038/icb.2015.48
42. Jordao MJC, Sankowski R, Brendecke SM, Sagar G, Tai YH, Tay TL, et al. Prinz: Single-Cell Profiling Identifies Myeloid Cell Subsets With Distinct Fates During Neuroinflammation. *Science* (2019) 363(6425). doi: 10.1126/science.aat7554
43. Krasemann S, Madore C, Cialic R, Baufeld C, Calcagno N, El Fatimy R, et al. The TREM2-APOE Pathway Drives the Transcriptional Phenotype of Dysfunctional Microglia in Neurodegenerative Diseases. *Immunity* (2017) 47(3):566–81.e9. doi: 10.1016/j.immuni.2017.08.008
44. Dong Y, D'Mello C, Pinsky W, Lozinski BM, Kaushik DK, Ghorbani S, et al. Oxidized Phosphatidylcholines Found in Multiple Sclerosis Lesions Mediate Neurodegeneration and Are Neutralized by Microglia. *Nat Neurosci* (2021) 24(4):489–503. doi: 10.1038/s41593-021-00801-z
45. Yeh FL, Hansen DV, Sheng M. TREM2, Microglia, and Neurodegenerative Diseases. *Trends Mol Med* (2017) 23(6):512–33. doi: 10.1016/j.molmed.2017.03.008
46. Burguillos MA, Svensson M, Schulte T, Boza-Serrano A, Garcia-Quintanilla A, Kavanagh E, et al. Microglia-Secreted Galectin-3 Acts as a Toll-Like Receptor 4 Ligand and Contributes to Microglial Activation. *Cell Rep* (2015) 10(9):1626–38. doi: 10.1016/j.celrep.2015.02.012
47. Tan Y, Zheng Y, Xu D, Sun Z, Yang H, Yin Q. Galectin-3: A Key Player in Microglia-Mediated Neuroinflammation and Alzheimer's Disease. *Cell Biosci* (2021) 11(1):78. doi: 10.1186/s13578-021-00592-7
48. Siew JJ, Chen HM, Chen HY, Chen HL, Chen CM, Soong BW, et al. Galectin-3 Is Required for the Microglia-Mediated Brain Inflammation in a Model of Huntington's Disease. *Nat Commun* (2019) 10(1):3473. doi: 10.1038/s41467-019-11441-0
49. Ochocka N, Segit P, Walentynowicz KA, Wojnicki K, Cyranowski S, Swatler J, et al. Single-Cell RNA Sequencing Reveals Functional Heterogeneity of Glioma-Associated Brain Macrophages. *Nat Commun* (2021) 12(1):1151. doi: 10.1038/s41467-021-21407-w
50. Xia C, Braunstein Z, Toomey AC, Zhong J, Rao X. S100 Proteins As an Important Regulator of Macrophage Inflammation. *Front Immunol* (1908) 82017):1908. doi: 10.3389/fimmu.2017.01908
51. Kanner AA, Marchi N, Fazio V, Mayberg MR, Koltz MT, Siomin V, et al. Serum S100beta: A Noninvasive Marker of Blood-Brain Barrier Function and Brain Lesions. *Cancer* (2003) 97(11):2806–13. doi: 10.1002/cncr.11409
52. Cristovao JS, Gomes CM. S100 Proteins in Alzheimer's Disease. *Front Neurosci* (2019) 13:463. doi: 10.3389/fnins.2019.00463
53. Donato R, Sorci G, Giambanco I. S100A6 Protein: Functional Roles. *Cell Mol Life Sci* (2017) 74(15):2749–60. doi: 10.1007/s00018-017-2526-9
54. Olson OC, Joyce JA. Cysteine Cathepsin Proteases: Regulators of Cancer Progression and Therapeutic Response. *Nat Rev Cancer* (2015) 15(12):712–29. doi: 10.1038/nrc4027
55. Chen Z, Feng X, Herting CJ, Garcia VA, Nie K, Pong WW, et al. Cellular and Molecular Identity of Tumor-Associated Macrophages in Glioblastoma. *Cancer Res* (2017) 77(9):2266–78. doi: 10.1158/0008-5472.CAN-16-2310
56. Luo P, Chu SF, Zhang Z, Xia CY, Chen NH. Fractalkine/CX3CR1 Is Involved in the Cross-Talk Between Neuron and Glia in Neurological Diseases. *Brain Res Bull* (2019) 146:12–21. doi: 10.1016/j.brainresbull.2018.11.017
57. Griciuc A, Serrano-Pozo A, Parrado AR, Lesinski AN, Asselin CN, Mullin K, et al. Alzheimer's Disease Risk Gene CD33 Inhibits Microglial Uptake of Amyloid Beta. *Neuron* (2013) 78(4):631–43. doi: 10.1016/j.neuron.2013.04.014
58. Lemke G. Biology of the TAM Receptors. *Cold Spring Harb Perspect Biol* (2013) 5(11):a009076. doi: 10.1101/cshperspect.a009076
59. Fourgeaud L, Traves PG, Tufail Y, Leal-Bailey H, Lew ED, Burrola PG, et al. TAM Receptors Regulate Multiple Features of Microglial Physiology. *Nature* (2016) 532(7598):240–4. doi: 10.1038/nature17630
60. Weinger JG, Brosnan CF, Loudig O, Goldberg MF, Macian F, Arnett HA, et al. Loss of the Receptor Tyrosine Kinase Axl Leads to Enhanced Inflammation in the CNS and Delayed Removal of Myelin Debris During Experimental Autoimmune Encephalomyelitis. *J Neuroinflamm* (2011) 8:49. doi: 10.1186/1742-2094-8-49
61. Tanaka M, Siemann DW. Gas6/Axl Signaling Pathway in the Tumor Immune Microenvironment. *Cancers (Basel)* (2020) 12(7). doi: 10.3390/cancers12071850
62. Cheng S, Li Z, Gao R, Xing B, Gao Y, Yang Y, et al. A Pan-Cancer Single-Cell Transcriptional Atlas of Tumor Infiltrating Myeloid Cells. *Cell* (2021) 184(3):792–809 e23. doi: 10.1016/j.cell.2021.01.010
63. Pei L, Castrillo A, Tontonoz P. Regulation of Macrophage Inflammatory Gene Expression by the Orphan Nuclear Receptor Nur77. *Mol Endocrinol* (2006) 20(4):786–94. doi: 10.1210/me.2005-0331
64. Liu Z, Gu Y, Chakarov S, Bleriot C, Kwok I, Chen X, et al. Fate Mapping *via* Ms4a3-Expression History Traces Monocyte-Derived Cells. *Cell* (2019) 178(6):1509–25.e19. doi: 10.1016/j.cell.2019.08.009
65. Hollingworth P, Harold D, Sims R, Gerrish A, Lambert JC, Carrasquillo MM, et al. Common Variants at ABCA7, MS4A6A/MS4A4E, EPHA1, CD33 and CD2AP Are Associated With Alzheimer's Disease. *Nat Genet* (2011) 43(5):429–35. doi: 10.1038/ng.803

66. Sedgwick JD, Ford AL, Foulcher E, Airriess R. Central Nervous System Microglial Cell Activation and Proliferation Follows Direct Interaction With Tissue-Infiltrating T Cell Blasts. *J Immunol* (1998) 160(11):5320–30.
67. Icer MA, Gezmen-Karadag M. The Multiple Functions and Mechanisms of Osteopontin. *Clin Biochem* (2018) 59:17–24. doi: 10.1016/j.clinbiochem.2018.07.003
68. Liddelow SA, Guttenplan KA, Clarke LE, Bennett FC, Bohlen CJ, Schirmer L, et al. Neurotoxic Reactive Astrocytes Are Induced by Activated Microglia. *Nature* (2017) 541(7638):481–7. doi: 10.1038/nature21029
69. Zhou Y, Song WM, Andhey PS, Swain A, Levy T, Miller KR, et al. Human and Mouse Single-Nucleus Transcriptomics Reveal TREM2-Dependent and TREM2-Independent Cellular Responses in Alzheimer's Disease. *Nat Med* (2020) 26(1):131–42. doi: 10.1038/s41591-019-0695-9
70. Boire A, Zou Y, Shieh J, Macalinao DG, Pentsova E, Massague J. Complement Component 3 Adapts the Cerebrospinal Fluid for Leptomeningeal Metastasis. *Cell* (2017) 168(6):1101–13.e13. doi: 10.1016/j.cell.2017.02.025
71. Quail DF, Bowman RL, Akkari L, Quick ML, Schuhmacher AJ, Huse JT, et al. The Tumor Microenvironment Underlies Acquired Resistance to CSF-1R Inhibition in Gliomas. *Science* (2016) 352(6288):aad3018. doi: 10.1126/science.aad3018
72. Qiao S, Qian Y, Xu G, Luo Q, Zhang Z. Long-Term Characterization of Activated Microglia/Macrophages Facilitating the Development of Experimental Brain Metastasis Through Intravital Microscopic Imaging. *J Neuroinflamm* (2019) 16(1):4. doi: 10.1186/s12974-018-1389-9
73. Thomas RP, Nagpal S, Iv M, Soltys SG, Bertrand S, Pelpola JS, et al. Macrophage Exclusion After Radiation Therapy (MERT): A First in Human Phase I/II Trial Using a CXCR4 Inhibitor in Glioblastoma. *Clin Cancer Res* (2019) 25(23):6948–57. doi: 10.1158/1078-0432.CCR-19-1421
74. Molgora M, Esaulova E, Vermi W, Hou J, Chen Y, Luo J, et al. TREM2 Modulation Remodels the Tumor Myeloid Landscape Enhancing Anti-PD-1 Immunotherapy. *Cell* (2020) 182(4):886–900.e17. doi: 10.1016/j.cell.2020.07.013
75. Di Tacchio M, Macas J, Weissenberger J, Sommer K, Bahr O, Steinbach JP, et al. Tumor Vessel Normalization, Immunostimulatory Reprogramming, and Improved Survival in Glioblastoma With Combined Inhibition of PD-1, Angiopoietin-2, and VEGF. *Cancer Immunol Res* (2019) 7(12):1910–27. doi: 10.1158/2326-6066.CIR-18-0865
76. Bohn KA, Adkins CE, Nounou MI, Lockman PR. Inhibition of VEGF and Angiopoietin-2 to Reduce Brain Metastases of Breast Cancer Burden. *Front Pharmacol* (2017) 8:193. doi: 10.3389/fphar.2017.00193
77. Leone JP, Emblem KE, Weitz M, Gelman RS, Schneider BP, Freedman RA, et al. Phase II Trial of Carboplatin and Bevacizumab in Patients With Breast Cancer Brain Metastases. *Breast Cancer Res* (2020) 22(1):131. doi: 10.1186/s13058-020-01372-w
78. Kumthekar P, Dixit K, Grimm SA, Lukas RV, Schwartz MA, Rademaker A, et al. A Phase II Trial of Bevacizumab in Patients With Recurrent Solid Tumor Brain Metastases Who Have Failed Whole Brain Radiation Therapy (WBRT). *J Clin Oncol* (2019) 37(15_suppl):2070–0. doi: 10.1200/JCO.2019.37.15_suppl.2070
79. Patsialou A, Wyckoff J, Wang Y, Goswami S, Stanley ER, Condeelis JS. Invasion of Human Breast Cancer Cells *In Vivo* Requires Both Paracrine and Autocrine Loops Involving the Colony-Stimulating Factor-1 Receptor. *Cancer Res* (2009) 69(24):9498–506. doi: 10.1158/0008-5472.CAN-09-1868
80. Andreou KE, Soto MS, Allen D, Economopoulos V, de Bernardi A, Larkin JR, et al. Anti-Inflammatory Microglia/Macrophages As a Potential Therapeutic Target in Brain Metastasis. *Front Oncol* (2017) 7:251. doi: 10.3389/fonc.2017.00251
81. Liu SC, Alomran R, Chernikova SB, Lartey F, Stafford J, Jang T, et al. Blockade of SDF-1 After Irradiation Inhibits Tumor Recurrences of Autochthonous Brain Tumors in Rats. *Neuro Oncol* (2014) 16(1):21–8. doi: 10.1093/neuonc/not149
82. Litvinchuk A, Wan YW, Swartzlander DB, Chen F, Cole A, Propson NE, et al. Complement C3aR Inactivation Attenuates Tau Pathology and Reverses an Immune Network Deregulated in Tauopathy Models and Alzheimer's Disease. *Neuron* (2018) 100(6):1337–53.e5. doi: 10.1016/j.neuron.2018.10.031
83. Schulz M, Salamero-Boix A, Niesel K, Alekseeva T, Sevenich L. Microenvironmental Regulation of Tumor Progression and Therapeutic Response in Brain Metastasis. *Front Immunol* (2019) 10:1713. doi: 10.3389/fimmu.2019.01713
84. Wasilewski D, Priego N, Fustero-Torre C, Valiente M. Reactive Astrocytes in Brain Metastasis. *Front Oncol* (2017) 7:298. doi: 10.3389/fonc.2017.00298
85. Doron H, Amer M, Ershaid N, Blazquez R, Shani O, Lahav TG, et al. Inflammatory Activation of Astrocytes Facilitates Melanoma Brain Tropism *via* the CXCL10-CXCR3 Signaling Axis. *Cell Rep* (2019) 28(7):1785–98.e6. doi: 10.1016/j.celrep.2019.07.033
86. Priego N, Zhu L, Monteiro C, Mulders M, Wasilewski D, Bindeman W, et al. STAT3 Labels a Subpopulation of Reactive Astrocytes Required for Brain Metastasis. *Nat Med* (2018) 24(7):1024–35. doi: 10.1038/s41591-018-0044-4
87. Guttenplan KA, Weigel MK, Adler DI, Couthouis J, Liddelow SA, Gitler AD, et al. Knockout of Reactive Astrocyte Activating Factors Slows Disease Progression in an ALS Mouse Model. *Nat Commun* (2020) 11(1):3753. doi: 10.1038/s41467-020-17514-9
88. Mattiola I, Tomay F, De Pizzol M, Silva-Gomes R, Savino B, Gulic T, et al. The Macrophage Tetraspan MS4A4A Enhances Dectin-1-Dependent NK Cell-Mediated Resistance to Metastasis. *Nat Immunol* (2019) 20(8):1012–22. doi: 10.1038/s41590-019-0417-y
89. Ulland TK, Song WM, Huang SC, Ulrich JD, Sergushichev A, Beatty WL, et al. TREM2 Maintains Microglial Metabolic Fitness in Alzheimer's Disease. *Cell* (2017) 170(4):649–63.e13. doi: 10.1016/j.cell.2017.07.023
90. Kienast Y, von Baumgarten L, Fuhrmann M, Klinkert WE, Goldbrunner R, Herms J, et al. Real-Time Imaging Reveals the Single Steps of Brain Metastasis Formation. *Nat Med* (2010) 16(1):116–22. doi: 10.1038/nm.2072

Conflict of Interest: The authors declare that the research was conducted in the absence of any commercial or financial relationship that could be construed as a potential conflict of interest.

frontiers in Immunology

ORIGINAL RESEARCH
published: 18 October 2021
doi: 10.3389/fimmu.2021.750407

New Artificial Intelligence Score and Immune Infiltrates as Prognostic Factors in Colorectal Cancer With Brain Metastases

*Violaine Randrian[1,2], Amandine Desette[2,3], Sheik Emambux[2,4], Valentin Derangere[5], Pauline Roussille[6], Eric Frouin[7,8], Julie Godet[7], Lucie Karayan-Tapon[2,3,9], François Ghiringhelli[5,10] and David Tougeron[1,2]**

[1] Hepato-Gastroenterology Department, CHU Poitiers, Poitiers, France, [2] Université de Poitiers, CHU Poitiers, INSERM, PRODICET, Poitiers, France, [3] Université de Poitiers, CHU Poitiers, INSERM, LNEC, Poitiers, France, [4] Medical Oncology Department, CHU Poitiers, Poitiers, France, [5] Plateforme de Transfert en Biologie Cancérologique, Département de Biologie et de Pathologie des Tumeurs, Centre de Lutte Contre le Cancer Georges-François Leclerc, Dijon, France, [6] Radiotherapy Department, CHU Poitiers, Poitiers, France, [7] Pathology Department, CHU Poitiers, Poitiers, France, [8] Université de Poitiers, CHU Poitiers, LITEC, Poitiers, France, [9] Cancer Biology Department, CHU Poitiers, Poitiers, France, [10] INSERM U1231, Dijon, France

Incidence of brain metastases has increased in patients with colorectal cancer (CRC) as their survival has improved. CD3 T-cells and, lately, DGMate (DiGital tuMor pArameTErs) score, have been identified as prognostic factors in locally advanced CRC. Until now, there is no data concerning the prognostic value of these markers in patients with CRC-derived brain metastases. All consecutive patients with CRC-derived brain metastases diagnosed between 2000 and 2017 were retrospectively included. Staining for CD3, CD8, PD-1, PD-L1 and DGMate analyses were performed using tissue micro-array from primary tumors and, if available, brain metastases. All in all, 83 patients were included with 80 primary tumor samples and 37 brain metastases samples available. CD3 and CD8 T-cell infiltration was higher in primary tumors compared to brain metastases. We observed a significant higher DGMate score in rectal tumors compared to colon tumors (p=0.03). We also noted a trend of higher CD3 T-cell infiltration in primary tumors when brain metastases were both supra and subtentorial compared to brain metastases that were only subtentorial or supratentorial (p=0.36 and p=0.03, respectively). No correlation was found between CD3 or CD8 infiltration or DGMate score in primary tumors or brain metastases and overall survival (OS) in the overall population. In patients with rectal tumors, a high DGMate score in brain metastases was associated with longer OS (13.4 ± 6.1 months versus 6.1 ± 1.4 months, p=0.02). High CD3 T-cell infiltration in brain metastases was associated with lower OS in patients with supratentorial brain metastases (9.8 ± 3.3 months versus 16.7 ± 5.9 months, p=0.03). PD-L1

OPEN ACCESS

Edited by:
Manuel Sarmiento Soto, Sevilla University, Spain

Reviewed by:
Calin Cainap, Iuliu Haţieganu University of Medicine and Pharmacy, Romania
Stefano Ugel, University of Verona, Italy

***Correspondence:**
David Tougeron
davidtougeron@hotmail.fr;
david.tougeron@chu-poitiers.fr
orcid.org/0000-0002-8065-9635

Specialty section:
This article was submitted to Cancer Immunity and Immunotherapy, a section of the journal Frontiers in Immunology

Received: *30 July 2021*
Accepted: *29 September 2021*
Published: *18 October 2021*

Citation:
Randrian V, Desette A, Emambux S, Derangere V, Roussille P, Frouin E, Godet J, Karayan-Tapon L, Ghiringhelli F and Tougeron D (2021) New Artificial Intelligence Score and Immune Infiltrates as Prognostic Factors in Colorectal Cancer With Brain Metastases. Front. Immunol. 12:750407. doi: 10.3389/fimmu.2021.750407

overexpression was rare, both in primary tumors and brain metastases, but PD-L1 positive primary tumors were associated with worse OS (p=0.01). In contrast to breast and lung cancer derived brain metastases, CD3 and CD8 infiltration and DGMate score are not major prognostic factors in patients with CRC-derived brain metastases.

Keywords: colorectal cancer, brain metastases, anti-tumoral immunity, tumor infiltrated lymphocytes (TILs), prognostic factors, CD3

INTRODUCTION

The prognosis of patients with metastatic colorectal cancer (mCRC) has improved and median overall survival (OS) is now about three years. In parallel to this OS improvement, the incidence of unusual metastatic sites such as brain metastases (BM) has increased (1). Mostly metachronous, BMs derived from CRC are diagnosed about two years after the primary tumor diagnosis and are usually associated with a *RAS* mutation (2, 3). CRC-derived BMs remain associated with a poor prognosis with 5 months of median OS (4).

Immune infiltration is a known prognostic factor in locally advanced CRC and will perhaps be used in the near future as a prognostic factor to determine modalities of adjuvant chemotherapy (5, 6). The percentage of CD3+ T cells at the invasive margin of locally advanced CRC is also a predictive factor of metachronous metastases (7). It also remains a robust prognostic factor at the metastatic stage (8). Furthermore, CD3+ T lymphocytes are the main type of tumor-infiltrating lymphocytes (TIL) identified in BMs of various primary tumors. This infiltration correlates with prolonged OS in BMs derived from lung cancer, breast cancer, melanoma or renal cell cancer (9). In CRC-derived BMs, data are lacking since BMs from CRC are rare (1 to 5% of CRC) (3). This is of great interest as prognosis in mCRC is correlated with infiltration of the least-immune infiltrated metastases and BMs are supposed to be poorly infiltrated by immune cells (10). Therefore, more biological insight is needed to characterize dynamic and prognostic significance of immune infiltration, especially by CD3+ T cells, in this rare subgroup of CRC with BMs.

An artificial intelligence software device, using a LASSO algorithm called DiGital tuMour pArameTErs (DGMate), was shown in the PETACC08 study to predict the prognosis of locally advanced colon cancers (stage III) (11). DGMate score is a set of texture parameters extracted from the CRC tissue. When combined with CD3 staining, it overwhelms immune score performance in predicting the outcome of locally advanced colon cancer. Indeed, a predictive nomogram based on DGMate, CD3 TIL and clinical variables has identified a group of patients with less than 10% relapse risk and another group with a 50% relapse risk in stage III CRC. These tools are not yet validated in mCRC. We analyzed both CD3 infiltration and DGMate score in a rare series of CRC-derived BM to assess whether CD3 infiltration and/or DGMate score were prognostic factors in CRC-derived BMs.

MATERIALS AND METHODS

Patients

This study was conducted on samples available from patients included in the study previously published by Roussille P et al. (2, 3). All consecutive patients with BM from CRC, diagnosed from 2001 to 2016, were identified in our institution using our clinical report database. Inclusion criteria were age over 18 years, histologically confirmed CRC and histologically or radiologically confirmed BM by computed tomography scan (CT-scan) and/or magnetic resonance imaging (MRI) were included. Our institution's Ethics Committee approved the study (DC-2008-565). The study was performed according to the principles of the Declaration of Helsinki.

Microsatellite stable/instable status (MSS/MSI), *KRAS*, *NRAS* and *BRAF V600E* mutational statuses were determined as previously described (2).

Tissue Microarray Construction and Immunohistochemistry

Formalin-fixed paraffin-embedded (FFPE) blocks were used for tissue microarray (TMA) construction using four biopsy cores of 1 mm diameter per tumor in the tumor center (MTA Booster© version 1.01, Alphelys, Paris, France). Both primary tumors (PT) and BMs, if available, were included in the TMA.

IHC was carried out on paraffin-embedded 3-µm thick TMA sections with antibodies directed against Programmed death-1 (PD-1) (clone NAT105, Roche©), Programmed death-ligand 1 (PD-L1) (clone SP263, Roche©), CD3 (clone F7.2.38, Agilent©) and CD8 (clone C8144B, Dako©) according to the manufacturer's instructions. Once counterstained and permanently mounted, slides were scanned with a Nanozoomer HT2.0 (Hamamatsu Photonics) at ×20 magnification to generate a whole slide imaging (WSI) file in ndpi format (**Figure 1**).

For each TMA core, CD3 positive cells were detected using QuPath© software (12) and exported as a number of positive cells by mm² (TMA core area = 1,13 mm²). DGMate score was calculated for each tumor core as described by Reichling and colleagues (11). Briefly, using QuPath© software, the whole slide was tiled using a DoG superpixel strategy. For each tile QuPath© is able to measure and export 127 parameters related to color, texture or pixel environment within the tile. These parameters are used in a random forest prediction model, called Coloclass (11), to classify tiles in several tissue classes such as tumor, immune patch, healthy and stroma for instance. Next, restricting information to tiles classified as tumors, a score predictive of

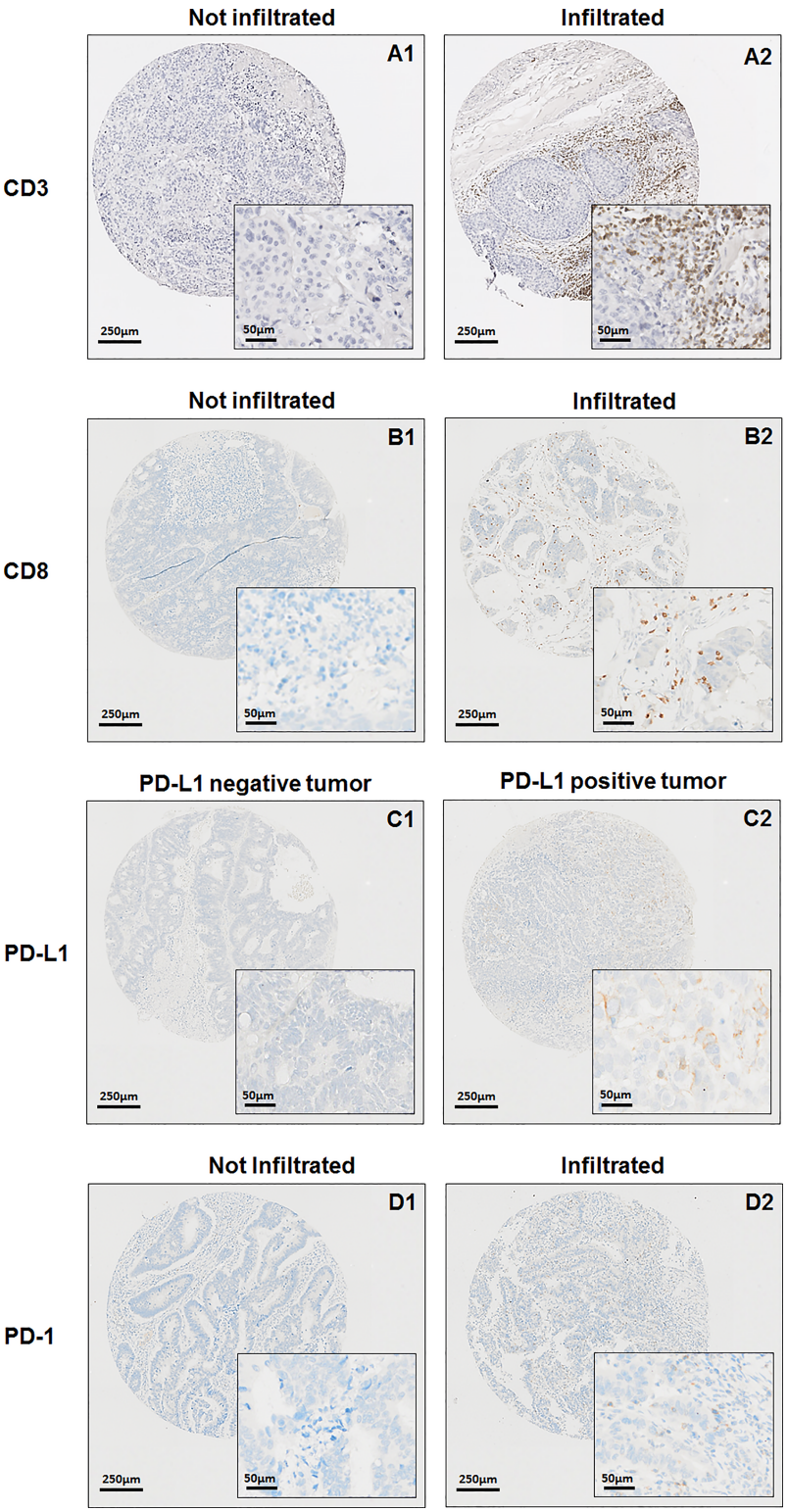

FIGURE 1 | Median overall survival after brain metastases diagnosis. Kaplan-Meier method was used to determine OS.

relapse-free survival in stage III colon cancer, coined DGMate, was estimated through a Cox regression model with lasso method to select a minimum set of predictive parameters. The CD3 lymphocyte surface area and DGMate were quantified automatically both in the tumor core of PT and BM.

PD-1 IHC was considered positive when ≥1% of intra-epithelial tumor infiltrating lymphocytes (TILs) were stained. PD-L1 immunostaining was considered positive when ≥1% of tumor cells had membranous staining. CD3 and CD8 staining were also analyzed as the percentage of both intra-tumoral and stromal CD3 and CD8 positive lymphocytes over the total immune cells (13).

Statistical Analysis

Continuous variables were described with median, standard deviation (SD) and range. Qualitative variables were described with frequency and percentage. Comparisons of characteristics were performed with the non-parametric Mann-Whitney (2 groups) or Kruskall-Wallis (3 groups or more) tests for continuous variables and the chi-square test or Fisher's exact test for qualitative variables. Correlation was determined calculating Spearman's rank-order coefficient.

The primary endpoint was OS, defined by the time between BM diagnosis and death, whatever the causes. Survival curves and 95% confidence intervals (CI) were determined using the Kaplan-Meier method. Predictive factors of OS were evaluated using the log-rank test for univariate analysis and variables with p values ≤0.10 in univariable analyses were included in multivariate analysis using a Cox regression model.

The level of significance was set at a p value of 0.05. All statistical tests were two-sided. Statistical analyses were performed using Statview© 4.0 software (SAS Institute Inc., Cary, NC, USA).

RESULTS

Population

Eighty-three patients were included with PT samples available in 80 cases and BMs tissues available for 37 patients. Samples from both PT and BMs were available for staining analysis for 34 patients. Median age at BM diagnosis was 66.8 years old (**Table 1**). Most patients had a T3 (64.0%) or a T4 (25.3%) tumor with lymph nodes invasion (72.4%). At CRC diagnosis most tumors were stage III or IV (79.2%). *RAS* was mutated in 61.5% of cases and *BRAF* was mutated in 6.4% of cases.

Among the 83 patients included, 96.4% had neurologic symptoms that led to the BM diagnosis. At BM diagnosis most patients had extracranial metastases (ECM) (90.4%) and 81.9% had already received at least one line of chemotherapy for their metastatic disease. Most patients had metachronous BM from PT diagnosis (92.8%) or from ECM diagnosis (80.0%). A minority of patients had synchronous BM at diagnosis of metastatic disease (20.0%). Median interval between BM diagnosis and PT diagnosis was 35.1 ± 3.4 months. Median interval between BM diagnosis and ECM diagnosis was 21.2 ± 2.7 months.

About half of patients had single BM (50.6%), mostly supratentorial only (57.8%). At BM diagnosis half patients had an Eastern Cooperative Oncology Group performance status (ECOG PS) at 2 or more (47.5%).

All in all, 37 patients (44.6%) underwent BM surgery. Decision of BM surgery was decided during a multidisciplinary team meeting based on the performance status of the patient, the

TABLE 1 | Patients, primary tumors and brain metastases characteristics.

n = 83	n (%)
Age at BM diagnosis (median, min-max)	66.8 (36.8-87.1)
Gender	
Male	53 (63.9%)
Female	30 (36.1%)
Site of primary tumor	
Ascending colon	19 (22.9%)
Descending colon	26 (31.3%)
Rectum	34 (41.0%)
Bifocal tumor	4 (4.8%)
Tumor grade	
Well differentiated	24 (33.8%)
Moderately differentiated	38 (53.5%)
Poorly differentiated	9 (12.7%)
Missing data	12
Stage at initial CRC diagnostic	
I	4 (4.9%)
II	13 (15.9%)
III	28 (34.1%)
IV	37 (45.1%)
Missing data	1
Primary tumor resection	73 (88.0%)
ECOG performance status at BM diagnosis	
0	14 (17.5%)
1	28 (35.0%)
2	21 (26.3%)
3	17 (21.2%)
4	0
Missing data	3
Lung metastases at BM diagnosis	
Yes	59 (71.1%)
No	24 (28.9%)
Liver metastases at BM diagnosis	
Yes	36 (43.4%)
No	47 (56.6%)
Site of BM	
Supratentorial only	48 (57.8%)
Subtentorial only	17 (20.5%)
Supra and subtentorial	18 (21.7%)
Number of brain metastases	
Single	42 (50.6%)
Multiple	41 (49.4%)
Interval between primary tumor and BM diagnosis	
Synchronous	6 (7.2%)
Metachronous	77 (92.8%)
Interval between BM and extracranial disease (n=75)	
Synchronous	15 (20.0%)
Metachronous	60 (80.0%)
Molecular characteristics	
RAS: Wild-type/Mutated/Missing data	30 (38.5%)/48 (61.5%)/5
BRAF: Wild-type/Mutated/Missing data	73 (93.6%)/5 (6.4%)/5
MMR status: MSI/MSS/Missing data	4 (5.5%)/69 (94.5%)/10

CRC, colorectal cancer; BM, brain metastases; PT, primary tumor; SD, standard deviation; MMR, mismatch repair; MSS, microsatellite stable; MSI, microsatellite instability; ECOG, Eastern Cooperative Oncology Group.

expected OS, the number, size and location of BM. Most patients (83.0%) underwent radiotherapy of the BM. Among the patients treated with radiotherapy, 23.5% were treated by stereotactic radiosurgery and 69.1% were treated with whole brain radiotherapy. The remaining patients received local radiotherapy without using stereotactic radiosurgery. Among the patients with BM surgery, most have undergone previous chemotherapy for the metastatic disease (59.5%) and adjuvant radiotherapy after BM surgery (94.6%).

CD3 T-Cell Infiltration and DGMate Score in Primary Tumor and Brain Metastases

CD3 T-cell infiltration was higher in PT as compared to BM (78.9/mm^3 versus 19.1/mm^3, p=0.0071) (**Figure 2**). We observed no correlation of CD3 T-cell infiltration between BM and PT (Rho=0.29, p=0.13).

Concerning the rate of the DGMate score there was no statistical difference between PT and BM (p=0.86). We observed a strong correlation between the DGMate score in PT and the DGMate score BM (Rho=0.62, p=0.0004).

Correlation Between CD3 T-Cell Infiltration and DGMate Score With Patient and Tumor Characteristics

Age, gender, tumor grade, stage at initial CRC diagnostic, T stage, N stage, interval between metastases and PT diagnosis, interval between BM and PT diagnosis, interval between BM and ECM diagnosis, *RAS* status, *BRAF* status and MMR status were not associated with CD3 T-cell infiltration in PTs (**Table 2**). CD3 T-cell infiltration in PTs increased with T stage from 24.6/mm^3 for T1 to 100.7/mm^3 for T4 but was not significant (p=0.43). Concerning DGMate score in PTs, using the same patient and tumor characteristics, no statistically difference was observed. DGMate score in PTs increased with T stage from 1.85 for T1 to 1.98 for T4 but was not significant (p=0.31). There was no significant difference in CD3 infiltration or DGMate score in PTs according to the metachronous or synchronous status of the BM from the diagnosis of PT or ECM.

CD3 T-cell infiltration or DGMate score in BMs were not statistically different according to patient or tumor characteristics (**Table 2**).

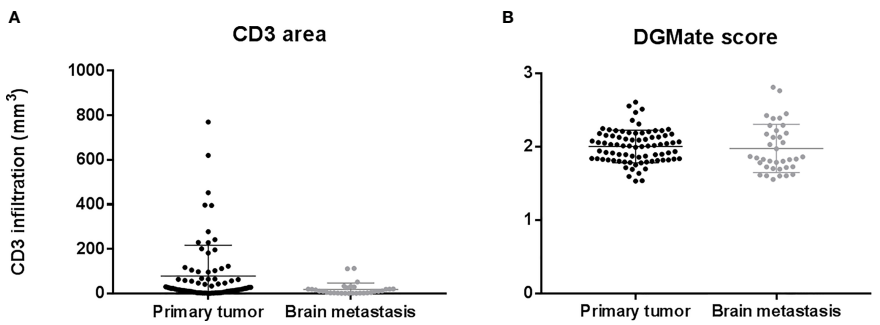

FIGURE 2 | CD3 infiltration **(A)** and DGMate **(B)** in primary tumor and brain metastases.

TABLE 2 | Correlation between CD3 T-cell infiltration and DGMate score with patient and tumor characteristics.

	CD3 area		DGMate score	
	Primary tumor (p value)	Brain metastasis (p value)	Primary tumor (p value)	Brain metastasis (p value)
Age (continuous variable)	0.81	0.09	0.84	0.41
Gender (male vs female)	0.37	0.58	0.22	0.92
Site of primary tumor (ascending colon vs descending colon vs rectum)	0.53	0.42	0.11	0.54
Tumor grade (well and moderately differentiated vs poorly differentiated)	0.08	0.10	0.21	0.26
Stage at initial CRC diagnostic (I vs II vs III vs IV)	0.74	0.94	0.99	0.43
T stage (T1 and T2 vs T3 vs T4)	0.43	0.31	0.44	0.65
N stage (N0 vs N1 vs N2)	0.39	0.22	0.24	0.55
Interval between metastases diagnosis and PT (continuous variable)	0.29	0.73	0.59	0.16
Interval between BM diagnosis and PT (continuous variable)	0.17	0.36	0.27	0.16
Interval between BM and ECM (continuous variable)	0.27	0.16	0.19	0.28
***RAS* status (mutated vs wild-type)**	0.68	0.43	0.70	0.30
***BRAF* status (mutated vs wild-type)**	0.37	0.58	0.79	0.11
MMR status (MSS vs MSI)	0.68	0.35	0.80	0.08

vs, versus; ECM, extracranial metastases; PT, primary tumor; BM, brain metastases; MMR, mismatch repair; MSI, microsatellite instability; MSS, microsatellite stability.

We observed non-significantly higher CD3 T-cell infiltration in rectal tumors compared to colon tumors (108.7 ± 30.4/mm^3 versus 54.9 ± 15.9/mm^3, p=0.26) and a significantly higher DGMate score (2.1 ± 0.1 versus 1.9 ± 0.1, p=0.03) (**Table 3**). When BMs were both supra and subtentorial, mean CD3 T-cell infiltration in PTs (137.1 ± 42.8/mm^3) was higher than when BMs were subtentorial only (85.7 ± 31.2/mm^3) or supratentorial only (53.9 ± 17.5/mm^3) (p=0.36 and p=0.03, respectively). The same trend was observed with CD3 T-cell infiltration in BMs. There was a non-significant increase of CD3 T-cell infiltration in PT and BM when BMs were multiple (p=0.40 and p=0.23, respectively) (**Table 3**). We also observed a trend of higher DGMate score in BM in patients with multiple BMs (2.2 ± 0.1 versus 1.9 ± 0.1, p=0.07).

CD8 T-Cell Infiltration and Expression of PD-L1 In Primary Tumor and Brain Metastases

PTs had CD8 positive T-cells in most cases (93.4%) with a mean of 13.7% CD8+ lymphocyte infiltrates (median 10.0%, range 0-70.0%). BM CD8 positive T-cells were less frequent (62.9%, n=22/35), with a mean of 8.6% of CD8+ lymphocyte infiltrates (median 3.0%, range 0-50.0%). While there was a correlation between CD8 T-cell infiltration in BM and PT (Rho=0.37, p=0.01), CD8 T-cell infiltration was higher in PT as compared to BM (p=0.03).

Primary tumors with PD-1 positive TILs were 13.3% but no BM with PD-1 positive TILs was found in the available samples. We observed only 6.8% PTs with PD-L1 positive TILs and there were two BMs with PD-L1 positive TILs (n=2/35, 5,7%). Both BMs with PD-L1 positive TILs had PTs with no PD-L1 positive TILs. Among the PTs with PD-L1 positive TILs, only one had an available BM sample and it was negative for PD-L1 TILs.

Prognostic Value of Immune T-Cell Infiltration and DGMate Score

Median OS after PT diagnosis was 41.0 ± 1.5 months. Median OS after BM diagnosis was 3.9 ± 0.5 months (**Figure 3**). Patient and tumor characteristics associated with OS after BM diagnosis were

TABLE 3 | CD3 T-cell infiltration and DGMate score in primary tumor and brain metastases according to BM site and BM numbers.

	Primary Tumor			Brain Metastases		
	n	CD3 area*	DGMate	n	CD3 area*	DGMate
Site of primary tumor						
Colon	42	54.9 ± 15.9	1.9 ± 0.1	24	16.0 ± 17.5	2.0 ± 0.1
Rectum	34	108.7 ± 30.4	2.1 ± 0.1	12	28.2 ± 12.5	2.0 ± 0.1
Site of BM						
Supratentorial only	46	53.9 ± 17.5	2.0 ± 0.1	23	15.3 ± 5.5	1.9 ± 0.1
Subtentorial only	16	85.7 ± 31.2	2.0 ± 0.1	13	17.4 ± 5.1	2.0 ± 0.1
Supra and subtentorial	18	137.1 ± 42.8	2.0 ± 0.1	1	113.2	2.2
Number of BM						
Unique BM	39	64.6 ± 21.3	2.0 ± 0.1	30	15.8 ± 4.7	1.9 ± 0.1
Multiple BM	41	92.1 ± 22.6	2.0 ± 0.1	7	32.9 ± 16.6	2.2 ± 0.1

** Mean CD3 infiltration was expressed by mm^3.*

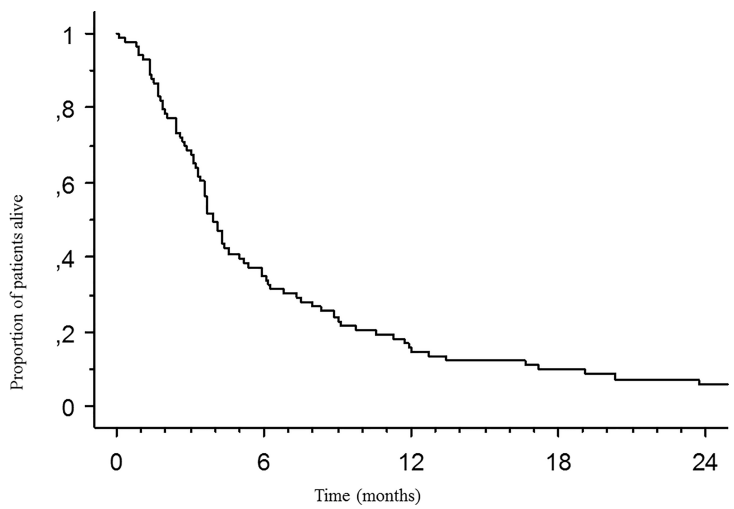

FIGURE 3 | Median overall survival (OS) after brain metastasis diagnosis. Kaplan Meier method was used to determine OS.

age, site of primary tumor, ECOG PS, *BRAF* status, site of BMs, number of BMs and lung metastases in univariate analysis (**Table 4**). Neither CD3 infiltration nor DGMate score in PT or BM was correlated with OS. In multivariate analysis, only ECOG PS 0-1 and absence of lung metastasis were associated with better OS.

Neither CD3 infiltration nor DGMate score in PT or BM was correlated with OS from CRC diagnosis (**Figures 4A, B**). In addition, CD3 infiltration or DGMate score in patients with metastatic or non-metastatic disease at CRC diagnosis had no prognostic impact.

Since CD3 T-cell infiltration and/or DGMate scores were different according to PT site, BMs location and BMs number, we looked for a potential prognostic impact in these subgroups. When DGMate score was divided in two groups according to the median, high DGMate score in BM was associated with longer OS in two subgroups: patients with multiple BMs (20.3 ± 3.8 months versus 3.7 ± 4.0 months, p=0.06) and patients with rectal tumor (13.4 ± 6.1 months versus 6.1 ± 1.4 months, p=0.02) (**Figures 5A, B**). When CD3 T-cell infiltration was divided in two groups according to the median, high CD3 T-cell infiltration in BM was associated with lower OS in two subgroups: patients with colon tumor (4.6 ± 2.3 months versus 12.0 ± 5.5 months, p=0.02) and patients with supratentorial BMs (9.8 ± 3.3 months versus 16.7 ± 5.9 months, p=0.03) (**Figures 6A, B**).

PD-L1 positive PTs were associated with worse OS from CRC diagnosis (10.1 ± 6.6 months versus 43.1 ± 1.6 months, p=0.01) (**Figure 4D**). CD8 T-cell infiltration in PT was not correlated with OS (**Figure 4C**). Nor PD-L1 positive BM or CD8 T-cell infiltration in BM was correlated with OS after BM diagnosis.

DISCUSSION

This large series of 83 CRC patients with BM displayed lower CD3 and CD8 T-cell infiltration in BMs compared with PTs. In PTs there was a trend of higher CD3 T-cell infiltration in rectal tumor, when BMs were both supra and subtentorial and when BMs were multiple. No correlation was found between CD3 or CD8 infiltration in PT or BM and OS in overall population. Patients with high CD3 T-cell infiltration in BMs had a lower OS in two subgroups: patients with colon tumor and patients with supratentorial BMs. In contrast to locally advanced CRC, CD3 and CD8 infiltration and DGMate score were not robust prognostic factor in CRC patients with BM. PD-L1 positive PTs or BMs were rare but PD-L1 positive PTs were associated with worse OS from CRC diagnosis.

Our series of 83 CRC patients with BM had similar patients and tumor characteristics as previously described, i.e. frequent rectal tumor, lung metastases, synchronous metastatic disease and *RAS*-mutated tumors (1, 3). In addition, CRCs are associated with different clinicopathological features according to the type of *RAS* mutation (14). Most CRC-derived BMs were metachronous (more than 90%) and with a median interval of more than 30 months from PT diagnosis (3, 15, 16).

For the first time we analyzed immune infiltrates in both PT and BM in a series of CRC-derived BMs. We determined CD3 infiltration using artificial intelligence and the validated DGMate score, as well as CD8 infiltration, PD-L1 and PD-1 positive tumors (11, 12). CD3 and CD8 T-cell infiltration were higher in PTs as compared to BMs. To our knowledge, no other study has evaluated correlations between lymphocyte infiltration in BM and PT in CRC. Nevertheless, lymphocytes are typically absent from the healthy brain parenchyma (17). Most primary brain tumors contain few TILs, but some reports have suggested the presence of dense TIL infiltrates in BMs of different cancer types (9). In this series, most PTs were lung or breast cancers and correlation between PT and BM infiltrates was not analyzed. In a series of 46 matched samples of breast primary tumors and breast-derived BMs, BMs were positive for TILs in only 36% of cases compared to 82% of primary breast tumors (18). No correlation was established between CD3 infiltration in BMs and PTs in our series of CRC. To our knowledge, only one study has evaluated PD-L1 expression in BMs as compared to PTs in breast cancer and no difference was found between the two sites (18). In our series of CRC-derived BMs, PD-L1 overexpression was rare in both BMs and PTs. Moreover, PD-L1 overexpression in BMs was not associated with PD-L1 overexpression in PTs and vice versa. Angelova et al. analyzed both the clonal tumor cell evolution and immune landscape between PT and metastatic sites in two patients with metastatic CRC (19). They studied immune disparity from one metastatic site to another and showed that immunoediting is at work at the metastatic stage of CRC. The studied patients did not present BM but, in contrast to lung, breast cancers and melanoma, BMs represent a terminal evolution of CRCs. Immune response is expected to evolve drastically between the PT and the BM. Different rounds of chemotherapy may affect immune effectors, especially after a long disease history, which is the case in most CRC-derived BMs (20). These points could explain the absence of correlation of CD3 infiltration between BM and PT in our series of CRC-derived BMs. The lower CD3 T-cell infiltrates in BMs as compared to primary CRCs confirms the difficulties of T-cell recruitment in BMs.

In CRC, CD3 T-cell infiltrate in PTs has been associated with patient and tumor characteristics. Higher T and N stages have been associated with lower T-cell infiltration (11, 21). By contrast, in our study, we observed in PTs a trend of higher CD3 T-cell infiltration in higher T stages and no correlation with N stages. We also noted a non-significantly higher CD3 T-cell infiltration in rectal tumors compared to colon tumors. Our series was a subgroup of rare CRCs with BM whose T-cell infiltration had never been evaluated before. Moreover, CD3 staining covered different types of effector T-cells and infiltrates are different between tumor center and invasion front but in our series, only tumor center was studied (5, 11, 21, 22). Reichling et al. (11) evaluated CD3 T-cell infiltrates with the same method but only in stage III colon cancer, which is a different series compared to ours.

To our knowledge, no study has previously evaluated the correlation of CD3 infiltration with BM characteristics. We observed that CD3 T-cell infiltration in PT was higher when BMs were both supra and subtentorial. In addition, there was a trend of more CD3 T-cell infiltration in PT and BM when BMs were multiple. Caution and confirmation on a larger cohort are

TABLE 4 | Prognostic factors of overall survival from brain metastases diagnosis.

Variables	n	Univariate analysis		Multivariate analysis		
		Median (months)	p value	HR	95% CI	p value
Gender			0.98*			0.67
Male	53	3.9		1		
Female	30	4.1		0.9	0.5-1.5	
Age at BM diagnosis#	83		0.03*	1.0	1.0-1.0	0.82
Site of primary tumor (n=79)			0.05*			0.20
Colon	45	4.6		1		
Rectum	34	2.8		1.4	0.8-2.4	
Tumor grade (n=71)			0.59			
Well or moderately differentiated	62	3.7				
Poorly differentiated	9	4.6				
Primary tumor resection			0.74			
Yes	73	3.7				
No	10	3.9				
ECOG PS at BM diagnosis			<0.01*			0.03
0 or 1	42	6.8		1		
2 or 3	38	3.1		2.1	1.1-4.0	
***RAS* status**			0.66			
Wild-type	30	3.6				
Mutant	48	4.1				
***BRAF* status**			0.04*			0.38
Wild-type	73	4.1		1		
Mutant	5	3.3		1.7	0.5-5.6	
Site of BM			0.01*			0.27
Supratentorial only	48	4.3		1		
Subtentorial only	17	4.6		0.6	0.3-1.3	
Supra and subtentorial	18	2.8		1.2	0.5-2.9	
Number of brain metastases			<0.01*			0.13
Single	42	6.2		1		
Multiple	41	3.1		1.7	0.9-3.2	
Interval between PT and BM diagnosis			0.20			
Synchronous	6	11.7				
Metachronous	77	3.9				
Interval between BM and extracranial disease (n=75)			0.11			
Synchronous	15	6.3				
Metachronous	60	3.7				
Lung metastases at BM diagnosis			<0.01*			0.02
No	24	8.9		1		
Yes	59	3.7		2.0	1.1-3.8	
Liver metastases at BM diagnosis						
No	47	4.1	0.17			
Yes	36	3.6				
CD3 T-cell infiltration in PT#	79		0.15			
CD3 T-cell infiltration in BM#	31		0.91			
DGMate score in PT#	80		0.71			
DGMate score in BM#	37		0.84			
CD3 T-cell infiltration in PT¤			0.45			
Low	40	3.7				
High	39	3.9				
CD3 T-cell infiltration in BM¤			0.23			
Low	14	10.6				
High	15	7.5				
DGMate score in PT¤			0.78			
Low	40	4.1				
High	40	3.3				
DGMate score in BM¤			0.92			
Low	19	8.0				
High	18	9.8				

HR, hazard ratio; BM, brain metastasis(es); PT, primary tumor; 95% CI, 95% confidence interval; ECOG PS, Eastern Cooperative Oncology Group score performances status.

**variables included in multivariate analysis.*

#analyses as continuous variable.

¤scores split at median.

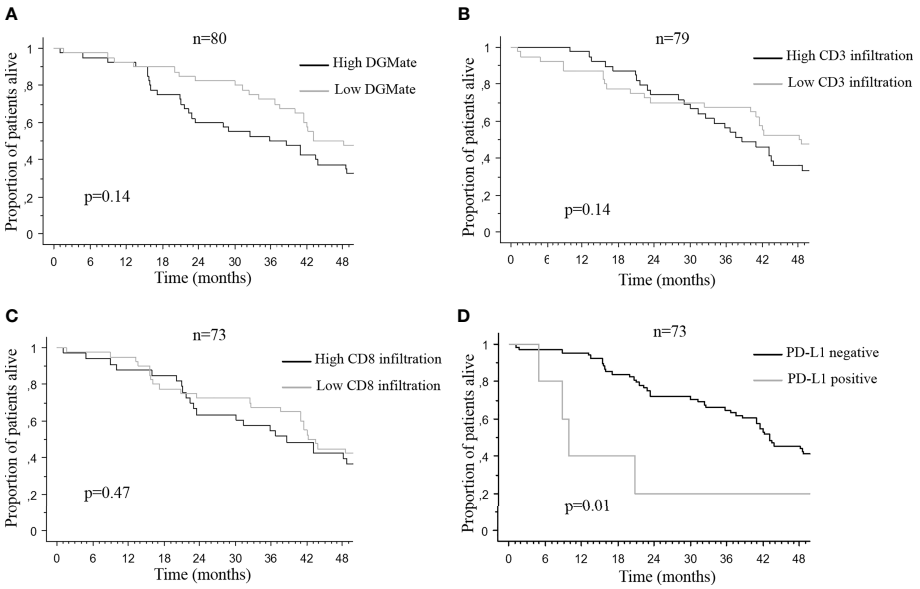

FIGURE 4 | Median overall survival after brain metastases diagnosis according to DGMate score **(A)**, CD3 infiltrating T-cells **(B)**, CD8 infiltrating T-cells **(C)**, and PDL1 positive tumors **(D)** in primary tumor. Kaplan-Meier method was used to determine OS. DGMate, CD3 and CD8 scores were split at median and p valuecalculated using the Logrank test.

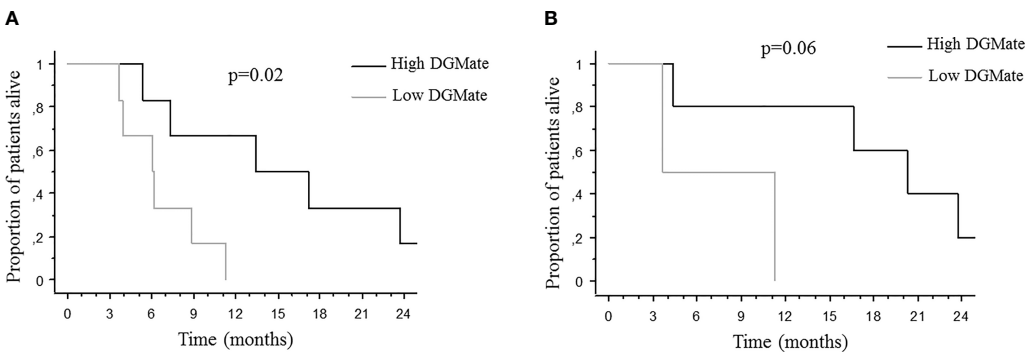

FIGURE 5 | Median overall survival after brain metastases diagnosis according to DGMate score in BM among patients with rectal tumor **(A)** and patients with multiple BMs **(B)**. Kaplan-Meier method was used to determine OS. DGMate score was split at median and p value calculated using the Logrank test.

required to interpret these data given the low number of patients in each subgroup. Higher T-cell infiltration in BM could represent microenvironment modification due to cancer cell aggressiveness, which correlates with their ability to colonize both the infra and supra-tentorial brain.

DGMate score was first built and validated in stage III colon cancers (11). In this setting, DGMate score increased with T and N stages. In our series, DGMate score did not differ between PT and BM. Furthermore, we observed a strong correlation between the DGMate score in PT and BM, suggesting that this prognostic score had no major change during tumor progression. Our results indicate that although the immune environment is reshaped from PT to BM, other tumor characteristics taken into account by the DGMate score were stable despite time evolution and treatments. As in the PETACC08 study, there was a trend of higher DGMate score in PT with higher T stage. DGMate score was also higher in rectal tumors as compared to colon tumors. We also observed a trend of higher DGMate score in BM in patients with multiple BMs. These correlations suggest that DGMate score could be a surrogate marker of tumor aggressiveness in CRC-derived BM, as is already described in stage III CRC.

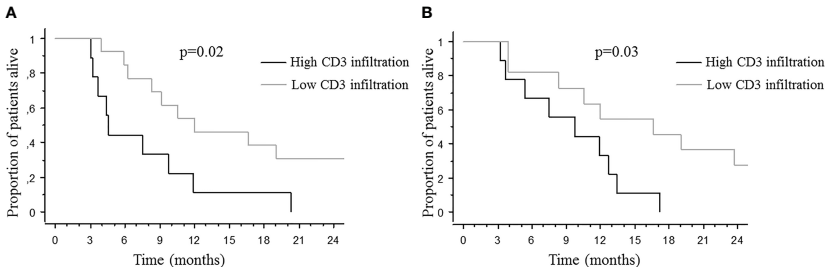

FIGURE 6 | Median overall survival after brain metastases diagnosis according to CD3 T-cell infiltration in BM among patients with colon cancer **(A)** and supratentorial BMs **(B)**. Kaplan-Meier method was used to determine OS. CD3 T-cell infiltration score was split at median and p value calculated using the Logrank test.

CD3 and/or CD8 T-cell infiltrates have been associated with CRC prognosis in many studies (5, 11, 21, 23). Nevertheless, in our series of CRC-derived BM, CD3 and CD8 infiltration in PT or BM did not correlate with OS. CD3 was questioned as a prognostic factor in locally advanced CRC and immune scores were developed to overcome the approximation linked to this single marker. More importantly, there is no strong evidence that CD3, CD8 or immune scores in PT of mCRC are predictive factors of OS. Several studies have shown discordance in immune cell infiltration between PT and metastases, but these studies focused mainly on liver or lung metastases (24–26). Moreover, some studies have suggested that the least immune-infiltrated metastasis predict OS in mCRC (10, 20, 26). These observations could explain why CD3 and CD8 infiltrates in PT or BM were not a prognostic factor in our series of mCRC with BM. As a positive CD3 staining covers different types of effector T-cells, some groups showed that a subgroup analysis of T-cells was required to establish a correlation of immune infiltration with prognosis at a metastatic stage, for instance in lung metastases (22). In contrast, in liver metastases, CD3 alone was correlated with OS (27). Furthermore, in a series of BMs derived from melanoma, lung, breast and renal cancers, the most frequently observed high immune infiltration involved CD3 positive cells and was associated with OS (9). In CRC, BM is a late event with poor prognosis. We analyzed only 37 BMs, which made correlations between T-cell infiltration in BM and OS difficult to establish. By contrast, PD-L1 positive PTs were associated with worse OS from CRC diagnosis. It is worth noting that only 5 PTs (6.8%) were PD-L1 positive. Our study showed comparable proportions of PD-L1 positive tumors when compared with other studies in the literature (28, 29). This association with OS should be interpreted with caution considering the small number of patients with PD-L1 positive tumors and potential tumor heterogeneity. High PD-L1 expression has been associated with longer OS in mCRC in some studies, but not all (30, 31). In addition, in lung cancers with BMs, PD-L1 expression has been associated with worse OS (30). Larger studies are needed to confirm the prognostic value of PD-L1 expression in cancer patients with BM.

DGMate score was associated with stage III colon cancer prognosis (11). In our cohort, DGMate score in PT did not correlate with OS. We hypothesized that the disease stage could account for this result since it was formed mainly of T3-T4 stage primary tumors (about 80%) and only stage III colon cancers by contrast to our series with only 34.1% of stage III CRC at diagnosis. At the BM site, DGMate score was not associated with OS. DGMate score is a tumor signature of 127 parameters whose interpretation might be intrinsic to each type of tissue and could differ from one type of tissue to another. Previously published prognostic factors in patients with BM from CRC were identified in our series, like ECOG PS and lung metastases (3).

Since CD3 T-cell infiltration and/or DGMate score were different according to PT site, BM site and BM number, we looked at a potential prognostic impact in these subgroups. High CD3 T-cell infiltration in BM was associated with lower OS in the subgroup of patients with supratentorial BMs. In addition, high DGMate score in BMs was associated with longer OS in two subgroups: patients with multiple BMs and patients with rectal tumor. Larger series are required to validate these associations. Supratentorial BMs were previously associated with better prognosis and multiple BMs with poor prognosis (3).

CONCLUSION

CD3 and CD8 infiltration, PD-L1 expression and DGMate score at the brain metastatic site do not predict OS in patients with BMs from CRC. Our results suggest that immune response in CRC-derived BM differs from other CRC metastatic sites and further basic research focused on these lesions is required.

DATA AVAILABILITY STATEMENT

The raw data supporting the conclusions of this article will be made available by the authors, without undue reservation.

ETHICS STATEMENT

The studies involving human participants were reviewed and approved by local ethics committee (DC-2008-565). Written informed consent for participation was not required for this

study in accordance with the national legislation and the institutional requirements.

AUTHOR CONTRIBUTIONS

VR, LT, FG, and DT performed study concept and design. AD, SE, VD, PR, and JG performed development of methodology and carried out the experiments. AD, JG, and EF contributed to sample preparation. VR, FG, and DT contributed to the interpretation of the results. DT and VR took the lead in writing the first draft of the manuscript. All authors contributed to the article and approved the submitted version.

FUNDING

This work was supported by a grant from the associations "Sport et Collection" and "Ligue Contre le Cancer, Comités départementaux de la Vienne, Charente et Charente-Maritime".

ACKNOWLEDGMENTS

The authors thank Jeffrey Arsham for English proofreading of the manuscript.

REFERENCES

1. Christensen TD, Spindler K-LG, Palshof JA, Nielsen DL. Systematic Review: Brain Metastases From Colorectal Cancer—Incidence and Patient Characteristics. *BMC Cancer* (2016) 16(1):260. doi: 10.1186/s12885-016-2290-5
2. Roussille P, Tachon G, Villalva C, Milin S, Frouin E, Godet J, et al. Pathological and Molecular Characteristics of Colorectal Cancer With Brain Metastases. *Cancers* (2018) 10(12):504. doi: 10.3390/cancers10120504
3. Roussille P, Auvray M, Vansteene D, Lecomte T, Rigault E, Maillet M, et al. Prognostic Factors of Colorectal Cancer Patients With Brain Metastases. *Radiother Oncol* (2021) 158:6773. doi: 10.1016/j.radonc.2021.02.006
4. Mege D, Sans A, Ouaissi M, Iannelli A, Sielezneff I. Brain Metastases From Colorectal Cancer: Characteristics and Management. *ANZ J Surg* (2018) 88 (3):1405. doi: 10.1111/ans.14107
5. Galon J, Costes A, Sanchez-Cabo F, Kirilovsky A, Mlecnik B, Lagorce-Pagès C, et al. Type, Density, and Location of Immune Cells Within Human Colorectal Tumors Predict Clinical Outcome. *Science* (2006) 313 (5795):19604. doi: 10.1126/science.1129139
6. Pagès F, André T, Taieb J, Vernerey D, Henriques J, Borg C, et al. Prognostic and Predictive Value of the Immunoscore in Stage III Colon Cancer Patients Treated With Oxaliplatin in the Prospective IDEA France PRODIGE-GERCOR Cohort Study. *Ann Oncol* (2020) 31(7):9219. doi: 10.1016/j.annonc.2020.03.310
7. Laghi L, Bianchi P, Miranda E, Balladore E, Pacetti V, Grizzi F, et al. CD3+ Cells at the Invasive Margin of Deeply Invading (Pt3-T4) Colorectal Cancer and Risk of Post-Surgical Metastasis: A Longitudinal Study. *Lancet Oncol* (2009) 10(9):87784. doi: 10.1016/S1470-2045(09)70186-X
8. Baldin P, Van den Eynde M, Mlecnik B, Bindea G, Beniuga G, Carrasco J, et al. Prognostic Assessment of Resected Colorectal Liver Metastases Integrating Pathological Features, RAS Mutation and Immunoscore. *J Pathol Clin Res* (2021) 7(1):2741. doi: 10.1002/cjp2.178
9. Berghoff AS, Fuchs E, Ricken G, Mlecnik B, Bindea G, Spanberger T, et al. Density of Tumor-Infiltrating Lymphocytes Correlates With Extent of Brain Edema and Overall Survival Time in Patients With Brain Metastases. *Oncoimmunology* (2016) 5(1):e1057388. doi: 10.1080/2162402X.2015.1057388
10. Mlecnik B, Van den Eynde M, Bindea G, Church SE, Vasaturo A, Fredriksen T, et al. Comprehensive Intrametastatic Immune Quantification and Major Impact of Immunoscore on Survival. *J Natl Cancer Inst* (2018) 110(1):97–108. doi: 10.1093/jnci/djx123
11. Reichling C, Taieb J, Derangere V, Klopfenstein Q, Le Malicot K, Gornet J-M, et al. Artificial Intelligence-Guided Tissue Analysis Combined With Immune Infiltrate Assessment Predicts Stage III Colon Cancer Outcomes in PETACC08 Study. *Gut* (2020) 69(4):68190. doi: 10.1136/gutjnl-2019-319292
12. Bankhead P, Loughrey MB, Fernández JA, Dombrowski Y, McArt DG, Dunne PD, et al. QuPath: Open Source Software for Digital Pathology Image Analysis. *Sci Rep* (2017) 7(1):16878. doi: 10.1038/s41598-017-17204-5
13. Tougeron D, Fauquembergue E, Rouquette A, Le Pessot F, Sesboüé R, Laurent M, et al. Tumor-Infiltrating Lymphocytes in Colorectal Cancers With Microsatellite Instability are Correlated With the Number and Spectrum of Frameshift Mutations. *Mod Pathol* (2009) 22(9):1186–95. doi: 10.1038/modpathol.2009.80
14. Rimbert J, Tachon G, Junca A, Villalva C, Karayan-Tapon L, Tougeron D. Association Between Clinicopathological Characteristics and RAS Mutation in Colorectal Cancer. *Mod Pathol* (2018) 31(3):517–26. doi: 10.1038/modpathol.2017.119
15. Tanriverdi O, Kaytan-Saglam E, Ulger S, Bayoglu IV, Turker I, Ozturk-Topcu T, et al. The Clinical and Pathological Features of 133 Colorectal Cancer Patients With Brain Metastasis: A Multicenter Retrospective Analysis of the Gastrointestinal Tumors Working Committee of the Turkish Oncology Group (TOG). *Med Oncol* (2014) 31(9):152. doi: 10.1007/s12032-014-0152-z
16. Berghoff AS, Schur S, Füreder LM, Gatterbauer B, Dieckmann K, Widhalm G, et al. Descriptive Statistical Analysis of a Real Life Cohort of 2419 Patients With Brain Metastases of Solid Cancers. *ESMO Open* (2016) 1(2):e000024. doi: 10.1136/esmoopen-2015-000024
17. Galea I, Bechmann I, Perry VH. What Is Immune Privilege (Not)? *Trends Immunol* (2007) 28(1):128. doi: 10.1016/j.it.2006.11.004
18. Ogiya R, Niikura N, Kumaki N, Yasojima H, Iwasa T, Kanbayashi C, et al. Comparison of Immune Microenvironments Between Primary Tumors and Brain Metastases in Patients With Breast Cancer. *Oncotarget* (2017) 8 (61):103671–81. doi: 10.18632/oncotarget.22110
19. Angelova M, Mlecnik B, Vasaturo A, Bindea G, Fredriksen T, Lafontaine L, et al. Evolution of Metastases in Space and Time Under Immune Selection. *Cell* (2018) 175(3):751–65.e16. doi: 10.1016/j.cell.2018.09.018
20. Van den Eynde M, Mlecnik B, Bindea G, Fredriksen T, Church SE, Lafontaine L, et al. The Link Between the Multiverse of Immune Microenvironments in Metastases and the Survival of Colorectal Cancer Patients. *Cancer Cell* (2018) 34(6):1012–26.e3. doi: 10.1016/j.ccell.2018.11.003
21. Pagès F, Berger A, Camus M, Sanchez-Cabo F, Costes A, Molidor R, et al. Effector Memory T Cells, Early Metastasis, and Survival in Colorectal Cancer. *N Engl J Med* (2005) 353(25):265466. doi: 10.1056/NEJMoa051424
22. Schweiger T, Berghoff AS, Glogner C, Glueck O, Rajky O, Traxler D, et al. Tumor-Infiltrating Lymphocyte Subsets and Tertiary Lymphoid Structures in Pulmonary Metastases From Colorectal Cancer. *Clin Exp Metastasis* (2016) 33 (7):72739. doi: 10.1007/s10585-016-9813-y
23. Mlecnik B, Bifulco C, Bindea G, Marliot F, Lugli A, Lee JJ, et al. Multicenter International Society for Immunotherapy of Cancer Study of the Consensus Immunoscore for the Prediction of Survival and Response to Chemotherapy in Stage III Colon Cancer. *J Clin Oncol* (2020) 38(31):363851. doi: 10.1200/JCO.19.03205
24. Halama N, Spille A, Lerchl T, Brand K, Herpel E, Welte S, et al. Hepatic Metastases of Colorectal Cancer are Rather Homogeneous But Differ From Primary Lesions in Terms of Immune Cell Infiltration. *Oncoimmunology* (2013) 2(4):e24116. doi: 10.4161/onci.24116
25. Van den Eynde M, Mlecnik B, Bindea G, Galon J. Multiverse of Immune Microenvironment in Metastatic Colorectal Cancer. *Oncoimmunology* (2020) 9(1):1824316. doi: 10.1080/2162402X.2020.1824316
26. Ahtiainen M, Elomaa H, Väyrynen JP, Wirta E-V, Kuopio T, Helminen O, et al. Immune Contexture of MMR-Proficient Primary Colorectal Cancer and Matched Liver and Lung Metastases. *Cancers (Basel)* (2021) 13(7). doi: 10.3390/cancers13071530
27. Donadon M, Hudspeth K, Cimino M, Di Tommaso L, Preti M, Tentorio P, et al. Increased Infiltration of Natural Killer and T Cells in Colorectal Liver Metastases Improves Patient Overall Survival. *J Gastrointest Surg* (2017) 21 (8):1226–36. doi: 10.1007/s11605-017-3446-6

28. Gatalica Z, Snyder C, Maney T, Ghazalpour A, Holterman DA, Xiao N, et al. Programmed Cell Death 1 (PD-1) and its Ligand (PD-L1) in Common Cancers and Their Correlation With Molecular Cancer Type. *Cancer Epidemiol biomark Prev* (2014) 23(12):2965–70. doi: 10.1158/1055-9965.EPI-14-0654
29. Lee LH, Cavalcanti MS, Segal NH, Hechtman JF, Weiser MR, Smith JJ, et al. Patterns and Prognostic Relevance of PD-1 and PD-L1 Expression in Colorectal Carcinoma. *Mod Pathol* (2016) 29(11):1433–42. doi: 10.1038/modpathol.2016.139
30. Téglási V, Reiniger L, Fábián K, Pipek O, Csala I, Bagó AG, et al. Evaluating the Significance of Density, Localization, and PD-1/PD-L1 Immunopositivity of Mononuclear Cells in the Clinical Course of Lung Adenocarcinoma Patients With Brain Metastasis. *Neuro-Oncology* (2017) 19(8):1058–67. doi: 10.1093/neuonc/now309
31. Droeser RA, Hirt C, Viehl CT, Frey DM, Nebiker C, Huber X, et al. Clinical Impact of Programmed Cell Death Ligand 1 Expression in Colorectal Cancer. *Eur J Cancer* (2013) 49(9):2233–42. doi: 10.1016/j.ejca.2013.02.015

Conflict of Interest: The authors declare that the research was conducted in the absence of any commercial or financial relationship that could be construed as a potential conflict of interest.

Publisher's Note: All claims expressed in this article are solely those of the authors and do not necessarily represent those of their affiliated organizations, or those of the publisher, the editors and the reviewers. Any product that may be evaluated in this article, or claim that may be made by its manufacturer, is not guaranteed or endorsed by the publisher.

frontiers in Oncology

REVIEW
published: 26 October 2021
doi: 10.3389/fonc.2021.711405

The Role of the Immune Response in Brain Metastases: Novel Imaging Biomarkers for Immunotherapy

Rasheed Zakaria[1,2], *Mark Radon*[3], *Samantha Mills*[3], *Drew Mitchell*[4], *Carlo Palmieri*[2], *Caroline Chung*[5] *and Michael D. Jenkinson*[2,6*]

[1] Department of Neurosurgery, University of Texas M.D.Anderson Cancer Center, Houston, TX, United States, [2] Faculty of Health and Life Sciences, University of Liverpool, Liverpool, United Kingdom, [3] Department of Radiology, Walton Centre NHS Foundation Trust, Liverpool, United Kingdom, [4] Department of Imaging Physics, University of Texas M.D.Anderson Cancer Center, Houston, TX, United States, [5] Department of Radiation Oncology, University of Texas M.D.Anderson Cancer Center, Houston, TX, United States, [6] Department of Neurosurgery, Walton Centre NHS Foundation Trust, Liverpool, United Kingdom

Brain metastases are a major clinical problem, and immunotherapy offers a novel treatment paradigm with the potential to synergize with existing focal therapies like surgery and radiosurgery or even replace them in future. The brain is a unique microenvironment structurally and immunologically. The immune response is likely to be crucial to the adaptation of systemic immune modulating agents against this disease. Imaging is frequently employed in the clinical diagnosis and management of brain metastasis, so it is logical that brain imaging techniques are investigated as a source of biomarkers of the immune response in these tumors. Current imaging techniques in clinical use include structural MRI (post-contrast T1W sequences, T2, and FLAIR), physiological sequences (perfusion- and diffusion-weighted imaging), and molecular imaging (MR spectroscopy and PET). These are reviewed for their application to predicting and measuring the response to immunotherapy in brain metastases.

Keywords: immune response, brain metastasis (BM), microenvironment, immunotherapy, biomarkers, MRI, PET

OPEN ACCESS

Edited by:
Frits Thorsen,
University of Bergen, Norway

Reviewed by:
Lisa Sevenich,
Georg Speyer Haus, Germany
Andreas Pircher,
Innsbruck Medical University, Austria

***Correspondence:**
Michael D. Jenkinson
michael.jenkinson@liverpool.ac.uk

Specialty section:
This article was submitted to Cancer Immunity and Immunotherapy, a section of the journal Frontiers in Oncology

Received: *18 May 2021*
Accepted: *30 September 2021*
Published: *26 October 2021*

Citation:
Zakaria R, Radon M, Mills S, Mitchell D, Palmieri C, Chung C and Jenkinson MD (2021) The Role of the Immune Response in Brain Metastases: Novel Imaging Biomarkers for Immunotherapy. Front. Oncol. 11:711405. doi: 10.3389/fonc.2021.711405

INTRODUCTION

The overall clinical burden from brain metastases (BM) is increasing, most likely to due to more widespread use of brain imaging, even in asymptomatic patients, and improved control of extracranial disease and survival in cancers that predispose to BM. Incidence increases with age and varies with the primary, being most common in non-small-cell lung cancer, breast cancer, and

Abbreviations: ADC, apparent diffusion coefficient; BM, brain metastases; CAR, chimeric antigen receptor; CBF, cerebral blood flow; CBV, cerebral blood volume; DCE-MRI, dynamic contrast enhanced MRI; DSC-MRI, dynamic susceptibility contrast MRI; DTI, diffusion tensor imaging; DWI, diffusion-weighted imaging; FA, fractional anisotropy; FDG, F-18 fluorodeoxyglucose; FLT, F-18 flourothymidine; FET, O-(2-[18F]fluoroethyl)-L-tyrosine; FLAIR, fluid attenuated inversion recovery; GBM, glioblastoma multiforme; ICI, immune checkpoint inhibitors; MD, mean diffusivity; NSCLC, non-small-cell lung cancer; PET, positron emission tomography; PWI, perfusion-weighted imaging; ROI, region of interest; RSI, restriction spectrum imaging; SUV, standard uptake value; T1W, T1 weighted; T2W, T2 weighted; TBR, tumor-to-brain ratio; VOI, volume of interest.

malignant melanoma. This has led to BM occupying substantially more of the neurosurgery, radiology, and oncology workload compared to other brain tumors in recent years (1).

Immunotherapy is a transformative field of treatment for cancer and encompasses a variety of therapeutics including vaccines, oncolytic viruses, cell-based therapies, and immune checkpoint inhibitors (ICI). A number of trials of ICI for solid organ cancers that have included patients with BM suggest a heterogeneous but robust response in the brain [(2) summary (3), for specific example in metastatic melanoma]. This has come on the background of increased investigation of the BM microenvironment and the understanding that this is an immunologically distinct rather than immune-isolated compartment (4, 5). The immune response to BM therefore requires further investigation, to elucidate both the underlying mechanism of this response and that of resistance to therapeutics. Imaging is frequently used in the diagnosis and management of BM, so it is logical that brain imaging techniques are used to investigate the immune response and as a possible source of biomarkers of the immune microenvironment in these tumors (6–9).

At the time of writing this report, there was insufficient data in this field for a systematic review applying PRISMA (10) guidelines; therefore, we have performed a narrative review and categorized the *clinically available* techniques in brain imaging—taking in studies from other brain tumors and therapies—to assess the prospects for the development of biomarkers of response to immunotherapy in BM.

CONVENTIONAL MRI BIOMARKERS OF EARLY TREATMENT RESPONSE

The radiological evaluation of BM response to therapy has fundamentally relied on tumor size on T1-weighted (T1W) contrast-enhanced MRI. Within the context of clinical trials—the Response Assessment in Neuro-Oncology Brain Metastases (RANO-BM) group guidance of 2015—up to five target lesions are identified and measured; these ideally should be large, easily evaluated, and not pretreated (11). There are a variety of definitions of what constitutes a measurable target lesion, but the group suggested these should be at least 10 mm in diameter. The intracranial response was recognized as being independent of extracranial response and accounts for this measured size plus clinical condition and corticosteroid dose. From a radiological perspective, the biomarker here is simply the tumor diameter in its longest axis. A percentage decrease (30% or more for partial response, 100% for complete response) or increase (20% or more for progressive disease) of the summed diameters is used as a surrogate of the true, unmeasurable biological disease response to therapy.

These current RANO methods are two-dimensional, but volume of disease may replace size for a variety of reasons in the future (12). Regarding thresholds, a volumetric change of 20% appears to be a reproducible figure between different readers and may be associated with neurological improvement (13, 14), although the RANO-BM group was more conservative and suggested a 65% volume decrease (corresponding to a 30% diameter reduction, subject to the assumption of a spherical lesion) as a safer cutoff for defining a partial response to therapy (11). In summary, tumor volume is not part of standard clinical reporting to assess response at present, but is useful because of emerging evidence it may better reflect prognosis compared to two-dimensional measurements and is an important metric to include in clinical trials.

The challenge with measuring sizes—either diameter or volume—is that immunotherapy-induced inflammation may mimic progression radiologically. This was already well documented in glioma as the "flare phenomenon," and in early immunotherapy trials, some extracranial metastases increased in size due to immune infiltration, or new areas of enhancement appeared whilst a response was mounted but disappeared later as there was no viable tumor there (15, 16). Despite these potential pitfalls, conventional RANO-BM was applied to an early ICI trial of pembrolizumab for non-small-cell lung cancer (NSCLC) and melanoma BM (there was no stratification by genetic mutations such as EGFR and BRAF), and the authors found good concordance with other response criteria, although noted that lowering the cutoff for measurable lesions to 5 mm would have included more patients (17). To address this issue of inflammation and size, the immune related Response Criteria (ir-RC) were devised by a different panel of experts for solid tumors (18). As immunotherapy became more widely applied to patients with BM (and glioma), these were reconsidered for neuro-oncology alongside the original RANO and RANO-BM criteria to generate the immunotherapy or iRANO criteria, which are summarized in **Figure 1** (19). Based on the available evidence, this group determined that major radiographic changes occurring after 6 months following the start of immunotherapy are likely to be progression, but *until this time* there should be two major differences in approach compared to other therapies in neuro-oncology. First, in patients with no significant clinical decline, new enhancing lesions should not define progressive disease, on the basis that they may represent inflammation that subsequently resolves. Second, in patients with no significant clinical decline, rather than obtaining a confirmation scan 4 weeks after the initial imaging that suggests progression, this should be done after 3 months to allow time for inflammatory changes to occur and potentially resolve. As in the original criteria, confirmation of progression is backdated to the initial scan that suggested this. The caveat was that the patient in both circumstances must be clinically well, with no new or worsened deficits (unless such deficits have a specific cause like medication or a comorbid event). Finally, the role of steroids in patients with BM undergoing immunotherapy is more complex than in other therapies as they may dampen the immune response and yet may be required to manage symptoms. Therefore, the group deemed that any patient with altered steroid requirement within 2 weeks of MRI should be classified as "non-evaluable" at that time point for response or progression.

Further guidance on endpoints in immunotherapy trials in BM —particularly the issue of separating out the intracranial and

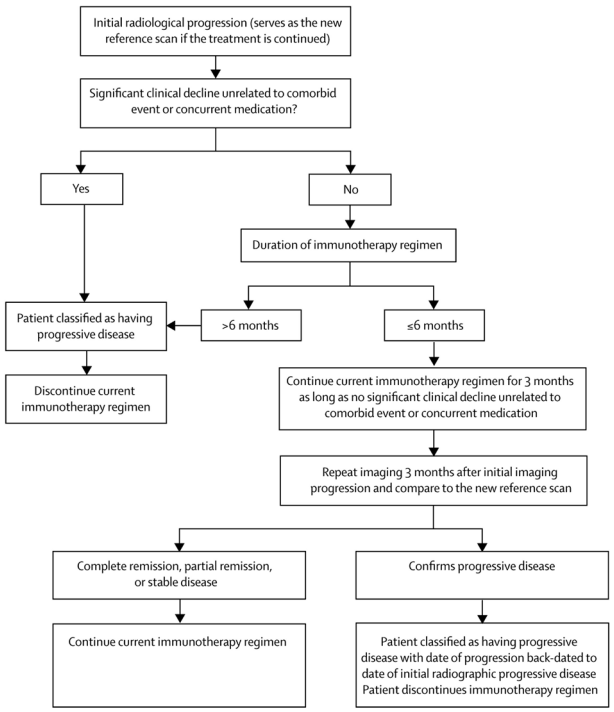

FIGURE 1 | Suggested algorithm for evaluation of progressive imaging findings among neuro-oncology patients undergoing immune-based therapies. Reproduced under Creative Commons license without modification (http://creativecommons.org/licenses/by/4.0/) from (19).

extracranial response—has been provided by the FDA (20). Whilst criteria are dynamic (21, 22), such guidance should reduce the over-reporting of progressive disease due to imaging immune responses and consensus guidelines—which are technically low-quality evidence—will invariably will be applied in trials going forward (23).

In summary, measuring size on post-contrast T1W MRI remains a major part of assessing response to treatment for BM, including immunotherapy. Volume is likely to increase in importance compared to 2-D measurements in the future. Despite being easily understood and established in clinical practice, there are significant problems when applying size measurements alone to BM receiving immunotherapy due to the inflammatory response affecting tumor size and shape. Modern guidelines and trial criteria are reflecting this uncertainty, but ultimately more advanced imaging techniques are needed and treating clinicians and radiologists must have information on the precise timing of immunotherapy, steroids, and the patient's clinical status to interpret the images.

BEYOND SIZE AND SHAPE: PERFUSION AND DIFFUSION

Diffusion-weighted imaging (DWI) has many advantages, being a quick, reproducible, and well-studied sequence in neuro-oncology, which is available on many standard scanners including in non-academic centers. In BM in particular, DWI parameters have been widely investigated as biomarkers of response to radiation and surgery (24) and may demonstrate biological change in both the tumor and the peritumoral region (25, 26), the latter being especially important in immunotherapy response (5).

Apparent diffusion coefficient (ADC) maps can be generated from standard DWI sequences and measured in voxels, regions, or volumes of interest. Diffusion tensor imaging (DTI) generally involves more directions and/or b-values and allows fractional anisotropy (FA) maps and thence putative white matter tracts to be derived. ADC may be a surrogate of cellularity, although for BM this will vary somewhat depending on the primary cancer type (26, 27). For a BM that is continuing to progress after the start of treatment to the point of follow-up imaging, it would be broadly expected for the ADC values within the BM to decrease as the cellularity increases, and this has been shown for specific histologic types, e.g., renal cell carcinoma (28). In a BM treated with immunotherapy, intratumoral infiltration by immune cells, necrosis, and edema could complicate this picture, and no studies have reported measuring ADC in BM undergoing immunotherapy yet. There are some indicators from the glioma literature; for example, a trial of dendritic cell vaccine therapy in eight patients with glioblastoma (GBM) found the minimum tumor ADC values (but not mean values) from the contrast-enhancing regions were lower in tumors that were about to progress or had already progressed compared to those that were stable or responding (29). This highlights another issue that will be relevant for BM studies, which is that clear definitions are needed of how individual biomarkers such as the ADC of the tumor or peritumoural region are recorded. For example, a study of 19 patients with recurrent GBM found increased relative ADC within contrast-enhancing tumor regions in 86% of those responding to ICI treatment within the first 6 months (30). Relative ADC was generated by normalizing the measured ADC to the contralateral white matter. Although this is a common methodological approach in brain tumor studies, it is notable that the small number of reports so far have all used different DWI metrics (e.g., minimum ADC, fractional increased ADC, intermediate ADC volume of interest). Variability in definition is a particular problem in BM, especially when considering multiple time points and multiple small BMs. Unlike glioma, the edema around BM is also largely not infiltrated by tumor cells; therefore, data on the use of ADC readings further out from the tumor border, in the region of FLAIR signal change, are also likely to be less relevant (31). One case report in GBM notably used restriction spectrum imaging (RSI), which applies multiple b-values and gradient directions to try and separate out different components of the diffusion signal, and this may be one option to overcome heterogeneity of signal, but again this has not yet been applied to BM (32).

Perfusion-weighted imaging (PWI), like DWI, has a strong basis in preclinical studies for detecting viable tumor specifically in BM (33). In clinical practice, necrosis, edema, steroids, and anti-angiogenic therapies prior to immunotherapy may confound the measurement of PWI. Logically, one would

expect increased blood flow, by whatever metric, to correlate with active tumor, and this has been investigated for patients with melanoma BM receiving ICI using two different dynamic contrast enhanced (DCE)-MRI metrics, the relative Vp90 and relative K^{trans} (34). DCE-MRI is one subtype of PWI that uses the T1 relaxation characteristics of gadolinium contrast agents to model the distribution of contrast between the vascular and interstitial space and indicates vascular permeability (for example, due to blood-brain barrier breakdown at the tumor interface). The other common PWI technique in neuro-oncology practice is dynamic susceptibility contrast (DSC)-MRI. This measures the signal loss on a T2 weighted sequence as contrast passes through the area of interest and is more informative of blood flow to a tumor.

The effects of radiation on PWI will complicate assessment further, and this is relevant since combination ICI with radiosurgery is a potentially valuable paradigm in treating BM. It has been shown that during this treatment, if there is no increase in the relative cerebral blood volume (rCBV, a PWI measure derived from DSC-MRI), this favors treatment effect over progressive tumor (35). Finally, the effects of anti-angiogenic agents on PWI will also need to be considered. A recent study of ICI in GBM found there was no predictive value of rCBV derived from DSC-perfusion or K^{trans} derived from DCE-perfusion on treatment response; however, crucially 5/19 patients had received and continued to receive anti-angiogenic treatment during the study, with inevitable effects on PWI (30). Given that up to approximately 10–20% of patients may experience radionecrosis (36), potentially more likely in the ICI with radiosurgery-treated patients, anti-angiogenic agents like bevacizumab may be even more frequently used (37). It remains to be seen if ICI affects the tumor and peritumoral region of BM in different ways compared to vaccine or cell-based immunotherapy or if PWI may have different value in BM from primaries where neo-angiogenesis is a particular feature such as NSCLC (38).

This final point is relevant more widely to imaging biomarkers in BM. Solid organ cancers generate BM with different biological behavior, potentially with different growth patterns and vulnerabilities. It remains to be seen to what extent the immune response to BM is brain-specific or tumor type specific and therefore to what extent these imaging techniques could be generalized across BM from different solid organ cancers. The only way forward is to include multiple cancer types and stratify or limit studies to single cancer types and document the molecular subtypes (e.g., BRAF status within melanoma BM), accepting this will lead to smaller studies.

In summary, PWI and DWI are both well-established techniques in clinical practice, which can be performed rapidly and reliably without additional hardware in many cases. Post processing, however, requires more specialist expertise and specific software packages in some instances. The techniques allow qualitative understanding of whether changes in tumor size or microenvironment (e.g., peritumoural edema) are reflective of viable tumor or inflammation. Further data are needed before measures from these sequences can be reliably equated to biological changes during immunotherapy and hence treatment response. They are currently surrogates of quite crude features of the tissue, such as cellular density for DWI or vascularity for PWI, and the underlying intratumoral and peritumoural microenvironment is clearly more complex.

THE POTENTIAL OF MOLECULAR IMAGING

Positron Emission Tomography (PET) imaging uses radioactive tracers to assess the metabolic and biochemical activity of tissues and is the most logical technique for assessing early treatment response in BM under immunotherapy treatment. In theory it could cut through much of the confounding effect of pretreatment and radiation effects likely to be seen in this group of patients. Availability and logistics are often challenging with this technique as radiotracers are produced on site and scans are accompanied by structural imaging in the form of CT or MRI.

Amino acid PET has advantages over the conventional F-18 fluorodeoxyglucose (FDG) tracer, particularly its background to noise ratio, and there are a small number of BM-specific studies already in the literature. One descriptive study of melanoma BM patients was conducted using F-18 flourothymidine (FLT) but only collected post-treatment data on two of five patients, making interpretation difficult (39). O-(2-[18F]fluoroethyl)-L-tyrosine (FET) has been used in neuro-oncology to assess amino acid transport in brain tumors and to distinguish immune-related treatment change from progressive disease in glioma (40). A small study of five patients applied FET-PET to those with melanoma BM receiving ICI who had progressive disease as defined by T1W contrast-enhanced MRI. The maximum tumor-to-brain ratio (TBR) of metabolic activity was calculated from the standard uptake value (SUV, a semiquantitative PET measurement of activity) map by comparing tumor ROI to the normal-appearing contralateral white matter. The TBR was higher in the progressive cases, whereas time-to-peak values were shorter. One patient with pseudoprogression could in theory have been identified by FET-PET 4 weeks earlier and continued ICI despite the contrary conventional MRI findings. To overcome the intralesional heterogeneity, this study took only the BM with the highest TBR and all the patients had been heavily pretreated, being on their 2^{nd} to 4^{th} cycle of ICI by the time of scan (41). Subsequently, a larger series of BM patients from NSCLC (n=11) and melanoma (n=29) primaries was investigated using the same technique in retrospective fashion and ROC analysis performed (42). Although this was a heterogeneous group in which radiation and targeted therapy were used as well as ICI, the mean TBR (note, not the maximum) from the most metabolically active appearing lesion was 94% specific and 70% sensitive for identifying progressive disease. Furthermore, metabolic "responders" (which the authors took as a relative reduction of 10% in the mean TBR) had a significantly longer stable clinical course (10.4 months *vs* 4 months) even when at odds with the conventional MRI assessed by RANO

criteria. 11-C methionine is another tracer that has been applied to BM (43) but not in those receiving immunotherapy. The same tracer has also been used in 14 patients with GBM receiving peptide based vaccination to inform treatment changes, although it required a voxel-wise method comparing pre- and post-treatment scans (likely due to the heterogeneity of GBM), and this might be difficult with most, smaller BM (44).

At an even more detailed and personalized level, specifically engineered PET tracers can be used as *in vivo* imaging tool to look at cell trafficking, which allows the unfolding immune response to be assessed. This technique has been applied in GBM (but not BM) in seven patients treated with engineered (chimeric antigen receptor or CAR) cytotoxic T-cells. The signal detected using a probe to image the subsequent infiltration of those cells into tumor was distinct from any disease progression (45, 46). CAR-T cell immunotherapy in GBM patients has also been assayed with MR spectroscopy, although this study combined this with other markers from DWI and PWI (47).

MR spectroscopy is a longstanding technique in brain imaging that has been very sparsely applied to monitoring immunotherapy responses, in BM or in brain tumors generally. It takes time to acquire, depending on anatomical coverage and resolution, which are severely limited, and is not easily applied to BM, which are often small lesions and multifocal. Generally, a defined set of metabolites such as choline (reflecting cell membrane turnover), N-acetyl aspartate (neuronal integrity), lactate (anaerobic metabolism), and lipid (necrosis) are compared to an internal control peak such as creatine or to one another with the ratios reflecting tumor or normal tissue. Although a wide range of methods and techniques exists that are beyond the scope of this review, ultimately there is much overlap of different tissue and tumor types. An older report of two patients with intratumoral IL4 injection into GBM used the MRS finding of low choline in the context of increasing enhancement to justify continuing observation and treatment, and the tumors subsequently regressed (48). The prospects of MRI spectroscopy being widely used in BM studies of immunotherapy response are seemingly limited, and although a number of studies report using it sporadically to distinguish pseudoprogression from viable tumor in BM treated with ICI in their methods, the sensitivity and specificity are not formally described (49).

Chemical exchange saturation transfer (CEST) imaging is a more recent technique based on the chemical composition of the tissue being assessed that detects certain compounds at very low concentrations by means of exchange of protons with the surrounding water molecules (50). The technique can detect both exogenous contrast agents as well as several endogenous substances. Amide proton transfer CEST imaging uses proteins and peptides as an endogenous contrast agent and has been applied to some common neuro-oncology problems such as distinguishing solitary BM from GBM (51) and radiation necrosis from BM progression (52). CEST may have a future role in assessing response to immune therapy due to a variety of endogenous agents that can be assessed as well as a broad scope for development of exogenous agents, including "responsive" agents capable of detecting pH, ion composition, and other tissue parameters (53, 54). Amide-proton transfer has recently become available as a commercially available software option on some clinical MRI systems, but other CEST techniques remain preclinical research tools.

In summary, spectroscopy is non-invasive and involves no ionizing radiation tracer but takes time, is subject to artefacts, and is poorly studied in BM and even more poorly studied in immunotherapy. With multiple BM often being treated, it is impractical to imagine that spectroscopy will be incorporated into clinical trials of immunotherapy for BM very widely. As a result, it is hard to correlate changes in different spectral peaks with any definite clinical change and to distinguish viable tumor from inflammation as there will not be a bank of data to analyze. PET imaging is only available in specialist centers and may require more tailored radioactive tracers to assess responses to immunotherapy, which makes the prospect of routine clinical use very distant. Nonetheless, the centers using immunotherapy for BM are likely to be specialist oncology departments and have ready access to PET compared to the community. Particularly, FET-PET does appear to demonstrate clear ability to assess the response of BM to immunotherapy regardless of changes in other MRI parameters.

All these techniques offer the tantalizing prospect of assessing the early response to therapy; however, perhaps a more pressing need is the development of imaging biomarkers that will predict treatment response before even starting therapy (8).

BIOMARKERS TO PREDICT RESPONSE

In large clinical trials to date, the response of BM to immunotherapy, especially ICI, is heterogenous, and those patients who do not respond may experience significant toxicity or adverse events. There is a clear clinical need for biomarkers that can predict the subsequent response to immunotherapy. The most logical way of doing this for ICI in BM would be demonstrating an immunologically favorable microenvironment before commencing treatment (4, 5).

Conventional Anatomic Imaging

Structural or anatomical imaging may have some value in this regard, in that T2 and FLAIR sequences can quantify the degree of peritumoral edema and inflammation. This varies greatly with the number and location of BM, the use of steroids, and the timing of any radiation treatments. Nonetheless, an analysis of 116 BM by conventional MRI and immunohistochemistry of the resected tumors found that the density of CD8+ tumor-infiltrating lymphocytes was correlated with the volume of peritumoral edema on preoperative MRI (55). Notably, these were all solitary BM, steroids did not seem to make any difference, and edema was graded in a novel fashion by radiologists, scoring its extent from the tumor margin on T2W images, <1 cm, >1 cm not crossing the midline and >1 cm crossing the midline. They suggest edema may be a surrogate marker of the immune response pretreatment in BM, but this needs to be more quantitatively investigated—most logically as a volume of interest on FLAIR and T2W images—and recorded

longitudinally in BM patients receiving immunotherapy, for example. It is was initially suggested that the interaction of radiation and ICI can cause a temporary increase in size and edema where SRS was given prior to ICI in some patients, but other studies with the same histology and agents have not reproduced this, showing instead a gradually declining volume of edema and tumor with response (56, 57). A recent paper used a mathematical model of immunotherapy efficacy based on conventional anatomic imaging to examine the response to ICI (ipilimumab and nivolumab) amongst patients with BM from different clinical trials (58). The BM growth rate at first restaging was as accurate as the retrospective determination of immune response at predicting response, and no additional imaging beyond the clinical structural scans were used. Ultimately, many terms in the model such as intrinsic growth rate of the tumor were determined from previous scans, but in the future, it might be possible to infer this from tissue or blood analysis. The advantage of conventional structural imaging is that it can be repeated quickly and reliably at multiple time points and analysis can potentially be automated, even if size and shape are not very specific.

Radiomics

One emerging method of deriving more information from conventional structural imaging is radiomics. This is a computational method for extracting many (potentially hundreds of) image features related to texture and shape. Multivariable regression or other machine learning techniques can then be used to develop a classification or prognostic model. Radiomics can be applied to any form of imaging, including both conventional anatomical imaging and DWI, PWI, and combinations of multiple modalities. Radiomics has already been used in extracranial disease (59) and melanoma BM (60). In the latter, pretreatment post-contrast T1W scans were manually assessed by a radiologist and target lesions segmented using freely available software (ITK-SNAP). Several features were associated with overall—although not progression-free—survival, and whilst these did not hold up in multivariate analysis, a Laplacian of Gaussian (LoG) feature was significant in a validation cohort, suggesting there was a biological signal. This technique has the advantage of not needing additional sequences or tracers and so could in theory be widely used, including retrospectively, e.g., in case-control or retrospective cohort studies. An illustration of this technique is given in **Figure 2**. There is limited evidence of repeatability and reproducibility of radiomics results, as well as limitations in the quality of reporting in the literature (62). As a result of these concerns, consensus guidelines and definitions have been proposed, with the aim of improving the quality of reporting (63).

Diffusion

Focusing on the peritumoral region but moving to advanced imaging, a series of 18 BM being removed surgically was investigated using image-guided samples from the peritumoral region, and a higher density of tumor-infiltrating lymphocytes was associated with prolonged overall survival regardless of primary. Additionally, higher CD3+ T cell density was also associated with a reduction in peritumoral FA, a measure of diffusion that is a surrogate of white matter tract integrity and has been widely investigated in other neuroinflammatory pathologies such as multiple sclerosis and radiation injury. This implies that the BM microenvironment could be assessed non-invasively, and studies are underway to determine if this is a biomarker of response to subsequent ICI in melanoma (64, 65). These results are illustrated in **Figure 3**. As with all BM, there is evidence of discordant mutations between the metastasis and the primary (66), and the impact of BM-specific changes—such as BRAF mutations in metastatic melanoma—on the imaging responses must also be investigated.

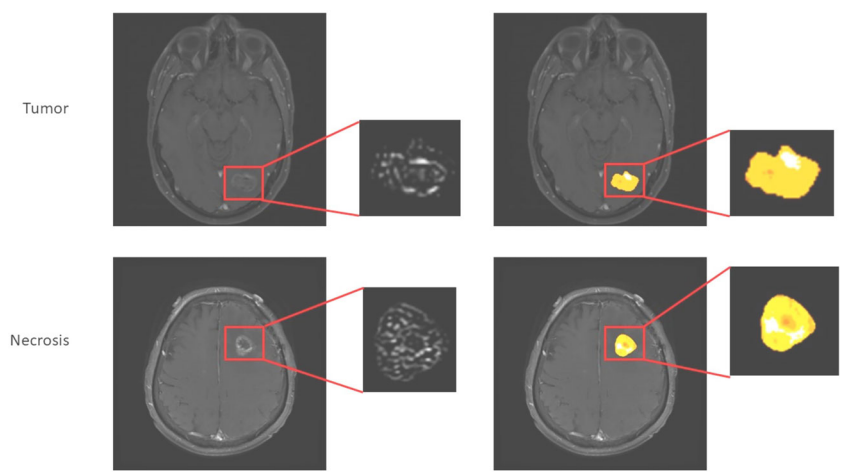

FIGURE 2 | Application of radiomics approach to melanoma brain metastases to distinguish tumor from necrosis/treatment effect (unpublished work, DM). This is similar to the approach used in (61), which found higher complexity in edge-filtered images of the sort seen on the left as well as higher entropy illustrated by various extracted features such as shown on the right in progressing BM after immunotherapy *versus* responding.

Molecular Imaging

Since PD-L1 expression correlates with response to ICI with targeted treatment, PET imaging with an engineered tracer has been used in patients with non-small-cell lung cancer to assay this. Uptake correlated with tumor positivity for PD-L1 at immunohistochemistry analysis and treatment response to the ICI agent nivolumab (61). Two of the 13 patients in this study had untreated BM, and both patients—but not all their BM—showed intracranial uptake, albeit with lower SUV values than in extracranial lesions. This is important as we know that due to the branched evolution of BM, the extracranial disease may not indicate the same susceptibilities to treatment as intracranial metastases (66).

Probes have been developed that are even more specific to the immune response and applied in other brain tumors but not yet in BM. 18-F CFA is a probe specifically developed to accumulate in proliferating T cells and was used in two patients to demonstrate immune activation after dendritic cell vaccination (67). Similarly, the effectiveness of vector-mediated HSV-1-tk gene expression in a phase I/II gene therapy trial for GBM was measured using a specific PET tracer ([124I]-FIAU) and correlated with therapeutic response (68).

The advantage of molecular imaging is thus that immunotherapy-specific tracers can be developed but with the problem that ever more specific tracers are harder to produce, less widely applicable, and less well studied.

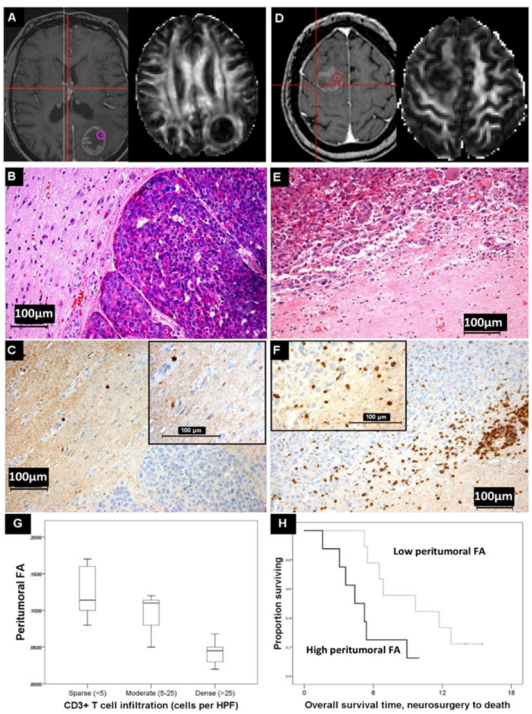

FIGURE 3 | Diffusion MRI changes and immune cell infiltration. **(A)** A lung adenocarcinoma brain metastasis which shows little peritumoural white matter disruption and has a high peritumoural fractional anisotropy (FA) value at the biopsy location shown. **(B)** H&E, **(C)** CD3-stained serial section showing sparse T cell infiltration in this same region (inset, magnified). This contrasts with the breast cancer brain metastasis in **(D)**, where there is more change in the peritumoural white matter and the FA value in the peritumoural region shown is lower. Here, there is dense peritumoural T cell infiltration [**(E, F)** and inset, magnified]. **(G)** The cases with a peritumoural FA >median (n=8, thick line) died sooner after neurosurgical resection of their metastasis than those with a lower peritumoural FA (n=9, dashed line) (log rank statistic = 4.566, p<0.05). **(H)** The FA values differentiated categories of peritumoural CD3+ T cell density (<5, 5–25, and >25 per high-power field) in the co-localized image-guided biopsy regions (Kruskal-Wallis, p<0.05), although such a relation is not seen with other immune cells such as CD68+ macrophages or CD20+ B cells, nor is it seen with other MRI measures, such as the mean diffusivity (MD). Reproduced by Creative Commons license from (65).

SUMMARY

Most of the published literature on imaging biomarkers of immunotherapy for brain tumors relates to glioma, particularly recurrent GBM, as these are the types of cases that enter such clinical trials. BM are an increasing target for such therapeutics, and novel biomarkers and techniques are needed to overcome the unique challenges in this disease. This includes the interaction of the BM with the native brain microenvironment, which is likely to vary for metastases from different primaries, as well as the differential intra- and extracranial disease responses to be assessed. The pros and cons of each technique are listed in **Table 1** and summarized below:

- Structural imaging will remain important—size, and ultimately volume, continues to be a crude marker of early response but not any indication before treatment. The radiomics approach may have use in incorporating large amounts of existing clinical imaging data in a useful manner.
- Physiological imaging is the most applicable and available advanced technique, diffusion is promising and well-studied, whilst perfusion also appears to reliably associate with tissue characteristics during treatment. These sequences are often included in the BM workup and treatment workflow so could be excellent for finding early markers after therapies start to affect the tumor tissue. In the peritumoral regions, such techniques may indicate an immune active microenvironment and could be a pretreatment marker.
- Molecular markers are highly specific, and many BM patients have PET studies as part of staging investigations, so this is an opportunity for investigating and defining pretreatment biomarkers. Tracers to look at the various ICI-targeted pathways are being developed and will need to be used in trials for intra- and extracranial disease with a variety of primary tumors.

FUTURE DIRECTIONS

There is a clear need for further investigation of imaging biomarkers of immunotherapy in BM; these may develop along with extracranial imaging techniques for assessing other metastases or arise from the existing intracranial techniques for

TABLE 1 | Summary of the current imaging techniques for predicting and measuring the response to immunotherapy in brain metastases.

Imaging method	Metrics investigated	Advantages	Disadvantages	Technique feasibility
Conventional MRI	Tumor diameter, volume from T1W post-contrast sequences. Peritumoral edema from T2, FLAIR sequences.	Quick, reproducible, widely available including non-specialist centers. Well-established guidelines for interpretation. Can potentially be integrated into radiomics models or automated, AI pipelines.	Rely on operator to take measurements if not automated, volumetric imaging is not widespread, very crude surrogate of biological behaviour.	Routine clinical use.
Diffusion MRI	ADC	Fast.	Cellularity may change due to tumor or inflammatory cells.	Routine clinical use in neuro-oncology and neurology.
	FA	Peritumoral changes may have prognostic value.		
	Restriction spectrum measures	May pick up more heterogeneity in future.	Novel technique with limited data. Software not readily available.	Preclinical research technique.
Perfusion MRI	CBV from dynamic contrast susceptibility MRI	Widely used in clinical practice, large amount of data on relation of perfusion to BM including from different primaries, high spatial resolution.	Post-processing software and expertise needed.	Routine clinical use in neuro-oncology.
	K^{trans} from dynamic contrast-enhanced MRI.		May be confounded by radiation, use of anti-angiogenic agents. Unclear how blood flow relates to cellular inflammation and BBB around tumor.	Routine clinical use in oncology for specific tumor types (e.g., breast, prostate), occasional use in neuro-oncology.
MR spectroscopy	Choline/creatine ratio	Well established in brain imaging, multivoxel in addition to single-voxel imaging improves spatial discrimination.	Time-consuming, poor spatial resolution given size of lesions in brain metastasis cases, not specific for inflammation *versus* viable tumor	Routine clinical use in neuro-oncology and other neurological conditions.
CEST MRI	Amide-proton transfer	Less confounded by radiation.	Limited availability	Translational research/early clinical technique.
		No contrast agent/tracer required.	Limited data	
			Time-consuming	
	Others	Wide research scope, including sensitivity to multiple endogenous metabolites and large variety of molecular tracers.	Little data.	Preclinical research technique.
PET	Various tracers, 18F-FET PET most widely studied	Not confounded by radiation, steroids. Combined with structural/conventional imaging. PD-L1 specific tracer may predict response to immune checkpoint inhibition.	Poor availability due to need to produce specific tracers and expertise, poor spatial resolution.	Specialist clinical technique.

assessing glioma. These may be novel sequences or probes or composites of existing ones. All must account for the unique brain microenvironment and the intralesional variation in response.

AUTHOR CONTRIBUTIONS

RZ and MJ devised the article and wrote the outline. RZ wrote the first draft; and CP, SM, DM, CC, and MR added specific sections and figures. All authors contributed to the article and approved the submitted version.

FUNDING

RZ receives funding from Cancer Research UK (C68514/A28190) and the Royal College of Surgeons of England (Pump Priming Grant for new investigators 2019).

REFERENCES

1. Jung J, Tailor J, Dalton E, Glancz LJ, Roach J, Zakaria R, et al. Management Evaluation of Metastasis in the Brain (MEMBRAIN)-A United Kingdom and Ireland Prospective, Multicenter Observational Study. *Neuro-oncol Pract* (2020) 7(3):344–55. doi: 10.1093/nop/npz063
2. Tan AC, Heimberger AB, Menzies AM, Pavlakis N, Khasraw M. Immune Checkpoint Inhibitors for Brain Metastases. *Curr Oncol Rep* (2017) 19(6):38. doi: 10.1007/s11912-017-0596-3
3. Tawbi HA, Forsyth PA, Algazi A, Hamid O, Hodi FS, Moschos SJ, et al. Combined Nivolumab and Ipilimumab in Melanoma Metastatic to the Brain. *N Engl J Med* (2018) 379(8):722–30. doi: 10.1056/NEJMoa1805453
4. Serres S, O'Brien ER, Sibson NR. Imaging Angiogenesis, Inflammation, and Metastasis in the Tumor Microenvironment With Magnetic Resonance Imaging. *Adv Exp Med Biol* (2014) 772:263–83. doi: 10.1007/978-1-4614-5915-6_12
5. Giridharan N, Glitza Oliva IC, O'Brien BJ, Parker Kerrigan BC, Heimberger AB, Ferguson SD. Targeting the Tumor Microenvironment in Brain

Metastasis. *Neurosurg Clinics North Am* (2020) 31(4):641–9. doi: 10.1016/j.nec.2020.06.011
6. Zakaria R, Das K, Bhojak M, Radon M, Walker C, Jenkinson MD. The Role of Magnetic Resonance Imaging in the Management of Brain Metastases: Diagnosis to Prognosis. *Cancer Imaging Off Publ Int Cancer Imaging Soc* (2014) 14:8. 10.1186/1470-7330-14-8
7. Mills SJ, Thompson G, Jackson A. Advanced Magnetic Resonance Imaging Biomarkers of Cerebral Metastases. *Cancer Imaging Off Publ Int Cancer Imaging Soc* (2012) 12(1):245–52. doi: 10.1102/1470-7330.2012.0012
8. Kasten BB, Udayakumar N, Leavenworth JW, Wu AM, Lapi SE, McConathy JE, et al. Current and Future Imaging Methods for Evaluating Response to Immunotherapy in Neuro-Oncology. *Theranostics* (2019) 9(17):5085–104. doi: 10.7150/thno.34415
9. Galldiks N, Lohmann P, Werner JM, Ceccon G, Fink GR, Langen KJ. Molecular Imaging and Advanced MRI Findings Following Immunotherapy in Patients With Brain Tumors. *Expert Rev Anticancer Ther* (2020) 20(1):9–15. doi: 10.1080/14737140.2020.1705788
10. Moher D, Liberati A, Tetzlaff J, Altman DG. Preferred Reporting Items for Systematic Reviews and Meta-Analyses: The PRISMA Statement. *Int J Surg* (2010) 8(5):336–41. doi: 10.1016/j.ijsu.2010.02.007
11. Lin NU, Lee EQ, Aoyama H, Barani IJ, Barboriak DP, Baumert BG, et al. Response Assessment Criteria for Brain Metastases: Proposal From the RANO Group. *Lancet Oncol* (2015) 16(6):e270–8. doi: 10.1016/S1470-2045(15)70057-4
12. Mills SJ, Radon MR, Baird RD, Hanemann CO, Keatley D, Lewis J, et al. Utilization of Volumetric Magnetic Resonance Imaging for Baseline and Surveillance Imaging in Neuro-Oncology. *Br J Radiol* (2019) 92 (1098):20190059. doi: 10.1259/bjr.20190059
13. Yang DY, Sheehan J, Liu YS, ChangLai SP, Pan HC, Chen CJ, et al. Analysis of Factors Associated With Volumetric Data Errors in Gamma Knife Radiosurgery. *Stereotact Funct Neurosurg* (2009) 87(1):1–7. doi: 10.1159/000177622
14. Pan HC, Cheng FC, Sun MH, Chen CC, Sheehan J. Prediction of Volumetric Data Errors in Patients Treated With Gamma Knife Radiosurgery. *Stereotact Funct Neurosurg* (2007) 85(4):184–91. doi: 10.1159/000101297
15. Smith MM, Thompson JE, Castillo M, Cush S, Mukherji SK, Miller CH, et al. MR of Recurrent High-Grade Astrocytomas After Intralesional Immunotherapy. *AJNR Am J Neuroradiol* (1996) 17(6):1065–71. doi: 0195-6108/96/1706 –1065
16. Aquino D, Gioppo A, Finocchiaro G, Bruzzone MG, Cuccarini V. MRI in Glioma Immunotherapy: Evidence, Pitfalls, and Perspectives. *J Immunol Res* (2017) 2017:5813951–. doi: 10.1155/2017/5813951
17. Qian JM, Mahajan A, Yu JB, Tsiouris AJ, Goldberg SB, Kluger HM, et al. Comparing Available Criteria for Measuring Brain Metastasis Response to Immunotherapy. *J Neurooncol* (2017) 132(3):479–85. doi: 10.1007/s11060-017-2398-8
18. Wolchok JD, Hoos A, O'Day S, Weber JS, Hamid O, Lebbé C, et al. Guidelines for the Evaluation of Immune Therapy Activity in Solid Tumors: Immune-Related Response Criteria. *Clin Cancer Res an Off J Am Assoc Cancer Res* (2009) 15(23):7412–20. doi: 10.1158/1078-0432.CCR-09-1624
19. Okada H, Weller M, Huang R, Finocchiaro G, Gilbert MR, Wick W, et al. Immunotherapy Response Assessment in Neuro-Oncology: A Report of the RANO Working Group. *Lancet Oncol* (2015) 16(15):e534–e42. doi: 10.1016/S1470-2045(15)00088-1
20. Administration USDoHaHSFaD. *Evaluating Cancer Drugs in Patients With Central Nervous System Metastases: Guidance for Industry. In: Excellence OCo, Editor.: U.S. Department of Health and Human Services: Food and Drug Administration*. (2020). pp. 53007–8(2 pages).
21. Nowosielski M, Wen PY. Imaging Criteria in Neuro-Oncology. *Semin Neurol* (2018) 38(1):24–31. doi: 10.1055/s-0038-1627468
22. Wen PY, Chang SM, Van den Bent MJ, Vogelbaum MA, Macdonald DR, Lee EQ. Response Assessment in Neuro-Oncology Clinical Trials. *J Clin Oncol Off J Am Soc Clin Oncol* (2017) 35(21):2439–49. doi: 10.1200/JCO.2017.72.7511
23. Le Rhun E, Wolpert F, Fialek M, Devos P, Andratschke N, Reyns N, et al. Response Assessment and Outcome of Combining Immunotherapy and Radiosurgery for Brain Metastasis From Malignant Melanoma. *ESMO Open* (2020) 5(4):1–18. doi: 10.1136/esmoopen-2020-000763
24. Zakaria R, Jenkinson MD. Diffusion Weighted MRI Is a Promising Imaging Biomarker in Brain Metastases. *J Neuro-Oncol* (2015) 121(2):421–2. doi: 10.1007/s11060-014-1642-8
25. Serres S, Martin CJ, Sarmiento Soto M, Bristow C, O'Brien ER, Connell JJ, et al. Structural and Functional Effects of Metastases in Rat Brain Determined by Multimodal MRI. *Int J Cancer* (2014) 134(4):885–96. doi: 10.1002/ijc.28406
26. Zakaria R, Das K, Radon M, Bhojak M, Rudland PR, Sluming V, et al. Diffusion-Weighted MRI Characteristics of the Cerebral Metastasis to Brain Boundary Predicts Patient Outcomes. *BMC Med Imaging* (2014) 14:26. doi: 10.1186/1471-2342-14-26
27. Hayashida Y, Hirai T, Morishita S, Kitajima M, Murakami R, Korogi Y, et al. Diffusion-Weighted Imaging of Metastatic Brain Tumors: Comparison With Histologic Type and Tumor Cellularity. *AJNR Am J Neuroradiol* (2006) 27 (7):1419–25. doi: 16908550
28. Chung C DB, Foltz W, Menard C, Jaffray D, Coolens C. *Differential Imaging Biomarker Response to Sunitinib Across Tumor Histologies in a Prospective Trial of Brain Metastases ISMRM 24th Annual Meeting & Exhibition 07-13 May 2016*. Singapore: ISMRM (2016).
29. Vrabec M, Van Cauter S, Himmelreich U, Van Gool SW, Sunaert S, De Vleeschouwer S, et al. MR Perfusion and Diffusion Imaging in the Follow-Up of Recurrent Glioblastoma Treated With Dendritic Cell Immunotherapy: A Pilot Study. *Neuroradiology* (2011) 53(10):721–31. doi: 10.1007/s00234-010-0802-6
30. Song J, Kadaba P, Kravitz A, Hormigo A, Friedman J, Belani P, et al. Multiparametric MRI for Early Identification of Therapeutic Response in Recurrent Glioblastoma Treated With Immune Checkpoint Inhibitors. *Neuro-Oncology* (2020) 22(11):1658–66. doi: 10.1093/neuonc/noaa066
31. Qin L, Li X, Stroiney A, Qu J, Helgager J, Reardon DA, et al. Advanced MRI Assessment to Predict Benefit of Anti-Programmed Cell Death 1 Protein Immunotherapy Response in Patients With Recurrent Glioblastoma. *Neuroradiology* (2017) 59(2):135–45. doi: 10.1007/s00234-016-1769-8
32. Daghighi S, Bahrami N, Tom WJ, Coley N, Seibert TM, Hattangadi-Gluth JA, et al. Restriction Spectrum Imaging Differentiates True Tumor Progression From Immune-Mediated Pseudoprogression: Case Report of a Patient With Glioblastoma. *Front Oncol* (2020) 10:24. doi: 10.3389/fonc.2020.00024
33. Larkin JR, Simard MA, de Bernardi A, Johanssen VA, Perez-Balderas F, Sibson NR. Improving Delineation of True Tumor Volume With Multimodal MRI in a Rat Model of Brain Metastasis. *Int J Radiat Oncol Biol Phys* (2020) 106(5):1028–38. doi: 10.1016/j.ijrobp.2019.12.007
34. Umemura Y, Wang D, Peck KK, Flynn J, Zhang Z, Fatovic R, et al. DCE-MRI Perfusion Predicts Pseudoprogression in Metastatic Melanoma Treated With Immunotherapy. *J Neuro-Oncol* (2020) 146(2):339–46. doi: 10.1007/s11060-019-03379-6
35. Du Four S, Janssen Y, Michotte A, Van Binst A-M, Van den Begin R, Duerinck J, et al. Focal Radiation Necrosis of the Brain in Patients With Melanoma Brain Metastases Treated With Pembrolizumab. *Cancer Med* (2018) 7(10):4870–9. doi: 10.1002/cam4.1726
36. Colaco RJ, Martin P, Kluger HM, Yu JB, Chiang VL. Does Immunotherapy Increase the Rate of Radiation Necrosis After Radiosurgical Treatment of Brain Metastases? *J Neurosurg JNS* (2016) 125(1):17. doi: n10.3171/2015.6.JNS142763
37. Glitza IC, Guha-Thakurta N, D'Souza NM, Amaria RN, McGovern SL, Rao G, et al. Bevacizumab as an Effective Treatment for Radiation Necrosis After Radiotherapy for Melanoma Brain Metastases. *Melanoma Res* (2017) 27 (6):580–4. doi: 10.1097/CMR.0000000000000389
38. Berghoff AS, Preusser M. Anti-Angiogenic Therapies in Brain Metastases. *Memo - Magazine Eur Med Oncol* (2018) 11(1):14–7. doi: 10.1007/s12254-018-0384-2
39. Nguyen NC, Yee MK, Tuchayi AM, Kirkwood JM, Tawbi H, Mountz JM. Targeted Therapy and Immunotherapy Response Assessment With F-18 Fluorothymidine Positron-Emission Tomography/Magnetic Resonance Imaging in Melanoma Brain Metastasis: A Pilot Study. *Front Oncol* (2018) 8:18. doi: 10.3389/fonc.2018.00018
40. Kristin Schmitz A, Sorg RV, Stoffels G, Grauer OM, Galldiks N, Steiger HJ, et al. Diagnostic Impact of Additional O-(2-[18F]Fluoroethyl)-L-Tyrosine ((18)F-FET) PET Following Immunotherapy With Dendritic Cell Vaccination in Glioblastoma Patients. *Br J Neurosurg* (2019) 13:1–7. doi: 10.1080/02688697
41. Kebir S, Rauschenbach L, Galldiks N, Schlaak M, Hattingen E, Landsberg J, et al. Dynamic O-(2-[18F]Fluoroethyl)-L-Tyrosine PET Imaging for the Detection of Checkpoint Inhibitor-Related Pseudoprogression in Melanoma

Brain Metastases. *Neuro-oncology* (2016) 18(10):1462–4. doi: 10.1093/neuonc/now154
42. Galldiks N, Abdulla DS, Scheffler M, Wolpert F, Werner JM, Huellner MW, et al. Treatment Monitoring of Immunotherapy and Targeted Therapy Using (18)F-FET PET in Patients With Melanoma and Lung Cancer Brain Metastases: Initial Experiences. *J Nucl Med* (2020) 62(4):464–70. doi: 10.2967/jnumed.120.248278
43. Stefano A, Comelli A, Bravatà V, Barone S, Daskalovski I, Savoca G, et al. A Preliminary PET Radiomics Study of Brain Metastases Using a Fully Automatic Segmentation Method. *BMC Bioinf* (2020) 21(8):325. doi: 10.1186/s12859-020-03647-7
44. Chiba Y, Kinoshita M, Okita Y, Tsuboi A, Isohashi K, Kagawa N, et al. Use of (11)C-Methionine PET Parametric Response Map for Monitoring WT1 Immunotherapy Response in Recurrent Malignant Glioma. *J Neurosurg* (2012) 116(4):835–42. doi: 10.3171/2011.12.JNS111255
45. Keu KV, Witney TH, Yaghoubi S, Rosenberg J, Kurien A, Magnusson R, et al. Reporter Gene Imaging of Targeted T Cell Immunotherapy in Recurrent Glioma. *Sci Transl Med* (2017) 9(373):eaag2196. doi: 10.1126/scitranslmed.aag2196
46. Yaghoubi SS, Jensen MC, Satyamurthy N, Budhiraja S, Paik D, Czernin J, et al. Noninvasive Detection of Therapeutic Cytolytic T Cells With 18F-FHBG PET in a Patient With Glioma. *Nat Clin Pract Oncol* (2009) 6(1):53–8. doi: 10.1038/ncponc1278
47. Wang S, O'Rourke DM, Chawla S, Verma G, Nasrallah MP, Morrissette JJD, et al. Multiparametric Magnetic Resonance Imaging in the Assessment of Anti-EGFRvIII Chimeric Antigen Receptor T Cell Therapy in Patients With Recurrent Glioblastoma. *Br J Cancer* (2019) 120(1):54–6. doi: 10.1038/s41416-018-0342-0
48. Floeth FW, Wittsack HJ, Engelbrecht V, Weber F. Comparative Follow-Up of Enhancement Phenomena With MRI and Proton MR Spectroscopic Imaging After Intralesional Immunotherapy in Glioblastoma. *Cent Eur Neurosurg* (2002) 63(01):23–8. doi: 10.1055/s-2002-31579
49. Thust SC, van den Bent MJ, Smits M. Pseudoprogression of Brain Tumors. *J Magn Reson Imaging* (2018) 48(3):571–89. doi: 10.1002/jmri.26171
50. Wu B, Warnock G, Zaiss M, Lin C, Chen M, Zhou Z, et al. An Overview of CEST MRI for non-MR Physicists. *EJNMMI Phys* (2016) 3(1):19–. doi: 10.1186/s40658-016-0155-2
51. Yu H, Lou H, Zou T, Wang X, Jiang S, Huang Z, et al. Applying Protein-Based Amide Proton Transfer MR Imaging to Distinguish Solitary Brain Metastases From Glioblastoma. *Eur Radiol* (2017) 27(11):4516–24. doi: 10.1007/s00330-017-4867-z
52. Mehrabian H, Desmond KL, Soliman H, Sahgal A, Stanisz GJ. Differentiation Between Radiation Necrosis and Tumor Progression Using Chemical Exchange Saturation Transfer. *Clin Cancer Res an Off J Am Assoc Cancer Res* (2017) 23(14):3667–75. doi: 10.1158/1078-0432.CCR-16-2265
53. Okuchi S, Hammam A, Golay X, Kim M, Thust S. Endogenous Chemical Exchange Saturation Transfer MRI for the Diagnosis and Therapy Response Assessment of Brain Tumors: A Systematic Review. *Radiol Imaging Cancer* (2020) 2(1):e190036. doi: 10.1148/rycan.2020190036
54. Hancu I, Dixon WT, Woods M, Vinogradov E, Sherry AD, Lenkinski RE. CEST and PARACEST MR Contrast Agents. *Acta Radiol* (2010) 51(8):910–23. doi: 10.3109/02841851.2010.502126
55. Berghoff AS, Fuchs E, Ricken G, Mlecnik B, Bindea G, Spanberger T, et al. Density of Tumor-Infiltrating Lymphocytes Correlates With Extent of Brain Edema and Overall Survival Time in Patients With Brain Metastases. *Oncoimmunology* (2016) 5(1):e1057388. doi: 10.1080/2162402X.2015.1057388
56. Kiess AP, Wolchok JD, Barker CA, Postow MA, Tabar V, Huse JT, et al. Stereotactic Radiosurgery for Melanoma Brain Metastases in Patients Receiving Ipilimumab: Safety Profile and Efficacy of Combined Treatment. *Int J Radiat OncologyBiologyPhys* (2015) 92(2):368–75. doi: 10.1016/j.ijrobp.2015.01.004
57. Diao K, Bian SX, Routman DM, Yu C, Kim PE, Wagle NA, et al. Combination Ipilimumab and Radiosurgery for Brain Metastases: Tumor, Edema, and Adverse Radiation Effects. *J Neurosurg JNS* (2018) 129(6):1397. doi: 10.3171/2017.7.JNS171286
58. Butner JD, Wang Z, Elganainy D, Al Feghali KA, Plodinec M, Calin GA, et al. A Mathematical Model for the Quantification of a Patient's Sensitivity to Checkpoint Inhibitors and Long-Term Tumour Burden. *Nat BioMed Eng* (2021) 5(4):297–308. doi: 10.1038/s41551-020-00662-0
59. Trebeschi S, Drago SG, Birkbak NJ, Kurilova I, Călin AM, Delli Pizzi A, et al. Predicting Response to Cancer Immunotherapy Using Noninvasive Radiomic Biomarkers. *Ann Oncol* (2019) 30(6):998–1004. doi: 10.1093/annonc/mdz108
60. Bhatia A, Birger M, Veeraraghavan H, Um H, Tixier F, McKenney AS, et al. MRI Radiomic Features Are Associated With Survival in Melanoma Brain Metastases Treated With Immune Checkpoint Inhibitors. *Neuro-Oncology* (2019) 21(12):1578–86. doi: 10.1093/neuonc/noz141
61. Niemeijer AN, Leung D, Huisman MC, Bahce I, Hoekstra OS, van Dongen G, et al. Whole Body PD-1 and PD-L1 Positron Emission Tomography in Patients With non-Small-Cell Lung Cancer. *Nat Commun* (2018) 9(1):4664. doi: 10.1038/s41467-018-07131-y
62. Traverso A, Wee L, Dekker A, Gillies R. Repeatability and Reproducibility of Radiomic Features: A Systematic Review. *Int J Radiat Oncol Biol Phys* (2018) 102(4):1143–58. doi: 10.1016/j.ijrobp.2018.05.053
63. Zwanenburg A, Vallières M, Abdalah MA, Aerts H, Andrearczyk V, Apte A, et al. The Image Biomarker Standardization Initiative: Standardized Quantitative Radiomics for High-Throughput Image-Based Phenotyping. *Radiology* (2020) 295(2):328–38. doi: 10.1148/radiol.2020191145
64. Zakaria R, Platt-Higgins A, Rathi N, Radon M, Das S, Das K, et al. T-Cell Densities in Brain Metastases Are Associated With Patient Survival Times and Diffusion Tensor MRI Changes. *Cancer Res* (2018) 78(3):610–6. doi: 10.1158/0008-5472.CAN-17-1720
65. UK CR. *BRITEMET Study* (2020). Available at: https://www.cancerresearchuk.org/about-cancer/find-a-clinical-trial/a-study-to-find-out-if-a-special-brain-mri-scan-can-predict-how-well-immunotherapy-will-work-for.
66. Brastianos PK, Carter SL, Santagata S, Cahill DP, Taylor-Weiner A, Jones RT, et al. Genomic Characterization of Brain Metastases Reveals Branched Evolution and Potential Therapeutic Targets. *Cancer Discov* (2015) 5(11):1164–77. doi: 10.1158/2159-8290.CD-15-0369
67. Antonios JP, Soto H, Everson RG, Moughon DL, Wang AC, Orpilla J, et al. Detection of Immune Responses After Immunotherapy in Glioblastoma Using PET and MRI. *Proc Natl Acad Sci USA* (2017) 114(38):10220–5. doi: 10.1073/pnas.1706689114
68. Jacobs A, Voges J, Reszka R, Lercher M, Gossmann A, Kracht L, et al. Positron-Emission Tomography of Vector-Mediated Gene Expression in Gene Therapy for Gliomas. *Lancet (London England)* (2001) 358(9283):727–9. doi: 10.1016/S0140-6736(01)05904-9

Conflict of Interest: The authors declare that the research was conducted in the absence of any commercial or financial relationships that could be construed as a potential conflict of interest.

frontiers in Immunology

CASE REPORT
published: 01 March 2022
doi: 10.3389/fimmu.2022.746869

Case Report: Immune Checkpoint Inhibitors Successfully Controlled Asymptomatic Brain Metastasis in Esophageal Squamous Cell Carcinoma

Linlin Xiao[1†], *Chi Lin*[2†], *Yueping Liu*[3], *Yajing Wu*[1] *and Jun Wang*[1*]

[1] Department of Radiation Oncology, The Fourth Hospital of Hebei Medical University, Shijiazhuang, China, [2] Department of Radiation Oncology, University of Nebraska Medical Center, Omaha, NE, United States, [3] Department of Pathology, The Fourth Hospital of Hebei Medical University, Shijiazhuang, China

OPEN ACCESS

Edited by:
Nicola Sibson,
University of Oxford, United Kingdom

Reviewed by:
Shuanghu Yuan,
Shandong University, China
Liu Hong,
Fourth Military Medical University, China

***Correspondence:**
Jun Wang
wangjunzr@163.com

[†]These authors have contributed equally to this work

Specialty section:
This article was submitted to Cancer Immunity and Immunotherapy, a section of the journal Frontiers in Immunology

Received: 25 July 2021
Accepted: 09 February 2022
Published: 01 March 2022

Citation:
Xiao L, Lin C, Liu Y, Wu Y and Wang J (2022) Case Report: Immune Checkpoint Inhibitors Successfully Controlled Asymptomatic Brain Metastasis in Esophageal Squamous Cell Carcinoma. Front. Immunol. 13:746869. doi: 10.3389/fimmu.2022.746869

Background: Brain metastases are the most common cause of intracranial malignancy, often resulting in significant morbidity and mortality. Brain metastases from esophageal squamous cell carcinoma (ESCC) are relatively rare, with a rate of generally less than 2%.

Case Report: In this article, we report a rare case of ESCC with asymptomatic brain metastasis. The combined positive score (CPS) of programmed cell death-ligand 1 (PD-L1) from the primary tumor was 2 by DAKO 22C3 and 3 by VENTANA SP263. The proportion of tumor infiltrating lymphocytes (TILs) was 1%. After receiving 15 cycles of immune checkpoint inhibitors (ICIs), the patient's brain metastatic lesion had disappeared and was replaced by a local necrotic area. He retains good cognitive function with a stable disease at the primary site.

Conclusions: This is the first to be reported in an ESCC patient whose brain metastatic lesion had a complete response to ICIs, which may provide supporting data for using ICIs as an option of treatment for ESCC patients with brain metastases.

Keywords: brain metastasis, esophageal carcinoma, PD-L1, immune checkpoint inhibitors, esophageal squamous cell carcinoma

INTRODUCTION

Brain metastases are the most common cause of intracranial malignancy, often resulting in significant morbidity and mortality (1). Brain metastases usually occur in lung cancer, breast cancer and melanoma, which account for approximately 67-80% of patients. Brain metastases from esophageal carcinoma (EC) are relatively rare, with a rate of generally less than 2% (2–4).

Recently, immune checkpoint inhibitors (ICIs) in the treatment of patients with EC was in full swing. The KEYNOTE-181, ATTRACTION-3 and ESCORT studies had demonstrated that ICIs could improve the overall survival (OS) with a manageable toxicity profile in previously treated patients with advanced or metastatic EC, representing a standard second-line treatment option for these patients (5–7). As the low incidence of brain metastases in patients with EC, the three studies did not include patients with brain metastases and there is no study on ICIs for these patients at

present. Here, we presented a case of asymptomatic brain metastasis from EC. The patient achieved intracranial complete response by the treatment of ICIs. Although this phenomenon had been reported in other cancers (8, 9), it is the first to be reported in EC, which may provide supporting data for using ICIs as one of options for management of brain metastases from esophageal cancer.

CASE REPORT

A 66-year-old male patient presented himself to our oncological outpatient clinic with odynophagia in February 2019. Esophagogastroduodenoscopy (EGD) revealed a lesion in the esophagus, about 20-26cm from the incisor. Biopsy of the lesion was positive for esophageal squamous cell carcinoma (ESCC). The combined positive score (CPS) of programmed cell death ligand 1 (PD-L1) was 2 by DAKO 22C3 and 3 by VENTANA SP263. The patient's baseline examination showed no abnormalities, including brain MRI (**Figure 1**), and the functional tests of thyroid, heart, lung, liver, and kidney. The patient was hospitalized and received a course of definitive radiotherapy to the primary tumor and regional lymph nodes to a dose of 60 Gy in 30 fractions concurrently with a chemotherapy regimen of paclitaxel and cisplatin. The patient developed severe myelosuppression during the course of chemoradiation therapy. Subsequently, he received four 3-week cycles of consolidative chemotherapy with fluorouracil and cisplatin. The last chemotherapy was received on July 5th, 2019.

On July 26th, 2019, the patient returned for follow up. Thoracic computed tomography (CT) showed that the tumor in the esophagus was stable. The patient reported no odynophagia. Unfortunately, the magnetic resonance imaging (MRI) of the brain revealed a new well-circumscribed enhancing nodular lesion in the left temporal lobe (**Figure 2**). Given that his ESCC was positive for PD-L1, toripalimab, one of ICIs, was recommended for his asymptomatic solitary brain metastasis. From August 2019 to October 2020, he received 15 3-week cycles of toripalimab. A follow-up brain MRI revealed that the brain metastasis was replaced by a necrotic area (**Figure 2**). No decline of cognitive function [mini-mental state examination (MMSE) and Loewenstein-cognitive function assessment (LOTCA)] or other acute toxicity have been found during the treatment. Physical examination, brain MRI, esophageal barium swallow, gastroscope, chest radiography, or CT from the neck to the upper abdomen were performed in the follow up. By the last revision of this article, the patient was still on toripalimab with a stable disease at the primary site as well as a good cognitive function.

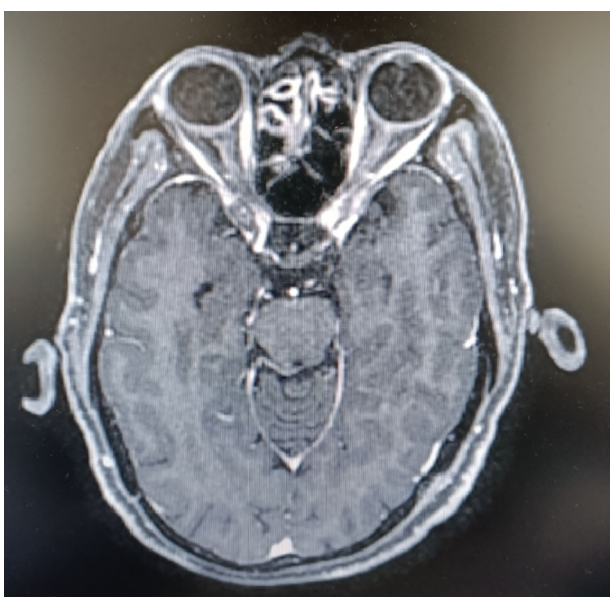

FIGURE 1 | The baseline brain MRI of the patient.

DISCUSSION

In this article, we report a case of asymptomatic brain metastasis from EC, which is very rare in itself. We found that the brain metastatic lesion had a complete response to ICIs and the lesion was replaced by a necrotic area after 15 cycles of ICIs. In addition, he is doing generally well with stable disease and good cognitive function. Due to the low incidence of brain metastasis in EC, it is difficult to conduct clinical trials in these patients. Therefore, this case report will add to the existing publications and provide supporting data for using ICIs to treat EC patients with brain metastases, especially for patients with asymptomatic brain metastases.

Surgery is a highly effective treatment for patients with symptomatic brain metastases, especially for patients with a solitary lesion, a good KPS score and a controlled extracranial tumor. Stereotactic radiosurgery (SRS) is also a standard treatment for patients with symptomatic brain oligometastases. Whole-brain radiation therapy (WBRT) is often used for patients who is not suitable for surgery or SRS, such as with multiple brain metastases, leptomeningeal disease or poor performance status. Systemic chemotherapeutic drugs have a limited therapeutic efficacy for brain metastases due to poor penetration of the blood–brain barrier. Targeted therapy has shown some value in certain tumors with brain metastases; for example, osimertinib in epidermal growth factor receptor (EGFR)-mutant non-small cell lung cancer (NSCLC) patients with brain metastases (10, 11) and alectinib in anaplastic lymphoma kinase (ALK)-rearrangements NSCLC patients with brain metastases (12). ICIs have also shown some preliminary evidence, mainly in brain metastases for patients with lung cancer, melanoma and renal cell carcinoma (13, 14).

In recent years, a variety of ICIs have entered the field of oncotherapy and have quickly reshaped management strategies for many types of cancers, such as NSCLC, SCLC, melanoma, lymphoma, esophagus cancer, breast cancer, renal cancer, liver cancer, and urothelium cancer. However, patients with active or untreated brain metastases usually are excluded from clinical trials (15, 16). Although some studies have included patients with

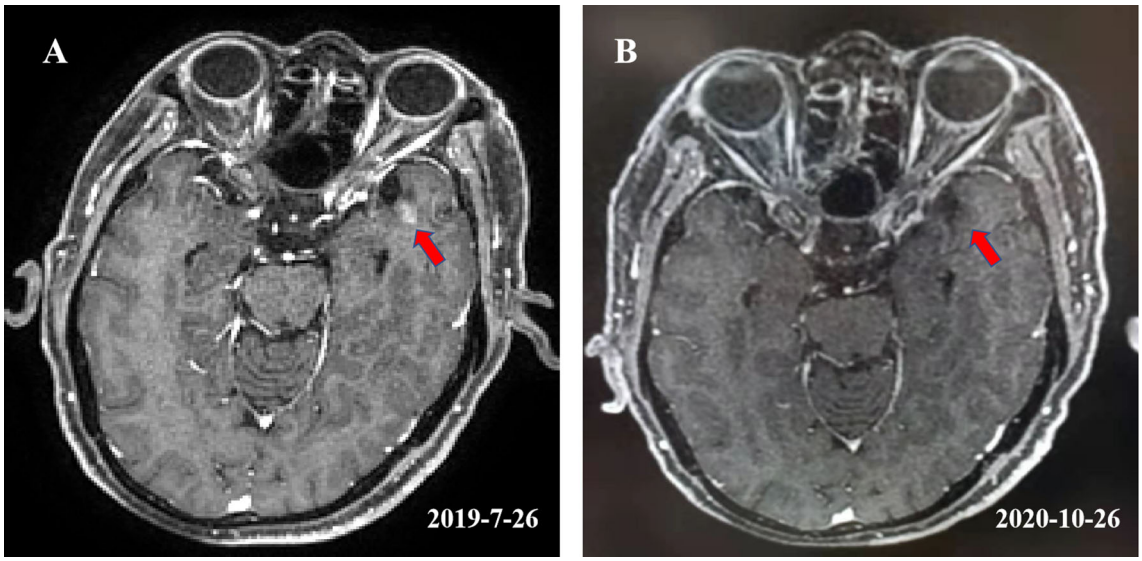

FIGURE 2 | **(A)** Showed a well-circumscribed enhancing nodular lesion with a maximum diameter of about 0.5 cm in the left temporal lobe. **(B)** Showed that the lesion was replaced by a necrotic area after receiving 15 cycles of toripalimab.

stable brain metastases, specific subgroup analyses have not been reported. At present, the research on the ICIs of brain metastases have been mainly focused on melanoma (14, 17–19). The results of these studies demonstrated that ICIs, especially ipilimumab have therapeutic activity in some patients with brain metastases, particularly in patients with small and asymptomatic metastases. The rate of intracranial responses was approximately 20%. In addition, some studies showed that double-drug combined ICI regimens may bring more benefits to these patients. In the study of CheckMate 204, for melanoma patients with asymptomatic untreated brain metastases, the rate of intracranial responses was 57% in patients treated with nivolumab and ipilimumab (14). A multicenter open-label randomized phase 2 trial demonstrated that nivolumab combined with ipilimumab could bring a higher rate of intracranial responses (46% vs. 20%) for patients with asymptomatic untreated brain metastases comparing with nivolumab alone (19). There are a few reports on brain metastasis from lung cancer treated with ICIs. A study from Italy analyzed the efficacy of nivolumab in 409 patients with asymptomatic, neurologically stable brain metastases from non-squamous non-small cell lung cancer. The results showed that the objective response rate (ORR) and the disease control rate (DCR) were 17% and 39% in these patients, with similar toxicity rates in the overall study population with or without brain metastases (9). An exploratory analysis of a phase III OAK study showed that atezolizumab could prolong the median OS (16.0 vs 11.9 months) of patients with asymptomatic, treated brain metastases compared with docetaxel (20). Activating the immune system is the mechanisms by which ICIs kill tumor cells, by which blood-brain barrier could not block.

Brain radiotherapy was an important treatment options for patients with brain metastases. Preclinical findings have suggested that the combined application of brain radiotherapy and ICIs could yield synergistic effects, bringing more benefits to patients (21, 22), while clinical studies on ICIs combined with radiotherapy are very limited, particularly in patients with brain metastases. Notably, many prospective trials often removed these patients with active brain metastases (23, 24). With respect to brain radiotherapy and ICIs in combination, favorable outcomes have been demonstrated in a few retrospective studies (25–27). The study of Pike et al. reported that brain radiation following the start of PD-1 inhibitors could benefit patients (26). Kotecha et al. evaluated the outcomes of 150 patients who received ICIs and SRS and demonstrated that concurrent radiotherapy and ICIs will maximize the benefits (27). Ahmed et al. found that delivery of brain radiotherapy prior to or during administration of PD-1/PD-L1 inhibitors would bring more survival benefits for patients compared to patients who received brain radiotherapy after ICIs (p=0.006) (25). The ability of concurrent radiotherapy and ICIs to improve patients' survival may be due to the fact that concurrent ICIs increased the durability of intracranial control that radiotherapy provided. In light of the controversy and limited data, further research on how to combine brain radiotherapy and ICIs are warranted to improve the management strategy for these patients.

On the other hand, with this combined approach, the question we need to ask would be: will the risk of brain radiotherapy-associated adverse events (AEs), especially, radiation necrosis, increase synchronously when combined with ICIs? Radiation necrosis can be a very serious complication for patients who received radiotherapy to brain metastases and may even be life-threatening (28). Combination of SRS and WBRT would increase the incidence of radiation necrosis of brain compared to SRS alone (29). Du Four et al. reported that three patients with brain metastases from

melanoma developed radiation necrosis of brain following brain radiotherapy and ipilimumab for the first time (30). Martin et al. found that addition of ICIs would increase the incidence of symptomatic radiation necrosis in patients that underwent stereotactic radiation for brain metastases, especially in patients with melanoma (31). In this study, 23 of 115 (20%) developed symptomatic necrosis in patients with ICIs, significantly higher than 25 of 365 (6.8%) in patients without ICIs. However, the available results are not always consistent. Hubbeling et al. investigated the safety of brain radiotherapy in NSCLC patients receiving PD-1/PD-L1 inhibitors and found that brain radiotherapy and ICIs in combination was not associated with an increase in brain-radiotherapy-associated AEs (32). A great challenge in current oncology practice is to achieve the best possible balance between benefits and adverse events of treatments. In the past, patients with brain metastases usually had a short survival time and had no chance to develop late complications from brain irradiation, such as radiation necrosis of the brain. In the era of immunotherapy, the survival time of these patients have been extended, which have exposed patients to a chance for more late adverse events.

In this study, we report a case of asymptomatic brain metastasis from EC, which had a complete response after 15 cycles of ICIs. The patient since has had stable disease at the primary site and good cognitive function. Similar results have been reported in the past. Flippot et al. had reported the first study assessing the activity of nivolumab in patients with asymptomatic brain metastases from metastatic clear cell renal cell carcinoma (8). In their study, there were 4 out of 34 patients that achieved intracranial complete response after treatment of nivolumab without radiotherapy. Notably, the longest diameter of the lesion in the four patients was less than 10 mm at baseline, which was similar to the patient in our report. Crinò et al. also reported a similar phenomenon in a patient with non-squamous NSCLC, who had two metastatic nodular lesions in the brain (9). After 3 years of treatment with nivolumab without radiotherapy, both metastases had disappeared. These studies suggest that for patients with limited intracranial tumor burden, ICIs may be a sufficient treatment for intracranial tumor control.

These thought-provoking study results invoke us to ask: could ICIs replace surgery or radiation therapy for treating a brain metastatic lesion? The answer was obviously: no. However, the safety profile of ICIs alone appears acceptable and ICIs seemed to control certain brain metastases, especially small and asymptomatic ones. Therefore, ICIs seemed to be appropriate to replace surgery or radiation therapy for patients with small, stable, and asymptomatic brain metastatic lesions. In the meantime, for patients with symptomatic brain metastases, brain surgery and radiotherapy are still the main treatment options. It is worthwhile to note that the use of corticosteroids may affect the efficacy of ICIs. A combination of ICIs and brain radiotherapy may bring favorable outcomes for patients, but we need to pay attention to potentially increased neurologic toxicities caused by this combined therapy.

In conclusion, for patients with asymptomatic brain metastasis, ICIs seem to be a favorable treatment option, while the best treatment options for patients with symptomatic brain metastases remains an open question. More clinical trials of ICIs in patients with brain metastases are warranted.

DATA AVAILABILITY STATEMENT

The original contributions presented in the study are included in the article/supplementary material. Further inquiries can be directed to the corresponding author.

ETHICS STATEMENT

Written informed consent was obtained from the individual(s) for the publication of any potentially identifiable images or data included in this article.

AUTHOR CONTRIBUTIONS

Conceptualization, JW. Data curation, LX and YW. Formal analysis, LX, YL, and JW. Resources, LX, YW, and YL. Validation, CL and JW. Writing-original draft, LX. Writing-review & editing, CL and JW. All authors contributed to the article and approved the submitted version.

REFERENCES

1. Nayak L, Lee EQ, Wen PY. Epidemiology of Brain Metastases. *Curr Oncol Rep* (2012) 14(1):48–54. doi: 10.1007/s11912-011-0203-y
2. Go PH, Klaassen Z, Meadows MC, Chamberlain RS. Gastrointestinal Cancer and Brain Metastasis: A Rare and Ominous Sign. *Cancer* (2011) 117 (16):3630–40. doi: 10.1002/cncr.25940
3. Weinberg JS, Suki D, Hanbali F, Cohen ZR, Lenzi R, Sawaya R. Metastasis of Esophageal Carcinoma to the Brain. *Cancer* (2003) 98(9):1925–33. doi: 10.1002/cncr.11737
4. Feng W, Zhang P, Zheng X, Chen M, Mao WM. Incidence and Treatment of Brain Metastasis in Patients With Esophageal Carcinoma. *World J Gastroenterol* (2015) 21(19):5805–12. doi: 10.3748/wjg.v21.i19.5805
5. Kojima T, Shah MA, Muro K, Francois E, Adenis A, Hsu CH, et al. Randomized Phase III KEYNOTE-181 Study of Pembrolizumab Versus Chemotherapy in Advanced Esophageal Cancer. *J Clin Oncol* (2020) 38 (35):4138–48. doi: 10.1200/JCO.20.01888
6. Kato K, Cho BC, Takahashi M, Okada M, Lin CY, Chin K, et al. Nivolumab Versus Chemotherapy in Patients With Advanced Oesophageal Squamous Cell Carcinoma Refractory or Intolerant to Previous Chemotherapy (ATTRACTION-3): A Multicentre, Randomised, Open-Label, Phase 3 Trial. *Lancet Oncol* (2019) 20(11):1506–17. doi: 10.1016/S1470-2045(19) 30626-6
7. Huang J, Xu J, Chen Y, Zhuang W, Zhang Y, Chen Z, et al. Camrelizumab Versus Investigator's Choice of Chemotherapy as Second-Line Therapy for Advanced or Metastatic Oesophageal Squamous Cell Carcinoma (ESCORT): A Multicentre, Randomised, Open-Label, Phase 3 Study. *Lancet Oncol* (2020) 21(6):832–42. doi: 10.1016/S1470-2045(20)30110-8
8. Flippot R, Dalban C, Laguerre B, Borchiellini D, Gravis G, Négrier S, et al. Safety and Efficacy of Nivolumab in Brain Metastases From Renal Cell

Carcinoma: Results of the GETUG-AFU 26 NIVOREN Multicenter Phase II Study. *J Clin Oncol* (2019) 37(23):2008–16. doi: 10.1200/JCO.18.02218
9. Crinò L, Bronte G, Bidoli P, Cravero P, Minenza E, Cortesi E, et al. Nivolumab and Brain Metastases in Patients With Advanced Non-Squamous Non-Small Cell Lung Cancer. *Lung Cancer* (2019) 129:35–40. doi: 10.1016/j.lungcan.2018.12.025
10. Mok TS, Wu Y-L, Ahn M-J, Garassino MC, Kim HR, Ramalingam SS, et al. Osimertinib or Platinum-Pemetrexed in EGFR T790M-Positive Lung Cancer. *N Engl J Med* (2017) 376(7):629–40. doi: 10.1056/NEJMoa1612674
11. Ballard P, Yates JW, Yang Z, Kim DW, Yang JC, Cantarini M, et al. Preclinical Comparison of Osimertinib With Other EGFR-TKIs in EGFR-Mutant NSCLC Brain Metastases Models, and Early Evidence of Clinical Brain Metastases Activity. *Clin Cancer Res* (2016) 22(20):5130–40. doi: 10.1158/1078-0432.CCR-16-0399
12. Peters S, Camidge DR, Shaw AT, Gadgeel S, Ahn JS, Kim DW, et al. Alectinib Versus Crizotinib in Untreated ALK-Positive Non-Small-Cell Lung Cancer. *N Engl J Med* (2017) 377(9):829–38. doi: 10.1056/NEJMoa1704795
13. Goldberg SB, Gettinger SN, Mahajan A, Chiang AC, Herbst RS, Sznol M, et al. Pembrolizumab for Patients With Melanoma or Non-Small-Cell Lung Cancer and Untreated Brain Metastases: Early Analysis of a Non-Randomised, Open-Label, Phase 2 Trial. *Lancet Oncol* (2016) 17(7):976–83. doi: 10.1016/S1470-2045(16)30053-5
14. Tawbi HA, Forsyth PA, Algazi A, Hamid O, Hodi FS, Moschos SJ, et al. Combined Nivolumab and Ipilimumab in Melanoma Metastatic to the Brain. *N Engl J Med* (2018) 379(8):722–30. doi: 10.1056/NEJMoa1805453
15. Mok TSK, Wu YL, Kudaba I, Kowalski DM, Cho BC, Turna HZ, et al. Pembrolizumab Versus Chemotherapy for Previously Untreated, PD-L1-Expressing, Locally Advanced or Metastatic Non-Small-Cell Lung Cancer (KEYNOTE-042): A Randomised, Open-Label, Controlled, Phase 3 Trial. *Lancet* (2019) 393(10183):1819–30. doi: 10.1016/S0140-6736(18)32409-7
16. Larkin J, Chiarion-Sileni V, Gonzalez R, Grob JJ, Cowey CL, Lao CD, et al. Combined Nivolumab and Ipilimumab or Monotherapy in Untreated Melanoma. *N Engl J Med* (2015) 373(1):23–34. doi: 10.1056/NEJMoa1504030
17. Margolin K, Ernstoff MS, Hamid O, Lawrence D, McDermott D, Puzanov I, et al. Ipilimumab in Patients With Melanoma and Brain Metastases: An Open-Label, Phase 2 Trial. *Lancet Oncol* (2012) 13(5):459–65. doi: 10.1016/S1470-2045(12)70090-6
18. Queirolo P, Spagnolo F, Ascierto PA, Simeone E, Marchetti P, Scoppola A, et al. Efficacy and Safety of Ipilimumab in Patients With Advanced Melanoma and Brain Metastases. *J Neurooncol* (2014) 118(1):109–16. doi: 10.07/s11060-014-1400-y
19. Long GV, Atkinson V, Lo S, Sandhu S, Guminski AD, Brown MP, et al. Combination Nivolumab and Ipilimumab or Nivolumab Alone in Melanoma Brain Metastases: A Multicentre Randomised Phase 2 Study. *Lancet Oncol* (2018) 19(5):672–81. doi: 10.1016/S1470-2045(18)30139-6
20. Gadgeel SM, Lukas RV, Goldschmidt J, Conkling P, Park K, Cortinovis D, et al. Atezolizumab in Patients With Advanced Non-Small Cell Lung Cancer and History of Asymptomatic, Treated Brain Metastases: Exploratory Analyses of the Phase III OAK Study. *Lung Cancer* (2019) 128:105–12. doi: 10.1016/j.lungcan.2018.12.017
21. Gong X, Li X, Jiang T, Xie H, Zhu Z, Zhou F, et al. Combined Radiotherapy and Anti-PD-L1 Antibody Synergistically Enhances Antitumor Effect in Non-Small Cell Lung Cancer. *J Thorac Oncol* (2017) 12(7):1085–97. doi: 10.1016/j.jtho.2017.04.014
22. Sharabi AB, Nirschl CJ, Kochel CM, Nirschl TR, Francica BJ, Velarde E, et al. Stereotactic Radiation Therapy Augments Antigen-Specific PD-1-Mediated Antitumor Immune Responses *via* Cross-Presentation of Tumor Antigen. *Cancer Immunol Res* (2015) 3(4):345–55. doi: 10.1158/2326-6066.CIR-14-0196
23. Reck M, Rodríguez-Abreu D, Robinson AG, Hui R, Csőszi T, Fülöp A, et al. Pembrolizumab Versus Chemotherapy for PD-L1-Positive Non-Small-Cell Lung Cancer. *N Engl J Med* (2016) 375(19):1823–33. doi: 10.1056/NEJMoa1606774
24. Carbone DP, Reck M, Paz-Ares L, Creelan B, Horn L, Steins M, et al. First-Line Nivolumab in Stage IV or Recurrent Non-Small-Cell Lung Cancer. *N Engl J Med* (2017) 376(25):2415–26. doi: 10.1056/NEJMoa1613493
25. Ahmed KA, Kim S, Arrington J, Naghavi AO, Dilling TJ, Creelan BC, et al. Outcomes Targeting the PD-1/PD-L1 Axis in Conjunction With Stereotactic Radiation for Patients With Non-Small Cell Lung Cancer Brain Metastases. *J Neurooncol* (2017) 133(2):331–8. doi: 10.1007/s11060-017-2437-5
26. Pike LRG, Bang A, Ott P, Balboni T, Taylor A, Catalano P, et al. Radiation and PD-1 Inhibition: Favorable Outcomes After Brain-Directed Radiation. *Radiother Oncol* (2017) 124(1):98–103. doi: 10.1016/j.radonc.2017.06.006
27. Kotecha R, Kim JM, Miller JA, Juloori A, Chao ST, Murphy ES, et al. The Impact of Sequencing PD-1/PD-L1 Inhibitors and Stereotactic Radiosurgery for Patients With Brain Metastasis. *Neuro Oncol* (2019) 21(8):1060–8. doi: 10.1093/neuonc/noz046
28. Giglio P, Gilbert MR. Cerebral Radiation Necrosis. *Neurologist* (2003) 9(4):180–8. doi: 10.1097/01.nrl.0000080951.78533.c4
29. Kocher M, Soffietti R, Abacioglu U, Villà S, Fauchon F, Baumert BG, et al. Adjuvant Whole-Brain Radiotherapy Versus Observation After Radiosurgery or Surgical Resection of One to Three Cerebral Metastases: Results of the EORTC 22952-26001 Study. *J Clin Oncol* (2011) 29(2):134–41. doi: 10.1200/JCO.2010.30.1655
30. Du Four S, Wilgenhof S, Duerinck J, Michotte A, Van Binst A, De Ridder M, et al. Radiation Necrosis of the Brain in Melanoma Patients Successfully Treated With Ipilimumab, Three Case Studies. *Eur J Cancer* (2012) 48(16):3045–51. doi: 10.1016/j.ejca.2012.05.016
31. sMartin AM, Cagney DN, Catalano PJ, Alexander BM, Redig AJ, Schoenfeld JD, et al. Immunotherapy and Symptomatic Radiation Necrosis in Patients With Brain Metastases Treated With Stereotactic Radiation. *JAMA Oncol* (2018) 4(8):1123–4. doi: 10.1001/jamaoncol.2017.3993
32. Hubbeling HG, Schapira EF, Horick NK, Goodwin KEH, Lin JJ, Oh KS, et al. Safety of Combined PD-1 Pathway Inhibition and Intracranial Radiation Therapy in Non-Small Cell Lung Cancer. *J Thorac Oncol* (2018) 13(4):550–8. doi: 10.1016/j.jtho.2018.01.012

Conflict of Interest: The authors declare that the research was conducted in the absence of any commercial or financial relationships that could be construed as a potential conflict of interest.

frontiers in Oncology

ORIGINAL RESEARCH
published: 10 March 2022
doi: 10.3389/fonc.2022.850656

Inhibition of Anti-Inflammatory Macrophage Phenotype Reduces Tumour Growth in Mouse Models of Brain Metastasis

Vasiliki Economopoulos, Maria Pannell, Vanessa A. Johanssen, Helen Scott, Kleopatra E. Andreou, James R. Larkin and Nicola R. Sibson *

Department of Oncology, MRC Oxford Institute for Radiation Oncology, University of Oxford, Oxford, United Kingdom

OPEN ACCESS

Edited by:
Michel Salzet, Lille University of Science and Technology, France

Reviewed by:
Marie Duhamel, Université de Lille, France
Salvatore J. Coniglio, Kean University, United States

***Correspondence:**
Nicola R. Sibson
nicola.sibson@oncology.ox.ac.uk

Specialty section:
This article was submitted to Cancer Immunity and Immunotherapy, a section of the journal Frontiers in Oncology

Received: *08 January 2022*
Accepted: *15 February 2022*
Published: *10 March 2022*

Citation:
Economopoulos V, Pannell M, Johanssen VA, Scott H, Andreou KE, Larkin JR and Sibson NR (2022) Inhibition of Anti-Inflammatory Macrophage Phenotype Reduces Tumour Growth in Mouse Models of Brain Metastasis. Front. Oncol. 12:850656. doi: 10.3389/fonc.2022.850656

Breast cancer brain metastasis is a significant clinical problem and carries a poor prognosis. Although it is well-established that macrophages are a primary component of the brain metastasis microenvironment, the role of blood-derived macrophages (BDM) and brain-resident microglia in the progression of brain metastases remains uncertain. The aim of this study, therefore, was to determine the role, specifically, of pro- and anti-inflammatory BDM and microglial phenotypes on metastasis progression. Initial *in vitro* studies demonstrated decreased migration of EO771 metastatic breast cancer cells in the presence of pro-inflammatory, but not anti-inflammatory, stimulated RAW 264.7 macrophages. *In vivo*, suppression of the anti-inflammatory BDM phenotype, specifically, *via* myeloid knock out of Krüppel-like Factor 4 (KLF4) significantly reduced EO771 tumour growth in the brains of C57BL/6 mice. Further, pharmacological inhibition of the anti-inflammatory BDM and/or microglial phenotypes, *via* either Colony Stimulating Factor 1 Receptor (CSF-1R) or STAT6 pathways, significantly decreased tumour burden in two different syngeneic mouse models of breast cancer brain metastasis. These findings suggest that switching BDM and microglia towards a more pro-inflammatory phenotype may be an effective therapeutic strategy in brain metastasis.

Keywords: neuro-oncology, tumour microenvironment, brain metastasis, microglia, tumour associated macrophages

1 INTRODUCTION

Brain metastasis is a devastating diagnosis for patients with primary breast cancer, and the prognosis is extremely poor; patient survival ranges from 2 to 23 months from diagnosis (1, 2). Many gaps exist in our knowledge regarding the pathogenesis of brain metastasis, but the role of the microenvironment, and cells of the innate immune system (monocytes/macrophages) in particular, remain a subject for debate.

In extracranial metastases, macrophages have been shown to promote disease progression. Gil-Bernabé et al. demonstrated that blood-derived macrophages are associated with arrested tumour

cells in the lung, and that depletion of myeloid cells in the transgenic CD11b-DTR mouse decreases tumour cell survival and prevents the establishment of micrometastases (3). Similarly, Qian et al. showed that depletion of the macrophage population, using clodronate liposomes, hinders the establishment of metastases in the lung (4). More specifically, Yao et al. found that inhibiting anti-inflammatory (M2) macrophage polarization, with the tyrosine kinase inhibitor imatinib, significantly reduced the number of nodules present in the lungs in a lung cancer model, in part due to STAT6 inhibition (5). Similarly, Binnemars-Postma et al. evaluated STAT6 inhibition *in vivo* and showed that inhibition in macrophages reduces tumour growth and development of the metastatic niche within the liver in a murine breast cancer model (6).

Given its unique environment, however, the role that macrophages are known to play in extracranial metastases and primary tumours may not be reflected in the brain. Nevertheless, there is evidence to suggest that the role of macrophages may be similar. In models of glioma, macrophage inhibition through targeting Colony Stimulating Factor-1 Receptor (CSF-1R) decreases tumour volume (7, 8). Since the CSF-1R pathway promotes anti-inflammatory M2 activation and expansion of macrophages and microglia (9–11), it seems likely that the phenotype of these macrophages/microglia is an important factor in brain tumour growth. Indeed, work by Rippaus et al. demonstrated that parenchymal brain metastases have a more anti-inflammatory M2-like phenotype (12), whilst recent work by Andreou et al. demonstrated that specific depletion of anti-inflammatory M2-like macrophages/microglia, using mannosylated clodronate liposomes, in a breast cancer brain metastasis model resulted in decreased tumour burden (13). However, there is also evidence to suggest that macrophages may have an anti-tumour effect; Galarneau et al. found that overall depletion of myeloid cells in CD11b-TK mice treated with ganciclovir actually increased glioma growth (14). Moreover, it is now well established that the dichotomous M1/M2 macrophage polarization paradigm does not fully capture the complexity of the macrophage/microglial activation states, especially when these cells are associated with tumours and experience a wide variety of pro-inflamamtory (M1) and anti-inflammatory (M2) stimuli simultaneously (10). Throughout this work, therefore, we will rather refer to M1 phenotypes and stimuli as pro-inflammatory, and M2 phenotypes and stimuli as anti-inflammatory.

Overall, therefore, uncertainty remains as to the role of macrophages/microglia in both primary and secondary brain tumours, although evidence points towards a pro-tumorigenic role for the predominantly anti-inflammatory polarised subpopulation. Further, it is unclear as to whether brain resident microglia and blood-derived macrophages recruited to brain tumours play differential roles in tumour progression. The primary aims of this study, therefore, were (i) to determine whether anti-inflammatory blood-derived macrophages (BDM) promote tumour cell migration *in vitro*, (ii) to determine whether there is significant infiltration of anti-inflammatory BDM into the microenvironment of breast cancer brain metastases *in vivo*, (iii) to determine whether suppression of anti-inflammatory BDM activation through genetic knock-out reduces brain metastasis growth, and (iv) whether pharmacologically inhibiting BDM and/or microglial populations, or switching them to a more pro-inflammatory phenotype, reduces brain metastasis growth.

2 MATERIALS AND METHODS

2.1 Cell Culture

The EO771 cell line (mouse metastatic medullary mammary carcinoma, C57BL/6 background (15), kindly provided by Prof. Mihaela Lorger, University of Leeds) was cultured in RPMI-1640 medium with 20% FBS, 1% L-Glutamine, 1% non-essential amino acids and 1% sodium pyruvate. The 4T1-GFP cell line [mouse metastatic mammary carcinoma, BALB/c background (16)] was purchased from ATCC and cultured in DMEM medium with 10% FBS and 1% L-Glutamine. The RAW 264.7 cell line (mouse macrophage, kindly provided by Prof. Xin Lu, University of Oxford) was cultured in DMEM medium with 10% FBS and 1% L-Glutamine. All cells were maintained at 37°C and in 5% CO_2.

2.2 Effect of Macrophage Phenotype on Tumour Invasion

RAW 264.7 cells were seeded into the bottom portion of 24-well Matrigel Transwell plate system (Corning) and allowed to adhere overnight. These cells were then treated with either the pro-inflammatory stimulus lipopolysaccharide (LPS; 10 μg/mL) or the anti-inflammatory stimulus interleukin-4 (IL-4; 20 ng/mL), or left untreated as a control for 24 hours. Subsequently, EO771 cells were seeded into the top portion of the Transwells, in wells containing either RAW cells or just the treatment media in the bottom portion. Invasion of the EO771 cells was measured 24 hours later by counting the number of cells that had crossed through the Transwell membrane normalized to the total number of cells on both the upper and lower sides of the Transwell insert (n = 6 for each condition).

The phenotype of the stimulated RAW 264.7 cells was assessed by immunofluorescent staining for the pro-inflammatory marker inducible nitric oxide synthase (iNOS) and the anti-inflammatory marker arginase 1 (Arg1), after 24 hours incubation with either LPS (10 μg/mL), IL-4 (20 ng/mL) or control media. Normalized staining areas were calculated by dividing the measured stained area of the marker by the number of nuclei present, as determined through DAPI staining. The ratio of normalized iNOS stained area to normalized Arg1 stained area was then calculated to determine the predominant phenotype of the stimulated cells.

2.3 Intracerebral Models of Brain Metastasis

All animal experiments were assessed by the University of Oxford Clinical Medicine Ethics Review Committee and approved by the UK Home Office (Animals [Scientific Procedures] Act 1986), and conducted in accordance with the

University of Oxford Policy on the Use of Animals in Scientific Research, the ARRIVE Guidelines and the Guidelines for the Welfare and Use of Animals in Cancer Research (17). All mice were maintained in a specific pathogen free environment and transgenic mice were obtained from in-house breeding colonies.

Mice were injected intracerebrally with EO771 cells in PBS into the left striatum, as described previously (18, 19). Briefly, mice were anaesthetised using 3% isoflurane in 30% oxygen and 70% nitrous oxide, mounted on a stereotactic frame and, subsequently, maintained at 2% isoflurane during surgery. An incision was made on the top of the scalp to expose the skull and a burr hole drilled 0.5 mm forward and 2 mm to the left of bregma. A pulled glass microcapillary (tip <75μm) was inserted stereotaxically through the burr hole to a depth of 2.5 mm from the surface of the brain. EO771 cells (500 cells in 0.5 μl) were injected over 5 min, and the microcapillary left in place for a further 5 min before withdrawing slowly and the scalp wound sutured. Animals were excluded from the study if evidence of extracranial tumour development was found during the course of the experiment. Animals were also excluded if the tumour was found on histological examination to have been injected within the ventricle. Pilot studies were conducted to optimize this injection model.

In order to be able to study a longer time-course of metastasis growth in the brain, it is necessary to use this intracerebral induction model rather than a systemically induced model, as the latter results in significant systemic metastasis burden and animal welfare issues; consequently, longer-term studies are precluded. Previous work by Serres et al. has demonstrated that intracerebral induction route produces similar growth patterns of metastatic colonies and inflammatory responses as an intracardiac injection model, and also recapitulates the microenvironment of human brain metastases (20). Whilst the intracerebral injection model used in that particular study was in rats, similar features are found in the mouse intracerebral injection models used in the current study.

2.3.1 Assessment of Blood-Derived Monocyte/Macrophage Recruitment to Brain Metastases *In Vivo*

Female Lys-GFP-ki transgenic mice (C57BL/6J background; 7-9 weeks) were used to assess recruitment of blood-derived macrophages (BDM) to the brain, as this strain possesses GFP expression in myeloid cells, but not microglia (21, 22). Mice were injected intracerebrally with EO771 cells, as described above, at day 0 and were perfusion-fixed 7, 14 or 21 days later for histological assessment (details below).

2.3.2 Suppression of Anti-Inflammatory Phenotype in Blood-Derived Monocytes/Macrophages

$LysM^{Cre/Cre}KLF4^{fl/fl}$ (C57BL/6J background; 7-9 weeks, kindly provided by Dr Xudong Liao, Case Western Reserve University) transgenic mice were used to assess the effect of BDM phenotype on brain metastasis growth. In these mice, the KLF4 transcription factor is knocked out in BDM (23), resulting in suppression of the anti-inflammatory phenotype through downstream inhibition of the STAT6 pathway. For these experiments, $LysM^{Cre/Cre}$ mice of the same background were used as controls. Blood-derived specificity of the KLF4 knock out was confirmed through genotyping of primary microglia and BDM isolated from the bone marrow of $LysM^{Cre/Cre}KLF4^{fl/fl}$ mice (**Figure S1**). Mice were injected intracerebrally, as above, with EO771 cells and perfusion-fixed 21 days later for histological assessment.

2.3.3 Pharmacological Inhibition of Macrophages/Microglia *In Vivo*

To further assess the roles of BDM/microglia, and the anti-inflammatory phenotype specifically, Lys-GFP-ki mice (as above) were treated with either macrophage inhibitory peptide (Tuftsin fragment 1-3, TKP, Bachem) or the CSF-1R neutralizing antibody (M279, Amgen). TKP has previously been shown to reduce overall macrophage/microglial activation, and to shift their transcriptional profile to more anti-inflammatory (Th2) in experimental autoimmune encephalomyelitis and spinal cord injury models (24, 25). In contrast, M279 has been shown to suppress the anti-inflammatory macrophage expansion (26) and to exert its effects on the CSF-1R pathway exclusively in BDM, and not brain-resident microglia (27). Control animals were treated with PBS. All treatments were delivered by osmotic minipump (100 μL 28 day release, model 1004 Alzet Osmotic Minipump, purchased through Charles River) which delivers its payload at a rate of 0.11μL/hour.

One week prior to intracerebral injection, animals underwent surgery to implant the minipump. Animals were anaesthetised with 3% isoflurane in 30% oxygen and 70% air, and subsequently maintained with 2% isoflurane. Immediately prior to surgery preparation, animals received a subcutaneous injection of Vetergesic (Buprenorphine, 0.1 mg/kg) and a local injection of Marcaine 0.25% (bupivacaine, 7.5 mg/kg) at the incision/implantation site. The fur at the back of the neck and on the upper back was then clipped and cleaned with a chlorhexidine preparation. An incision was made just below the base of the neck from the left to right of the animal and a sufficiently sized pocket was created under the skin on the back through the incision. A filled pump was placed nozzle-end first into the pocket, and a suture placed internally to secure the pump in the pocket. The incision was sutured closed.

After a 48 hour *in vivo* priming period, mice were treated for 5 days with either TKP (2.27 mM in PBS), M279 (50 mg/mL in PBS) or PBS alone, prior to cell injection. At day 7, mice were injected intracerebrally, as above, with EO771 cells, and were perfusion-fixed at day 28 post-minipump implantation (21 days post-cell injection) for histological assessment (details below).

2.4 Inhibition of Anti-Inflammatory Macrophages/Microglia in an Intracardiac Brain Metastasis Model

To assess the effects of inhibiting the anti-inflammatory BDM/microglia phenotype on brain metastasis development, a model that more closely mimics the natural development of brain metastases was used. Female BALB/cAnNCrl mice (7-9 weeks

old; Charles River, Margate, UK) were injected with 10^5 4T1-GFP cells in 100 μL of PBS *via* the left ventricle of the heart under ultrasound image guidance, as described previously (28), to allow haematogenous dissemination to the brain. One week after intracardiac injection, animals were implanted with subcutaneous osmotic minipumps, as above. Following 48 hours *in vivo* priming, mice were treated with either the STAT6 inhibitor AS1517499 (11.43 mg/mL; 10.6 mg/kg/week) or vehicle (50% DMSO in water) for 7 days from day 9 after intracardiac injection. AS1517499 is BBB penetrant (29) and, thus, will inhibit the STAT6 pathway in both BDM and microglia. Animals were perfusion-fixed at 16 days post-intracardiac injection and prepared for histological assessment (detailed below).

2.5 Immunofluorescence

For immunofluorescent analysis of macrophage/microglial infiltration and phenotype, animals were deeply anaesthetised with sodium pentobarbital (40 mg/mL; 0.2 mL injected i.p.) and transcardially perfusion-fixed with heparinised saline, followed by periodate-lysine-paraformaldehyde with 0.25% glutaraldehyde (PLP_{light}). The brains were removed, cryopreserved in 30% sucrose and frozen in OCT. Tissue sections were cut at a thickness of 10 μm and allowed to dry on the slides for 24 hours.

Sections were stained for a variety of antigens as either single, double or triple immunofluorescent stains. The following antigen targets were stained (see **Table S1** for antibody details): iNOS (rabbit anti-mouse) with Arg1, F4/80 with iNOS (rabbit anti-mouse), F4/80 with Arg1, TMEM119 with F4/80 and iNOS (mouse anti-mouse), TMEM119 with F4/80 and Arg1. In the case of iNOS two different antibodies were used as differentiated above. TMEM119 staining was used to differentiate microglia from BDM in the KLF4 knock out study (30–35). Using Lys-GFP-ki mice, we confirmed that there was minimal TMEM119 and GFP colocalization (**Figure S2**).

2.6 Fluorescent Image Acquisition and Analysis

Images of entire brain sections for volume calculation were acquired using a Nexelom Celigo image cytometer (Nexelom, Manchester, UK) using the slide scanning function. Cell culture plates were also imaged and analysed with this system using the expression analysis function. Tumour foci were identified and measured using DAPI stained sections.

In the intracardiac 4T1 model, DAPI stained images were used to measure tumour burden, which was calculated by measuring the total area of metastases within sections and then dividing by the total section area of analysed sections. The number of lesions per area was measured by dividing the number of metastases measured by the total section area of analysed sections. Average lesion area was calculated by dividing the total area of lesions by the total number of lesions.

All confocal images were acquired on a Zeiss LSM 710 inverted confocal microscope. Images were acquired as z-stacks with 10 slices and a spacing of 1.46 μm using a 20x objective, a software zoom of 1 and with 4 averages. Images were acquired from at least 3 separate tissue sections spaced 60 - 180 μm apart for each animal.

Co-localization analysis was performed on confocal images between immunostained markers and GFP using an automated in-house ImageJ plugin. All analyses were performed on raw, unprocessed images. In this analysis, the threshold for positive signal for each marker was defined as the average signal of the background plus 3 standard deviations, as determined from images specifically acquired of the background signal. The plugin calculated the areas of positive signal based on these thresholds for each marker, whilst tracking the area of co-localized pixels for each combination of markers present in the image. The co-localization between markers was calculated as the percentage of marker A area that co-localized with marker B, by dividing the area of co-localized pixels (A + B) by the total area of marker A. All calculations were performed by the automated inhouse ImageJ plugin with the calculated thresholds for each marker being fed into this software.

The colour thresholding tool was used to quantify the number of cells that were GFP+ and either F4/80+ or F4/80- using previously calculated thresholds. First, the GFP+ threshold was used to create a mask of all GFP+ cells and this was then used to block out any areas that were not GFP+. Next the F4/80+ threshold was used to create a second mask that highlighted areas of F4/80+ staining. Finally, the masks were overlapped to identify areas of GFP and F4/80 co-localization, and the number of cells that fell into the GFP+F4/80+ or GFP+F4/80- categories were counted.

2.7 Statistical Analysis

Sample sizes required for sufficient statistical power were calculated using pilot data. The details of these calculations are shown in **Table S2** and were performed using the methodology described by Kadam and Bhalerao (36). Analysis was performed on measurements taken from independent samples.

In the KLF4 knock out study, a two-tailed Student's t-test was used to compare tumour volume, cell infiltration and cell phenotype between the control and knockout groups. In the characterization study and the pharmacological inhibition study (TKP and M279), expression of histological markers was compared using a one-way ANOVA test, with Welch's ANOVA used where the standard deviation of data varied significantly between groups. The Tukey's and Dunnett's (Welch's ANOVA) post-tests were used when ANOVA results were significant, to compare individual groups. A two-way ANOVA was used to compare iNOS and Arg1 expression over time in the characterization study.

In the intracardiac 4T1-GFP model, a two-tailed Student's t-test was used to compare tumour burden, number of lesions/area and average lesion area between the AS1517499 treated and vehicle only treated groups. A two-tailed Student's t-test was also used to compare the expression of immunostained markers in both the KLF4 knock out model and the intracardiac 4T1-GFP model.

Normality testing was performed using the Shapiro-Wilk test and data that were found to not follow a normal distribution in

all experiments were analysed using non-parametric versions of the above tests (Mann-Whitney and Kruskal-Wallis tests). All sample sizes for groups in each study are reported within figure captions.

To ensure data reproducibility, we monitored the volume of the control groups in each experiment to ensure that these remained similar. Animals that received the various pharmacological treatments were distributed as evenly as possible between all cages to ensure that both control and treatment variability could be controlled. The researcher was blinded to treatment group and knock out status of animals during the analysis of the data, and animals were identified in a manner that only the particular experiment they were in could be known.

3 RESULTS

3.1 Effect of Macrophage Phenotype on Tumour Cell Invasion *In Vitro*

To determine whether macrophage phenotype alters tumour cell invasion *in vitro*, cultured macrophages were treated with either LPS to induce a pro-inflammatory phenotype or IL-4 to induce an anti-inflammatory phenotype. The phenotype of LPS stimulated, IL-4 stimulated and unstimulated control RAW264.7 cells was confirmed by determining the ratio of iNOS : Arg1 expression immunofluorescently (**Figure 1A**). Since the phenotype of macrophages exists as a continuum, rather than as discrete classes, the ratio of iNOS : Arg1 was used in addition to individual expression levels to assess shifts in macrophage and microglial phenotype. LPS stimulated cells showed a significantly higher iNOS : Arg1 ratio than control cells (**Figure 1B**; $p < 0.01$), indicating a predominantly pro-inflammatory phenotype. Conversely, the IL-4 stimulated cells showed a significantly reduced iNOS : Arg1 ratio compared to LPS stimulated cells ($p < 0.05$), indicating a more anti-inflammatory phenotype, although the ratio was not significantly different to control cells ($p = 0.1478$). In the Transwell invasion assay, significantly fewer EO771 cells passed through the Matrigel membrane in the wells with LPS stimulated macrophages in the bottom chamber, compared to both IL-4 stimulated and control macrophages (**Figure 1C**; $p < 0.05$). Increased EO771 invasion was also evident in IL4 stimulated ($p < 0.01$) and control ($p < 0.001$) wells where RAW macrophages were present, compared to the media + stimulus only wells (**Figure 1C**).

3.2 Infiltration of Blood-Derived Monocytes/Macrophages *In Vivo*

Infiltration of BDM into brain metastases *in vivo*, was assessed in the Lys-GFP-ki transgenic mice (**Figure 2A**), in which GFP is expressed in myeloid cells and not within microglia (21, 22). The percentage of GFP within metastasis foci in the brain increased significantly from day 7 to days 14 and 21 ($p < 0.001$; **Figure 2B**). Whilst overall expression of the mouse macrophage/microglial marker F4/80 as a percentage of tumour area did not change

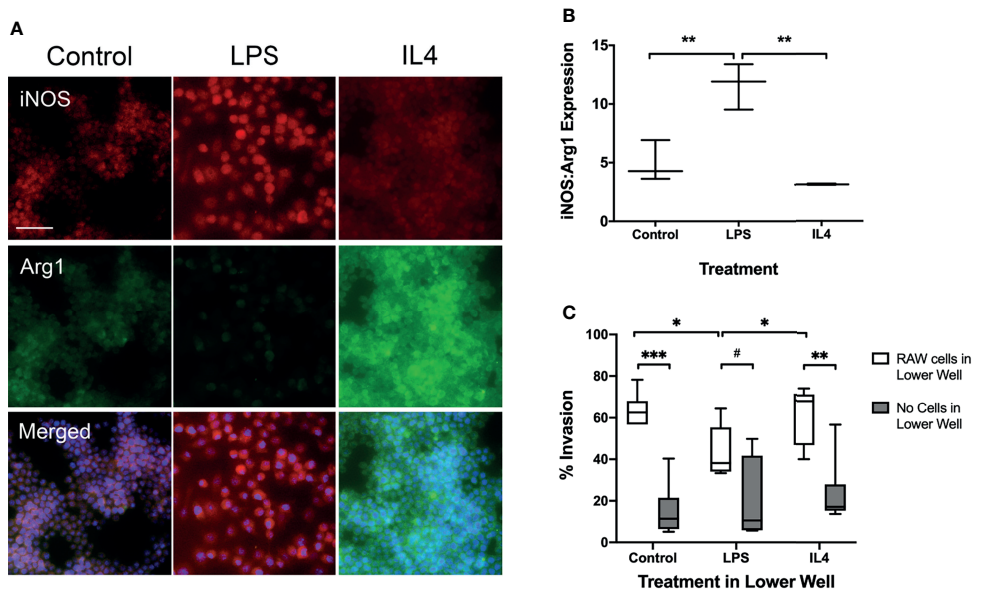

FIGURE 1 | Transwell migration assay with RAW 267.4 macrophages and EO771 metastatic tumour cells. **(A)** Immunofluorescent staining of pro-inflammatory marker iNOS and anti-inflammatory marker Arg1 in macrophages to assess phenotype following incubation with either the pro-inflammatory stimulus LPS or the anti-inflammatory cytokine IL4. Bottom panel of images also contains nuclear (DAPI) counterstain (blue). **(B)** Graph showing ratio of iNOS : Arg1 expression in macrophages treated with either LPS (n = 6) or IL4 (n = 6), compared to untreated macrophages (n = 6). **(C)** Graph showing percentage of EO771 tumour cells migrating through the Matrigel coated Transwell membrane in the presence of either LPS (n = 6) or IL4 (n = 6) stimulated or untreated (n = 6) macrophages (white bars), or the stimulus media alone without macrophages (grey bars). Data shown as box and whisker plots depicting full range of data points. Scale bar = 100 μm. *$p < 0.05$, **$p < 0.01$, ***$p < 0.001$, $^{\#}p = 0.0756$".

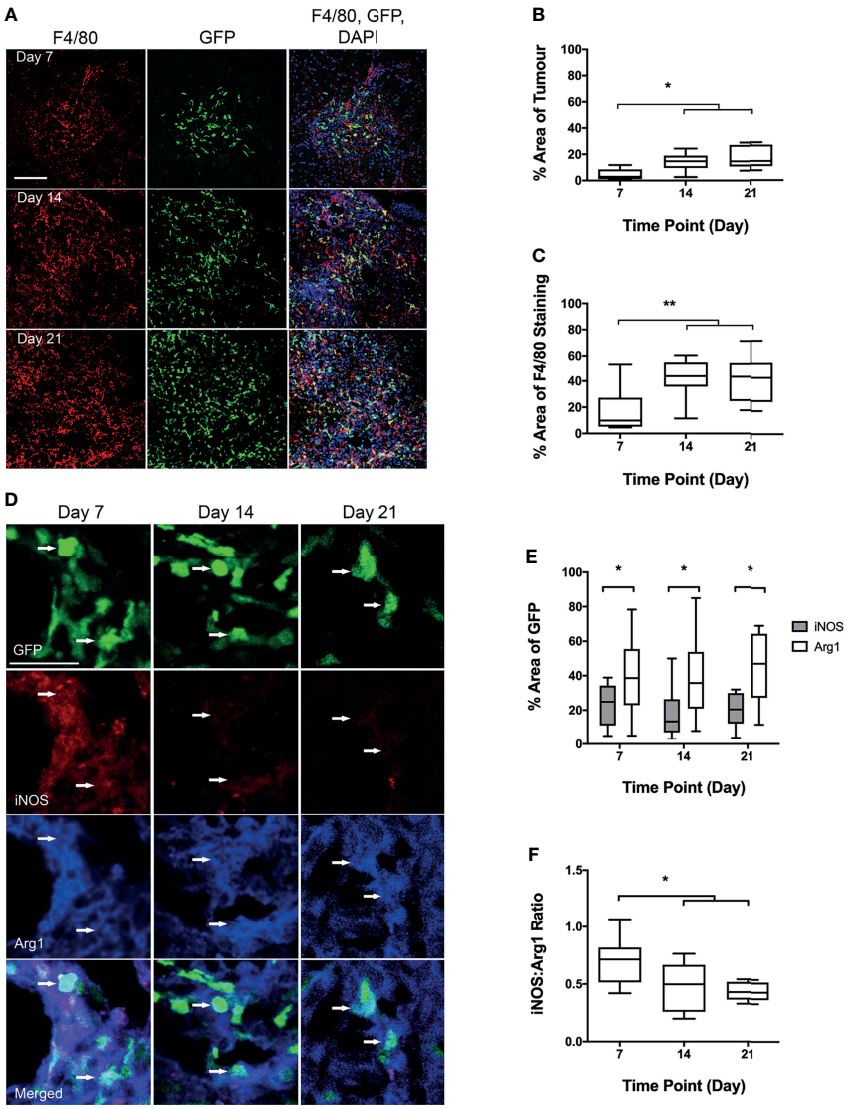

FIGURE 2 | Analysis of blood-derived macrophage (BDM) infiltration and phenotype into tumour foci from Lys-GFP-ki mice injected intracerebrally with EO771 cells. **(A)** Co-localisation of GFP fluorescence (BDM; green) with immunofluorescent staining for F4/80 (all microglia/macrophages; red). Nuclei stained with DAPI (blue). Scale bar = 100 µm. **(B)** Graph showing percentage of tumour area that is GFP positive indicating infiltration of BDM. **(C)** Graph showing percentage of F4/80 staining that is GFP positive, indicating relative proportions of BDM and brain-resident microglia within the tumour foci. **(D)** Co-localisation of immunofluorescent staining for iNOS (pro-inflammatory; red) or Arg1 (anti-inflammatory; blue) with GFP in BDM. Arrows indicate GFP+ BDM with colocalization of iNOS and Arg1. Scale bar = 30 µm. **(E)** Graph showing percentage of GFP-positive area that is either iNOS (grey bars) or Arg1 (white bars) positive. **(F)** Graph showing ratio of iNOS : Arg1 in GFP-positive cells. N = 9 at day 7, n = 9 at day 14 and n = 10 at day 21. Data shown as box and whisker plots depicting full range of data points. *$p < 0.05$, **$p < 0.01$.

significantly, the percentage of F4/80 expressing cells that were also GFP positive increased significantly from day 7 to days 14 and 21 ($p < 0.01$; **Figure 2C**). The GFP positive area of the tumours correlated with tumour volume ($p < 0.0001$; **Figure S3**). The proportion of GFP positive cells that were also F4/80 positive was greater than 90% on average, indicating that they were predominantly monocytes/macrophages, and did not vary significantly between time points (**Figure S2A**). Interestingly, qualitative observation suggested that microglial recruitment was greater at the margins of the tumours, whilst BDM were evident throughout.

3.3 Immune Phenotype of Infiltrating Blood-Derived Monocytes/Macrophages

Tissue sections stained for both Arg1 and iNOS (**Figure 2D**), showed significantly higher levels of Arg1 co-localisation with GFP positive cells, than for iNOS ($p < 0.05$; **Figure 2E**). The ratio of iNOS/Arg1 on GFP positive cells decreased significantly from

day 7 to days 14 and 21 ($p < 0.05$; **Figure 2F**), indicating an increasingly anti-inflammatory phenotype in recruited blood-derived myeloid cells, predominantly monocytes/macrophages (see above).

3.4 Suppression of Anti-Inflammatory Phenotype in Blood-Derived Monocytes/Macrophages

Next, to determine the effect of anti-inflammatory BDM, specifically, on tumour growth, myeloid specific deletion of KLF4 was used to suppress STAT6-mediated anti-inflammatory macrophage activation (**Figure 3**). Representative images of tumours stained for F4/80 are shown in **Figure 3A**. Immunofluorescent images stained with F4/80 and TMEM119 with both iNOS and Arg1 are shown in **Figure 3B**. No significant differences were found between control and KLF4 knockout (KLF4-KO) mice for either the percentage of tumour area showing overall macrophage/microglia infiltration (F4/80 staining) or, specifically, microglial infiltration/activation (TMEM119+F4/80+) or BDM infiltration (TMEM119-F4/80+; **Figure S5**). The ratio of BDM to microglia was not significantly different between WT and KO animals (**Figure 3C**). A significant reduction in tumour volumes, however, was evident in the KLF4-KO group compared to control animals ($p < 0.05$; **Figure 3D**). In the TMEM119 positive microglial population, no significant difference was found between KLF4-KO and controls for either Arg1 or iNOS expression (**Figure S4**), and the ratio of iNOS : Arg1 was not significantly different (**Figure 3E**). In contrast, the level of Arg1 expression was significantly reduced in BDM in the KLF4-KO group ($p < 0.05$), whilst the level of iNOS expression remained unchanged (**Figure S4**). Consequently, the iNOS : Arg1 ratio in BDM increased significantly in the KLF4-KO group ($p < 0.05$; **Figure 3F**).

3.5 Inhibition of Macrophages/Microglia *In Vivo*

We next assessed the effects of inhibiting pro- and anti-inflammatory BDM/microglial phenotypes through TKP and M279 treatment, respectively. Again, the Lys-GFP-ki mouse strain was used, to enable differentiation between BDM and brain-resident microglia. Immunofluorescent staining for F4/80, iNOS and Arg1 demonstrated changes in infiltration and phenotype in the BDM and microglial populations according to treatment (**Figure 4**). Overall levels of F4/80 staining within tumours was significantly higher in mice treated with M279 (CSF-1R mAb) compared to TKP treatment mice ($p < 0.05$; **Figure 4A**). Whilst no differences were observed between groups for GFP positive myeloid cell infiltration (**Figure 4B**), microglial infiltration was significantly higher in M279 treated mice compared to both PBS and TKP treated mice ($p < 0.05$; **Figure 4C**). The proportion of GFP positive cells that were also F4/80 positive did not vary between treatment groups and remained above 90% as for the previous study, indicating that the majority of recruited myeloid cells were BDM (**Figure S2B**). Colocalization analysis of iNOS expression (**Figure 4D**) and Arg1 (**Figure 4E**) demonstrated changes in phenotype of BDM. iNOS expression did not vary significantly between groups in any macrophage/microglial population (**Figure 4F**). In contrast, Arg1 expression in GFP positive BDM was significantly lower in M279 treated mice compared to the TKP treated group ($p < 0.05$; **Figure 4G**). Although, there appeared to be a trend towards a reduction in iNOS : Arg1 in all populations from the M279 treated group compared to the TKP treated group (**Figure 4H**), the ratio of iNOS : Arg1 expression was not significantly different between groups in any cell population, likely owing to inter-animal variability particularly in the M279 treated group. Measurements of tumour volume from immunofluorescent stained sections (**Figure 5A**), showed a significant decrease in M279 treated animals compared to both PBS and TKP treated groups (**Figure 5B**).

3.6 Inhibition of Anti-Inflammatory Macrophages/Microglia in An Intracardiac Brain Metastasis Model

Finally, the effect of inhibiting the anti-inflammatory phenotype of BDM/microglia was determined in animals injected intracardially with 4T1-GFP cells and treated with either the STAT6 inhibitor AS1517499 or vehicle. *In vitro* culture of 4T1-GFP cells with AS1517499 showed no negative effects on tumour cell growth or viability (**Figure S5**). Immunostaining for F4/80 and TMEM119 with Arg1 or iNOS (**Figure 6A**) demonstrated a decrease in Arg1 expression in TMEM119+F4/80+ microglia in the AS1517499 treated group compared to the vehicle control group ($p < 0.05$; **Figure 6B**). Arg1 expression in total F4/80 and BDM also demonstrated a similar trend ($p = 0.0667$ for both). No significant changes were observed in iNOS expression (**Figure 6C**) or the ratio of iNOS : Arg1 expression (**Figure 6D**) in each cell population. Tumour burden was found to be significantly lower in the AS1517499 treated group ($3000 \pm 800\ \mu m^2/mm^2$) compared to the vehicle controls ($5600 \pm 550\ \mu m^2/mm^2$; $p < 0.05$; **Figure 6E**). Whilst the average lesion area was not significantly different between groups (**Figure 6F**), a trend towards a decrease in the number of lesions per mm^2 was evident ($p = 0.075$, **Figure 6G**).

4 DISCUSSION

Macrophages are known to impact systemic tumour progression and extracranial metastasis, and have also been implicated in glioma and breast cancer brain metastasis (4, 7, 13, 37, 38). There is mounting evidence that macrophages/microglia, and their different phenotypes, play an important role in brain metastasis progression, with an increasing number of studies suggesting a role for the anti-inflammatory phenotype specifically. In this study, initial *in vitro* experiments demonstrated that macrophage phenotype affects migration of metastatic breast cancer cells, with anti-inflammatory phenotype (IL-4-stimulated) leading to increased migration compared to pro-inflammatory phenotype (LPS-stimulated). Subsequent *in vivo* studies demonstrated that infiltration of blood-derived myeloid cells (predominantly macrophages; BDM) into brain

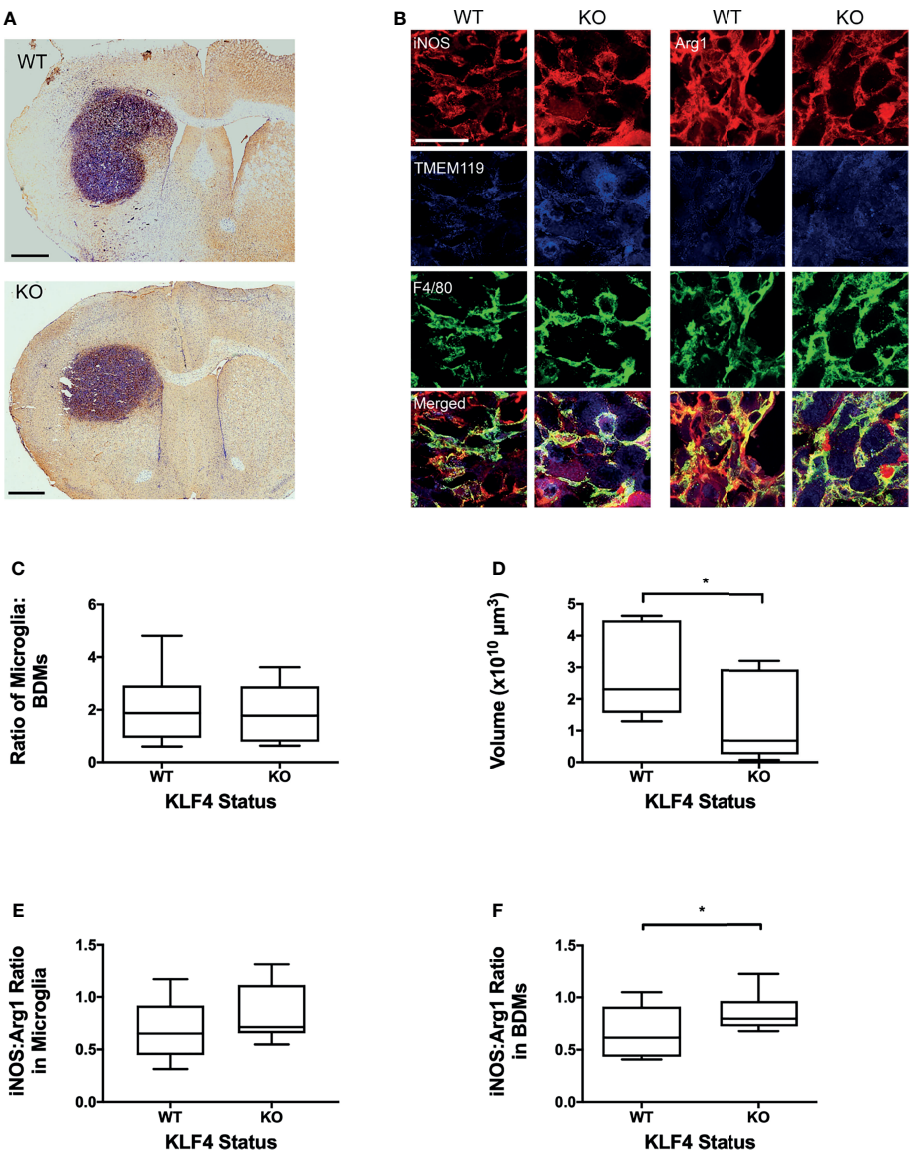

FIGURE 3 | Effect of KLF4 knock out in myeloid cells on phenotype of blood-derived macrophages (BDM) and microglia in brain metastases and tumour growth. **(A)** Representative IHC images showing F4/80 staining in metastases for wild-type (upper panel, n = 9) and knock-out (lower panel, n = 8) mice. Sections counterstained with cresyl violet. Scale bars = 1 mm. **(B)** Immunofluorescent staining of F/480 (total macrophage/microglia; green), TMEM119 (microglia; blue) with either iNOS (left panels, red) or Arg1 (right panels, red) in WT and KLF4-KO mice. Scale bar = 50 µm. **(C)** Graph showing ratio of microglia (TMEM119+ F4/80+) to BDM (TMEM- F4/80+) in WT and KLF4-KO mice. **(D)** Graph showing tumour volumes in WT and KLF4-KO mice. **(E, F)** Graphs showing ratios of iNOS : Arg1 expression, in WT and KLF4-KO mice, in **(E)** microglia (p = 0.152) and **(F)** BDM (p = 0.036). Data shown as box and whisker plots depicting full range of data pointspoints. *p < 0.05.

metastases increased over time, and with an increasingly anti-inflammatory phenotype. Moreover, suppression of the anti-inflammatory phenotype in BDM, either through BDM specific KLF4 knock-out or antibody blockade of CSFR1, resulted in a significant reduction in brain metastasis growth. Finally, inhibition of the anti-inflammatory microglial phenotype *via* STAT6 inhibition, in a model of haematogenously disseminated brain metastases, also significantly reduced brain tumour burden. Together these data suggest that modulation of both BDM and microglial phenotype towards a pro-inflammatory profile has substantial therapeutic potential in brain metastasis.

Our *in vitro* work has demonstrated that an anti-inflammatory macrophage phenotype promotes breast cancer cell invasiveness. Previous work by Green et al. demonstrated an increase in colorectal (CT26) tumour cell migration and invasiveness in the presence of unstimulated RAW 264.7 macrophages or their conditioned media, as well as increases in transcription of genes associated with increased tumour aggressiveness (39). However,

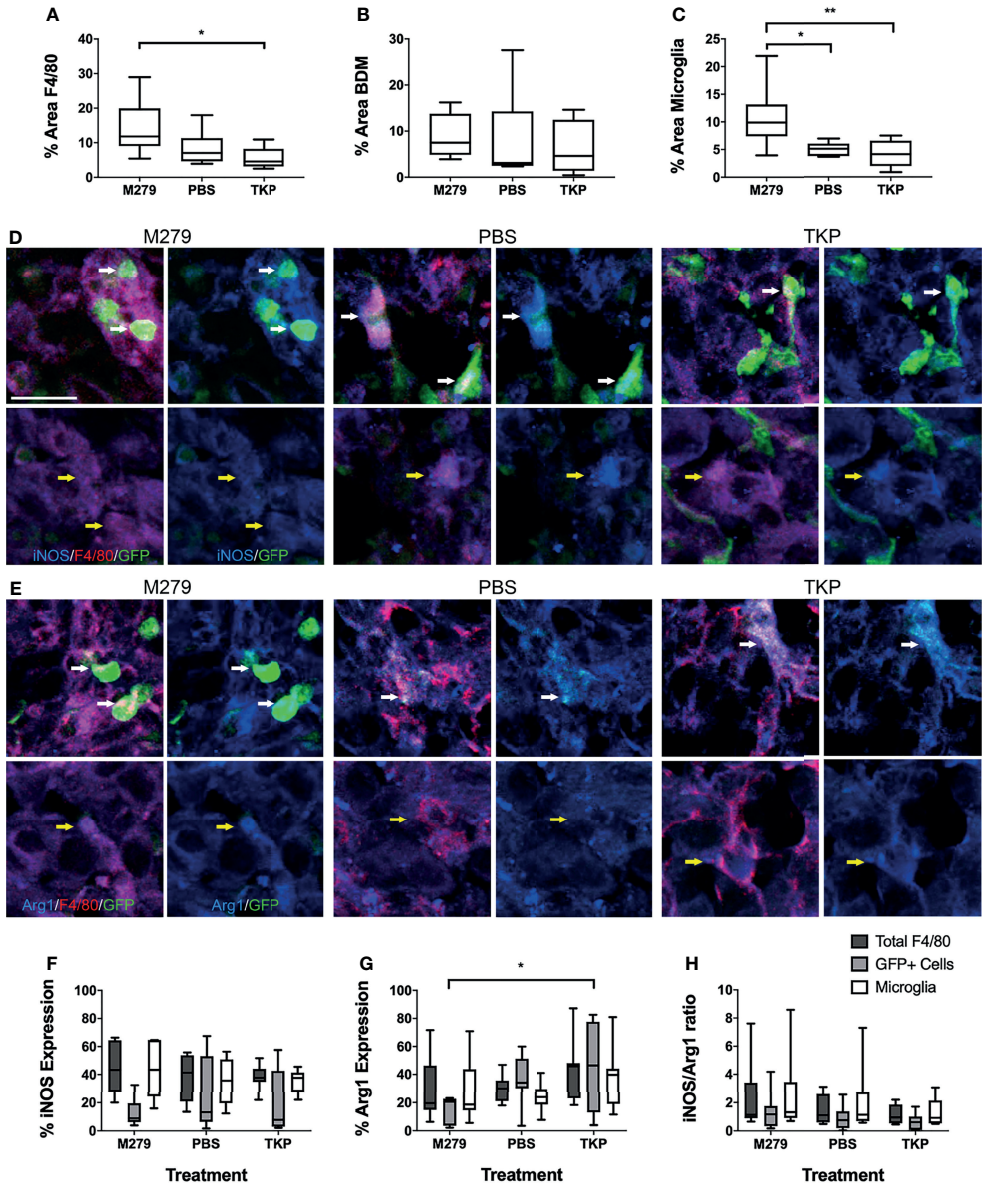

FIGURE 4 | Effect of phenotype modulation of microglia and blood-derived macrophages (BDM) with TKP and the CSF-1R neutralizing antibody, M279. **(A–C)** Graphs showing percentage of tumour area that is stained for **(A)** all F4/80+ cells, **(B)** GFP+ BDM and **(C)** GFP- microglia. **(D, E)** Immunofluorescent staining of F4/80 (red) with **(D)** iNOS or **(E)** Arg1 (blue) and endogenous GFP in M279 (n = 7), PBS (n = 7) and TKP (n = 8) treated mice. In each panel, the upper rows are highlighting GFP+ BDM (white arrows), whilst the lower rows are highlighting GFP- microglia (yellow arrows). **(F–H)** Graphs showing expression of **(E)** iNOS, **(F)** Arg1 and **(G)** ratio of iNOS : Arg1 expression in all F4/80+ cells (dark grey bars), GFP+ BDM (light grey bars) and microglia (white bars). Data shown as box and whisker plots depicting full range of data points. Scale bar = 20 μm. *$p < 0.05$.

no information on the phenotype of the macrophages was reported. Macrophage TNF and TGFβ1 present within co-cultures have also been shown to increase the migration of MDA-231 breast cancer cells in a 3D culture model through MMP1 and MT1-MMP, respectively (40). This finding conflicts with our results as TNF is known to be a pro-inflammatory cytokine. However, the phenotype of activated macrophages is complex, potentially expressing a combination of pro- and anti-inflammatory markers and cytokines, dependent upon the specific environment surrounding the macrophages (10).

Our initial *in vivo* studies indicated significant recruitment of BDM to brain metastases, which not only increased over time but also became more anti-inflammatory in phenotype, with a decrease in the expression of iNOS relative to Arg1. It is important to recognise, however, that the phenotype of macrophages/microglia do not fall into discrete classes of

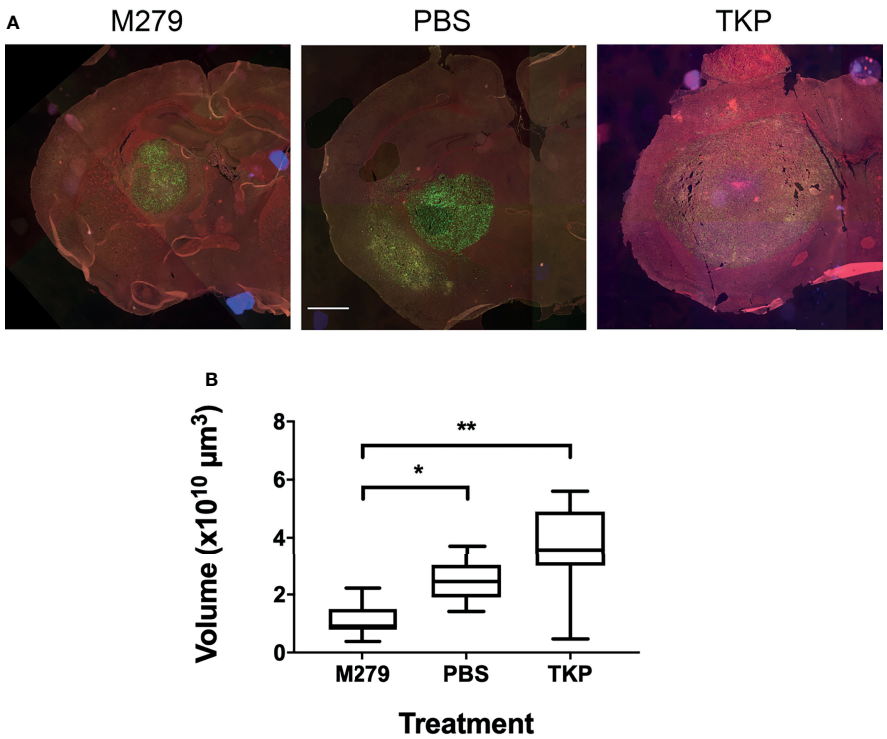

FIGURE 5 | Effect of TKP and M279 treatment on tumour volume. **(A)** Representative images of brain sections from M279 (CSF-1R mAb), PBS and TKP treated mice. Scale bar = 1 mm. **(B)** Graph of tumour volumes in M279 (n = 7), PBS (n = 7) and TKP (n = 8) treated groups. Data shown as box and whisker plots depicting full range of data points. *p < 0.05, **p < 0.01.

pro-inflammatory or anti-inflammatory, but exist on a spectrum where both pro- and anti-inflammatory phenotype markers may be expressed within the same cell, or population of cells, but to differing degrees (10, 41). Our previous work demonstrated that anti-inflammatory macrophages and microglia, expressing Arg1 and the mannose receptor MRC-1 (CD206), are present within brain metastases and that these markers also tend to increase as the metastases progress (13). The current study builds on that work by differentially looking at the phenotype of BDM specifically, rather than the mixed population of BDM/microglia. Rippaus et al. previously evaluated the phenotype of macrophages and microglia in parenchymal and dural brain metastases. Their findings showed that BDM and microglia in parenchymal metastases have a more anti-inflammatory phenotype with a decrease in iNOS expression and an increase in CD206 expression, and that there is a phenotypic difference in BDM between dural and parenchymal metastases (12). In that study, microglia and BDM were identified based on relative expression of macrophage specific markers, which may not stratify BDM and microglia entirely. To address this potential limitation, and further assess the phenotype of BDM recruited to metastases, we have used a model that specifically expresses GFP in myeloid cells. Whilst the GFP expression occurs in all myeloid cells, we have found that in the brain metastasis model used here the contribution of non-BDM cells (GFP+F4/80-) to the overall GFP+ infiltrating population was <10%. Thus, our results predominantly reflect infiltrating BDM, although we cannot exclude a minor contribution from granulocytes. This finding is consistent with previous studies, in which the major infiltrating population in parenchymal brain metastases were CD11b+F4/80+ cells (12, 42). Overall, the results of this study are consistent with previous reports and demonstrate increasing infiltration of anti-inflammatory BDM, specifically, over time.

Given the increasingly anti-inflammatory phenotype of recruited BDM in the above study, our next aim was to determine the impact of this phenotype on brain metastasis growth. The transcription factor KLF4 has been shown to be a key regulator of macrophage polarization in models of both prostate (43) and breast cancer (6), and is activated through STAT6 signaling; this, in turn, is triggered through IL-4 signaling and participates in limiting the pro-inflammatory response (44). Here, we have shown that in KLF4 knock-out animals the anti-inflammatory response of BDM, but not brain-resident microglia, is significantly suppressed, and that this is associated with a reduction in brain metastasis growth. Subsequent studies, using the more clinically relevant antibody-mediated inhibition of anti-inflammatory BDM, further confirmed the above finding, and together these data support the notion that anti-inflammatory BDM recruited to brain metastases are pro-tumorigenic. These results are in accord with our previous work, in which mannosylated clodronate liposomes were used to deplete the total anti-inflammatory BDM/microglia population in an intracerebral brain metastasis model, using 4T1-GFP cells in

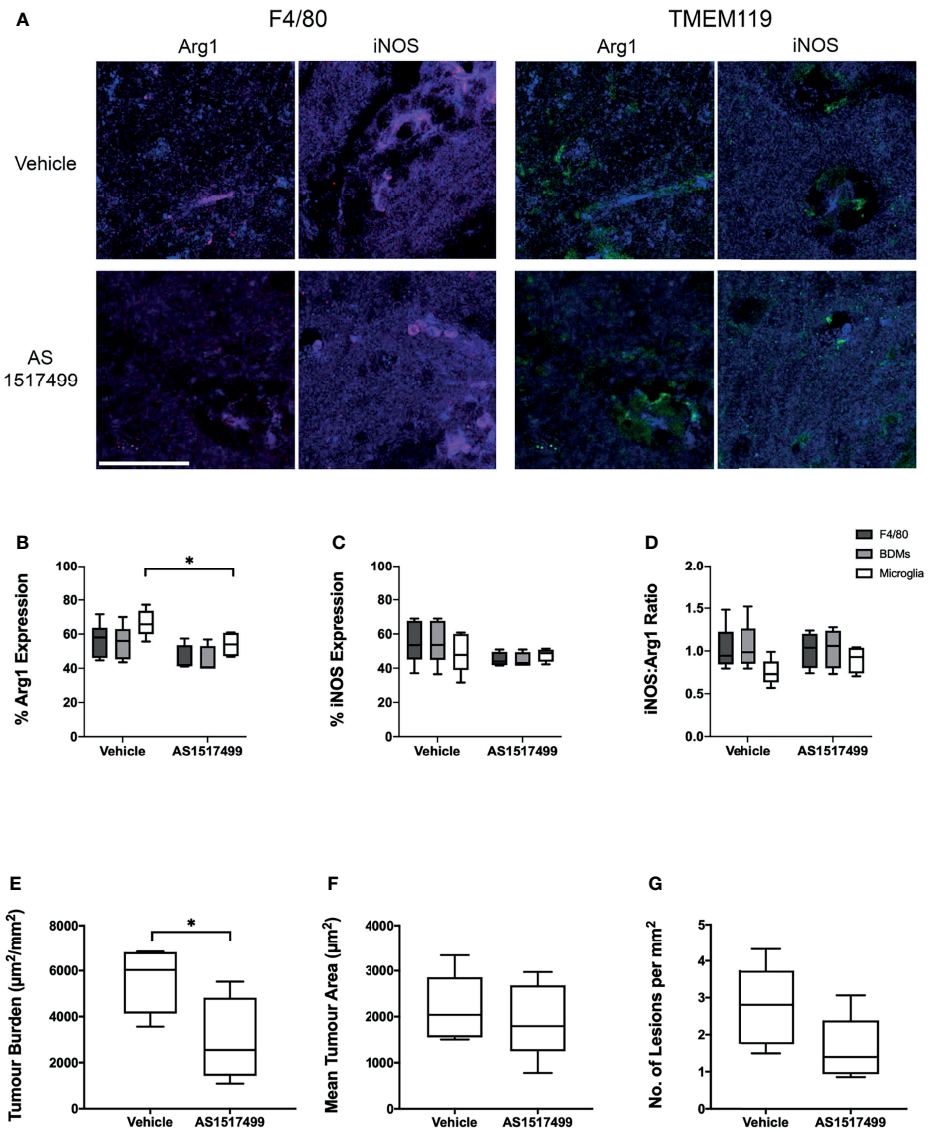

FIGURE 6 | Effect of STAT6 Inhibition in BALB/c mice injected intracardially with 4T1-GFP cells. **(A)** Representative immunofluorescence images from vehicle and AS1517499 treated mice depicting co-expression of F4/80 (red, left panel) with Arg1 and iNOS (blue), and TMEM119 (green, right panel) with Arg1 and iNOS (blue). Scale bar = 40 μm. **(B–D)** Graphs showing **(B)** expression of Arg1, **(C)** expression of iNOS and **(D)** the ratio of iNOS : Arg1 expression in all F4/80+ cells (dark grey bars), microglia (TMEM119+F4/80+ cells, light grey bars) and BDM (TMEM119-F4/80+ cells, white bars) for vehicle (n = 6) and AS1517499 (n = 5) treated mice. **(E–G)** Graphs showing **(E)** tumour burden measured as total area of metastases divided by total tissue area analysed, **(F)** average tumour area, and **(G)** average number of metastases per square mm of tissue analysed. Data shown as box and whisker plots depicting full range of data points. *p < 0.05.

BALB/c mice. In that work, we observed a significant decrease in anti-inflammatory BDM/microglia, together with a reduction in tumour growth (13).

In accord with our findings, the antibody used in our studies, M279, which does not readily cross the BBB, has previously been shown not to alter the resident microglial phenotype when administered systemically (26, 27), and to inhibit anti-inflammatory monocyte/macrophage activation without affecting pro-inflammatory activation (26). The above findings are also in agreement with previous studies showing that inhibition targeting the CSF-1R pathway shifted the phenotype of activated tumour-associated macrophages (TAMs) towards a more pro-inflammatory phenotype, resulting in reduced tumour growth in glioblastoma models (7, 8), as well as in extracranial models of breast and cervical cancer (45). Moreover, it has also been shown that the addition of CSF-1R pathway inhibition to adoptive cell therapy in preclinical melanoma models can improve the anti-tumour response (46). However, those studies used small molecule inhibitors of CSF-1R, such as BLZ495 and PLX3397, which are known to be BBB penetrant. Interestingly, in contrast to the current work, studies with such molecules have shown an overall decrease in macrophage and/or microglial recruitment (7, 47), although a decrease in M2

(anti-inflammatory) genes has also been observed, which is consistent with our work (7). As M279, could not act directly on microglia in our study, the observed increase in microglial recruitment may reflect paracrine signaling from other cells within the microenvironment (48, 49).

Interestingly, whilst others have shown that TKP is capable of attenuating activation of both BDM and microglia (24, 25), in the current study we found no significant changes in either BDM/microglia numbers or phenotype following TKP treatment. These differences may reflect the models used in those previous studies, which were predominantly pro-inflammatory (e.g. experimental autoimmune encephalomyelitis (EAE), spinal cord injury and intracerebral ischemic hemorrhage) (24, 25, 50) and, consequently, represent an entirely different immune environment to cancer. At the same time, the relatively short time-course of the treatment and inter-animal variability may have reduced sensitivity to the effects of TKP in the current study; there is some minor suggestion of a movement towards reduced numbers of both BDM/microglia and pro-inflammatory phenotype in the TKP treated group when compared to the controls, and a possible increase in tumour volume. Nevertheless, none of these changes reach significance and further work would be required to confirm or refute these observations.

Finally, we wanted to test the hypothesis that inhibition of the anti-inflammatory macrophage/microglial phenotype reduces brain metastasis volume in a more physiologically representative model, induced *via* haematogenous tumour cell dissemination to the brain. In this study, treatment with the STAT6 inhibitor AS1517499 was associated with a significant decrease in Arg1 expression in microglia and a significant reduction in brain tumour burden. Notably, AS1517499 did not reduce 4T1-GFP cell proliferation or viability *in vitro* (**Figure S7**), indicating that the observed reduction in tumour growth does not reflect a direct effect of AS1517499 on the tumour cells' viability themselves. Nevertheless, we cannot exclude an effect of AS1517499 on the tumour cells' transcriptional profile, which could in turn impact tumour progression through changes in secreted factors and paracrine interactions with the microenvironment. Although there was also a trend towards reduced Arg1 expression in BDM, this did not quite reach significance. Together, these data suggest that the anti-inflammatory phenotype of brain-resident microglia may also be pro-tumorigenic and, hence, contribute to brain metastasis progression. Similarly, previous studies have demonstrated that STAT6 inhibition with AS1517499 suppresses the anti-inflammatory macrophage phenotype *in vitro*, whilst leading to reduced primary breast tumour volume and lower incidence of liver metastasis *in vivo* (6).

Together the above findings suggest that targeting the anti-inflammatory phenotype of microglia/macrophages may provide an effective treatment strategy for brain metastasis, most likely in combination with other currently available therapies. Drugs targeting the CSF-1 signalling pathway are currently in development and many are in clinical trial. Several of these drugs have shown great promise, but are susceptible to acquiring tumour resistance (51). Inhibition of the CSF-1 pathway can be overcome by IL-4 stimulation of TAMs within the tumour microenvironment. Quail et al. have demonstrated that this IL-4 stimulation leads to IGF-1 secretion by TAMs, which in turn activates IGF-1R and PI3K signalling in tumour cells driving tumour relapse (8). Those authors also demonstrated that regrowth could be curbed by adding inhibitors that target the IGF-1R and PI3K pathways as well as targeting STAT6 directly after the initial CSF-1R targeted therapy (8). Moreover, studies by Pradel et al. of Emactuzumab (Humanized IgG1 anti-CSF-1R antibody) have shown that *in vitro* IL-4 stimulation can overcome CSF-1R inhibition in macrophages (52). Thus, combining CSF-1 and IL-4 pathway inhibition with additional therapies may be important and have a synergistic effect. CSF-1/CSF-1R blockade has also been shown to reprogram tumour associated macrophages, and enhance the response to checkpoint immunotherapy in a pancreatic ductal adenocarcinoma model (53). A preclinical study of CSF-1R inhibition with BRAF inhibitors demonstrated that these therapies complement each other and produce a robust anti-tumour effect (46). Finally, Quail et al. have shown that AS1517499 inhibition of STAT6 in combination with CSF-1R inhibition reduces CSF-1R resistant glioblastoma regrowth (8).

The current work has focused predominantly on systemically derived BDMs. However, the results of the final study suggest that microglia may also influence metastasis progression. In support of this notion, whilst not significant, we did note trends towards changes in inflammatory marker expression in microglia that followed those observed in BDM in both the KLF4 knockout and pharmacological inhibition studies. These observations may reflect paracrine signalling between BDM and microglia, and possibly other cells within the environment, such as astrocytes and endothelial cells. The microenvironment of brain metastases is complex, with many different cell types potentially contributing to, or inhibiting, progression (48, 49). Additional studies where both populations are inhibited, as well as microglia specifically, will be invaluable in determining the exact contributions of each macrophage population, and how they interact with other components of the tumour microenvironment.

In conclusion, inhibition of the anti-inflammatory phenotype in blood-derived macrophages and/or brain-resident microglia, through targeting of CSF-1R or STAT6/KLF4, reduces metastasis growth in the brain. This work provides strong support for the concept that modulating the inflammatory phenotype of both blood-derived macrophages and microglia towards a more pro-inflammatory phenotype may have significant therapeutic benefits in brain metastasis, particularly in combination with other therapies, and may significantly improve prognosis for patients with brain metastasis.

DATA AVAILABILITY STATEMENT

The raw data supporting the conclusions of this article will be made available by the authors, without undue reservation.

ETHICS STATEMENT

The animal study was reviewed and approved by the University of Oxford Clinical Medicine Ethics Review Committee and

approved by the UK Home Office (Animals [Scientific Procedures] Act 1986).

AUTHOR CONTRIBUTIONS

VE and NS designed the research. VE, MP, VJ, HS, and KA performed the research. VE performed the analysis. KA assisted with model development. JL contributed to statistical analysis. VE and NS wrote the manuscript. All authors contributed to reviewing the work and revising it critically for important intellectual content. All authors approved the version to be published and agree to be accountable for all aspects of the work.

FUNDING

This work was supported by an MSCA fellowship (MSCA-IF-EF-ST-654985) from the European Commission to VE, Cancer Research UK (C5255/A15935), Breast Cancer Now (2016NovPRB31), the Engineering and Physical Sciences Research Council (EP/L 024012/1), and a Cancer Research UK studentship to KA.

ACKNOWLEDGMENTS

The authors thank Claire Bristow for assistance with immunohistochemistry, Karla Watson and Magda Hutchins for assistance with animal care, and Dr Alexandros Zervas and Dr Henri Bertrand for training in surgical procedures.

SUPPLEMENTARY MATERIAL

The Supplementary Material for this article can be found online at: https://www.frontiersin.org/articles/10.3389/fonc.2022.850656/full#supplementary-material

REFERENCES

1. Frisk G, Svensson T, Bäcklund LM, Lidbrink E, Blomqvist P, Smedby KE. Incidence and Time Trends of Brain Metastases Admissions Among Breast Cancer Patients in Sweden. *Br J Cancer* (2012) 106(11):1850–3. doi: 10.1038/bjc.2012.163
2. Leone JP, Leone BA. Breast Cancer Brain Metastases: The Last Frontier. *Exp Hematol Oncol* (2015) 4:33. doi: 10.1186/s40164-015-0028-8
3. Gil-bernabé AM, Ferjancic S, Tlalka M, Zhao L, Allen PD, Im JH, et al. Recruitment of Monocytes/Macrophages by Tissue Factor-Mediated Coagulation Is Essential for Metastatic Cell Survival and Premetastatic Niche Establishment in Mice. *Blood* (2012) 119(13):3164–75. doi: 10.1182/blood-2011-08-376426
4. Qian B, Deng Y, Im JH, Muschel RJ, Zou Y, Li J, et al. A Distinct Macrophage Population Mediates Metastatic Breast Cancer Cell Extravasation, Establishment and Growth. *PloS One* (2009) 4(8):e6562. doi: 10.1371/journal.pone.0006562
5. Yao Z, Zhang J, Zhang B, Liang G, Chen X, Yao F, et al. Imatinib Prevents Lung Cancer Metastasis by Inhibiting M2-Like Polarization of Macrophages. *Pharmacol Res* (2018) 133:121–31. doi: 10.1016/j.phrs.2018.05.002
6. Binnemars-Postma K, Bansal R, Storm G, Prakash J. Targeting the Stat6 Pathway in Tumor-Associated Macrophages Reduces Tumor Growth and Metastatic Niche Formation in Breast Cancer. *FASEB J* (2018) 32(2):969–78. doi: 10.1096/fj.201700629R
7. Pyonteck SM, Akkari L, Schuhmacher AJ, Bowman RL, Sevenich L, Quail DF, et al. CSF-1R Inhibition Alters Macrophage Polarization and Blocks Glioma Progression. *Nat Med* (2013) 19(10):1264–72. doi: 10.1038/nm.3337
8. Quail DF, Bowman RL, Akkari L, Quick ML, Schuhmacher AJ, Huse JT, et al. The Tumor Microenvironment Underlies Acquired Resistance to CSF-1R Inhibition in Gliomas. *Science* (2016) 352(6288):aad3018. doi: 10.1126/science.aad3018
9. Wang Y, Szretter KJ, Vermi W, Gilfillan S, Rossini C, Cella M, et al. IL-34 Is a Tissue-Restricted Ligand of CSF1R Required for the Development of Langerhans Cells and Microglia. *Nat Immunol* (2012) 13(8):753–60. doi: 10.1038/ni.2360
10. Martinez FO, Gordon S. The M1 and M2 Paradigm of Macrophage Activation: Time for Reassessment. *F1000Prime Rep* (2014) 6:13. doi: 10.12703/P6-13
11. Amici SA, Dong J, Guerau-de-Arellano M. Molecular Mechanisms Modulating the Phenotype of Macrophages and Microglia. *Front Immunol* (2017) 8:1–18. doi: 10.3389/fimmu.2017.01520
12. Rippaus N, Taggart D, Williams J, Andreou T, Wurdak H, Wronski K, et al. Metastatic Site-Specific Polarization of Macrophages in Intracranial Breast Cancer Metastases. *Oncotarget* (2016) 7:41473–87. doi: 10.18632/oncotarget.9445
13. Andreou KE, Soto MS, Allen D, Economopoulos V, de Bernardi A, Larkin JR, et al. Anti-Inflammatory Microglia/Macrophages As a Potential Therapeutic Target in Brain Metastasis. *Front Oncol* (2017) 7:251. doi: 10.3389/fonc.2017.00251
14. Galarneau H, Villeneuve J, Gowing G, Julien J-P, Vallières L. Increased Glioma Growth in Mice Depleted of Macrophages. *Cancer Res* (2007) 67(18):8874–81. doi: 10.1158/0008-5472.CAN-07-0177
15. Ewens A, Mihich E, Ehrke MJ. Distant Metastasis From Subcutaneously Grown E0771 Medullary Breast Adenocarcinoma. *Anticancer Res* (2005) 25(6B):3905–15 Available at: http://www.ncbi.nlm.nih.gov/pubmed/16312045.
16. Pulaski BA, Ostrand-Rosenberg S. Mouse 4T1 Breast Tumor Model. *Curr Protoc Immunol* (2000) 39(1):20.2.1–20.2.16. doi: 10.1002/0471142735.im2002s39
17. Workman P, Aboagye EO, Balkwill F, Balmain A, Bruder G, Chaplin DJ, et al. Guidelines for the Welfare and Use of Animals in Cancer Research. *Br J Cancer* (2010) 102(11):1555–77. doi: 10.1038/sj.bjc.6605642
18. Sarmiento Soto M, Serres S, Anthony DC, Sibson NR. Functional Role of Endothelial Adhesion Molecules in Early Stages of Brain Metastasis. *Neuro Oncol* (2014) 16(4):540–51. doi: 10.1093/neuonc/not222
19. O'Brien ER, Kersemans V, Tredwell M, Checa B, Serres S, Soto MS, et al. Glial Activation in the Early Stages of Brain Metastasis: TSPO as a Diagnostic Biomarker. *J Nucl Med* (2014) 55(2):275–80. doi: 10.2967/jnumed.113.127449
20. Serres S, Martin CJ, Sarmiento Soto M, Bristow C, O'Brien ER, Connell JJ, et al. Structural and Functional Effects of Metastases in Rat Brain Determined by Multimodal MRI. *Int J Cancer* (2014) 134(4):885–96. doi: 10.1002/ijc.28406
21. Faust N, Varas F, Kelly LM, Heck S, Graf T. Insertion of Enhanced Green Fluorescent Protein Into the Lysozyme Gene Creates Mice With Green Fluorescent Granulocytes and Macrophages. *Blood* (2000) 96(2):719–26. doi: 10.1182/blood.V96.2.719
22. Oweida AJ, Dunn EA, Karlik SJ, Dekaban GA, Foster PJ. Iron-Oxide Labeling of Hematogenous Macrophages in a Model of Experimental Autoimmune Encephalomyelitis and the Contribution to Signal Loss in Fast Imaging Employing Steady State Acquisition (FIESTA) Images. *J Magn Reson Imaging* (2007) 26(1):144–51. doi: 10.1002/jmri.21005
23. Liao X, Sharma N, Kapadia F. Krüppel-Like Factor 4 Regulates Macrophage Polarization. *J Clin Invest* (2011) 121(7):2736–49. doi: 10.1172/JCI45444
24. Emmetsberger J, Tsirka SE. Microglial Inhibitory Factor (MIF/TKP) Mitigates Secondary Damage Following Spinal Cord Injury. *Neurobiol Dis* (2012) 47(3):1–27. doi: 10.1016/j.nbd.2012.05.001

25. Bhasin M, Wu M, Tsirka SE. Modulation of Microglial/Macrophage Activation by Macrophage Inhibitory Factor (TKP) or Tuftsin (TKPR) Attenuates the Disease Course of Experimental Autoimmune Encephalomyelitis. *BMC Immunol* (2007) 8(1):10. doi: 10.1186/1471-2172-8-10
26. MacDonald KPA, Palmer JS, Cronau S, Seppanen E, Olver S, Raffelt NC, et al. An Antibody Against the Colony-Stimulating Factor 1 Receptor Depletes the Resident Subset of Monocytes and Tissue- and Tumor-Associated Macrophages But Does Not Inhibit Inflammation. *Blood* (2010) 116 (19):3955–63. doi: 10.1182/blood-2010-02-266296
27. Sauter KA, Pridans C, Sehgal A, Tsai YT, Bradford BM, Raza S, et al. Pleiotropic Effects of Extended Blockade of CSF1R Signaling in Adult Mice. *J Leukoc Biol* (2014) 96(2):265–74. doi: 10.1189/jlb.2A0114-006R
28. Balathasan L, Beech JS, Muschel RJ. Ultrasonography-Guided Intracardiac Injection: An Improvement for Quantitative Brain Colonization Assays. *Am J Pathol* (2013) 183(1):26–34. doi: 10.1016/j.ajpath.2013.03.003
29. olde Heuvel F, Holl S, Chandrasekar A, Li Z, Wang Y, Rehman R, et al. STAT6 Mediates the Effect of Ethanol on Neuroinflammatory Response in TBI. *Brain Behav Immun* (2019) 81:228–46. doi: 10.1016/j.bbi.2019.06.019
30. Bowman RL, Klemm F, Akkari L, Pyonteck SM, Sevenich L, Quail DF, et al. Macrophage Ontogeny Underlies Differences in Tumor-Specific Education in Brain Malignancies. *Cell Rep* (2016) 17(9):2445–59. doi: 10.1016/j.celrep.2016.10.052
31. Bennett FC, Bennett ML, Yaqoob F, Mulinyawe SB, Grant GA, Hayden Gephart M, et al. A Combination of Ontogeny and CNS Environment Establishes Microglial Identity. *Neuron* (2018) 98(6):1170–83.e8. doi: 10.1016/j.neuron.2018.05.014
32. Butovsky O, Jedrychowski MP, Moore CS, Cialic R, Lanser AJ, Gabriely G, et al. Identification of a Unique TGF-β-Dependent Molecular and Functional Signature in Microglia. *Nat Neurosci* (2014) 17(1):131–43. doi: 10.1038/nn.3599
33. Kaiser T, Feng G. Tmem119-EGFP and Tmem119-Creert2 Transgenic Mice for Labeling and Manipulating Microglia. *eNeuro* (2019) 6(4):1–18. doi: 10.1523/ENEURO.0448-18.2019
34. Ruan C, Sun L, Kroshilina A, Beckers L, De Jager P, Bradshaw EM, et al. A Novel Tmem119-Tdtomato Reporter Mouse Model for Studying Microglia in the Central Nervous System. *Brain Behav Immun* (2020) 83:180–91. doi: 10.1016/j.bbi.2019.10.009
35. Jordão MJC, Sankowski R, Brendecke SM, Sagar, Locatelli G, Tai Y-H, et al. Single-Cell Profiling Identifies Myeloid Cell Subsets With Distinct Fates During Neuroinflammation. *Science* (2019) 363(6425):eaat7554. doi: 10.1126/science.aat7554
36. Kadam P, Bhalerao S. Sample Size Calculation. *Int J Ayurveda Res* (2010) 1 (1):55–7. doi: 10.4103/0974-7788.59946
37. Ries CH, Cannarile MA, Hoves S, Benz J, Wartha K, Runza V, et al. Targeting Tumor-Associated Macrophages With Anti-CSF-1R Antibody Reveals a Strategy for Cancer Therapy. *Cancer Cell* (2014) 25(6):846–59. doi: 10.1016/j.ccr.2014.05.016
38. Zhai H, Heppner FL, Tsirka SE. Microglia/macrophages Promote Glioma Progression. *Glia* (2011) 59(3):472–85. doi: 10.1002/glia.21117
39. Green CE, Liu T, Montel V, Hsiao G, Lester RD, Subramaniam S, et al. Chemoattractant Signaling Between Tumor Cells and Macrophages Regulates Cancer Cell Migration, Metastasis and Neovascularization. *PloS One* (2009) 4 (8):e6713. doi: 10.1371/journal.pone.0006713
40. Li R, Hebert JD, Lee TA, Xing H, Boussommier-Calleja A, Hynes RO, et al. Macrophage-Secreted Tnfα and TGFβ1 Influence Migration Speed and Persistence of Cancer Cells in 3D Tissue Culture *via* Independent Pathways. *Cancer Res* (2017) 77(2):279–90. doi: 10.1158/0008-5472.CAN-16-0442
41. Lawrence T, Natoli G. Transcriptional Regulation of Macrophage Polarization: Enabling Diversity With Identity. *Nat Rev Immunol* (2011) 11 (11):750–61. doi: 10.1038/nri3088
42. Schulz M, Michels B, Niesel K, Stein S, Farin H, Rödel F, et al. Cellular and Molecular Changes of Brain Metastases-Associated Myeloid Cells During Disease Progression and Therapeutic Response. *iScience* (2020) 23(6):101178. doi: 10.1016/j.isci.2020.101178
43. Barakat DJ, Suresh R, Barberi T, Pienta KJ, Simons W, Friedman AD. Absence of Myeloid Klf4 Reduces Prostate Cancer Growth With Pro-Atherosclerotic Activation of Tumor Myeloid Cells and Infiltration of CD8 T Cells. *PloS One* (2018) 13:e0191188. doi: 10.1371/journal.pone.0191188
44. Van Overmeire E, Laoui D, Keirsse J, Van Ginderachter JA, Sarukhan A. Mechanisms Driving Macrophage Diversity and Specialization in Distinct Tumor Microenvironments and Parallelisms With Other Tissues. *Front Immunol* (2014) 5:127. doi: 10.3389/fimmu.2014.00127
45. Strachan DC, Ruffell B, Oei Y, Bissell MJ, Coussens LM, Pryer N, et al. CSF1R Inhibition Delays Cervical and Mammary Tumor Growth in Murine Models by Attenuating the Turnover of Tumor-Associated Macrophages and Enhancing Infiltration by CD8+ T Cells. *Oncoimmunology* (2013) 2(12): e26968. doi: 10.4161/onci.26968
46. Mok S, Koya RC, Tsui C, Xu J, Robert L, Wu L, et al. Inhibition of CSF-1 Receptor Improves the Antitumor Efficacy of Adoptive Cell Transfer Immunotherapy. *Cancer Res* (2014) 74(1):153–61. doi: 10.1158/0008-5472.CAN-13-1816
47. Coniglio SJ, Eugenin E, Dobrenis K, Stanley ER, West BL, Symons MH, et al. Microglial Stimulation of Glioblastoma Invasion Involves Epidermal Growth Factor Receptor (EGFR) and Colony Stimulating Factor 1 Receptor (CSF-1R) Signaling. *Mol Med* (2012) 18(1):519–27. doi: 10.2119/molmed.2011.00217
48. Lorger M. Tumor Microenvironment in the Brain. *Cancers* (2012) 4(1):218–43. doi: 10.3390/cancers4010218
49. Hamilton A, Sibson NR. Role of the Systemic Immune System in Brain Metastasis. *Mol Cell Neurosci* (2013) 53:42–51. doi: 10.1016/j.mcn.2012.10.004
50. Wang J, Tsirka SE. Tuftsin Fragment 1-3 Is Beneficial When Delivered After the Induction of Intracerebral Hemorrhage. *Stroke* (2005) 36(3):613–8. doi: 10.1161/01.STR.0000155729.12931.8f
51. Quail DF, Joyce JA. Molecular Pathways: Deciphering Mechanisms of Resistance to Macrophage-Targeted Therapies. *Clin Cancer Res* (2017) 23 (4):876–84. doi: 10.1158/1078-0432.CCR-16-0133
52. Pradel LP, Ooi CH, Romagnoli S, Cannarile MA, Sade H, Reuttinger D, et al. Macrophage Susceptibility to Emactuzumab (RG7155) Treatment. *Mol Cancer Ther* (2016) 15(12):3077–86. doi: 10.1158/1535-7163.MCT-16-0157
53. Zhu Y, Knolhoff BL, Meyer MA, Nywening TM, West BL, Luo J, et al. CSF1/CSF1R Blockade Reprograms Tumor-Infiltrating Macrophages and Improves Response to T-Cell Checkpoint Immunotherapy in Pancreatic Cancer Models. *Cancer Res* (2014) 74(18):5057–69. doi: 10.1158/0008-5472.CAN-13-3723

Conflict of Interest: Author MP is currently employed by OxSonics Ltd.

The remaining authors declare that the research was conducted in the absence of any commercial or financial relationships that could be construed as a potential conflict of interest.

Publisher's Note: All claims expressed in this article are solely those of the authors and do not necessarily represent those of their affiliated organizations, or those of the publisher, the editors and the reviewers. Any product that may be evaluated in this article, or claim that may be made by its manufacturer, is not guaranteed or endorsed by the publisher.

Advantages of publishing in Frontiers

OPEN ACCESS
Articles are free to read for greatest visibility and readership

FAST PUBLICATION
Around 90 days from submission to decision

HIGH QUALITY PEER-REVIEW
Rigorous, collaborative, and constructive peer-review

TRANSPARENT PEER-REVIEW
Editors and reviewers acknowledged by name on published articles

Frontiers
Avenue du Tribunal-Fédéral 34
1005 Lausanne | Switzerland

Visit us: www.frontiersin.org
Contact us: frontiersin.org/about/contact

REPRODUCIBILITY OF RESEARCH
Support open data and methods to enhance research reproducibility

DIGITAL PUBLISHING
Articles designed for optimal readership across devices

FOLLOW US
@frontiersin

IMPACT METRICS
Advanced article metrics track visibility across digital media

EXTENSIVE PROMOTION
Marketing and promotion of impactful research

LOOP RESEARCH NETWORK
Our network increases your article's readership